

https://dspace.org/

Examination of the metatarsal diaphyseal nutrient foramina: Implications for forensic analysis and morpho-functional adaptations in 19th and 20th century individuals

Manjatika, Arthur Tsalani

2024
University of the Witwatersrand, Johannesburg
https://hdl.handle.net/10539/47177
Manjatika, Arthur Tsalani . (2024). Examination of the metatarsal diaphyseal nutrient foramina: Implications for forensic analysis and morpho-functional adaptations in 19th and 20th century individuals [PHD thesis, University of the Witwatersrand, Johannesburg]. WIReDSpace. https://hdl.handle.net/10539/47177

Downloaded from a DSpace repository. https://dspace.org/

Examination of the metatarsal diaphyseal nutrient foramina: Implications for forensic analysis and morpho-functional adaptations in 19th and 20th century individuals

Student name: Arthur Tsalani Manjatika

Student number: 2228141

Degree: Doctor of Philosophy in Anatomical Sciences

School of Anatomical Sciences, Faculty of Health Sciences, University of the Witwatersrand, South Africa.

Supervisor

Dr Joshua Gabriel Davimes, PhD. Senior Lecturer

School of Anatomical Sciences, Faculty of Health Sciences, University of the Witwatersrand, South Africa

Joshua.Davimes@wits.ac.za

Co-supervisor

Dr Pedzisai Mazengenya, PhD. Associate Professor

College of Medicine, Ajman University, United Arab Emirates

p.mazengenya@ajman.ac.ae

Thesis submitted to the Faculty of Health Sciences, University of the Witwatersrand, Johannesburg, in fulfilment of the requirements for the degree of Doctor of Philosophy in Anatomical Sciences.

Johannesburg

29 October 2024.

Declarations

I, Arthur Tsalani Manjatika (Student number: 2228141), declare that this Thesis is my own, unaided work. It is being submitted for the Doctor of Philosophy in Anatomical Sciences degree at the University of the Witwatersrand, Johannesburg. It has not been submitted before for any degree or examination at any other University.



(Signature of candidate)

On the 29 of October 2024, in Johannesburg, South Africa.

Presentations arising from this research

1. **Manjatika, AT.,** Mazengenya, P., Davimes, JG. Topographical anatomy and clinical implications of the metatarsal diaphyseal nutrient foramina across South African populations. XXVIII International Symposium on Morphological Sciences (ISMS). 5-8 August 2023, South Africa. Oral presentation. ***First author Role***: Presenter.

2. **Manjatika, AT.,** Mazengenya, P., Davimes, JG. Sex estimation using dimensions around the metatarsal diaphyseal nutrient foramen in South African population: Application of discriminant function analysis and logistic regression models. The 21st Congress of the International Federation of Associations of Anatomists (IFAA). 5-8 September, 2024, South Korea. Accepted Oral presentation. ***First author Role***: Presenter.

Publications arising from this research project

1. **Manjatika, A. T.,** Mazengenya, P., Davimes, J. G. (2023) Topographical anatomy and clinical implications of the metatarsal diaphyseal nutrient foramina across South African populations. *Surgical and Radiologic Anatomy.* 45:1213–1226 https://doi.org/10.1007/s00276-023-03233-5.

2. **Manjatika, A. T.,** Davimes, J. G., Mazengenya, P. (2024) Estimation of sex using dimensions around the metatarsal diaphyseal nutrient foramen: Application of discriminant function analysis and logistic regression models. *Legal Medicine.* 68:102417. https://doi.org/10.1016/j.legalmed.2024.102417.

3. **Manjatika, A. T.,** Mazengenya, P., Davimes, J. G. (2024) Utility of the metatarsal diaphyseal nutrient foramen in estimating sex in the South African Africans population. *Translational Research in Anatomy.* 37:100327. https://doi.org/10.1016/j.tria.2024.100327.

4. **Manjatika, A. T.,** Davimes, J. G., Mazengenya, P. (2024) Application of discriminant function analysis and logistic regression models to estimate sex using the dimensions around the metatarsal diaphyseal nutrient foramen in the South Africans of Mixed ancestry. *Australian Journal of Forensic Sciences*. Pp.1-15, https://doi.org/10.1080/00450618.2024.2394419.

5. **Manjatika, A. T.,** Hutchinson, E. F., Mazengenya, P., Davimes, J. G. (***Under review-Journal of Biomechanics***) Age-related trabecular bone structure changes around the metatarsal diaphyseal nutrient foramina: implications for risk of fracture assessment.

6. **Manjatika, A. T.,** Hutchinson, E. F., Davimes, J. G., Mazengenya, P. (***Under review-Journal of Human Evolution***) Morpho-functional adaptations of the trabecular microarchitecture around the metatarsal diaphyseal nutrient foramina of the 19th and 20th century individuals.

Author contributions to the published works

Paper 1: The first author developed the protocol, secured the research funds, collected the data, conducted data analysis and drafted the manuscript. The second and third co-authors supervised the project and critically reviewed the manuscript.

Paper 2: The first author developed the protocol, secured the research funds, collected the data, conducted data analysis and drafted the manuscript. The second and third co-authors supervised the project and critically reviewed the manuscript.

Paper 3: The first author developed the protocol, secured the research funds, collected the data, conducted data analysis and drafted the manuscript. The second and third co-authors supervised the project and critically reviewed the manuscript.

Paper 4: The first author developed the protocol, secured the research funds, collected the data, conducted data analysis and drafted the manuscript. The second and third co-authors supervised the project and critically reviewed the manuscript.

Paper 5: The first author developed the protocol, secured the research funds, collected the data, conducted data analysis and drafted the manuscript. The second author critically reviewed the manuscript. The third and fourth co-authors supervised the project and critically reviewed the manuscript.

Paper 6: The first author developed the protocol, secured the research funds, collected the data, conducted data analysis and drafted the manuscript. The second author critically reviewed the manuscript. The third and fourth co-authors supervised the project and critically reviewed the manuscript.

Abstract

Metatarsal fractures occurring at the nutrient foramen (NF) level are debilitating and result in poor healing patterns due to disturbed blood flow. Variations in the topographical anatomy of the NF, which may be population-specific, make it challenging to understand its role in fracture development. The area around the NF is considered weak as the nutrient canal may reduce the structural integrity of the bone, predisposing the bone to a high risk of fracture development. However, there are no previous studies that examined the trabecular microarchitecture around the metatarsal diaphyseal NF to determine its fragility. In forensic settings, the NF of upper and lower limb long bones aids in the sex estimation of unknown individuals. However, the usefulness of the measurements around the metatarsal diaphyseal NF is unknown. This study aimed to examine the topography, morphometry and trabecular microarchitecture around the NF in 19th and 20th century South African populations.

The study utilised 4284 dry cadaveric metatarsal bones (first to fifth, from the left and right sides) of South African populations, including South African Africans (SAA), South Africans of Mixed Ancestry (SAMA) and South Africans of European descent (SAED) that are housed in the Raymond A. Dart Collection of Modern Human Skeletons housed in the School of Anatomical Sciences, University of the Witwatersrand. The metatarsals were obtained from 438 individuals aged between 18 and 65 years (mean age 46.78 ± 13.29 years). The metatarsal bones were examined for topographical variations (i.e. location, position, number, size) of the NF. For sex estimation**,** five dimensions around the region of the NF (total length of the bone, distance from the proximal end to NF, circumference at the level of the NF, and mediolateral and dorsoplantar diameters at the level of the NF) were measured from 876 metatarsals from 186 individuals of the SAED, 995 metatarsal bones from 200 individuals of SAA, and 248 metatarsal bones from 51 individuals of the SAMA population. The direct and stepwise discriminant function (DFA) analysis and logistic regression (LRA) analysis were then used to generate functions for sex estimation from these measurements. For the analysis of age-related trabecular microarchitecture changes among the three modern populations (20th century) of South Africa, 88 metatarsal bones from 44 first and 44 fifth metatarsal bones were utilised. The age range for the specimens was 0-40 years. The bones were scanned using µCT to examine the trabecular microarchitectural parameters including bone surface volume (BS/BV), bone volume fraction (BV/TV), trabecular number (TbN), trabecular spacing (TbSp), trabecular thickness (TbTh), and local bone density for trabecular bone strength. Finally, 32 first and 32 fifth metatarsal bones were selected from SAA individuals from the

age-matched (18-65 years) 19th and 20th century populations in order to determine secular changes in the trabecular microarchitectural parameters using µCT.

Topographically, the NF was observed in 99.4% of all the metatarsal bones. Most (84.5%) of the metatarsals had a single NF. The highest number of NF observed on a single bone was 5. The NF were primarily (97.4%) located in the middle third of the metatarsal bones. The position of the NF exhibited variations depending on the bone. The first metatarsal bones had predominantly dominant-sized NF, while the second, third, fourth and fifth metatarsal bones had predominantly small-sized NF. Overall, there were no significant population topographical variations of the NF *(P>0.05)*. Morphometrically, the dimensions around the NF exhibited sexual dimorphism in all populations. In the SAED, the classification accuracies for multivariable DFA and LRA ranged from 83.1-88.7%. In the SAA, the classification accuracies for multivariable DFA and LRA ranged from 75-80.5%. In the SAMA, the classification accuracies for multivariable DFA and LRA ranged from 75-83.7%. The BV/TV and TbTh showed higher values, and the BS/BV, TbN and TbSp showed lower values around the NF than at the proximal and distal diaphyses in all population groups *(P<0.001)*. In the 20th century SAA, SAED and SAMA, the BV/TV and TbTh were highest, and the BS/BV, TbSp, and TbN were lowest in the 21-30 years group. In the 19th and 20th century SAA, the BS/BV, TbSp and TbN gradually increased while the BV/TV and TbTh gradually decreased from 18-29 to 50-65 years. Overall, there were no significant population differences in the trabecular microarchitecture between 19th and 20th century SAA individuals or across the 20th century SAA, SAED and SAMA.

The present study found that the topographical anatomy of the metatarsal diaphyseal NF exhibits no significant population variations. The measurements around the metatarsal NF are sexually dimorphic. The DFA and LRA functions yielded high classification accuracies for sex estimation appropriate for forensic use in the SAED, but the functions can be cautiously applied in the SAA and SAMA for estimating sex in forensic and archeological settings due to low discriminatory power. The study demonstrated that the region around the metatarsal diaphyseal NF exhibits high BV/TV, TbTh, but low BS/BV, TbN and TbSp indicating high trabecular bone quality in the NF region compared to other parts of the metatarsal diaphysis across all age groups and the different populations examined. The study also demonstrated that there are no significant secular trabecular microarchitecture changes between 19th and 20th century individuals. Comprehensive knowledge of the NF is essential to understanding

fracture development and repair patterns clinically and for use in estimating sex in forensic settings.

Acknowledgements

So many people have directly and indirectly contributed to my success in acquiring a Doctorate degree. Most specifically, I am grateful to the following:

My supervisors: Associate Professor Pedzisai Mazengenya and Dr Joshua Gabriel Davimes. Prof Mazengenya conceived the idea, which, under his and Dr Davimes' guidance, I was able to develop this PhD thesis. Dr Davimes was always there to ensure the research was going according to plan, and he also provided all the supporting letters when I was applying for conferences, scholarships, ethics and permission letters to study sites.

I am also grateful to Associate Professor Erin Hutchinson for her technical advice during the data collection phases. Prof Hutchinson also gave me lecturing roles to ensure I am well grounded in research and teaching experiences. I am also grateful to Associate Professor Tanya Augustine for volunteering and offering me professional mentorship throughout the study. I also would like to thank Professor Paul Manger for providing me with the office space when it was needed the most.

I would also like to express my gratitude for the support I received from the following: Dr Brendon Billings, Dr Anja Meyer, Dr Benhard Zipfel, Dr Nicholas Bacci, and Mr Mashudu Mulaudzi. Thanks to the Faculty of Health Sciences Biostatistics department for all the help with statistical analysis training and consultations.

Am also grateful to my employer, Kamuzu University of Health Sciences, for the study leave and scholarship. Am also grateful to the J.J.J. Smieszek fellowship (2022, 2023) and the Faculty of Health Sciences research grants (2023) for the financial assistance towards the research costs associated with this project. I also extend my gratitude to the University of the Witwatersrand for the Postgraduate Merit Award (2022-2024) that supported my tuition fees throughout my PhD studies. I also extend my gratitude to the International Federation Association of Anatomists (IFAA) for the research travel grant to present my PhD research work at the 21st Congress in South Korea at the 21st Congress of the International Federation of Associations of Anatomists (IFAA), 2024.

Special thanks go to my guardians, Mr Justins Pahuwa and Mrs Mary Pahuwa, for constantly checking on me and for all the encouragements during the study. I am also grateful to all my relatives, friends and colleagues for their encouragements and emotional support: Dr Anthony

Mwakikunga, Masauli Manjatika, Richard Manjatika, Tinyade Pahuwa, Justins Pahuwa Jnr, Jacqueline Jangale, Phunziro Pahuwa, Zuziwe Zama Ntini, Xolisiwe Mhlathi, Godfrey Kadzuwa, Michael Chinguo, Thom Kaledzera, Charles Nyasa, Dr Elna Owembabazi, Dr Ujaddughe Moses.

Table of contents

Declarations……ii

Presentations arising from this research……..iii

Publications arising from this research project……iv

Author contributions to the published works……...v

Abstract……vi

Acknowledgements……..viii

Table of contents……x

List of figures……xiii

List of tables……xix

List of abbreviations……xxii

Chapter 1: Introduction

1.1 Background……1

1.2 Topography of the metatarsal nutrient foramina (NF)……4

1.2.1 Anatomy of the foot and metatarsal diaphyseal nutrient foramina (NF)……..4

1.2.2 Topographical variations of the metatarsal diaphyseal nutrient foramen (NF)…8

1.3 Sex estimation using nutrient foramina (NF) of the metatarsal bones……11

1.3.1 Methods of sex estimation from skeletal material and population specificity….11

1.3.2 Usefulness of measurements around the nutrient foramen (NF) in sex estimation……13

1.4 Bone morphology and functional adaptations……15

1.4.1 Bone morphology……15

1.4.2 Trabecular bone morpho-functional adaptation……...17

1.5 Study hypothesis……20

1.6 Aims and objectives……21

1.6.1 Aim……...21

1.6.2 Objectives……21

1.7 Outline of the thesis……21

1.8 References……...22

Chapter 2: Topographical anatomy and clinical implications of the metatarsal diaphyseal nutrient foramina across South African populations……36

Chapter 3: Estimation of sex using dimensions around the metatarsal diaphyseal nutrient foramen: Application of discriminant function analysis and logistic regression models……50

Chapter 4: Utility of the metatarsal diaphyseal nutrient foramen in estimating sex in the South African Africans population ……60

Chapter 5: Application of discriminant function analysis and logistic regression models to estimate sex using the dimensions around the metatarsal diaphyseal nutrient foramen in the South Africans of Mixed ancestry……70

Chapter 6: Age-related trabecular bone structure changes around the metatarsal diaphyseal nutrient foramina: implications for risk of fracture assessment ……86

Chapter 7: Morpho-functional adaptations of the trabecular microarchitecture around the metatarsal diaphyseal nutrient foramina of the 19th and 20th century individuals …….144

Chapter 8: Discussion and conclusion……195

8.1 Introduction……...195

8.2 Topographical variation of the metatarsal diaphyseal nutrient foramina (NF)…….195

8.3 The utility of the dimension around the nutrient foramina (NF) in estimating sex ……196

8.4 Trabecular microarchitectural changes around the metatarsal diaphyseal nutrient foramen (NF)……...199

8.5 Study limitations……204

8.6 Recommendations for further studies…….……..205

8.7 Conclusions, novelty and significance of the current study ……206

8.8 References ……..…….208

Appendices: ……...215

Appendix 1: Ethical clearance waiver…….215

Appendix 2: Turnitin report……..……218

Appendix 3: Co-authorship agreement form……219

Appendix 4: Journal permissions to reuse publications for thesis……224

List of figures

Chapter 1

Figure 1: An x-ray photograph (anteroposterior view) of the right foot showing the three main divisions of the foot: Forefoot, midfoot and hindfoot. 1= First metatarsal bone, 2= Second metatarsal bone, 3= Third metatarsal bone, 4= Forth metatarsal bone, 5= Fifth metatarsal bone. This is the researcher's own X-ray photograph……6

Figure 2: A photograph of the metatarsal bones showing the location of the nutrient foramina on the diaphysis. 1= First metatarsal bone, 2= Second metatarsal bone, 3= Third metatarsal bone, 4= Forth metatarsal bone, 5= Fifth metatarsal bone. The nutrient foramina are located on the lateral surfaces in bones 1-4, and the medial surface in bone 5.……7

Figure 3: A plate of photographs showing the patency of the diaphyseal nutrient canal on the fifth metatarsal bones. A=x-ray patency confirmation. B=physical patency confirmation….7

Chapter 2

Figure 1: A plate of the metatarsal bones showing sex and side classification for each South African population group. The metatarsals are arranged from medial (1) to lateral (5). A= Metatarsal bones of the South African Africans (SAA), B= Metatarsals of the South Africans of European descent (SAED), C= Metatarsals of the South Africans of Mixed Ancestry (SAMA). 1= First metatarsal bone, 2= Second metatarsal bone, 3= Third metatarsal bone, 4= Fourth metatarsal bone, 5= Fifth metatarsal bone…….38

Figure 2: A photograph of the first metatarsal bones with arrows showing the number of diaphyseal nutrient foramina in the South African populations. A= right first metatarsal with one nutrient foramen on the lateral surface, B= right first metatarsal with two nutrient foramina on the lateral surface, C= Left first metatarsal with four nutrient foramina on the lateral surface……..41

Figure 3: A photograph of the left and right side metatarsal bones showing the location of nutrient foramina. The two dashed lines divides the metatarsals into the proximal, middle and distal thirds. Arrows are pointing at the nutrient foramina located in the middle third of different surfaces of the metatarsal bones. MT 1= first metatarsal, MT 2= second metatarsal, MT 3= third metatarsal, MT 4= fourth metatarsal, MT 5= fifth metatarsal…….43

Figure 4: A graphs showing the foramina index means and standard deviations across populations. L=Left side, R=Right side, SAA=South African Africans, SAED=South Africans of European descent, SAMA=South Africans of Mixed ancestry. Mt=Metatarsal bone. Mm=Millimetres. *=significant median difference (Kruskal Wallis test p-value <0.05), as the FI on Mt 2 were not normally distributed…….46

Figure 5: A plate of graphs showing the distribution of position of the nutrient foramen on the surfaces of metatarsal diaphysis. Upper graph=distribution of the nutrient foramen in the South African Africans, Middle graph=distribution of the nutrient foramen in the South Africans of European descent, Lower graph=distribution of the nutrient foramen in the South Africans of Mixed ancestry. Mt=Metatarsal bone…….47

Figure 6: A photograph of the first through fifth metatarsal bones of the right foot with a needle showing the direction of the nutrient canal. MT1= first metatarsal, MT2= second metatarsal, MT3= third metatarsal, MT4= fourth metatarsal, MT5= fifth metatarsal……48

Chapter 3

Figure 1: Photographs of the first metatarsal bones showing the measurements that were utilized in the study. The black arrow indicates the nutrient foramen. Cir=Circumference, DP=Dorsoplantar diameter, ML=Mediolateral diameter, NFPE=Distance from proximal end to the nutrient foramen, TL=Total length……51

Chapter 4

Figure 1: Photographs of the second metatarsal bones showing the measurements that were utilized in the study. The black arrow indicates the nutrient foramen. Cir=Circumference, DP=Dorsoplantar diameter, ML=Mediolateral diameter, NFPE=Distance from proximal end to the nutrient foramen, TL=Total length…….62

Chapter 5

Figure 1: Photographs of the fourth metatarsal bones showing the measurements that were utilized in the study. The short black arrow indicates the nutrient foramen.

Cir=Circumference, DP=Dorsoplantar diameter, ML=Mediolateral diameter, NFPE=Distance from proximal end to the nutrient foramen, TL=Total length…….74

Chapter 6

Figure 1: A plate of graphs showing age-related trabecular structural changes at different levels and surfaces of the first metatarsal bone in the **A**. SAA (South African Africans), **B.** SAED (South Africans of European descent) and **C.** SAMA (South Africans of Mixed Ancestry) populations. Bars indicate median trabecular values. MT1= First metatarsal bone, BV/TV= Bone volume fraction, BS/BV= Bone surface volume, TbTh=Trabecular thickness, TbN=Trabecular number, TbSp= Trabecular spacing, mm= millimetres, %= Percentage, *= Significant median differences $p \leq 0.05$, HU= Hounsfield units…….116

Figure 2: A plate of graphs showing age-related trabecular structural changes at different levels and surfaces of the fifth metatarsal bone in the **A**. SAA (South African Africans), **B.** SAED (South Africans of European descent) and **C.** SAMA (South Africans of Mixed Ancestry) populations. Bars indicate median trabecular values. MT5= Fifth metatarsal bone, BV/TV= Bone volume fraction, BS/BV= Bone surface volume, TbTh=Trabecular thickness, TbN=Trabecular number, TbSp= Trabecular spacing, mm= millimetres, %= Percentage, *= Significant median differences $p \leq 0.05$, HU= Hounsfield units……..119

Figure 3: A plate of graphs showing trabecular quality at different levels of the metatarsal bones within each population group in pooled age groups. **A.** First metatarsal bone. **B.** Fifth metatarsal bone. Bars indicate median trabecular values. MT1= First metatarsal bone, BV/TV= Bone volume fraction, BS/BV= Bone surface volume, TbTh= Trabecular thickness, TbN= Trabecular number, TbSp= Trabecular spacing, SAA= South African Africans, SAED= South Africans of European descent, SAMA= South Africans of Mixed ancestry, *= Significant median differences $p \leq 0.05$, **= Significant median differences $p < 0.0001$….122

Figure 4: A plate of graphs showing variations of trabecular bone quality on the first and fifth metatarsal bone surfaces in a pooled population and age group. Bars indicate median trabecular values. MT1= First metatarsal bone, MT5= Fifth metatarsal bone, BV/TV= Bone volume fraction, BS/BV= Bone surface volume, TbTh= Trabecular thickness, TbN= Trabecular number, TbSp= Trabecular spacing. *= Significant median differences $p \leq 0.05$, **= Significant median differences $p < 0.0001$…….124

Figure 5: A plate of µCT photographs showing local bone densities (colour maps) of the trabeculated bone at different levels of the metatarsal bones across different age groups. **A.** First metatarsal bone and the nutrient foramen is located on the lateral surface. **B.** Fifth metatarsal bone and the nutrient foramen is located on the medial surface. A higher mean gray value (reddish colour) indicates more dense areas, and a low mean gray value (blueish colour) indicates less dense areas. M= Medial surface, L= Lateral surface, D= Dorsal surface, P= Plantar surface……127

Chapter 7

Figure 1: A µCT photograph of the fifth metatarsal bone showing the medial surface and the levels of the bone where the transverse slices were taken. The dashed lines pass through the nutrient foramen level, and the arrowhead points at the insert box, showing the selected regions of interest on each surface of the bone. The coloured circled areas represent different regions of interest of the trabeculated bone with different local bone densities. NF= Nutrient foramina, Above= the area above the nutrient foramina, Below= the area below the nutrient foramina……153

Figure 2: A plate of graphs showing age-related trabecular structural changes at different levels and surfaces of the first metatarsal bone in the 19th century SAA population. Bars indicate median trabecular values. MT1= First metatarsal bone, BV/TV= Bone volume fraction, BS/BV= Bone surface volume, TbTh=Trabecular thickness, TbN=Trabecular number, TbSp= Trabecular spacing, SAA= South African Africans, mm= millimetres, %= Percentage, *= Significant median differences $p \leq 0.05$, HU= Hounsfield units……..166

Figure 3: A plate of graphs showing age-related trabecular structural changes at different levels and surfaces of the first metatarsal bone in the 20th century SAA population. Bars indicate median trabecular values. MT1= First metatarsal bone, BV/TV= Bone volume fraction, BS/BV= Bone surface volume, TbTh= Trabecular thickness, TbN= Trabecular number, TbSp= Trabecular spacing, SAA= South African Africans, mm= millimetres, %= Percentage, *= Significant median differences $p \leq 0.05$, HU=Hounsfield units…….168

Figure 4: A plate of graphs showing age-related trabecular structural changes at different levels and surfaces of the fifth metatarsal bone in the 19th century SAA population. Bars indicate median trabecular values. MT5= Fifth metatarsal bone, BV/TV= Bone volume

fraction, BS/BV= Bone surface volume, TbTh= Trabecular thickness, TbN= Trabecular number, TbSp= Trabecular spacing, SAA= South African Africans, mm= millimetres, %= Percentage, HU=Hounsfield units……169

Figure 5: A plate of graphs showing age-related trabecular structural changes at different levels and surfaces of the fifth metatarsal bone in the 20th century SAA population. Bars indicate median trabecular values. MT5= Fifth metatarsal bone, BV/TV= Bone volume fraction, BS/BV= Bone surface volume, TbTh= Trabecular thickness, TbN= Trabecular number, TbSp= Trabecular spacing, SAA= South African Africans, mm= millimetres, %= Percentage, HU=Hounsfield units…….171

Figure 6: A plate of graphs showing trabecular strength at different levels of the first metatarsal bone within the 19th century and 20th century population groups in pooled age groups. Bars indicate median trabecular values. BV/TV= Bone volume fraction, BS/BV= Bone surface volume, TbTh= Trabecular thickness, TbN= Trabecular number, TbSp= Trabecular spacing, SAA= South African Africans, *= Significant median differences $p \leq 0.05$, **= Significant median differences $p < 0.0001$……..173

Figure 7: A plate of graphs showing trabecular strength at different levels of the fifth metatarsal bone within the 19th century and 20th century population groups in pooled age groups. Bars indicate median trabecular values. BV/TV= Bone volume fraction, BS/BV= Bone surface volume, TbTh= Trabecular thickness, TbN= Trabecular number, TbSp= Trabecular spacing, SAA= South African Africans, *= Significant median differences $p \leq 0.05$, **= Significant median differences $p < 0.0001$……..174

Figure 8: A plate of graphs showing variations of bone strength on the first and fifth metatarsal bone surfaces in a pooled population and age group. Bars indicate median trabecular values. MT1= First metatarsal bone, MT5= Fifth metatarsal bone, BV/TV= Bone volume fraction, BS/BV= Bone surface volume, TbTh= Trabecular thickness, TbN= Trabecular number, TbSp= Trabecular spacing. *= Significant median differences $p \leq 0.05$, **= Significant median differences $p < 0.0001$……176

Figure 9: A plate of µCT photographs of the first metatarsal bone showing local bone densities (colour maps) at different levels of the metatarsal bone across different age groups within each population group. A higher mean gray value (reddish colour) indicates more dense areas and a low mean gray value (blueish colour) indicates less dense areas of the

trabeculated bone. The nutrient foramen is located on the lateral surface. M= Medial surface, L= Lateral surface, D= Dorsal surface, P= Plantar surface……178

Figure 10: A plate of µCT photographs of the fifth metatarsal bone showing local bone densities (colour maps) at different levels of the metatarsal bone across different age groups within each population group. A higher mean gray value (reddish colour) indicates more dense areas and a low mean gray value (blueish colour) indicates less dense areas of the trabeculated bone. The nutrient foramen is located on the medial surface. M= Medial surface, L= Lateral surface, D= Dorsal surface, P= Plantar surface……179

List of tables

Chapter 2

Table 1: Sample distribution of the South African populations…….37

Table 2: Number of the metatarsal diaphyseal nutrient foramina in the South African population groups……..40

Table 3: Size of the metatarsal diaphyseal nutrient foramina in the South African population groups……42

Table 4: Location of the metatarsal diaphyseal nutrient foramina in the South African population groups…….44

Table 5: Comparison of range and mean of the Foramina index the metatarsal diaphyseal nutrient foramina across populations……45

Chapter 3

Table 1: Descriptive statistics of the measurement parameters…….52

Table 2: Descriptive statistics of the foramina index (FI)…….53

Table 3: Direct discriminant coefficients, constants, and classification accuracies for individual measurements of the metatarsals……53

Table 4: Stepwise discriminant function coefficients, constants, and classification rates for a combination of measurements for multiple metatarsals……..54

Table 5: Direct discriminant function coefficients, constants, and classification rates for a combination of measurements for multiple metatarsals…….55

Table 6: Stepwise logistic regression coefficients, constants, and classification rates for a combination of measurements for multiple metatarsals……56

Table 7: Direct logistic regression coefficients, constants, and classification rates for a combination of measurements for multiple metatarsals…….57

Chapter 4

Table 1: Descriptive statistics of the measured parameters…….62

Table 2: Descriptive statistics of the foramina index (FI)……63

Table 3: Direct discriminant coefficients, constants and classification accuracies for individual measurements of the metatarsals……63

Table 4: Stepwise discriminant function coefficients, constants, and classification rates for a combination of measurements for multiple metatarsals……64

Table 5: Direct discriminant function coefficients, constants, and classification rates for a combination of measurements for multiple metatarsals…….65

Table 6: Stepwise logistic regression coefficients, constants, and classification rates for a combination of measurements for multiple metatarsals……66

Table 7: Direct logistic regression coefficients, constants, and classification rates for a combination of measurements for multiple metatarsals……..67

Chapter 5

Table 1: Descriptive statistics of the measured parameters in the South Africans of Mixed ancestry population…….73

Table 2: Descriptive statistics of the foramina index (FI) in the South Africans of Mixed ancestry population……76

Table 3: Direct discriminant function coefficients, constants and classification accuracies for individual measurements of the metatarsals……76

Table 4: Stepwise discriminant function coefficients, constants, and classification rates for a combination of measurements for multiple metatarsals……77

Table 5: Direct discriminant function coefficients, constants, and classification rates for a combination of measurements for multiple metatarsals……78

Table 6: Stepwise logistic regression coefficients, constants, and classification rates for a combination of measurements for multiple metatarsals…….79

Table 7: Direct logistic regression coefficients, constants, and classification rates for a combination of measurements for multiple metatarsals…….80

Chapter 6

Table 1: Sample distribution of the metatarsal bones across different age and population groups……91

Table 2: Age matched comparisons of trabecular structure parameters on different surfaces of the bone across population groups in the 0-10-year group……97

Table 3: Age matched comparisons of trabecular structure parameters on different surfaces of the bone across population groups in the 11-20-year group……101

Table 4: Age matched comparisons of trabecular structure parameters on different surfaces of the bone across population groups in the 21-30-year group……105

Table 5: Age matched comparisons of trabecular structure parameters on different surfaces of the bone across population groups in the 31-40-year group……109

Chapter 7

Table 1: Sample distribution of the metatarsal bones across different age and population groups……..151

Table 2: Age matched comparisons of trabecular morphologic parameters on different surfaces of the metatarsal bone across the 19th century and 20th century population groups in the 18-29-year group……156

Table 3: Age matched comparisons of trabecular morphologic parameters on different surfaces of the metatarsal bone across 19th century and 20th century population groups in the 30-49-year group……159

Table 4: Age matched comparisons of trabecular morphologic parameters on different surfaces of the metatarsal bone across 19th century and 20th century population groups in the 50-65-year group……162

List of abbreviations

ANF= Above nutrient foramina region

ANOVA= Analysis of variance

BCE= Before common era

BNF= Below nutrient foramina region

BS/BV= Bone surface to bone volume ratio

BV/TV= Bone volume to tissue volume ratio

CE= Common era

CI= Confidence interval

CNF= Circumference at the level of the nutrient foramen

DA= Degree of anisotropy

DFA= Discriminant function analysis

DPNF= Dorso-plantar diameter at the level of the nutrient foramen

LRA= Logistic regression analysis

MT= Metatarsal bone

MLNF= Mediolateral diameter at the nutrient foramen

NF= Nutrient foramina/foramen

TA= Total subperiosteal area

TbN= Trabecular number

TbSp= Trabecular spacing

TbTh= Trabecular thickness

TL= Total length

NFPE= Proximal end to nutrient foramen

Chapter 1: Introduction

1.1 Background

Metatarsal fractures are a significant cause of foot injuries and pain. They represent about 35% of all foot-related injuries and 6% of all skeletal injuries (Buddecke et al., 2010; Cakir et al., 2011; Sarpong et al., 2018). They are twice as common in children than in adults since the growing bones in children have low bone density, weak cortical and trabecular bone networks, predisposing them to fractures than in mature bones of adults (Rammelt et al., 2004; Moore, 2018). In the adult population, metatarsal fractures are common in physically active individuals (e.g., military personnel, athletes, or industrial workers), leading to disability, pain and reduced quality of life (Petrisor et al., 2006; Kothapalli, 2018). Most metatarsal fractures like overuse or repetitive stress fractures are observed in persons under 50 years of age possibly due to high levels of physical activity and increased exposure to traumatic injuries during sporting activities (Petrisor et al., 2006; Sarpong et al., 2018). These fracture patterns suggest that age is a potential risk factor for metatarsal fracture development, possibly due to differences in development, lifestyle, and physical activity levels (Moore, 2018; Sarpong et al., 2018). The first and fifth metatarsal bone fractures collectively have an incidence of about 61% (Cakir et al., 2011). The fractures of the first and fifth metatarsal bones usually occur in isolation. However, those of the second, third and fourth metatarsal bones rarely occur in isolation, suggesting that the relative position of the metatarsal bone in the foot may also be a predisposing factor (Petrisor et al., 2006). Simple metatarsal fractures are treated conservatively, but compound/complex metatarsal fractures require stabilization using internal fixation or bone grafting surgical procedures (Sarpong et al., 2018).

Metatarsal fractures can occur on the base or head of the bone, proximal, middle, or distal segments of the diaphysis, or in the vicinity of the nutrient foramen/foramina (NF) on the diaphysis (Dameron Jr, 1975; Craig et al., 2003; Rammelt et al., 2004; Cakir et al., 2011; DeVries et al., 2015; Moore, 2018). Unlike other fracture sites, fractures around the NF are of great concern as they may damage the nutrient artery, leading to non-union of the fracture site and poor healing patterns (Kizilkanat et al., 2007). The NF are external openings leading to the nutrient canal. The nutrient canal carries nutrient arteries and veins for the nutrition of the long bones (Götzen et al., 2003; Singla et al., 2017; Kothapalli, 2018). Blood supply to the bone is essential for the survival of bone cells such as osteocytes and osteoblasts during bone

development and growth, fracture union and healing (Monreal-Redondo and Fernández-Camacho, 2003; Kothapalli, 2018, Mazengenya and Fasemore, 2015, Mazengenya and Billings, 2016; Singla et al., 2017).

Clinically, topographical knowledge of the NF is essential to preserve circulation in bone graft surgical procedures when managing complex fractures (Anamika et al., 2015; Kothapalli, 2018). The topographical anatomy of the NF is also important in understanding the development of fractures, healing patterns and fracture site reconstruction in long bones like the metatarsals (Kothapalli, 2018). The topographical anatomy of the NF of the metatarsal bones is variable, and limited studies have described these variations (Singh, 1960; Patake and Mysorekar, 1977; Monreal-Redondo and Fernández-Camacho, 2003; Malukar and Joshi, 2011; Anamika et al., 2015; Kothapalli, 2018). From these studies, a comprehensive description of the anatomical variations of the metatarsal diaphyseal NF is still lacking due to the different methodologies employed and small sample sizes. It also remains unclear whether these variations exhibit population specificity, laterality or sexual dimorphism, as previous studies did not clearly describe the characteristics of the studied sample populations. If not properly comprehended, the topographical variations may pose a challenge to the diagnosis and treatment of metatarsal fractures. This may result in delayed healing or non-union of fractures and poor patient outcomes (Monreal-Redondo and Fernández-Camacho, 2003; Murlimanju et al., 2011; Mazengenya and Fasemore, 2015). To comprehensively understand the variations of the metatarsal diaphyseal NF, it is crucial to describe the topographical anatomy and morphometry of the NF using skeletal samples of known population affinity, age and sex. There is a paucity of information on the topography and morphometry of the NF of the metatarsal bones in South African populations. South African population groups show notable postcranial osteological feature variations and may serve as an ideal sample for determining population-specific variations (Mokoena et al., 2017; Bidmos et al., 2021).

Numerous topographical studies have extensively studied variations of the NF in many long bones of the limb including the hands and feet (Gümüsburun et al., 1994; Kizilkanat et al., 2007; Mazengenya and Fasemore, 2015; Mazengenya and Billings, 2016; Kothapalli, 2018). These studies concluded that the NF is a potentially weak area as the nutrient canal may reduce the structural integrity of the bone, thereby predisposing the long bone to a high risk of fracture development. However, limited studies describe the internal bone morphology around the NF, making it unclear whether the NF is weaker compared to other regions of the

diaphysis of the long bones. The internal bone morphology is divided into cortical and trabecular bone (Stock and Pfeiffer, 2001; Komza, 2017). Götzen et al. (2003) examined the cortical bone around the NF of the equine metacarpal bones and found no degree of cortical bone weakening. This study, however, did not examine the trabecular structure around the NF. Notably, the internal bone structure like cortical thickness and trabecular structure, as well as the loading mechanisms in equine (quadrupeds) is different from that of humans (bipeds), making it difficult to determine if the NF structure in humans may resemble that of the equine (Götzen et al., 2003). The trabecular bone has higher environmental plasticity than the cortical bone, making it a good model for understanding bone architecture and quality (Agarwal et al., 2004). It is important to note that the trabecular bone morphometry cannot directly be used as a proxy for bone strength since bone strength is influenced by multiple factors like cortical bone thickness, bone shape or geometry and bone mineral density (Stock and Pfeiffer, 2001; Götzen et al., 2003; Hagihara and Nara, 2018). However, the trabecular morphometric parameters, like the bone volume fraction (BV/TV), trabecular thickness (TbTh), trabecular number (TbN) and trabecular spacing (TbSp), can be correlated with bone strength (Agarwal et al., 2004). Thus, examining the trabecular microarchitecture of the bone diaphysis is important to understand the fragility of the area around the NF. This is because the trabecular structure is a well-known predictor of bone fragility and risk of fracture development (Stock and Pfeiffer, 2001; Agarwal et al., 2004). Given that no studies examined the trabecular structure around the NF, it remains unknown whether the trabecular structure around the NF is more fragile compared to other regions/areas of the diaphysis, such as the proximal and distal ends of the diaphysis. The effects of age, sex, population specificity and mechanical loading factors like habitual locomotor behaviours on the trabecular structure are also unknown, making it difficult to determine if some populations or age groups are at a high risk of fracture development.

Besides their clinical importance, the NF are also of archaeological and forensic importance in medico-legal cases where identifying unknown individuals is required (Mokoena et al., 2017; Fasemore et al., 2018). Measurement around the NF of the lower limb and upper limb long bones are known to aid in the sex estimation of individuals in different population groups worldwide (Mokoena et al., 2017; Fasemore et al., 2018; Sallie et al., 2022). Due to high crime and murder cases in South Africa, victim identification from exhumed skeletons is challenging (Steyn, 2005; Mokoena et al., 2017; Bidmos et al., 2021). It is very unlikely to find all the known sexually dimorphic bones in their intact and unbroken state in forensic and

archaeological settings (Bidmos et al., 2021). In many exhumed skeletal remains, the bones are poorly preserved and are usually recovered in a decomposed or broken state, making it very difficult to use in identifying unknown individuals (Bidmos et al., 2021). There is a need to generate new methods of estimating the parameters of the biological profile like sex using the metatarsal skeletal remains to ensure accurate human identification in the diverse South African populations (İşcan and Steyn, 1999; Mokoena et al., 2017; Bidmos et al., 2021). It is unclear whether the morphometry around the NF of the metatarsals can be used to estimate an individual's sex globally or locally in the South African populations.

In general, few studies examined the NF of the metatarsal bones with a limited focus on the clinical applications (Singh, 1960; Patake and Mysorekar, 1977; Monreal-Redondo and Fernández-Camacho, 2003; Malukar and Joshi, 2011; Anamika et al., 2015; Sandhya and Singh, 2017; Kothapalli, 2018). To date, the utility of the measurements around the NF of the metatarsal bones in sex estimation remains unclear. Additionally, the morpho-functional adaptations of the trabecular bone around the NF and their role in determining the risk of bone fragility and fracture development remain elusive. The current thesis therefore aimed to examine the topography, morphometric and trabecular microarchitecture around the metatarsal diaphyseal NF of the South African population groups to fill this knowledge gap.

This chapter gives the general background to the study and will critically review the literature on the topographical variations of the metatarsal diaphyseal NF. It will also provide literature underpinning the use of NF in estimating sex and the role of trabecular bone in determining bone strength. This will be followed by the research hypothesis, research aims and objectives, and finally, the outline of the thesis.

1.2 Topography of the metatarsal nutrient foramina (NF)

1.2.1 Anatomy of the foot and metatarsal diaphyseal nutrient foramina (NF)

The human foot has seven tarsal bones, five metatarsal bones, fourteen phalangeal bones and two sesamoid bones (Moore et al., 2018). The foot is divided into three regions: hind-, mid-, and forefoot (Figure 1). The hindfoot is made up of the calcaneus and talus bones. In contrast, the midfoot comprises the remaining five tarsal bones: the navicular, cuboidal and the three (lateral, intermediate and medial) cuneiform bones. The metatarsal, phalangeal and sesamoid bones make up the forefoot region (Standring, 2015; Moore et al., 2018). Clinically, the foot

bones are further classified into three columns: medial, central and lateral, based on the mobility of the associated bones and joints (Sarpong et al., 2018). The medial column is mobile and includes the navicular, talus, medial cuneiform, first metatarsal and phalangeal bones. The central group comprises the intermediate and lateral cuneiforms, the second to fourth metatarsal, and their associated phalangeal bones, and it is less mobile than the medial column. The least mobile lateral column comprises the calcaneus, cuboidal and fifth metatarsal bones (Sarpong et al., 2018).

Metatarsal bones are miniature long bones in the forefoot (Moore et al., 2018). External metatarsal features include the base proximally, the shaft or diaphysis centrally, and the head distally (Standring, 2015; Moore et al., 2018). The metatarsal bones have four reference surfaces: the dorsal (anterior), plantar (posterior), medial, and lateral. The five metatarsal bones in each foot are numbered first to fifth (1-5) from the medial to the lateral side of the foot (Figure 1), and each of them has distinct morphological features (Moore et al., 2018). The first metatarsal bone is the thickest and shortest, while the second metatarsal bone is the longest. The third metatarsal bone has two medial facets on its base. The fourth metatarsal bone has an oval-shaped base. The fifth metatarsal bone has a large tuberosity that protrudes laterally and proximally (Standring, 2015; Moore et al., 2018). Unlike other long bones, metatarsals have only one epiphysis. The epiphysis of the first metatarsal bone is on the proximal end of the bone, while that of the second metatarsal through to the fifth metatarsal bone is on the distal ends (Monreal-Redondo and Fernández-Camacho, 2003).

These regions of the foot are fundamental when considering the different phases of human gait and how each region is exposed to mechanical loading forces. The human bipedal gait is divided into stance and swing phases (Moore et al., 2018). The foot is not in contact with the ground in the swing phase, but it is in contact with the ground in the stance phase. During the stance phase, there is a mediolateral shift of weight onto the supporting limb (Hagihara and Nara, 2018). The weight on the supporting limb is absorbed by the foot's medial and lateral longitudinal arches before toeing off. Thus, there is high mechanical loading of the metatarsals during the stance phase (Nagel et al., 2008).

Interestingly, the foot columns also correspond with the incidence patterns of metatarsal fractures, with high incidence in the metatarsals in the lateral column, followed by the central and medial columns (Sarpong et al., 2018), suggesting that the mobility of each metatarsal bone is a predisposing factor to fracture development. The fact that most fractures are site-

specific on the metatarsal bones also suggests that there are other predisposing factors to high incidences of metatarsal fractures (Cakir et al., 2011). For instance, most metatarsal fractures occur at the proximal or distal diaphyses or NF, suggesting that these areas have intrinsic characteristics, i.e., less or poorly developed cortical and trabecular bone structure, predisposing them to a high risk of fracture development (Cakir et al., 2011). The NF is located on the metatarsals' diaphysis or shaft (Kothapalli, 2018) (Figure 2). Nutrient arteries are the primary source of blood supply to the diaphysis of the long bones, though some additional blood supply may come from the epiphyseal and periosteal nutrient arteries (Götzen et al., 2003; Kothapalli, 2018). To avoid confusing the NF with the other smaller foramina, the patency of the NF is confirmed by inserting a fine hypodermic needle and taking radiological images, as shown in Figure 3.

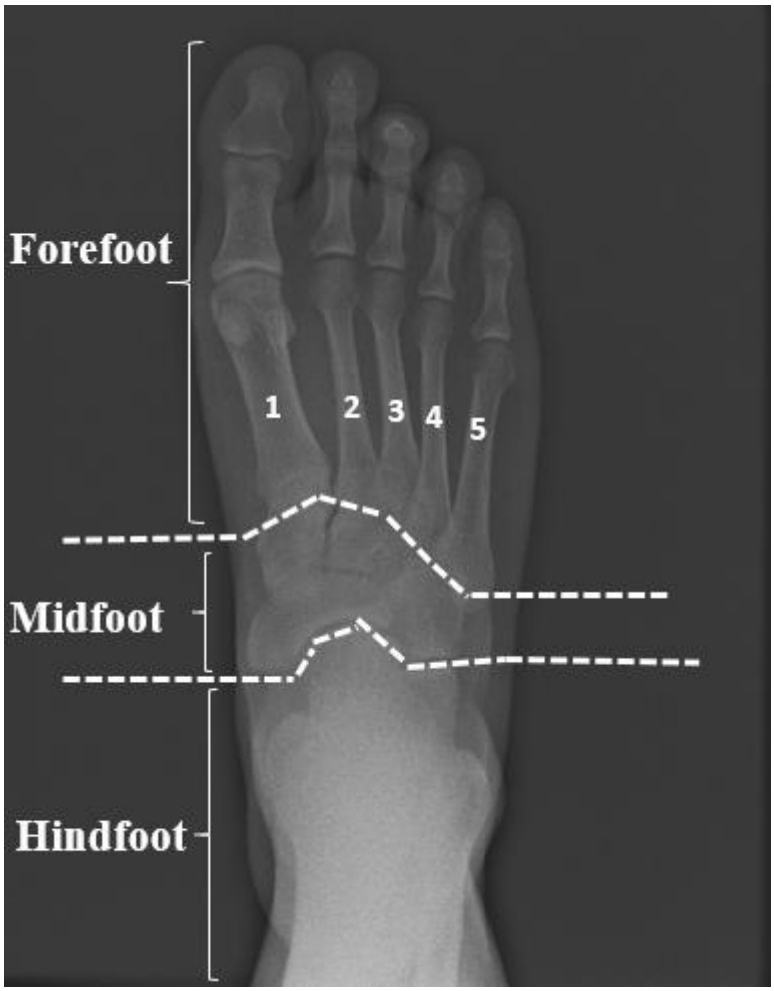


Figure 1: An X-ray photograph (anteroposterior view) of the right foot showing the three main divisions of the foot: forefoot, midfoot and hindfoot. 1= First metatarsal bone, 2= Second metatarsal bone, 3= Third metatarsal bone, 4= Forth metatarsal bone, 5= Fifth metatarsal bone. This is the researcher's own X-ray photograph.

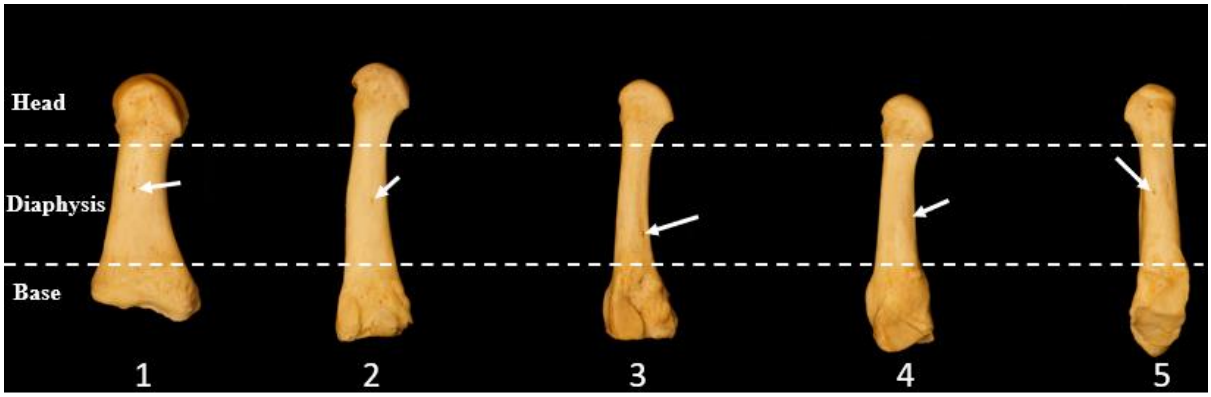


Figure 2: A photograph of the metatarsal bones showing the location of the nutrient foramina on the diaphysis (indicated by white arrows). 1= First metatarsal bone, 2= Second metatarsal bone, 3= Third metatarsal bone, 4= Forth metatarsal bone, 5= Fifth metatarsal bone. The nutrient foramina are located on the lateral surfaces in bones 1-4, and the medial surface in bone 5.

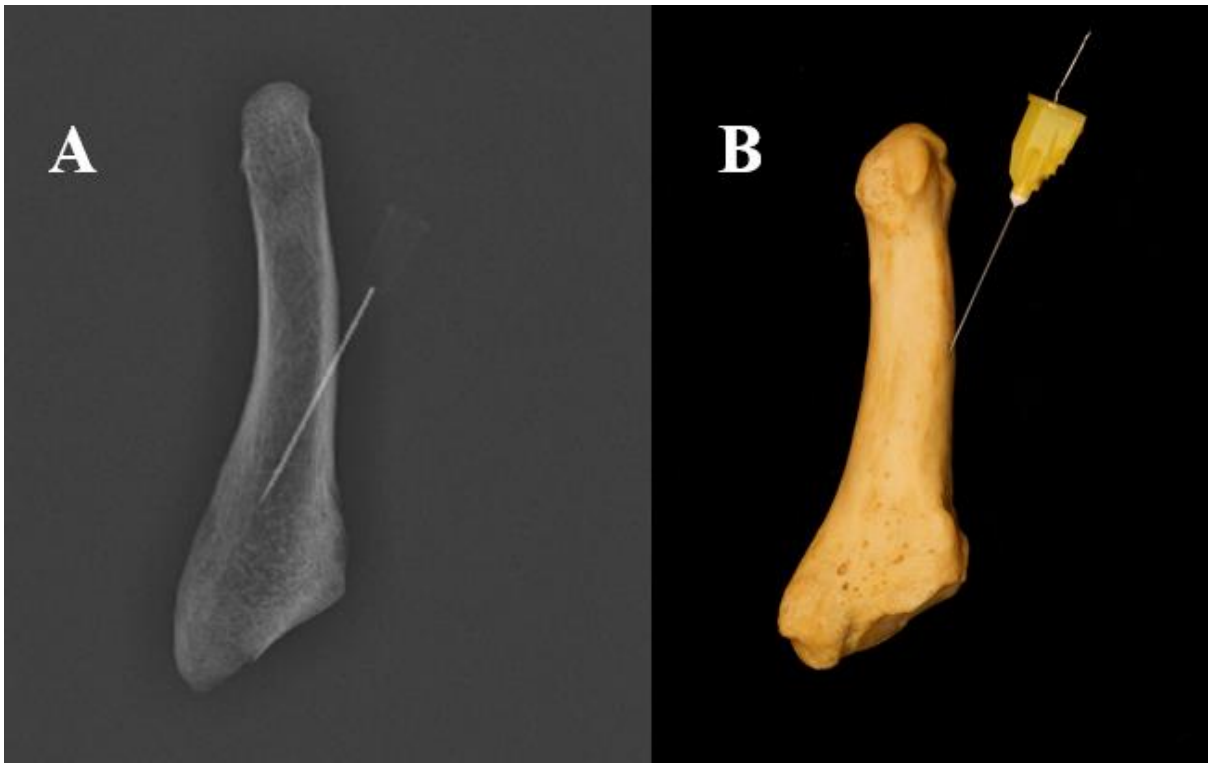


Figure 3: A plate of photographs showing the patency of the diaphyseal nutrient canal on the fifth metatarsal bones. A=x-ray patency confirmation. B=physical patency confirmation.

1.2.2 Topographical variations of the metatarsal diaphyseal nutrient foramen (NF)

Preoperatively, diagnostic imaging is usually done to rule out possible known anatomical variations related to the bones of the foot (Singla et al., 2017). During preoperative imaging, undescribed variations are found and the descriptions of such variations are limited because radiographic studies are not exploratory. Additionally, some unrecognised or unknown variations may still be misinterpreted as pathological, especially if the patient's presenting complaints correlate with the area of the variation. For instance, a large-sized NF may be misinterpreted as a fracture in children (Bixby, 2019). The study of dry cadaveric bones offers an ideal opportunity to identify any possible variations. This is because it is exploratory, and the sample size may be large enough to make meaningful descriptions of any identified variations. Previous studies have described some topographical variations of the metatarsal diaphyseal NF in terms of position, location, number and direction of the nutrient canal (Singh, 1960; Patake and Mysorekar, 1977; Monreal-Redondo and Fernández-Camacho, 2003; Malukar and Joshi, 2011; Anamika et al., 2015; Sandhya and Singh, 2017; Kothapalli, 2018).

Clinically, the position of the NF aids in identifying the safe surface for surgical procedures to prevent iatrogenic arterial injuries (Shrestha et al., 2019). Notably, NFs are barely visible on plain radiographs and they often mimic fractures in advanced imaging modalities like computed tomography (CT) and magnetic resonance imaging (MRI) (Bixby, 2019), making it imperative to have a comprehensive description of their topography. The typical position of the metatarsal NF is on the plantar or flexor surface of the diaphysis (Monreal-Redondo and Fernández-Camacho, 2003). However, variations in the positions of the NF have not been comprehensively reported in the literature, making it challenging for clinicians to determine its position. For instance, Singh (1960) identified NF on the plantar, dorsal, lateral, and medial surfaces of all the metatarsal bones. Another author, Kothapalli (2018), sampled an Indian population and reported that the NF were positioned on the lateral surface of the shaft of the first through third metatarsals and the medial surface of the fourth and fifth metatarsals diaphysis. This suggests that the position variation may occur within or between population groups. From these studies, it remains unclear as to what extent these variations are population-specific or sexually dimorphic, as the demographic characteristics of the sampled populations were not described. Given that the position of the NF on the metatarsal bones of the South African populations is unknown, it is essential to utilise the South African

population groups to determine if within and across population variations exist and if they are clinically significant.

The location of the NF helps determine areas of the bone that may be susceptible to non-union of fractures and avascular necrosis during midshaft metatarsal osteotomies (Monreal-Redondo and Fernández-Camacho, 2003; McKeon et al., 2013). The NF location showed variation patterns depending on the metatarsal bone and population group studied (Monreal-Redondo and Fernández-Camacho, 2003; Kothapalli, 2018). The NF was located in the middle third of the first metatarsal bones in the Spanish populations (Monreal-Redondo and Fernández-Camacho, 2003). Kothapalli (2018) observed that the NF was distributed throughout the metatarsal diaphysis in the Indian populations. It is important to note that Monreal-Redondo and Fernández-Camacho (2003) studied a limited sample (47 first metatarsals only) using a dissecting microscope while Kothapalli (2018) studied a relatively larger sample (first to fifth metatarsals, 80 bones each) using the naked eye. These sample size and methodology differences may also explain the observed differences besides population specificity. Other studies described the location of the NF but did not describe the population characteristics of their study samples (Anamika et al., 2015). Therefore, to understand the variations of the NF in terms of location, it is imperative to utilise skeletal samples with known demographics, like those of the South African populations in the Raymond A. Dart Collection of Modern Human Skeletons (Dayal et al., 2009).

The number of metatarsal diaphyseal NF reported so far is also variable, ranging from zero to three (Singh, 1960; Monreal-Redondo and Fernández-Camacho, 2003; Kothapalli, 2018). Singh (1960) reported that the first through third metatarsal bones have zero to two NF, while the fourth and fifth metatarsal bones have up to three NF in the Indian populations. From previous studies, it is unclear whether the length or robusticity of the bone may determine the number of NF in metatarsal diaphyses. Furthermore, some studies reported a high absence of the metatarsal diaphyseal NF, these studies simply utilized the naked eye without any magnifying tools (Patake and Mysorekar, 1977; Malukar and Joshi, 2011; Anamika et al., 2015). Furthermore, it was also not specified under which criteria the NF were excluded or considered non-viable or absent. The skeletal remains are macerated and preserved differently, and some NF may be obscured in the process especially when some soft tissues are still present, giving an impression of a false absence. Therefore, it is imperative to utilise a magnifying glass or loupe and a fine hypodermic needle when examining the presence and

number of NF on dry skeletons, as this may ensure the identification of small NF not clearly visible to an unaided eye.

The NF and its associated nutrient canal direction indicate the bone's dominant growing end (Cunningham et al., 2016). During foetal life, the NF and its associated nutrient canal is horizontally directed due to parallel growth and development at the ends of the diaphysis before the appearance of the epiphysis and changes as bones grow, usually following the growing-end theory, which states that the nutrient canal is directed distally or away from the dominant growing epiphysis (Craig et al., 2003). In long bones with two epiphyses like the humerus, radius, ulnar, femur, tibia and fibular, the direction of the nutrient canal is highly variable, indicating an altered developmental pattern (Lütken, 1950; Hughes, 1952; Mysorekar, 1967; Mazengenya and Fasemore, 2015; Mazengenya and Billings, 2016). From the few studies that reported the direction of the nutrient canal in the metatarsal bones, the variations were not reported, but these studies utilised a small sample size, making it difficult to detect any variations (Monreal-Redondo and Fernández-Camacho, 2003; Anamika et al., 2015; Kothapalli, 2018). It remains unclear from previous studies whether the direction of the nutrient canal varies in the metatarsal bones and whether the number of epiphyses may play a role in these variations (Anamika et al., 2015; Kothapalli, 2018).

The size of the NF helps determine the dominant blood supply to the bone. This is important in cases where the metatarsal bone has more than one NF. Few studies described the sizes of the NF (Patake and Mysorekar, 1977), making it clinically challenging to determine the volume and flow rate of blood going to each metatarsal bone and whether the blood supply from that source may be sufficient to aid in fracture healing processes.

In general, a few studies have previously examined the topographical variations of the metatarsal diaphyseal NF using dry bones (Patake and Mysorekar, 1977; Monreal-Redondo and Fernández-Camacho, 2003; Malukar and Joshi, 2011; Anamika et al., 2015; Sandhya and Singh, 2017; Kothapalli, 2018). These studies all present with some limitations, making it challenging to comprehensively understand the NF variations. The sample size for these studies was relatively small (47-811 metatarsal bones), and small sample-sized studies pose a bias in making meaningful interpretations and generalisations of the findings for a wider population. Uncovering all the clinically and anatomically relevant variations is also challenging when using a small sample-sized study. These studies were also limited in describing their sample's population characteristics. Whether the observed/reported variations

result from population-specific differences or arise from varied methodologies is unclear. Cross-sectionally, the population-specific variations can best be studied using two or more population groups with known skeletal biology variability, like South African populations (Steyn and İşcan, 1999; Patriquin et al., 2003). The laterality (side of the body) and sex-related variations were also not addressed in these studies; hence, it is unknown if the NF topographic and morphometric variations exhibit sexual dimorphism. Sex-related variations, especially for the metatarsal bones, are important and may explain why the prevalence of metatarsal fractures is higher in females than in males (Sarpong et al., 2018). Thus, overall, there is a lack of detailed, comprehensive topographical and morphometric descriptions of the variations of the NF on each metatarsal bone, which is why this study was conducted.

1.3 Sex estimation using nutrient foramina (NF) of the metatarsal bones

1.3.1 Methods of sex estimation from skeletal material and population specificity

In forensic and archaeological cases, skeletal individuation is an important step in approaching the skeletal remains of unknown individuals. This implies assessing the sex, age, stature and population affinity of unknown individuals from the skeletal remains to determine the biological profile (Steyn and Patriquin, 2009). Consequent methods of estimating age, stature and population affinity might be sex-specific, as thus, accurate sex estimation is crucial to ensure reliable demographic information for the other aspects of the biological profile (Mokoena et al., 2017; Bidmos et al., 2021). Depending on the prior probability of the sex of unidentified persons in a reference population, accurate sex estimation can also aid in reducing the number of potential victims, as sexual dimorphism exists as either biological male or female. Given its fundamental importance in aiding the accurate estimation of other biological markers, efforts have been dedicated to developing sex estimation standards from skeletonized remains (Dabbs and Moore-Jansen, 2010; Bozdag et al., 2022; Kiskira et al., 2022; Sallie et al., 2022; Nogueira et al., 2023; Curate et al., 2024). Sex estimation is performed on the understanding that there are distinct morphological (shape) and metric (size) differences between males and females within species. Thus, sex estimation using dry skeletons or radiological imaging employs morphological (Krogman and İşçan, 1986), metric (Moneim et al., 2008; Rodríguez et al., 2014; Ujaddughe et al., 2024) and geometric morphometric methods (López-Lázaro et al., 2020).

The morphological methods use anatomical features on bones that reveal sexual dimorphism. These qualitative methods are quick to apply depending on the experience of the observer. For instance, the female pelvis is evolved for parturition, making the pelvic bones of females distinct from those of males (Steyn and Patriquin, 2009; Klales, 2020a). However, the identification of sexually distinct anatomical features is dependent on the examiner's experience, expertise and the available skeletal material, making this approach subjective (Klales, 2020a; Bidmos et al., 2021). Although some methods incorporate scoring systems to quantify the observations of the anatomical features, the observer errors are still higher than the traditional linear measurements (Klales et al., 2020b). Identification of distinct sexually dimorphic features requires the specific sexually dimorphic skeletal features that are used for scoring (e.g., femoral condyle or ischiopubic ramus) to be recovered in an intact state, free from taphonomic and scavenging activities (Bidmos et al., 2021), and this scenario is implausible as the burial environment always has an effect on the skeletons. However, some skeletal features like the sciatic notch of the hip bone (os coxae) can be used though with lower sex estimation accuracy if the bone is fragmented or affected by taphonomic changes (Bruzek, 2002). Morphological methods also limit the utility of other bones with no obvious sexually dimorphic morphological features, like foot bones designed for walking and weight-bearing, a universal activity done by both males and females. The morphological methods may also be challenging to utilise in settings like South Africa, where there are few forensic and archaeological experts (Mokoena et al., 2019).

Unlike the morphological method, the metric (size) method involves taking reproducible measurements around specific bony landmarks like the length, breadth or height of the head or base of long bones (Robling and Ubelaker, 1997; Case and Ross, 2007; Bidmos et al., 2021). Recently, the development of metric methods for sexing skeletal remains has been on the rise (Bidmos et al., 2021; Bozdag et al., 2022; Sallie et al., 2022; Kiskira et al., 2022; Nogueira et al., 2023; Curate et al., 2024). This is because the techniques used are objective and require minimal expertise. Additionally, the measurements are subjected to various statistical models to be validated, and subsequently, sex estimation equations/functions are developed (Mokoena et al., 2019; Bidmos et al., 2021). The main drawback of metric standards is that some statistical assumptions must be met to determine the correct statistical test. For instance, the linear distribution of the measured variables needs to be considered to determine whether to use discriminant function analysis (DFA) or logistic regression analysis (LRA) statistical models (Pohar et al., 2004; Walker, 2008; Bartholdy et al., 2020). Thus,

when developing new metric standards, it is important to utilise both DFA and LRA models to determine the feasibility of those new standards, regardless of the data distribution.

Skeletal biology variations across different population groups have been described extensively (Robling and Ubelaker, 1997; Steyn and İşcan, 1999; Bidmos et al., 2021) as they undergo constant remodelling, which is affected by genetic variations, age, climate and environmental adaptations (Hill, 1998; Agarwal, 2021). Thus, it is important to develop population-specific standards, especially when using skeletal material with no obvious sexually dimorphic features. It has also been demonstrated that high sex estimation classification accuracy rates are achieved when population-specific equations are applied to the population they were developed from (İşcan and Steyn, 2013; Mokoena et al., 2019; Bidmos et al., 2021). In South African populations in particular, sex estimation classification accuracies are variable when using the exact bone measurements in South African Africans (also known as black South Africans), South Africans of Mixed ancestry (also known as coloured South Africans) and South Africans of European descent (also known as white South Africans) population groups (Bidmos and Dayal, 2003; Krüger et al., 2017; Mokoena et al., 2017; Bidmos and Mazengenya, 2021). Considering the high crime rate, limited forensic experts available, and extensive case backlog in South Africa (Steyn, 2005; Steyn and Brits, 2019), it is important to generate accessible methods of estimating sex for each South African population group.

1.3.2 Usefulness of measurements around the nutrient foramina (NF) in sex estimation

The dimensions around the diaphyseal NF of long upper and lower limb bones have proven effective in sexing skeletal remains in different population groups (Garcia, 2012; Krüger et al., 2017; Mokoena et al., 2017; Fasemore et al., 2018; Mokoena et al., 2019; Bidmos and Mazengenya, 2021; Sallie et al., 2022). As previously defined, diaphyseal NF are external openings to the nutrient canal, and the nutrient canal carries nutrient arteries and veins for the nutrition of the long bones (Gümüsburun et al., 1994; Götzen et al., 2003; Kothapalli, 2018). The NF are easily identifiable in diaphyses as they are marked by a raised margin surrounding an opening that leads to the nutrient canal (Kothapalli, 2018). The measurements around the NF may be considered similar to midshaft measurements as the NF is usually located in the middle of the bone diaphysis (Mazengenya and Fasemore, 2015; Sallie et al., 2022). However, the midshaft measurements cannot be utilised in cases where exhumed

skeletons are recovered in the fragmented or broken state as it may be challenging to determine the midshaft reference point with precision (Mokoena et al., 2017; Bidmos and Mazengenya, 2021). In contrast, measurements around the NF can be used in intact and fragmented skeletal remains because their identification is independent of other bone features, making them an ideal anatomical landmark to explore further in other bones.

Conventional bones for sex estimation, like the pelvis and cranium, may be susceptible to fragmentation and damage during the exhumation of skeletal remains (Steyn and Patriquin, 2009; Mokoena et al., 2017). These bones may also be missing in dismemberment cases, and this may complicate forensic investigations. Lower limb long bones that are also known to be sexually dimorphic, like the femur, tibia, and fibula, are highly susceptible to fragmentation compared to the miniature long bones (Mokoena et al., 2017; Bidmos and Mazengenya, 2021; Bidmos et al., 2021). Miniature long bones, particularly the metatarsals, are usually well preserved in exhumed skeletal remains compared to other long bones and may be reliable sex estimators, especially when an isolated foot is recovered (Mokoena et al., 2017; Bidmos et al., 2021). Metatarsal bones also pose a numerical advantage over other lower limb long bones, thereby increasing the chances of being recovered in high numbers. The metatarsal bones can also resist taphonomical and environmental degradation changes, as most individuals are usually buried with shoes on (Mountrakis et al., 2010; Bidmos et al., 2021). Thus, there is a need and an opportunity to explore and develop sex estimation standards further using metatarsal bones.

Previous studies formulated sex estimation methods that are of use in forensic settings utilising measurements around the head, midshaft, base and length of the metatarsal bones but did not include the measurements around the NF (Robling and Ubelaker, 1997; Case and Ross, 2007; Moneim et al., 2008; Mountrakis et al., 2010; Rodríguez et al., 2014; Gibelli et al., 2017; Bidmos et al., 2021). To date, there are no studies that examined the measurements of the NF of the metatarsal bones to generate equations or functions for sex estimation globally.

In general, the importance of accurate sex estimation in forensic and archaeological settings cannot be overemphasized. Numerous metric sex estimation equations have been developed using different postcranial skeletal elements, including the metatarsal bones. However, the utility of the measurements around the metatarsal diaphyseal NF is yet to be determined. Suppose the measurements around metatarsal diaphyseal NF prove to be sexually dimorphic.

In that case, they may be used independently or in combination with other known sexually dimorphic bones, especially in settings with high crime rates like South Africa, hence the purpose of conducting this study.

1.4 Bone morphology and functional adaptations

1.4.1 Bone morphology

Bones are dynamic organs that are constantly undergoing remodelling. The remodelling process replaces the old bone tissue with a new one, maintaining normal function and bone strength (Hill, 1998; Bartl et al., 2017). Bone strength entails bone quantity and quality. Bone quantity refers to the mineral content, e.g., bone mineral density. In contrast, bone quality implies the characteristic of internal bone morphology (Agarwal et al., 2004). The internal bone structure is classified into cortical (outer) and trabecular (inner) bones (Stock and Pfeiffer, 2001). The cortical bone consists of closely packed osteons and lamellae that give the cortical bone a compact bone appearance (Cooper et al., 2016). The fundamental building blocks of the trabecular bone include the trabecular struts or rods and trabecular plates (Oftadeh et al., 2015). The trabecular rods are cylindrical structures that are oriented perpendicular to the bone surface while trabecular plates are flat structures that are oriented parallel to the bone surface. Connections between the trabecular rods and plates leave some spaces in between, thereby giving the trabecular bone a spongy bone appearance (Turunen et al., 2013; Oftadeh et al., 2015). The amount of cortical and trabecular bone varies due to different local biomechanical demands of the bone and remodelling rates, and this depends on the anatomical site of the bone and age (Turunen et al., 2013; Chirchir et al., 2015). For instance, the epiphyses of the long bones have more trabecular bone than the cortical bone, while the diaphyses have more cortical bone than trabecular bone. Cortical bone strength indicators include the total subperiosteal area (TA), polar section modulus and shape ratio (Armelagos et al., 1972; Van Gerven et al., 1985; Rewekant, 2001; Götzen et al., 2003; Hagihara and Nara, 2018). In contrast, trabecular bone fragility indicators are the bone surface volume (BS/BV), bone volume fraction (BV/TV), trabecular number (TbN), trabecular thickness (TbTh), trabecular spacing and interconnectedness (TbSp) (Odgaard, 1997; Stock and Pfeiffer, 2001; Ketcham and Ryan, 2004; Bouxsein et al., 2010; Kivell, 2016). Areas with high values of BV/TV and TbTh, together with low values of BS/BV, TbN

and TbSp are correlated with greater trabecular bone quality, which suggests that the area of the bone is less fragile and less prone to fracturing (Agarwal et al., 2004; Saers et al., 2016).

Previously, the trabecular bone was given less attention in bone quality and fragility studies due to a lack of appropriate scanning modalities and technical demands (e.g., isolating the trabecular bone from cortical bone) when analysing the trabecular parameters (Agarwal et al., 2004). Micro-computed tomography (µCT) is an advanced form of scanning radiology that provides high-resolution images that allow detailed analysis of the trabecular structure (Hutchinson et al., 2017; Komza, 2017). Additionally, the associated µCT analysis software calculates only the trabecular bone morphometric properties within the selected regions or volumes of interest, and the cortical bone is excluded automatically, making it easier to study the trabecular bone strength (Bouxsein et al., 2010). Due to these advantages, some researchers have extensively utilised µCT in demonstrating trabecular structural differences due to mechanical loading between humans as well as primates using bones like the metatarsal head and base (Komza, 2017), talus (DeSilva and Devlin, 2012; Su et al., 2013), calcaneus (Maga et al., 2006; Zeininger et al., 2016), tibia (Tommy, 2018) and femur (Ryan and Shaw, 2012; Scherf et al., 2013). The µCT methodology has not yet been applied to determine the trabecular structure along the diaphysis of the metatarsal bones.

The term skeletal gracilization is used to imply any form of reduction in the bone strength indicators and bone mass (Chirchir et al., 2015). Evidence of the skeletal gracilization process across the human lineage has been demonstrated when comparing the prehistoric (3 million to 3000 BCE), historic (3000 BCE to 1492 CE) and modern populations (1492 CE to 1789 CE) (Vogel et al., 1990; Ruff et al., 1993; Kneissel et al., 1997; Brickley and Howell, 1999; Agarwal et al., 2004; Stock, 2006; Chirchir et al., 2015, 2017; Ryan and Shaw, 2015; Saers et al., 2016). However, little is known regarding these trends in contemporary (1789 CE to present) populations, especially those living centuries apart and exposed to different habitual locomotory behaviours. Most of the previous studies on bone strength and fragility utilised the diaphyseal cortical bone (Armelagos et al., 1972; Van Gerven et al., 1985; Rewekant, 2001; Griffin and Richmond, 2005; Griffin et al., 2010; Hagihara and Nara, 2018), with some utilising the epiphyseal trabecular structure (Ryan and Shaw, 2012; Scherf et al., 2013; Chirchir et al., 2015; Komza, 2017). This leaves the trabecular structure along the diaphyses of long bones like the metatarsals, unexplored. Hence, the role of the diaphyseal trabecular bone in determining bone strength and risk of bone fragility is unclear.

1.4.2 Trabecular bone morpho-functional adaptation

Trabecular bone shows more epigenetic response than cortical bone. Trabecular bone has a faster remodelling rate of 25% annual turnover compared to cortical bone with 2-3% (Eriksen, 2010; Barak et al., 2011; Komza, 2017). This enables the trabecular bone to display localised patterns of bone fragility and functional adaptations more than cortical bone, hence, it is an ideal model for this study (Lieberman, 1997; Komza, 2017). Genetic and non-genetic factors determine bone morpho-functional adaptations. Genetic factors entail a defined internal bone structure in a foetus, which may be attributable to a specific population (Skedros et al., 2004). The epigenetic factors can also alter the differentiation of bone cells (e.g., osteoclasts, osteoblasts and osteocytes), thereby altering the rate of bone modelling and remodelling (Eriksen, 2010; Barak et al., 2011). Non-genetic factors entail changes based on age, hormonal differences between sexes, and environmental conditions (Lieberman, 1997; Komza, 2017). Environmental conditions include climate, diet or nutrition, lifestyle, and biomechanical loading of the bones through habitual locomotor behaviours (Pearson, 2000; Stock, 2006). Biomechanical influence on the trabecular structural adaption is core owing to the plasticity of the trabecular bone (Trinkaus, 1997; Trinkaus and Ruff, 1999; Pontzer et al., 2006; Barak et al., 2011; Harrison et al., 2011). The mechanically induced bone changes are systemic, unlike pure localization of the loading factors (Lieberman, 1996). Notably, the bone is more susceptible to the effect of mechanical loading during the modelling phases before skeletal maturity as opposed to the remodelling phases (Kannus et al., 1995); hence, the biomechanical effects on the trabecular can best be studied using skeletal material that represents the modelling and remodelling phases. It should be noted that long bones, like metatarsal bones, are good indicators of biomechanical signatures due to their high load-carrying capacity, making them useful indicators of the physical activities and lifestyle of an individual (Agarwal, 2021).

To comprehend the effect of age or ontogeny on the trabecular structure, it is important to consider bone modelling and remodelling. Bone modelling is the process of forming and shaping bone during development and growth. It involves bone deposition, resorption and reshaping which occurs as the bone adapts to changing mechanical loads or during fracture repairs (Langdahl et al., 2016; Bartl et al., 2017). Bone remodelling is the process that involves bone resorption through osteoclastic activity, and bone formation through osteoblastic activity in order to maintain bone health and integrity throughout life (Hill, 1998; Bartl et al., 2017). Bone remodelling aids in repairing micro-fractures, removing old bone

tissue and adapting to the mechanical loads. Bone modelling occurs mainly during growth phases though it can also occur in adulthood during fracture repairs. On the other hand, bone remodelling is a lifelong process (Hill, 1998; Bartl et al., 2017; Agarwal, 2021). Thus, the juvenile populations mainly represent the modelling phase, and adult populations mainly represent the maintenance and remodelling phases. Usually, most bones reach peak bone mass around 21-30 years of age (Agarwal, 2021). Due to limited studies exploring the trabecular structure of the metatarsal bones using clearly defined age groups, the skeletal maturity (when the bone reaches peak strength) of the trabecular structure of the metatarsal diaphysis is unknown. Moreover, the ontogenetic-related trabecular structural changes along the diaphysis and around the NF of the metatarsal bones are unknown. Most ontogenetic-related bone loss or osteoporosis is evident after the seventh decade of life (Agarwal et al., 2004). As such, it is imperative to study population groups of less than 70 years old to fully comprehend the effect of age on the trabecular structure along many anatomical sites. Studying populations under 70 years is also advantageous clinically, as most metatarsal fractures occur within the first five decades of life (Moore, 2018; Sarpong et al., 2018).

Studies on osteoporosis have shown that different population groups exhibit different incidence rates, suggesting that an individual's population or genetic makeup may be a predisposing factor to bone loss and a risk rate of fracture development (Hochberg, 2007; Cauley, 2011; Paruk et al., 2017; Paruk et al., 2021; Ward et al., 2024). Additionally, previous studies have demonstrated population-specific trabecular structural differences (Schnitzler et al., 1990; Saers et al., 2016). For example, the highly mobile forager populations were associated with higher bone volume fraction, and thicker and fewer trabecular compared to the sedentary agriculturist populations (Saers et al., 2016). However, these studies were limited as the studied populations lived in different environmental and climatic conditions, e.g., the United States of America versus East Africa (Saers et al., 2016), making it difficult to attribute the observed changes to result from differences in the genetic make-up, diet or environmental conditions. It is unclear whether the trabecular structure along the metatarsal diaphysis and around the NF may exhibit population differences.

The relationship between influencing factors and skeletal changes is complex. This shows that other factors that can influence bone morphology must be carefully considered and controlled to avoid their confounding effect in interpreting the skeletal changes in response to these factors. For instance, using South African populations to study the trabecular changes may reduce the effect of environmental factors as these individuals may have lived in a

similar environment with a common climate. Despite sharing a similar environment, some variations, e.g., lifestyle or habitual locomotor behaviour, can exist among different groups and may need to be considered to accurately interpret the skeletal findings (Zipfel, 2004; Komza, 2017). When comparing populations, the sample size and inclusion criteria are to be considered, and the sample should have an equal number of samples in each group being compared. The proportions of the sample source should also reflect those of the general population. The ideal comparison is a large sample size with equal males to females, left to right, and for each population and all age groups.

The Raymond A. Dart Collection of Modern Human Skeletons, housed at the University of the Witwatersrand, South Africa, is the largest modern human skeletal collection, with over 5000 complete cranial and postcranial skeletons (Dayal et al., 2009). It has accurate and up-to-date demographic data of each human skeleton, including the sex, population affinity, date of death, and actual or estimated age at death. The accuracy of age at death is dependent on the sources of the human skeletons. Previously, most human skeletons were sourced from unclaimed bodies, but recently, the skeletal materials have been sourced from individuals under the body donation programs and these details are available in the Raymond A. Dart Collection of Modern Human Skeletons catalogue. Accurate demographic data are crucial and form the basis of anatomical and anthropological studies. Thus, the Raymond A. Dart Collection of Modern Human Skeletons is an ideal source of skeletal material for studying the metatarsal bones' topography, morphometry, and trabecular structure with respect to factors like age, sex, and population affinity variations. The Raymond A. Dart Collection of Modern Human Skeletons also enables a strong historical and cultural contextualization integral to understanding and accurately interpreting the findings of skeletal remains (Agarwal, 2021).

In general, few studies have examined the metatarsal epiphyseal trabecular structure of humans and compared them with primates like great apes (Griffin et al., 2010; Chirchir et al., 2015), but such comparisons pose a limitation in the interpretation of the findings and age was not considered. To our knowledge, there are no studies that examined how the trabecular structure varies along the diaphyses of the metatarsal bones and how these structural variations are affected by genetic (population affinity differences), age, sex, and locomotory behaviours in contemporary populations, e.g., 19th century and 20th century South African populations.

1.5 Study hypothesis

There is a limited understanding of metatarsal fracture development, healing, and repair patterns globally. A detailed anatomical study of metatarsal NF is crucial to providing this understanding and subsequently managing metatarsal fractures. However, the NF of the metatarsal bones present anatomical variations that are believed to be population-specific, making it challenging to determine the topography of NF from previous studies. There is an apparent need for further development of osteological metric standards to aid human identification, especially in settings with high murder cases and high rates of unidentified victims from skeletal remains like South Africa (Steyn, 2005; Mokoena et al., 2017). The usefulness of the measurements around the NF of the metatarsals to estimate sex is yet to be investigated globally. The trabecular bone morphology is a good source for estimating bone fragility and risk of fracture development. The role of the trabecular microarchitecture around the NF of the metatarsal bones in predisposing some individuals to a high risk of fracture development remains unclear. This study aimed to evaluate the metatarsal diaphyseal NF to determine the topographical variations, their sex estimation utility and the trabecular structure variations in the South African populations. Therefore, this study had four hypotheses based on prior literature:

1. The topographical anatomy of the metatarsal diaphyseal NF will vary among the South African Africans (SAA), South Africans of mixed ancestry (SAMA) and South Africans of European descent (SAED) population groups. This hypothesis is based on the concept that most postcranial skeletal elements of these populations show considerable variations (Işcan and Steyn, 1999; Mokoena et al., 2017).

2. The dimensions around the metatarsal diaphyseal NF will be sexually dimorphic and potentially useful in the sex estimation of individuals of the SAED, SAA, and SAMA populations. The sex estimation functions will possibly produce higher accurate classification rates in the SAED than in the SAA and SAMA. This hypothesis is based on the literature that shows that the SAED has higher sex estimation accuracies than the SAA and SAMA populations using other postcranial elements (Stull et al., 2014; Krüger et al., 2017).

3. The trabecular microarchitecture in the age-matched samples of the 20th century South African populations will demonstrate ontogenetic changes, sex and population differences. This hypothesis is based on literature that some ontogenetic-related trabecular variations exist among population groups (Schnitzler et al., 1990; Agarwal et al., 2004; Cole et al., 2015).

4. The trabecular microarchitecture around the NF of the metatarsal diaphysis will demonstrate substantial trabecular strength adaptations in the 19th century SAA compared with the 20th century SAA. This hypothesis is based on the understanding that trabecular structural differences exist among populations with different inferred habitual footwear (Saers et al., 2016).

1.6 Aims and Objectives

1.6.1 Aim

To evaluate the topography, estimate sex estimation potential, and examine the trabecular structure of the metatarsal diaphyseal NF in three South African population groups.

1.6.2 Objectives

1. To determine the topographical variations (number, location, position, size and direction) of the metatarsal diaphyseal NF in South African Africans (SAA), South Africans of Mixed Ancestry (SAMA), and South Africans of European descent (SAED) population groups (Chapter 2).

2. To determine the usefulness of the measurements around the metatarsal diaphyseal NF in estimating sex using discriminant function analysis and logistic regression analysis in 20th century SAED (Chapter 3), SAA (Chapter 4), and SAMA (Chapter 5) populations.

3. To determine the effect of age and population on the trabecular structure around the NF of the first and fifth metatarsals (bones that support the foot medial and lateral longitudinal arches, respectively) in 20th century individuals of SAA, SAED and SAMA populations using µCT scans (Chapter 6).

4. To determine the morpho-functional trabecular structural variations around the NF of the first and fifth metatarsal bones between the 19th century (habitually variably unshod/barefoot) and 20th century (habitually shod) SAA individuals (Chapter 7) using µCT scans.

1.7 Outline of the thesis

This thesis is presented using original published research articles. It has been organised into eight chapters. Chapter 1 (this chapter) describes the general background of the study, a

critical review of the literature, a research hypothesis, and the aims and objectives. Chapter 2 addresses objective 1 regarding topographical variations and clinical implications of the metatarsal diaphyseal NF in South Africa through an original published article. Chapter 3 addresses objective 2 regarding the utility of the dimensions around the metatarsal diaphyseal NF in South Africans of European descent (SAED) through an original published article. Chapter 4 addresses objective 2 regarding the utility of the dimensions around the NF in South African Africans (SAA) through an original published article, while Chapter 5 addresses objective 2 regarding the sex estimation potential of the dimensions around the metatarsal diaphyseal NF in South Africans of Mixed Ancestry (SAMA) (article in press). Chapter 6 addresses objective 3 regarding the trabecular structural variations in relation to age and population differences in 20th century individuals. Chapter 7 addresses objective 4 regarding the trabecular changes in relation to inferred habitual locomotory behaviours in 19th and 20th century SAA individuals. Chapter 8 discusses the main study findings with respect to the study objectives. It also presents conclusions, recommendations for future works, and general study limitations.

1.8 References

Agarwal, S. C. (2021) What is normal bone health? A bioarchaeological perspective on meaningful measures and interpretations of bone strength, loss, and aging. *American Journal of Human Biology,* 33(5)**,** pp. 23647.

Agarwal, S. C., Dumitriu, M., Tomlison, G. A. & Grynpas, M. D. (2004) Medieval trabecular bone architecture: the influence of age, sex, and lifestyle. *American Journal of Physical Anthropology.* 124(1)**,** pp. 33-44.

Anamika, K., Murlimanju, B., Divya, P., Prabhu, L. V., Saralaya, V., Rai, A. R. & Joy, T. (2015) Morphology of nutrient foramina in human metatarsals and their clinical importance. *Medicine & Health,* 10(1)**,** pp. 37-47.

Armelagos, G. J., Mielke, J. H., Owen, K. H., Van Gerven, D. P., Dewey, J. R. & Mahler, P. E. (1972) Bone growth and development in prehistoric populations from Sudanese Nubia. *Journal of Human Evolution,* 1(1)**,** pp. 89-119.

Barak, M. M., Lieberman, D. E. & Hublin, J. J. (2011) A Wolff in sheep's clothing: trabecular bone adaptation in response to changes in joint loading orientation. *Bone,* 49(6)**,** pp. 1141-1151.

Bartholdy, B. P., Sandoval, E., Hoogland, M. L. & Schrader, S. A. (2020) Getting rid of dichotomous sex estimations: Why logistic regression should be preferred over discriminant function analysis. *Journal of Forensic Sciences,* 65(5)**,** pp. 1685-1691.

Bartl, R., Bartl, C., Bartl, R. & Bartl, C. (2017) Modelling and remodelling of bone. *Bone Disorders: Biology, Diagnosis, Prevention, Therapy***,** Springer, pp. 21-30.

Bidmos, M., Adebesin, A., Mazengenya, P., Olateju, O. & Adegboye, O. (2021) Estimation of sex from metatarsals using discriminant function and logistic regression analyses. *Australian Journal of Forensic Sciences,* 53(5)**,** pp. 543-556.

Bidmos, M. A. & Dayal, M. R. (2003) Sex determination from the talus of South African whites by discriminant function analysis. *The American Journal of Forensic Medicine and Pathology,* 24(4)**,** pp. 322-328.

Bidmos, M. A. & Mazengenya, P. (2021) Accuracies of discriminant function equations for sex estimation using long bones of upper extremities. *International Journal of Legal Medicine,* 135**,** pp. 1095-1102.

Bixby, S. D. (2019) Pitfalls in pediatric trauma and microtrauma. *Magnetic Resonance Imaging Clinics,* 27(4)**,** pp. 721-735.

Bouxsein, M. L., Boyd, S. K., Christiansen, B. A., Guldberg, R. E., Jepsen, K. J. & Müller, R. (2010) Guidelines for assessment of bone microstructure in rodents using micro-computed tomography. *Journal of Bone and Mineral Research,* 25(7)**,** pp. 1468-1486.

Bozdag, M., Er, A., Kranioti, E., Basa, C. D., Oztop, B., Kacmaz, E., Moghaddam, N., Ekizoglu, O. & Grabherr, S. (2022) Sex estimation in a modern Turkish population using the clavicle: a computed tomography study. *Australian Journal of Forensic Sciences,* 54(2)**,** pp. 187-198.

Brickley, M. & Howell, P. (1999) Measurement of changes in trabecular bone structure with age in an archaeological population. *Journal of Archaeological Science,* 26(2)**,** pp. 151-157.

Bruzek, J. (2002) A method for visual determination of sex, using the human hip bone. *American Journal of Physical Anthropology,* 117(2), pp.157-168.

Buddecke, D. E., Polk, M. A. & Barp, E. A. (2010) Metatarsal fractures. *Clinics in Podiatric Medicine and Surgery,* 27(4)**,** pp. 601-624.

Cakir, H., Van Vliet-Koppert, S., Van Lieshout, E., De Vries, M., Van Der Elst, M. & Schepers, T. (2011) Demographics and outcome of metatarsal fractures. *Archives of Orthopaedic and Trauma Surgery,* 131**,** pp. 241-245.

Case, D. T. & Ross, A. H. (2007) Sex determination from hand and foot bone lengths. *Journal of Forensic Sciences,* 52(2)**,** pp. 264-270.

Cauley, J. A. (2011) Defining ethnic and racial differences in osteoporosis and fragility fractures. *Clinical Orthopaedics and Related Research®,* 469(7)**,** pp. 1891-1899.

Chirchir, H., Kivell, T. L., Ruff, C. B., Hublin, J.-J., Carlson, K. J., Zipfel, B. & Richmond, B. G. (2015) Recent origin of low trabecular bone density in modern humans. *Proceedings of the National Academy of Sciences,* 112(2)**,** pp. 366-371.

Chirchir, H., Ruff, C. B., Junno, J. A. & Potts, R. (2017) Low trabecular bone density in recent sedentary modern humans. *American Journal of Physical Anthropology,* 162(3)**,** pp. 550-560.

Cole, T. J., Rousham, E. K., Hawley, N. L., Cameron, N., Norris, S. A. & Pettifor, J. M. (2015) Ethnic and sex differences in skeletal maturation among the birth to twenty cohort in South Africa. *Archives of Disease in Childhood,* 100(2)**,** pp. 138-143.

Cooper, D. M. L., Kawalilak, C. E., Harrison, K., Johnston, B. D. & Johnston, J. D. (2016) Cortical bone porosity: what is it, why is it important, and how can we detect it? *Current Osteoporosis Reports*, *14*, pp.187-198.

Craig, J. G., Widman, D. & Van Holsbeeck, M. (2003) Longitudinal stress fracture: patterns of edema and the importance of the nutrient foramen. *Skeletal Radiology,* 32**,** pp. 22-27.

Cunningham, C., Scheuer, L. & Black, S. (2016) *Developmental juvenile osteology*, Academic Press.

Curate, F., Alves, I., Rodrigues, T. & Garcia, S. J. (2024) Assigned sex estimation with the clavicle and scapula: a study in a Portuguese reference sample. *Medicine, Science and the Law*, 64(1), pp. 15-22.

Dabbs, G. R. & Moore-Jansen, P. H. (2010) A method for estimating sex using metric analysis of the scapula. *Journal of Forensic Sciences*, 55(1), pp. 149-152.

Dameron Jr, T. B. (1975) Fractures and anatomical variations of the proximal portion of the fifth metatarsal. *Journal of Bone and Joint Surgery*, 57(6), pp. 788-792.

Dayal, M. R., Kegley, A. D., Štrkalj, G., Bidmos, M. A. & Kuykendall, K. L. (2009) The history and composition of the Raymond A. Dart Collection of human skeletons at the University of the Witwatersrand, Johannesburg, South Africa. *American Journal of Physical Anthropology*, 140(2), pp. 324-335.

Desilva, J. M. & Devlin, M. J. (2012) A comparative study of the trabecular bony architecture of the talus in humans, non-human primates, and Australopithecus. *Journal of Human Evolution*, 63(3), pp. 536-551.

Devries, J. G., Taefi, E., Bussewitz, B. W., Hyer, C. F. & Lee, T. H. (2015) The fifth metatarsal base: anatomic evaluation regarding fracture mechanism and treatment algorithms. *The Journal of Foot and Ankle Surgery*, 54(1), pp. 94-98.

Eriksen, E. F. (2010) Cellular mechanisms of bone remodelling. *Reviews in Endocrine and Metabolic Disorders*, 11, pp. 219-227.

Fasemore, M. D., Bidmos, M. A., Mokoena, P., Imam, A., Billings, B. K. & Mazengenya, P. (2018) Dimensions around the nutrient foramina of the tibia and fibula in the estimation of sex. *Forensic Science International*, 287, pp. 222. e1-222. e7.

Garcia, S. (2012) Is the circumference at the nutrient foramen of the tibia of value to sex determination on human osteological collections? Testing a new method. *International Journal of Osteoarchaeology*, 22(3), pp. 361-365.

Gibelli, D., Poppa, P., Cummaudo, M., Mattia, M., Cappella, A., Mazzarelli, D., Zago, M., Sforza, C. & Cattaneo, C. (2017) Sex assessment from the volume of the first metatarsal bone: a comparison of linear and volume measurements. *Journal of Forensic Sciences,* 62(6)**,** pp. 1582-1585.

Götzen, N., Cross, A. R., Ifju, P. G. & Rapoff, A. J. (2003) Understanding stress concentration about a nutrient foramen. *Journal of Biomechanics,* 36(10)**,** pp. 1511-1521.

Griffin, N. L., D'août, K., Ryan, T. M., Richmond, B. G., Ketcham, R. A. & Postnov, A. (2010) Comparative forefoot trabecular bone architecture in extant hominids. *Journal of Human Evolution,* 59(2)**,** pp. 202-213.

Griffin, N. L. & Richmond, B. G. (2005) Cross-sectional geometry of the human forefoot. *Bone,* 37(2)**,** pp. 253-260.

Gümüsburun, E., Yücel, F., Ozkan, Y. & Akgün, Z. (1994) A study of the nutrient foramina of lower limb long bones. *Surgical and Radiologic Anatomy,* 16(4)**,** pp. 409-412.

Hagihara, Y. & Nara, T. (2018) Diaphyseal cross-sectional geometry of the metatarsal bones in the Jomon population. *American Journal of Physical Anthropology,* 166**,** pp. 745-752.

Harrison, L. C., Nikander, R., Sikiö, M., Luukkaala, T., Helminen, M. T., Ryymin, P., Soimakallio, S., Eskola, H. J., Dastidar, P. & Sievänen, H. (2011) MRI texture analysis of femoral neck: Detection of exercise load-associated differences in trabecular bone. *Journal of Magnetic Resonance Imaging,* 34(6)**,** pp. 1359-1366.

Hill, P. (1998) Bone remodelling. *British Journal of Orthodontics,* 25**,** pp. 101-107.

Hochberg, M. C. (2007) Racial differences in bone strength. *Transactions of the American Clinical and Climatological Association,* 118**,** pp. 305-315.

Hughes, H. (1952) The factors determining the direction of the canal for the nutrient artery in the long bones of mammals and birds. *Cells Tissues Organs,* 15(3)**,** pp. 261-280.

Hutchinson, E. F., Farella, M., Hoffman, J. & Kramer, B. (2017) Variations in bone density across the body of the immature human mandible. *Journal of Anatomy,* 230(5)**,** pp. 679-688.

Işcan, M. Y. & Steyn, M. (2013) *The Human Skeleton in Forensic Medicine,* Charles C Thomas Publisher.

Işcan, M. Y. & Steyn, M. (1999) Craniometric determination of population affinity in South Africans. *International Journal of Legal Medicine,* 112**,** pp. 91-97.

Kannus, P., Haapasalo, H., Sankelo, M., Sievanen, H., Pasanen, M., Heinonen, A., Oja, P. & Vuori, I. (1995) Effect of starting age of physical activity on bone mass in the dominant arm of tennis and squash players. *Annals of Internal Medicine,* 123(1)**,** pp. 27-31.

Ketcham, R. & Ryan, T. (2004) Quantification and visualization of anisotropy in trabecular bone. *Journal of Microscopy,* 213(2)**,** pp. 158-171.

Kiskira, C., Eliopoulos, C., Vanna, V. & Manolis, S. K. (2022) Biometric sex assessment from the femur and tibia in a modern Greek population. *Legal Medicine,* 59**,** pp. 102126.

Kivell, T. L. (2016) A review of trabecular bone functional adaptation: what have we learned from trabecular analyses in extant hominoids and what can we apply to fossils? *Journal of Anatomy,* 228(4)**,** pp. 569-594.

Kizilkanat, E., Boyan, N., Ozsahin, E. T., Soames, R. & Oguz, O. (2007) Location, number and clinical significance of nutrient foramina in human long bones. *Annals of Anatomy,* 189(1)**,** pp. 87-95.

Klales, A. R. (2020a) Sex estimation using pelvis morphology. *In Sex Estimation of the Human Skeleton.* Academic Press, pp. 75-93.

Klales, A. R., Garvin, H., Gocha, T. P., Lesciotto, K. M. & Walls, M. (2020b) Examining the Reliability of Morphological Traits for Sex Estimation: Implications for the Walker (2008) and Klales et al.(2012) Methods. *Forensic Anthropology (University of Florida), 3*(3), pp. 139-150.

Kneissel, M., Roschger, P., Steiner, W., Schamall, D., Kalchhauser, G., Boyde, A. & Teschler-Nicola, M. (1997) Cancellous bone structure in the growing and ageing lumbar spine in a historic Nubian population. *Calcified Tissue International,* 61**,** pp. 95-100.

Komza, K. (2017) A unique form of locomotion in Swartkrans hominins: An analysis of the trabecular structure of the first metatarsal. Master's thesis, University of Kent, United Kingdom.

Kothapalli, J. (2018) Nutrient foramina architecture in metacarpal and metatarsal bones. *International Journal of Anatomy Research,* 6(4)**,** pp. 5848-5852.

Krogman, W. M. & Isçan, M. Y. (1986) The human skeleton in forensic medicine, Charles C. *Thomas, Springfield, IL,* 15**,** pp. 202-08.

Krüger, G. C., L'abbé, E. N. & Stull, K. E. (2017) Sex estimation from the long bones of modern South Africans. *International Journal of Legal Medicine,* 131**,** pp. 275-285.

Langdahl, B., Ferrari, S. & Dempster, D. W. (2016) Bone modelling and remodelling: potential as therapeutic targets for the treatment of osteoporosis. *Therapeutic Advances in Musculoskeletal Disease,* 8(6), pp. 225-235.

Lieberman, D. E. (1996) How and why humans grow thin skulls: experimental evidence for systemic cortical robusticity. *American Journal of Physical Anthropology,* 101(2)**,** pp. 217-236.

Lieberman, D. E. (1997) Making behavioural and phylogenetic inferences from hominid fossils: considering the developmental influence of mechanical forces. *Annual Review of Anthropology,* 26(1)**,** pp. 185-210.

López-Lázaro, S., Pérez-Fernández, A., Alemán, I. & Viciano, J. (2020) Sex estimation of the humerus: A geometric morphometric analysis in an adult sample. *Legal Medicine, 47,* pp. 101773.

Lütken, P. (1950) Investigation into the position of the nutrient foramina and the direction of the vessel canals in the shafts of the humerus and femur in man. *Cells Tissues Organs,* 9(1)**,** pp. 57-68.

Maga, M., Kappelman, J., Ryan, T. M. & Ketcham, R. A. (2006) Preliminary observations on the calcaneal trabecular microarchitecture of extant large-bodied hominoids. *American Journal of Physical Anthropology,* 129(3)**,** pp. 410-417.

Malukar, O. & Joshi, H. (2011) Diaphysial nutrient foramina in long bones and miniature long bones. *National Journal of Integrated Research in Medicine,* 12**,** pp. 14-17.

Mazengenya, P. & Billings, B. (2016) Topographic and morphometric features of the nutrient foramina of the fibula in the South African mixed-ancestry population group and their surgical relevance. *European Journal of Anatomy,* 20(4)**,** pp. 329-336.

Mazengenya, P. & Fasemore, M. D. (2015) Morphometric studies of the nutrient foramen in lower limb long bones of adult black and white South Africans. *European Journal of Anatomy,* 19(2)**,** pp. 155-163.

Mckeon, K. E., Johnson, J. E., Mccormick, J. J. & Klein, S. E. (2013) The intraosseous and extraosseous vascular supply of the fifth metatarsal: implications for fifth metatarsal osteotomy. *Foot & Ankle International,* 34(1)**,** 117-123.

Mokoena, P., Billings, B. K., Bidmos, M. A. & Mazengenya, P. (2017) Sex estimation using dimensions around the nutrient foramen of the long bones of the arm and forearm in South Africans. *Forensic Science International,* 278**,** pp. 404. e1-404. e5.

Mokoena, P., Billings, B. K., Gibbon, V., Bidmos, M. A. & Mazengenya, P. (2019) Development of discriminant functions to estimate sex in upper limb bones for mixed ancestry South Africans. *Science & Justice,* 59(6)**,** pp. 660-666.

Moneim, W. M. A., Hady, R. H. A., Maaboud, R. M. A., Fathy, H. M. & Hamed, A. M. (2008) Identification of sex depending on radiological examination of foot and patella. *The American Journal of Forensic Medicine and Pathology,* 29(2)**,** pp. 136-140.

Monreal-Redondo, D. & Fernández-Camacho, F. (2003) Diaphyseal nutrient foramina in the first metatarsals in normal and hallux valgus feet: location and surgical implications. *Surgical and Radiologic Anatomy,* 25**,** pp. 234-240.

Moore, K. L., Agur, A. M. R. & Dalley, A. F. (2018) *Clinically oriented anatomy,* Wolters Kluwer.

Moore, N. F. (2018) Metatarsal fracture management. *Orthopaedics and Trauma,* 32**,** pp. 428-436.

Mountrakis, C., Eliopoulos, C., Koilias, C. G. & Manolis, S. K. (2010) Sex determination using metatarsal osteometrics from the Athens collection. *Forensic Science International,* 200**,** pp. 178. e1-178. e7.

Murlimanju, B., Prashanth, K., Prabhu, L. V., Saralaya, V. V., Pai, M. M. & Rai, R. (2011) Morphological and topographical anatomy of nutrient foramina in human upper limb long bones and their surgical importance. *Romanian Journal of Morphology and Embryology,* 52(3)**,** pp. 859-862.

Mysorekar, V. (1967) Diaphysial nutrient foramina in human long bones. *Journal of Anatomy,* 101(4)**,** 813-822.

Nagel, A., Fernholz, F., Kibele, C. & Rosenbaum, D. (2008) Long distance running increases plantar pressures beneath the metatarsal heads: a barefoot walking investigation of 200 marathon runners. *Gait & Posture,* 27(1)**,** pp. 152-155.

Nogueira, L., Santos, F., Castier, F., Knecht, S., Bernardi, C. & Alunni, V. (2023) Sex assessment using the radius bone in a French sample when applying various statistical models. *International Journal of Legal Medicine,* 137(3)**,** pp. 925-934.

Odgaard, A. (1997) Three-dimensional methods for quantification of cancellous bone architecture. *Bone,* 20(4)**,** pp. 315-328.

Oftadeh, R., Perez-Viloria, M., Villa-Camacho, J. C., Vaziri, A. & Nazarian, A. (2015) Biomechanics and mechanobiology of trabecular bone: a review. *Journal of Biomechanical Engineering*, *137*(1), p.010802.

Paruk, F., Matthews, G. & Cassim, B. (2017) Osteoporotic hip fractures in Black South Africans: a regional study. *Archives of Osteoporosis,* 12**,** pp. 1-6.

Paruk, F., Tsabasvi, M. & Kalla, A. (2021) Osteoporosis in Africa—where are we now. *Clinical Rheumatology,* 40(9)**,** pp. 3419-3428.

Patake, S. & Mysorekar, V. (1977) Diaphysial nutrient foramina in human metacarpals and metatarsals. *Journal of Anatomy,* 124(2)**,** pp. 299-304.

Patriquin, M. L., Loth, S. & Steyn, M. (2003) Sexually dimorphic pelvic morphology in South African whites and blacks. *Homo,* 53(3)**,** pp. 255-262.

Pearson, O. M. (2000) Activity, climate, and postcranial robusticity: implications for modern human origins and scenarios of adaptive change. *Current Anthropology,* 41(4)**,** pp. 569-607.

Petrisor, B. A., Ekrol, I. & Court-Brown, C. (2006) The epidemiology of metatarsal fractures. *Foot & Ankle International,* 27(3)**,** pp. 172-174.

Pohar, M., Blas, M. & Turk, S. (2004) Comparison of logistic regression and linear discriminant analysis: a simulation study. *Metodoloski zvezki,* 1(1)**,** pp. 143-161.

Pontzer, H., Lieberman, D. E., Momin, E., Devlin, M. J., Polk, J., Hallgrimsson, B. & Cooper, D. (2006) Trabecular bone in the bird knee responds with high sensitivity to changes in load orientation. *Journal of Experimental Biology,* 209(1)**,** pp. 57-65.

Rammelt, S., Heineck, J. & Zwipp, H. (2004) Metatarsal fractures. *Injury,* 35(2)**,** pp. 77-86.

Rewekant, A. (2001) Do environmental disturbances of an individual's growth and development influence the later bone involution processes? A study of two mediaeval populations. *International Journal of Osteoarchaeology,* 11(6)**,** pp. 433-443.

Robling, A. G. & Ubelaker, D. H. (1997) Sex estimation from the metatarsals. *Journal of Forensic Science,* 42(6)**,** pp. 1062-1069.

Rodríguez, S., González, A., Simón, A., Rodríguez-Calvo, M. S., Febrero-Bande, M., Cordeiro, C. & Muñoz-Barús, J. I. (2014) The use of computerized tomography in determining stature and sex from metatarsal bones. *Legal Medicine,* 16(5)**,** pp. 252-257.

Ruff, C., Trinkaus, E., Walker, A. & Larsen, C. S. (1993) Postcranial robusticity in Homo. I: Temporal trends and mechanical interpretation. *American Journal of Physical Anthropology,* 91(1)**,** pp. 21-53.

Ryan, T. M. & Shaw, C. N. (2012) Unique suites of trabecular bone features characterize locomotor behavior in human and non-human anthropoid primates. *PloS One,* 7(7)**,** pp. e41037.

Ryan, T. M. & Shaw, C. N. (2015) Gracility of the modern Homo sapiens skeleton is the result of decreased biomechanical loading. *Proceedings of the National Academy of Sciences,* 112(2)**,** pp. 372-377.

Saers, J. P., Cazorla-Bak, Y., Shaw, C. N., Stock, J. T. & Ryan, T. M. (2016) Trabecular bone structural variation throughout the human lower limb. *Journal of Human Evolution,* 97**,** pp. 97-108.

Sallie, S., Bidmos, M. A. & Mazengenya, P. (2022) Estimation of sex from the metacarpal dimensions at the nutrient foramen in white South Africans. *Australian Journal of Forensic Sciences,* 54(4)**,** pp. 533-545.

Sandhya, K. & Singh, K. (2017) A morphometric study on the nutrient foramen of metatarsal bones in the Jharkhand population. *Journal of Dental and Medical Sciences,* 16(6)**,** pp. 31-34.

Sarpong, N. O., Swindell, H. W., Trupia, E. P. & Vosseller, J. T. (2018) Metatarsal fractures. *Foot & Ankle Orthopaedics,* 3(3)**,** pp. 1-8.

Scherf, H., Harvati, K. & Hublin, J.-J. (2013) A comparison of proximal humeral cancellous bone of great apes and humans. *Journal of Human Evolution,* 65(1)**,** pp. 29-38.

Schnitzler, C., Pettifor, J., Mesquita, J., Bird, M., Schnaid, E. & Smyth, A. (1990) Histomorphometry of iliac crest bone in 346 normal black and white South African adults. *Bone and Mineral,* 10(3)**,** pp. 183-199.

Shrestha, P., Mehta, D. K., Shrestha, S. & Shrestha, A. (2019) Variations of the nutrient foramen of femur and its clinical implications. *Journal of Lumbini Medical College,* 7(2)**,** pp. 61-64.

Singh, I. (1960) Variations in the metatarsal bones. *Journal of Anatomy,* 94(3)**,** pp. 345-350.

Singla, A., Kalsi, G., Masih, N., Gupta, T. & Sharma, M. (2017) Morphological and topographical anatomy of nutrient foramens in human metacarpals and their surgical importance. *Surgical and Radiologic Anatomy,* 39**,** pp. 1227-1233.

Skedros, J. G., Hunt, K. J. & Bloebaum, R. D. (2004) Relationships of loading history and structural and material characteristics of bone: development of the mule deer calcaneus. *Journal of Morphology,* 259(3)**,** pp. 281-307.

Standring, S. (2015) *Gray's Anatomy: The anatomical basis of clinical practice,* Elsevier Health Sciences.

Steyn, M. (2005) Muti murders from South Africa: a case report. *Forensic Science International,* 151**,** pp. 279-287.

Steyn, M. & Brits, D. (2019) Dismemberment in South Africa: case studies. *Dismemberments.* Academic Press.

Steyn, M. & İşcan, M. Y. (1999) Osteometric variation in the humerus: sexual dimorphism in South Africans. *Forensic Science International,* 106(2)**,** pp. 77-85.

Steyn, M. & Patriquin, M. (2009) Osteometric sex determination from the pelvis—does population specificity matter? *Forensic Science International,* 191**,** pp. 113. e1-113. e5.

Stock J. (2006) Hunter-gatherer postcranial robusticity relative to patterns of mobility, climatic adaptation, and selection for tissue economy. *American Journal of Physical Anthropology,* 131(2)**,** pp. 194-204.

Stock, J. & Pfeiffer, S. (2001) Linking structural variability in long bone diaphyses to habitual behaviors: foragers from the Southern African later stone age and the Andaman Islands. *American Journal of Physical Anthropology,* 115**,** pp. 337-348.

Stull, K. E., Kenyhercz, M. W. & L'abbé, E. N. (2014) Ancestry estimation in South Africa using craniometrics and geometric morphometrics. *Forensic Science International,* 245**,** pp. 206. e1-206. e7.

Su, A., Wallace, I. J. & Nakatsukasa, M. (2013) Trabecular bone anisotropy and orientation in an Early Pleistocene hominin talus from East Turkana, Kenya. *Journal of Human Evolution,* 64(6)**,** pp. 667-677.

Tommy, K. A. (2018) A Comparative Study of Trabecular Architecture in the Distal Tibia of Humans, Hominoids and Australopiths from South Africa. Doctoral dissertation, University of the Witwatersrand, Faculty of Science, South Africa.

Trinkaus, E. (1997) Appendicular robusticity and the paleobiology of modern human emergence. *Proceedings of the National Academy of Sciences,* 94(24)**,** pp. 13367-13373.

Trinkaus, E. & Ruff, C. B. (1999) Diaphyseal cross-sectional geometry of near Eastern Middle Palaeolithic humans: the tibia. *Journal of Archaeological Science,* 26(4)**,** pp. 1289-1300.

Turunen, M. J., Prantner, V., Jurvelin, J. S., Kröger, H. & Isaksson, H. (2013) Composition and microarchitecture of human trabecular bone change with age and differ between anatomical locations. *Bone, 54*(1), pp.118-125.

Ujaddughe, O. M., Haberfeld, J., Bidmos, M. A. & Olateju, O. I. (2024) Cranial measurements obtained by three-dimensional computed tomography technique in the estimation of sex of contemporary Black South Africans. *Forensic Imaging*, 37**,** pp. 200585.

Van Gerven, D. P., Hummert, J. R. & Burr, D. B. (1985) Cortical bone maintenance and geometry of the tibia in prehistoric children from Nubia's Batn el Hajar. *American Journal of Physical Anthropology,* 66(3)**,** pp. 275-280.

Vogel, M., Hahn, M., Caselitz, P., Woggan, J., Pompesius-Kempa, M. & Delling, G. (1990) Comparison of trabecular bone structure in man today and an ancient population in Western Germany. *Bone Morphometry***,** Japan, Nishimura Co, pp. 220-223.

Walker, P. L. (2008) Sexing skulls using discriminant function analysis of visually assessed traits. *American Journal of Physical Anthropology,* 136(1)**,** pp. 39-50.

Ward, K. A., Madanhire, T., Marenah, K., Micklesfield, L. K. & Gregson, C. L. (2024) Disparities in fragility fracture and osteoporosis care in Africa. *The Lancet Diabetes & Endocrinology,* 12(5)**,** pp. 294-296.

Zeininger, A., Patel, B. A., Zipfel, B. & Carlson, K. J. (2016) Trabecular architecture in the StW 352 fossil hominin calcaneus. *Journal of Human Evolution,* 97**,** pp. 145-158.

Zipfel, B. (2004) Morphological variation in the metatarsal bones of selected recent and pre-pastoral humans from South Africa. Doctoral dissertation, University of the Witwatersrand, South Africa.

Surgical and Radiologic Anatomy (2023) 45:1213–1226
https://doi.org/10.1007/s00276-023-03233-5

ORIGINAL ARTICLE

Topographical anatomy and clinical implications of the metatarsal diaphyseal nutrient foramina across South African populations

Arthur Tsalani Manjatika[1,2] · **Pedzisai Mazengenya**[3,4] · **Joshua Gabriel Davimes**[1]

Received: 12 April 2023 / Accepted: 10 August 2023 / Published online: 22 August 2023
© The Author(s), under exclusive licence to Springer-Verlag France SAS, part of Springer Nature 2023

Abstract

Purpose Metatarsal fractures often occur around the diaphyseal nutrient foramina (NF) which vary in topography depending on population affinity. Topographical and morphometrical knowledge of the NF is crucial in understanding fracture development and fracture site healing patterns. The current study aimed to describe the topography and the morphometry of the metatarsal diaphyseal NF in South African Africans (SAA), South Africans of European descent (SAED) and South Africans of Mixed Ancestry (SAMA).

Methods The study examined 4284 dry cadaveric metatarsals from both sexes and sides of these populations for NF topography and morphometry, including the presence, number, location, position, size and direction of the NF on the metatarsal bones.

Results The NF was present in 99.4% of the metatarsals. Most (84.5%) metatarsals examined had a single NF. Most (97.4%) NF were located in the middle third of the metatarsal bones. The median foramina index (FI) of the second metatarsal exhibited population affinity and significant differences were found both on the left second metatarsal ($P=0.043$), and the right second metatarsal ($P=0.046$). The position of NF was predominantly lateral on the first (92.4%), second (64.9%) and third (59.1%) metatarsals, whilst the position was predominantly medial on the fifth (65.1%) metatarsals. The NF positions on the fourth metatarsals showed the greatest population variability. The first metatarsals had primarily dominant-sized and distally directed NF whilst the second through fifth had primarily secondary-sized and proximally directed NF.

Conclusion The topographical anatomy of the metatarsal diaphyseal NF appears similar across the South African populations. Metatarsal bones are highly vascularized bones presenting with multiple nutrient foramina.

Keywords Diaphyseal nutrient foramen · Fractures · Metatarsal bones · Morphometry · South African populations · Topography

Introduction

Metatarsal fractures are the most commonly presenting foot problems in primary healthcare settings [3, 10, 21, 25], they are common in children, athletes, dancers, military personnel and industrial workers, leading to reduced mobility and productivity [14, 21]. They are also associated with the development of diabetic osteopathy [6]. Metatarsal bones are common sites of stress fractures due to weight-bearing, and these fractures are usually in the vicinity of the diaphyseal nutrient foramen [5, 21, 26]. Nutrient foramina are external openings to the nutrient canal on the bone diaphysis that conveys blood vessels (nutrient vessels) and nerves [8, 14]. Blood supply to the bone is crucial for metabolic processes, haematopoiesis, mineral banking, and the survival of osteocytes and osteoblasts [11, 14, 20]. The nutrient artery

✉ Pedzisai Mazengenya
p.mazengenya@ajman.ac.ae

1 School of Anatomical Sciences, University of the Witwatersrand, Parktown, Johannesburg, South Africa

2 School of Life Sciences and Allied Health Professions, Anatomy Division, Kamuzu University of Health Sciences, Blantyre, Malawi

3 College of Medicine, Ajman University, Ajman, United Arab Emirates

4 Center of Medical and Bio-allied Health Sciences Research, Ajman University, Ajman, United Arab Emirates

is the main source of blood supply to the long bone and is essential in primary ossification, bone growth and fracture healing [14, 20]. Knowledge of the number, location, position, size and direction of the nutrient foramina is vital for the preservation of blood supply to long bones during bone grafting and fracture repair [1, 13, 14, 17, 20]. In addition, the information is crucial in understanding fracture development in long bones since the nutrient foramen site represents the weak area on the long bone diaphysis [5, 14, 18].

The variation in the topography and morphometry of the nutrient foramina (NF) of long bones and the metatarsal bones, in particular, is population-specific [1, 14, 20, 29]. These variations may pose difficulties in the accurate diagnosis and management of metatarsal fractures leading to delayed fracture healing and poor patient outcomes [2, 16, 20, 22]. In children, for example, the unknown variations of the NF, especially the size of the NF, may be misdiagnosed as fractures when using magnetic resonance imaging [2]. To date, a comprehensive topographical and morphometric description of the NF of each metatarsal bone is lacking from previous studies on metatarsals [8, 15, 20, 24, 29]. It is unclear whether the metatarsal diaphyseal NF variations may exhibit sexual dimorphism as previous studies predominantly used samples of unknown sex [1, 14, 24, 27]. Additionally, there is a paucity of information describing the topographic and morphometric variations of the nutrient foramen in different population groups sharing the same geographic location [1, 14, 20, 29]. South Africa has three main population groups and their representation in the Raymond A. Dart Modern Skeletal Collection reflects that of the current South African general population. The three population groups show considerable variations in the postcranial skeletal elements [19]. The purpose of the current study was to determine the topography and morphometric variations of the metatarsal diaphyseal NF in South African Africans (SAA), South Africans of European descent (SAED), and South Africans of mixed ancestry (SAMA). Topographical and morphometrical knowledge of the NF may help in understanding fracture development and fracture site healing patterns and this may lead to improved management of metatarsal fractures.

Materials and methods

Study population

The current cross-sectional study was conducted on the dry metatarsal bones of the twentieth century individuals that are housed in the Raymond A. Dart Modern Skeletal Collection in the School of Anatomical Sciences, University of the Witwatersrand, South Africa. The study was conducted under the ethical clearance waiver number W-CBP-220504-01 obtained from the Faculty of Health Sciences, University of the Witwatersrand. The study utilised the first to fifth metatarsal bones of the right and left sides from both males and females. The metatarsal bones were from individuals aged between 18 and 65 years (mean age 46.78 ± 13.29 years). Metatarsal bones that presented with fractures, gross pathological deformities, malformed deformations, gross evidence of any genetic diseases and any evidence of surgical interventions were excluded from the study. The previous medical and occupational history of the cadaveric specimens were not recorded in the Raymond A. Dart collection catalogue; hence, the non-evident macroscopic genetic diseases and occupational history were not exclusion factors. A total of 4284 metatarsal bones from 438 skeletons were used. The skeletons were obtained from cadavers of both the unclaimed and donated bodies from the body donator programme at the university of the Witwatersrand. The study sample was stratified according to population groups as shown in Table 1.

Table 1 Sample distribution of the South African populations

Group	SAA				SAED				SAMA				Total
Sex	Male ($n=100$)		Female ($n=100$)		Male ($n=100$)		Female ($n=87$)		Male ($n=28$)		Female ($n=23$)		$n=438$
Bone	R	L	R	L	R	L	R	L	R	L	R	L	
Mt 1	100	100	100	100	99	96	86	86	27	27	21	23	865
Mt 2	100	100	100	100	98	93	85	85	28	27	23	23	862
Mt 3	100	100	100	100	98	94	82	81	27	27	23	23	855
Mt 4	100	100	100	100	96	93	82	81	28	28	23	23	854
Mt 5	100	100	100	100	93	90	82	83	28	26	23	23	848
Total	500	500	500	500	484	466	417	416	138	135	113	115	4284

n, total number of individuals; L, Left side; R, Right side; Mt 1, first metatarsal bone; Mt 2, second metatarsal bone; Mt 3, third metatarsal bone; Mt 4, fourth metatarsal bone; Mt 5, fifth metatarsal bone; SAA, South African Africans; SAED, South Africans of European descent; SAMA, South Africans of Mixed ancestry

Topography and morphometry of the metatarsal diaphyseal nutrient foramina

The metatarsal bones (first–fifth) from the three population groups were identified and categorised into right and left sides (Fig. 1a–c). A magnifying glass was used to identify the nutrient foramina on the diaphysis. A diaphyseal nutrient foramen was identified as a raised margin that surrounds the opening of a groove leading into the foramen [19]. All viable nutrient foramina were counted and recorded. Nutrient foramina that were non-viable and indistinguishable were considered as absent nutrient foramina. The position of the nutrient foramina was classified as being on the dorsal, plantar, lateral and or medial surfaces of the bone. A fine wire was used to determine the direction of the nutrient canal and this was classified as either towards the proximal or distal

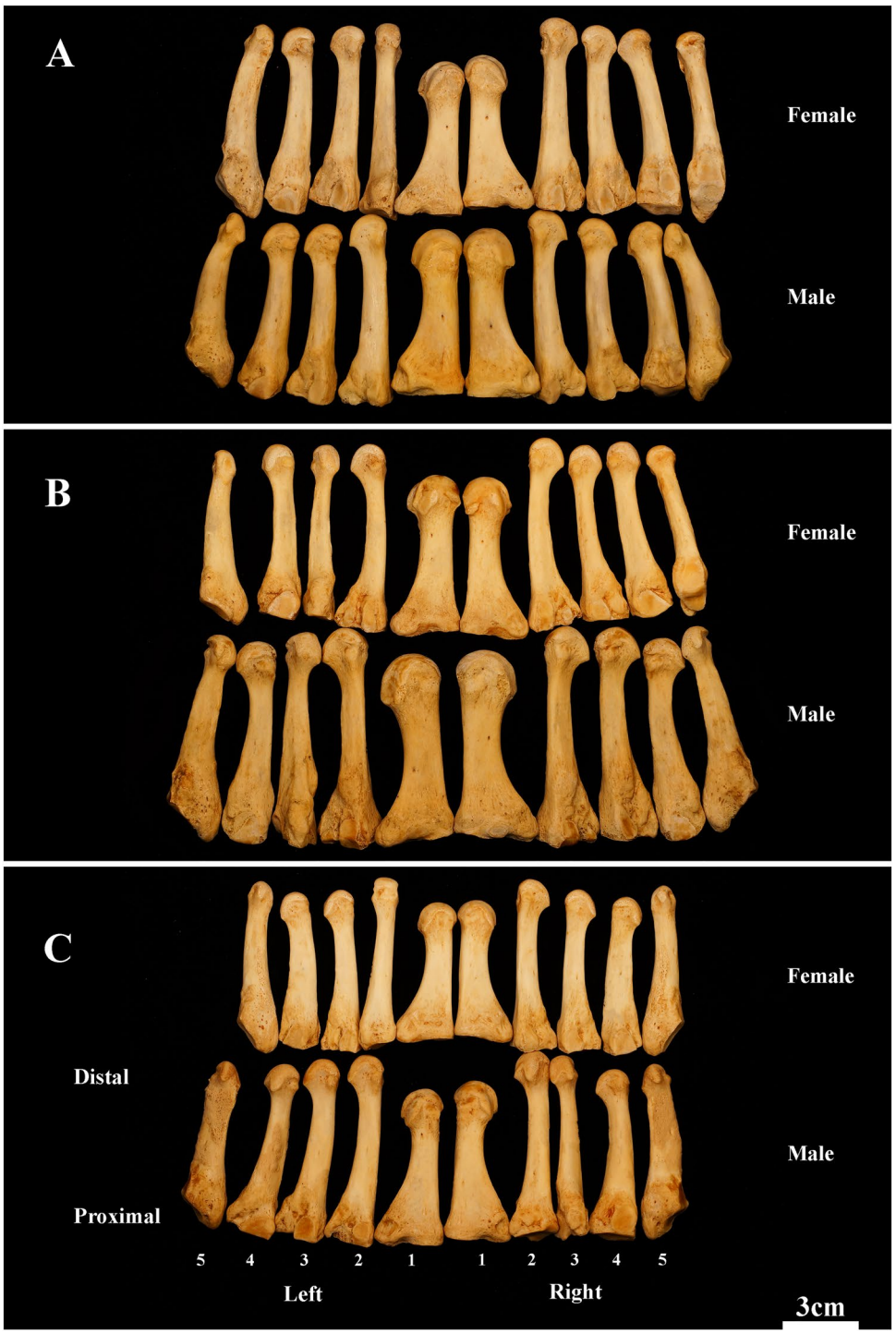


Fig. 1 A plate of the metatarsal bones showing sex and side classification for each South African population group. The metatarsals are arranged from medial (1) to lateral (5). **A** Metatarsal bones of the South African Africans (SAA), **B** metatarsals of the South Africans of European descent (SAED), **C** metatarsals of the South Africans of Mixed Ancestry (SAMA). 1, First metatarsal bone; 2, Second metatarsal bone; 3, Third metatarsal bone; 4, Fourth metatarsal bone; 5, Fifth metatarsal bone

ends of the bone. The size of the nutrient foramina was categorised as dominant or secondary using a 28-gauge hypodermic needle (0.362 mm outer diameter). A dominant-sized nutrient foramen was any foramen that allowed the passage of a 28-gauge hypodermic needle whilst a secondary-sized nutrient foramen was any visible foramen that did not allow needle passage. The largest nutrient foramen on each metatarsal was considered the main nutrient foramen.

If a metatarsal had only one nutrient foramen that could not allow the passage of a 28-gauge hypodermic needle, it was still categorised as a secondary-sized nutrient foramen though it was the main foramen of that bone and all morphometric parameters were measured from it. In cases of multiple nutrient foramina on a single bone, the largest (main) nutrient foramen was used to take measurements and to categorise its topography. To determine the location of the nutrient foramina, the total length (TL) of the metatarsal bone from the proximal end to the distal end was measured using a mini osteometric board (Paleo Tech Concepts, accuracy = 0.02 mm, resolution = 0.01 mm, repeatability = 0.01 mm), and the distance from the proximal end of the metatarsal bone to the nutrient foramina (NFPE) was measured using a digital sliding calliper (Mastercraft™ Africa, accuracy = 0.02 mm, resolution = 0.01 mm, repeatability = 0.01 mm). Foramina index (FI) is the percentage of the total length of the bone that is represented by the distance between the proximal end and the nutrient foramen. The location of the nutrient foramina on the metatarsal was categorised as proximal, middle or distal thirds, determined using the FI according to the Hughes formula [12]: $FI = (NFPE/TL) \times 100$. All photographs were taken using a Sony digital camera (60–150 mm focal distance, *f*/11 aperture, 1/60 s, ISO-400, florescent white balance, 18 megapixels) on a fixed camera stand.

Data analysis

The data were managed in Microsoft Excel Office 365 (Microsoft Corporation) and analysed with IBM® SPSS® version 23 (IBM Corp., Armonk, NY, USA). All the categorical variables were presented as frequencies and percentages. Chi-square tests were used to test for association between nutrient foramina parameters (number, location, position, size and direction) and sex, side of the body and population affinity. The morphometric data were presented as mean and standard deviations. The normality of the morphometric data was determined using the Kolmogorov–Smirnov test and Histograms. For the parametric data within each population group, the independent sample student's *t*-tests were done to determine significant differences in mean values between the sides of the body and sex. The Mann–Whitney *U* test was done for the non-parametric data to determine significant median differences between the sides of the body and sex. The one-way analysis of variance (ANOVA) was done to test significant mean differences across population groups for the parametric data whilst the Kruskal–Wallis test was done for the non-parametric data. For the significant population differences, the Bonferroni post hoc test was done. A significance level of $p \leq 0.05$ was used for all comparisons.

Results

A total of 4284 metatarsal bones were examined and 99.4% (4260) of them showed the presence of nutrient foramina (NF) whilst 0.6% had an absence of NF. The presence of NF did not vary across all three populations, sex and side of the body ($P > 0.05$). The presence of the NF was 99.7% in the SAA, 99.2% in the SAED and 99.4% in the SAMA. The absence of the NF was observed on the third and fourth metatarsal bones in the SAA and in males; second through fifth metatarsals in the SAED with no significant sex and side of the body associations ($P > 0.05$); and second and third metatarsals in the SAMA populations with no significant sex and side of the body associations ($P > 0.05$). The most predominant number of NF on the metatarsal bones did not vary across all populations, sex and side of the body ($P > 0.05$). The majority (84.5%) of metatarsal bones examined had a single NF (Table 2). The highest number of NF observed for a single bone was five and was observed on the first metatarsal on the left side in an SAA male. The highest number of NF in the SAMA was four and was observed on the first metatarsal in males only whilst the highest number of NF in SAED was also four and was observed on the first metatarsals mostly in males (5 males, 1 female). The highest number of NF observed on the same surface of a single bone was four (Fig. 2).

The predominant size of the main NF on each metatarsal bone did not vary across all populations, sex and side of the body ($P > 0.05$). The proportions of the dominant-sized NFs on the fifth metatarsal bones exhibited population affinity. Across all population groups, the first metatarsals had the majority of dominant-sized NF whilst the second through fifth metatarsals had predominantly secondary-sized NF with no significant sex and side of the body associations ($P > 0.05$) (Table 3). In the SAA and SAMA, the left and right fifth metatarsal bones had a relatively higher proportion (33%) of dominant-sized NF than the second through fourth metatarsal bones (Table 3).

The most dominant location of the NF did not vary across all populations, sex and side of the body ($P > 0.05$). The majority of the NF were located in the middle third of the metatarsal bones (97.4%) (Fig. 3), followed by the proximal third (2.1%), and lastly, the distal third (0.5%) (Table 4). The SAA had the highest proportions of distally located NF followed by the SAED and then SAMA. The

Table 2 Number of the metatarsal diaphyseal nutrient foramina in the South African population groups

SAA	Right foot					Left foot				
Mt bone	1st	2nd	3rd	4th	5th	1st	2nd	3rd	4th	5th
No of NF										
0	–	–	–	2 (1%)	–	–	–	2 (1%)	3 (1.5%)	–
1	149 (74.5%)	180 (90%)	184 (92%)	183 (91.5%)	181 (90.5%)	147 (73.5%)	180 (90%)	189 (94.5%)	180 (90%)	186 (93%)
2	48 (24%)	20 (10%)	16 (8%)	15 (7.5%)	19 (9.5%)	44 (22%)	18 (9%)	9 (4.5%)	17 (8.5%)	12 (6%)
3	3 (1.5%)	–	–	–	–	8 (4%)	2 (1%)	–	–	2 (1%)
4	–	–	–	–	–	–	–	–	–	–
5	–	–	–	–	–	1 (0.5%)	–	–	–	–
Total sample	200 (100%)	200 (100%)	200 (100%)	200 (100%)	200 (100%)	200 (100%)	200 (100%)	200 (100%)	200 (100%)	200 (100%)
SAED										
0	–	2 (1%)	2 (1.1%)	2 (1.1%)	1 (0.6%)	–	1 (0.6%)	3 (1.7%)	3 (1.7%)	–
1	126 (68.1%)	150 (82%)	147 (81.7%)	157 (88.2%)	166 (94.9%)	115 (63.2%)	138 (77.5%)	149 (85.1%)	141 (81%)	154 (89%)
2	54 (29.2%)	27 (14.8%)	29 (16.1%)	18 (10.1%)	8 (4.5%)	58 (31.9%)	39 (21.9%)	22 (12.6%)	29 (16.7%)	18 (10.4%)
3	3 (1.6%)	4 (2.2%)	2 (1.1%)	–	–	7 (3.8%)	–	–	1 (0.6%)	1 (0.6%)
4	2 (1.1%)	–	–	1 (0.6%)	–	2 (1.1%)	–	1 (0.6%)	–	–
Total sample	185 (100%)	183 (100%)	180 (100%)	178 (100%)	175 (100%)	182 (100%)	178 (100%)	175 (100%)	174 (100%)	173 (100%)
SAMA										
0	–	–	1 (2%)	–	–	–	1 (2%)	1 (2%)	–	–
1	33 (68.8%)	41 (80.4%)	39 (78%)	41 (80.4%)	42 (82.4%)	30 (60%)	40 (80%)	37 (74%)	47 (92.2%)	49 (100%)
2	12 (25%)	9 (17.6%)	10 (20%)	9 (17.6%)	8 (15.7%)	19 (38%)	8 (16%)	12 (24%)	3 (5.9%)	–
3	2 (4.2%)	1 (2%)	–	1 (2%)	–	–	1 (2%)	–	–	–
4	1 (2%)	–	–	–	1 (1.9%)	1 (2%)	–	–	1 (1.9%)	–
Total sample	48 (100%)	51 (100%)	50 (100%)	51 (100%)	51 (100%)	50 (100%)	50 (100%)	50 (100%)	51 (100%)	49 (100%)

NF, Nutrient foramina; Mt, Metatarsal bone; SAA, South African Africans; SAED, South African of European descent; SAMA, South African of Mixed ancestry. Values in brackets refer to percentage of total sample per metatarsal



Fig. 2 A photograph of the first metatarsal bones with arrows showing the number of diaphyseal nutrient foramina in the South African populations. **A** Right first metatarsal with one nutrient foramen on the lateral surface, **B** right first metatarsal with two nutrient foramina on the lateral surface, **C** Left first metatarsal with four nutrient foramina on the lateral surface

foramina index (FI) of the first through fifth metatarsal bones ranged from 25.2 to 83% (Table 5). There were no significant mean or median FI differences between the right and left sides in the SAA, SAED or SAMA for the first through fifth metatarsal bones ($P > 0.05$). The right second metatarsal bones in the SAED had a higher median FI as compared to that of the SAA ($P = 0.046$). The left second metatarsal bones in the SAMA had a lower median FI as compared to that of the SAA and SAED ($P = 0.043$) (Fig. 4). For all the metatarsal bones, there were no significant mean or median FI differences between the sexes within and amongst SA population groups ($P > 0.05$).

Except for the fourth metatarsal bones, there were no population, sex or side of the body variations regarding the predominant position of the main NF ($P > 0.05$). Across all populations, the position of the NF was predominantly lateral on the first (92.4%), second (64.9%) and third (59.1%) metatarsal bones, whilst the position on the fifth metatarsal bones was predominantly medial (65.1%) (Fig. 5). The position of the NF on the fourth metatarsal was predominantly medial in SAA (49%), lateral in SAED (44%), and equal proportions of medial and lateral surfaces in the SAMA (35%). These proportional differences were not significantly different ($P > 0.05$). The direction of the nutrient canal did not vary across all populations, sex and side of the body. The nutrient canals were directed towards the distal ends for all first metatarsal bones and directed towards the proximal ends for all the second through fifth metatarsals (Fig. 6).

Discussion

The current study examined the topography and morphometry of the metatarsal diaphyseal nutrient foramina (NF) across the South African populations. The metatarsal NF ranged from 0 to 5 in number on the metatarsal bones across the studied South African population groups. However, previous studies indicated a range of 0–3 NF per metatarsal bone in the various population groups examined [1, 14, 15, 20, 24, 27, 29]. These variations in the number of the NF on the metatarsal bones may be due to differences in the methodology. The use of the magnifying glass in the current study could lead to the identification of small foramina that may be indistinguishable and ignored without visual aids in dry metatarsal bones. Previous studies that reported large numbers of NF (5 and above) on a single bone were done on the femur [9, 16]. Singh [29] acknowledged that more than two NF may be present on a single surface of a metatarsal diaphysis without specifying the maximum number. Our findings suggest that the maximum number of NF on a single metatarsal diaphyseal surface is four and this was observed on the first metatarsal bone in the SAED population. The highest number of NF per bone in all the current studied population groups was associated more with males than females but no previous studies have reported this observation. From the total length of the bone measurements, males had longer bones than females and the presence of more than one NF on

Table 3 Size of the metatarsal diaphyseal nutrient foramina in the South African population groups

SAA	Right foot					Left foot				
MT bone	1st	2nd	3rd	4th	5th	1st	2nd	3rd	4th	5th
Size of NF										
Dominant	184 (92%)	21 (10.5%)	21 (10.5%)	28 (14.1%)	51 (25.5%)	186 (93%)	22 (11%)	24 (12.1%)	35 (17.8%)	66 (33%)
Secondary	16 (8%)	179 (89.5%)	179 (89.5%)	170 (85.9%)	149 (74.5%)	14 (7%)	178 (89%)	174 (87.9%)	162 (82.2%)	134 (67%)
Total sample	200 (100%)	200 (100%)	200 (100%)	198 (100%)	200 (100%)	200 (100%)	200 (100%)	198 (100%)	197 (100%)	200 (100%)
SAED										
Dominant	177 (95.7%)	31 (17.1%)	20 (11.2%)	18 (10.2%)	38 (21.8%)	172 (94.5%)	33 (18.6%)	17 (9.9%)	19 (11.1%)	26 (15%)
Secondary	8 (4.3%)	150 (82.9%)	158 (88.8%)	158 (89.8%)	136 (78.2%)	10 (5.5%)	144 (81.4%)	155 (90.1%)	152 (88.9%)	147 (85%)
Total sample	185 (100%)	181 (100%)	178 (100%)	176 (100%)	174 (100%)	182 (100%)	177 (100%)	172 (100%)	171 (100%)	173 (100%)
SAMA										
Dominant	43 (89.6%)	7 (13.7%)	6 (12.2%)	6 (11.8%)	17 (33.3%)	45 (90%)	7 (14.3%)	7 (14.3%)	3 (5.9%)	16 (32.7%)
Secondary	5 (10.4%)	44 (86.3%)	43 (87.8%)	45 (88.2%)	34 (66.7%)	5 (10%)	42 (85.7%)	42 (85.7%)	48 (94.1%)	33 (67.3%)
Total sample	48 (100%)	51 (100%)	49 (100%)	51 (100%)	51 (100%)	50 (100%)	49 (100%)	49 (100%)	51 (100%)	49 (100%)

NF, Nutrient foramina; MT, Metatarsal bone; SAA, South African Africans; SAED, South African of European descent; SAMA, South African of Mixed ancestry; Dominant nutrient foramina, allows passage of a 28-gauge hypodermic needle (0.362 mm outer diameter); Secondary nutrient foramina, does not allow needle passage. Values in brackets refer to percentage of total sample per metatarsal

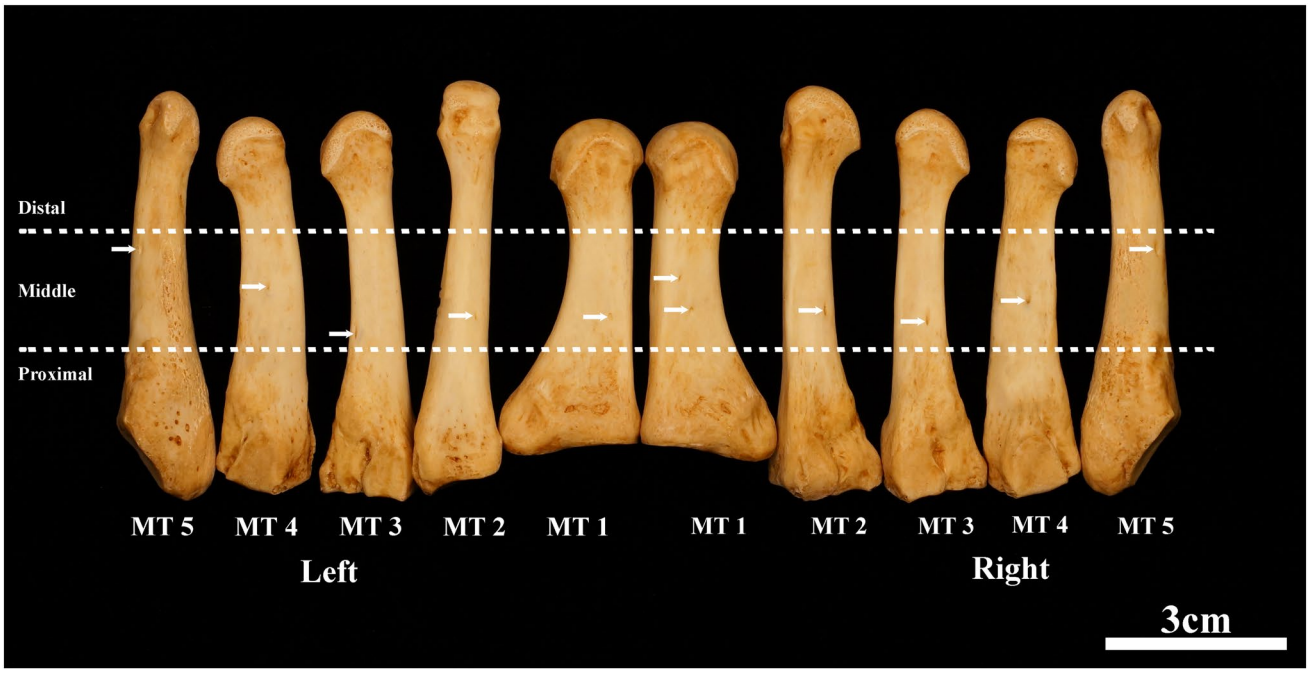


Fig. 3 A photograph of the left and right-side metatarsal bones showing the location of nutrient foramina. The two dashed lines divides the metatarsals into the proximal, middle and distal thirds. Arrows are pointing at the nutrient foramina located in the middle third of different surfaces of the metatarsal bones. MT 1, first metatarsal; MT 2, second metatarsal; MT 3, third metatarsal; MT 4, fourth metatarsal; MT 5, fifth metatarsal

male metatarsal bone surfaces indicates high vascularity that compliments the bone size [10]. The first metatarsals exhibited the highest numbers of NF per bone compared to the second through fifth metatarsals in all populations examined. High vascularity indicates a good prognosis for first metatarsal fractures since fracture healing requires a good blood supply [1, 24]. In contrast, few studies have reported an absence of NF on the first metatarsal bone [1, 14, 24].

In the current study, 0.6% of the metatarsal bones showed the absence of NF on their diaphysis. The absence of NF was marked on the third metatarsal bone across all three populations. Previous studies reported a 6–10.4% absence of NFs on the metatarsal bones in the Indian populations [1, 15, 24]. In case of the absence of NF, periosteal and epiphyseal blood vessels supply the diaphysis, but this source of blood supply is less sufficient compared to NFs [1, 14, 24]. Thus, the absence of NF on the metatarsal diaphysis may delay fracture healing and repair.

Few studies have characterised the size of the main NF on the metatarsals based on diameter measurements into dominant and secondary [24]. However, the characterisation is widely reported in other long bones [13, 16]. In the present study, the majority of the NF on the first metatarsal bones admitted the 28-gauge hypodermic needle and were all classified as dominant size whereas second to fifth metatarsal bones exhibited a majority of smaller-sized (secondary) NFs. This is likely due to the differences in the size of the metatarsal bones with large metatarsal bones having large-sized NF than smaller metatarsal bones [1]. The large-sized NF may ensure adequate blood supply to the bone which is essential for bone growth, healing and union of fractures [11, 14, 20]. The fifth metatarsals had a relatively more dominant-sized NF than the second through fourth metatarsals. Dominant-sized NF may supply more blood than smaller-sized NF as the vessel diameter is a better indicator of the amount of blood being carried to an organ. The fifth metatarsal bone may require more blood supply for metabolic activities since it forms and supports the lateral longitudinal arch of the foot and is subjected to dynamic loading during locomotion. Additionally, the fifth metatarsal bone is more mobile and has more muscle attachments that are involved in foot and ankle mobility and stability than the other metatarsal bones, and increased muscle activity during locomotion may increase the metabolic demands of the bone which may require more blood supply [4, 23, 30].

The location of NF along the long bone diaphysis helps to determine the parts of the bone that may be affected by non-union of fractures and avascular necrosis during diaphyseal metatarsal osteotomies [17, 18, 20]. In addition, it aids in the identification of the ideal sites on the diaphysis for the harvesting of free vascularised bone grafts [17]. The findings in the current study agree with previous studies that described the middle third of the metatarsal diaphysis to be

Table 4 Location of the metatarsal diaphyseal nutrient foramina in the South African population groups

SAA	Right foot					Left foot				
MT bone	1st	2nd	3rd	4th	5th	1st	2nd	3rd	4th	5th
Location of NF										
Proximal	4 (2%)	7 (3.5%)	7 (3.5%)	1 (0.5%)	–	4 (2%)	10 (5%)	7 (3.5%)	–	–
Middle	190 (95%)	193 (96.5%)	193 (96.5%)	197 (99.5%)	200 (100%)	188 (94%)	190 (95%)	190 (96%)	197 (100%)	200 (100%)
Distal	6 (3%)	–	–	–	–	8 (4%)	–	1 (0.5%)	–	–
Total sample	200 (100%)	200 (100%)	200 (100%)	198 (100%)	200 (100%)	200 (100%)	200 (100%)	198 (100%)	197 (100%)	200 (100%)
SAED										
Proximal	10 (5.4%)	10 (5.5%)	3 (1.7%)	1 (0.6%)	–	1 (0.5%)	10 (5.6%)	3 (1.7%)	1 (0.6%)	–
Middle	175 (94.6%)	170 (93.9%)	175 (98.3%)	174 (99.4%)	174 (100%)	177 (97.3%)	167 (94.4%)	169 (98.3%)	171 (99.4%)	173 (100%)
Distal	–	1 (0.6%)	–	–	–	4 (2.2%)	–	–	–	–
Total sample	185 (100%)	181 (100%)	178 (100%)	175 (100%)	174 (100%)	182 (100%)	177 (100%)	172 (100%)	172 (100%)	173 (100%)
SAMA										
Proximal	1 (2%)	4 (7.8%)	–	–	–	–	3 (6.1%)	2 (4%)	–	–
Middle	47 (98%)	47 (92.2%)	49 (100%)	51 (100%)	51 (100%)	49 (98%)	46 (93.9%)	47 (96%)	51 (100%)	49 (100%)
Distal	–	–	–	–	–	1 (2%)	–	–	–	–
Total sample	48 (100%)	51 (100%)	49 (100%)	51 (100%)	51 (100%)	50 (100%)	49 (100%)	49 (100%)	51 (100%)	49 (100%)

NF, Nutrient foramina; Mt, Metatarsal bone; SAA, South African Africans; SAED, South African of European descent; SAMA, South African of Mixed ancestry. Values in brackets refer to percentage of total sample per metatarsal

Table 5 Comparison of range and mean of the Foramina index the metatarsal diaphyseal nutrient foramina across populations

Study (year and author)	Patake and Mysorekar [24]	Anamika et al. [1]	Sandhya and Singh [27]	Kothapalli [14]	Present study					
Population	–	–	Jharkhand	Indian	SAA		SAED		SAMA	
Side	R and L	R and L	R and L	R and L	R	L	R	L	R	L
	Min–Max	(Mean ± SD)	Min–Max	Min–Max	Min–Max (Mean ± SD)	Min–Max (Mean ± SD)	Min–Max (Mean ± SD)	Min–Max (Mean ± SD)	Min–Max (Mean ± SD)	Min–Max (Mean ± SD)
MT 1	30.5–81.7	(65.3)	32.8–71.2	25.1–73.6	25.2–68.8 (51.5 ± 10.1)	29.4–70.8 (53.1 ± 10)	30.7–66.5 (50.4 ± 10.2)	29.5–71.8 (51.4 ± 9.7)	29.7–65.5 (50.3 ± 10.6)	33.9–69.4 (51.8 ± 9.7)
MT 2	25.4–55.6	(43.6)	17.9–63.3	28.2–70.7	27.5–59.7 (43.5 ± 6.6)	28.5–61.6 (44.4 ± 6.9)	29.1–74.7 (45.4 ± 7.5)	28.3–59.5 (44.3 ± 6.7)	26.9–57.8 (43.1 ± 7.1)	25.8–54.6 (41.8 ± 6.8)
MT 3	31.4–59.1	(44.4)	29.6–56.9	30.1–81.3	29–60 (44 ± 6.1)	29.9–83 (43.6 ± 6.4)	29.5–61 (43.8 ± 5.6)	28.5–61.1 (44.9 ± 6.1)	33.5–52.3 (44.8 ± 4.9)	30.4–54 (43.1 ± 6.1)
MT 4	36.4–62.9	(45.3)	30.8–63.3	29.9–72.2	25.9–61.1 (46.9 ± 5.5)	34–71.1 (46.4 ± 5.9)	32.9–66.6 (47.9 ± 5.8)	33.2–58.6 (47.1 ± 5.2)	39.6–57.6 (47.8 ± 4.4)	36.4–58.5 (47 ± 5.4)
MT 5	37.3–71.7	(47.5)	14.3–49.2	28.6–75.4	38.6–62.8 (51.7 ± 4.7)	38.9–63.1 (51.4 ± 4.9)	42.8–63 (52.5 ± 4.5)	40–60.8 (51.6 ± 4.6)	41.7–61.3 (52 ± 4.6)	41.4–60.7 (51.2 ± 4.9)

MT, Metatarsal bone; L, Left side; R, Right side; SAA, South African Africans; SAED, South African of European descent; SAMA, South African of Mixed ancestry. Ranges are reported in percentages. The dashed line (–) represent missing population data for the cited studies

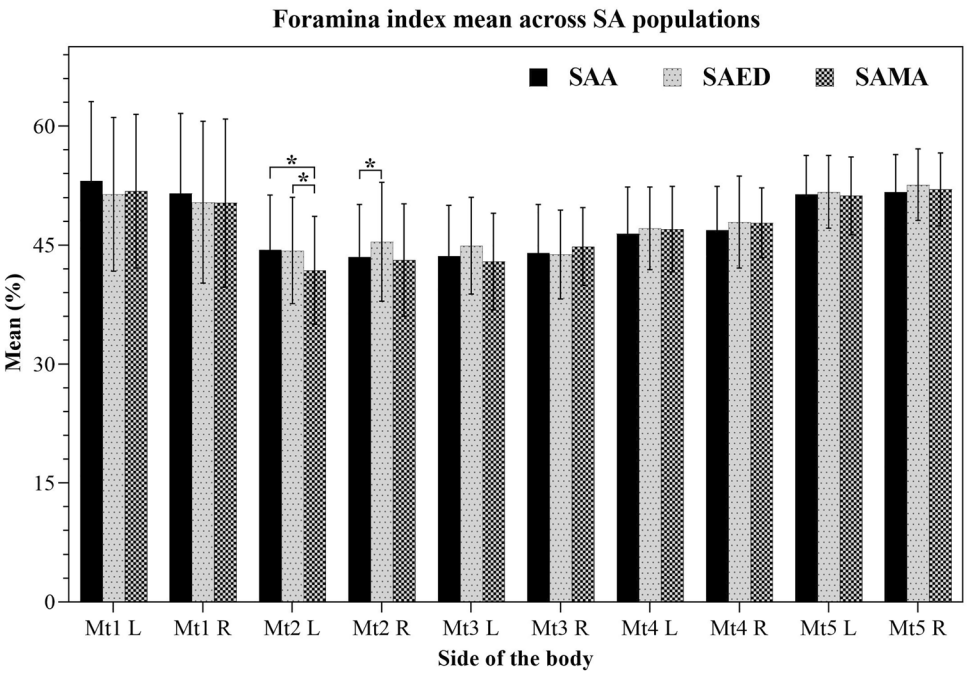


Fig. 4 A graph showing the foramina index means and standard deviations across populations. L, Left side; R, Right side; SAA, South African Africans; SAED, South Africans of European descent; SAMA, South Africans of Mixed ancestry; Mt, Metatarsal bone; %, Percentage; *, significant median difference (Kruskal–Wallis test p-value < 0.05), as the FI on Mt 2 were not normally distributed

the predominant location of the NF [1, 14, 20], although in a few bones NF were observed in the proximal and distal thirds. This observation contradicts that of Kothapalli [14], who observed NF across the proximal, middle and distal thirds of the diaphysis in the first through fifth metatarsals. Similar to previous studies, the mean and median foramina index (FI) in the current study did not show any significant side of the body and sex differences within all the population groups [1]. The median FI of the second metatarsal bones demonstrates significant differences across populations. The SAMA exhibited lower left side median FI of the second metatarsal bones as compared to the left side median FI of the SAA and SAED populations. Conversely, the right-side median FI of the second metatarsal bones were higher in the SAED as compared to the right-side median FI of the SAA population.

Knowledge of the most likely NF position on metatarsals helps to determine the safest surface for surgical procedures to prevent iatrogenic arterial injuries and to optimise fracture healing [17, 28]. The typical position of the NF on the metatarsal diaphysis is known to be on the plantar surface [20]. In the Indian populations, the NF were predominantly on the lateral surface of the diaphysis of the first, second and third metatarsals, and on the medial surface of the fourth and fifth metatarsals [14]. The current study supports this observation for all the studied South African populations on all the metatarsal bones except for the fourth metatarsal bone. On the fourth metatarsal bones, the predominant position of the NF was medial in the SAA, lateral in the SAED, and equal proportions of medial and lateral in the SAMA. Though not statistically significant proportional differences, the variable predominant positions of the fourth metatarsal NF in the current study may suggest across-population variability. Singh [29] identified NF on the dorsal, plantar, medial and lateral surfaces of all the metatarsals in the Indian populations. The findings from the current study indicate that the NF may be found in any position for the second, third and fourth metatarsals only, regardless of sex, side of the body or population affinity. The bone surfaces free from NF and vessels are suitable for surgical procedures in order to prevent iatrogenic arterial injuries [28] whereas surfaces occupied by NF may be considered for free vascularised bone grafting [17].

During foetal life, the nutrient canal is directed horizontally due to parallel growth at the ends of the shaft before epiphyseal appearance [14, 24]. Before birth, the direction of the nutrient canal undergoes modification, which may lead to some nutrient canals taking a different direction [20]. The metatarsals have one epiphysis and their nutrient canal is directed away from the epiphyseal end (growing end) [1, 7, 15]. The epiphysis of the first metatarsal is on the proximal end of the bone, whilst that of the second through fifth metatarsals is on the distal ends [20]. Nutrient canals of long bones tend to be directed away (opposite) from the epiphyseal end of the bone due to unequal growth rates of the diaphyseal ends and this is referred to as the growing-end theory [5, 7, 20]. The findings in the current study showed that the nutrient canals in all the metatarsal bones obeyed this theory whereby the nutrient canals were directed away from epiphysis. Similarly, studies in the Indian populations identified a similar trend [1, 14].

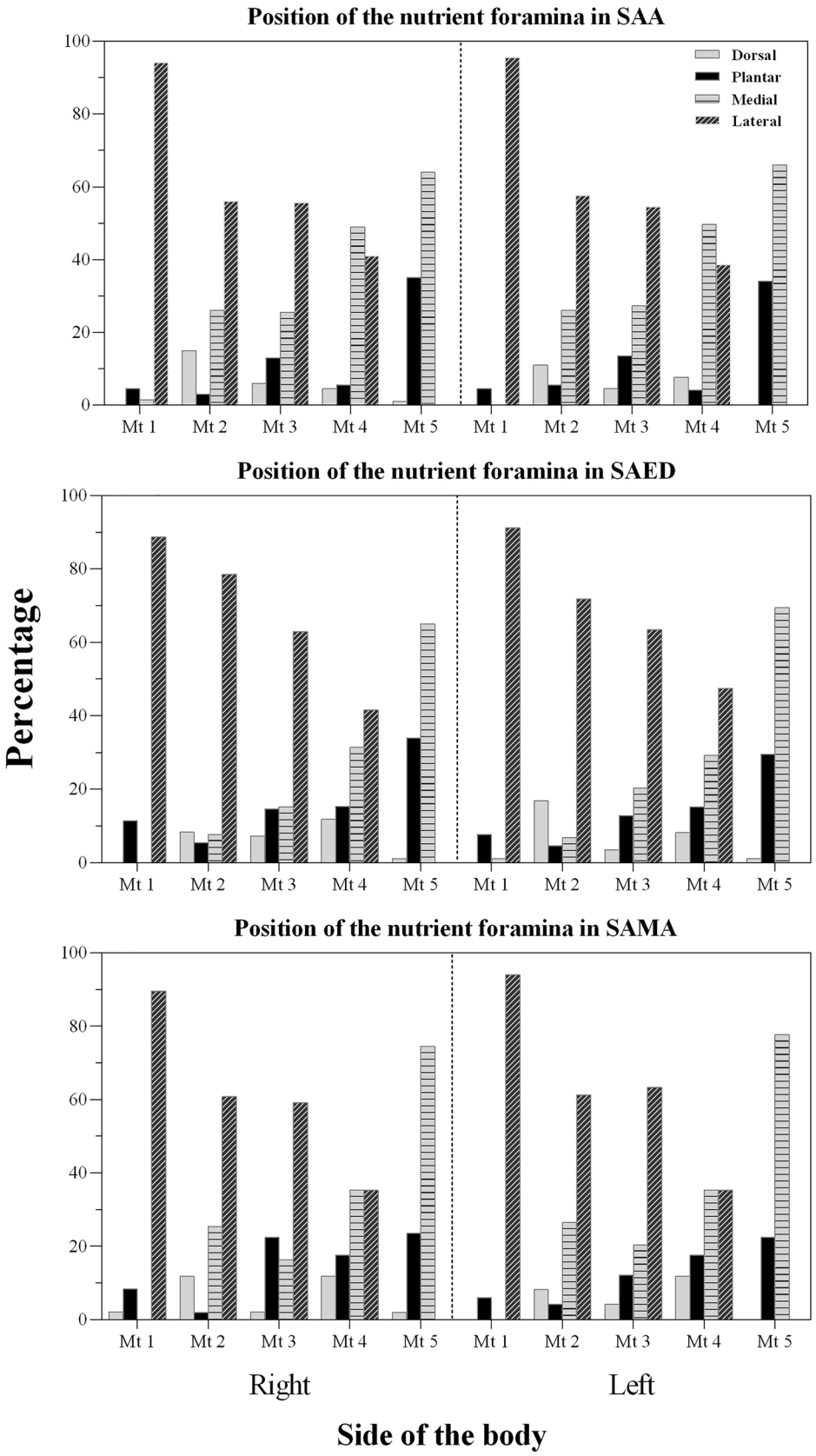


Fig. 5 A plate of graphs showing the distribution of the position of the nutrient foramen on the surfaces of the metatarsal diaphysis. Upper graph, distribution of the nutrient foramen in the South African Africans; Middle graph, distribution of the nutrient foramen in the South Africans of European descent; Lower graph, distribution of the nutrient foramen in the South Africans of Mixed ancestry, Mt, Metatarsal bone



Fig. 6 A photograph of the first through fifth metatarsal bones of the right foot with a needle showing the direction of the nutrient canal. MT1, first metatarsal; MT2, second metatarsal; MT3, third metatarsal; MT4, fourth metatarsal; MT5, fifth metatarsal

The generalisability of the current findings needs to be seen in the light of some limitations. First, there was a limited representation of the minority South African populations such as those of Asian/Indian ancestry. Since their numbers in the Raymond A. Dart collection were too low for statistical measurements, the study focussed only on the three main South African population groups. Second, the study focussed only on the adult population and thereby disregarding the young population who are more at risk of metatarsal fractures.

Conclusion

The current study has shown that the topographical and morphometric patterns regarding the metatarsal diaphyseal NF are similar across the South African populations, with some minimal variations. To date, this is the largest sample-sized and population-specific study on the metatarsal diaphyseal NF and the findings provide a new understanding of their number and size distributions. The implications of the findings from the current study may aid in the successful management of metatarsal fractures.

Acknowledgements The authors are grateful to Dr. N. Bacci, Dr. B. Billings and Mr. M. Mulaudzi for the help with accessing the skeletal materials from the Raymond A. Dart Modern Skeletal Collection, School of Anatomical Science, University of the Witwatersrand. The authors also sincerely thank those who donated their bodies to science so that anatomical research could be performed. Results from such research can potentially increase mankind's overall knowledge that can improve patient care. Therefore, these donors and their families deserve our highest gratitude.

Author contributions ATM: Project development, data collection, data analysis, manuscript writing. JGD: Project development, manuscript writing. PM: Project development, manuscript writing. All authors have read and approved the final manuscript.

Funding This study was undertaken with funding from the J.J.J. Smieszek fellowship awarded to A.T. Manjatika.

Availability of data and materials All data are kept in the institutional repository in line with institutional research ethics guidelines and it can only be available upon formal request.

Declarations

Conflict of interest No competing or conflict of interest regarding the undertaking of this research and publication of the results.

Ethical approval The study was conducted under the ethical clearance waiver number W-CBP-220504-01 obtained from the Faculty of Health Sciences, University of the Witwatersrand.

References

1. Anamika K, Murlimanju B, Divya P, Prabhu LV, Saralaya V, Rai AR, Joy T (2015) Morphology of nutrient foramina in human metatarsals and their clinical importance. Med Health 10:37–47
2. Bixby SD (2019) Pitfalls in pediatric trauma and microtrauma. Magn Reson Imaging Clin 27:721–735. https://doi.org/10.1016/j.mric.2019.07.009

3. Boutefnouchet T, Budair B, Backshayesh P, Ali SA (2014) Metatarsal fractures: a review and current concepts. Trauma 16:147–163. https://doi.org/10.1177/1460408614525738
4. Chan CW, Rudins A (1994) Foot biomechanics during walking and running. Mayo Clin Proc 16:448–461. https://doi.org/10.1016/S0025-6196(12)61642-5
5. Craig JG, Widman D, van Holsbeeck M (2003) Longitudinal stress fracture: patterns of edema and the importance of the nutrient foramen. Skeletal Radiol 32:22–27. https://doi.org/10.1007/s00256-002-0597-6
6. Cundy T, Edmonds M, Watkins P (1985) Osteopenia and metatarsal fractures in diabetic neuropathy. Diabet Med 2:461–464. https://doi.org/10.1111/j.1464-5491.1985.tb00683.x
7. Cunningham C, Scheuer L, Black S (2016) Developmental juvenile osteology. Academic Press, London
8. Götzen N, Cross AR, Ifju PG, Rapoff AJ (2003) Understanding stress concentration about a nutrient foramen. J Biomech 36:1511–1521. https://doi.org/10.1016/S0021-9290(03)00130-1
9. Gümüsburun E, Yücel F, Ozkan Y, Akgün Z (1994) A study of the nutrient foramina of lower limb long bones. Surg Radiol Anat 16:409–412. https://doi.org/10.1007/bf01627662
10. Hatch RL, Alsobrook J, Clugston JR (2007) Diagnosis and management of metatarsal fractures. Am Fam Physician 76:817–826
11. Hendriks M, Ramasamy SK (2020) Blood vessels and vascular niches in bone development and physiological remodeling. Front Cell Dev Biol 8:602278. https://doi.org/10.3389/fcell.2020.602278
12. Hughes H (1952) The factors determining the direction of the canal for the nutrient artery in the long bones of mammals and birds. Cells Tissues Organs 15:261–280. https://doi.org/10.1159/000140748
13. Kizilkanat E, Boyan N, Ozsahin ET, Soames R, Oguz O (2007) Location, number and clinical significance of nutrient foramina in human long bones. Ann Anat 189:87–95. https://doi.org/10.1016/j.aanat.2006.07.004
14. Kothapalli J (2018) Nutrient foramina architecture in metacarpal and metatarsal bones. Int J Anat Res 6:5848–5852. https://doi.org/10.16965/ijar.2018.359
15. Malukar O, Joshi H (2011) Diaphysial nutrient foramina in long bones and miniature long bones. Int J Integr Med Res 12:84
16. Mazengenya P, Fasemore MD (2015) Morphometric studies of the nutrient foramen in lower limb long bones of adult black and white South Africans. Eur J Anat 19:155–163
17. McKee NH, Haw P, Vettese T (1984) Anatomic study of the nutrient foramen in the shaft of the fibula. Clin Orth Relat Res 184:141–144
18. McKeon KE, Johnson JE, McCormick JJ, Klein SE (2013) The intraosseous and extraosseous vascular supply of the fifth metatarsal: implications for fifth metatarsal osteotomy. Foot Ankle Int 34:117–123. https://doi.org/10.1177/1071100712460227
19. Mokoena P, Billings BK, Bidmos MA, Mazengenya P (2017) Sex estimation using dimensions around the nutrient foramen of the long bones of the arm and forearm in South Africans. Forensic Sci Int 278:e401–e405. https://doi.org/10.1016/j.forsciint.2017.06.037
20. Monreal-Redondo D, Fernández-Camacho F (2003) Diaphyseal nutrient foramina in the first metatarsals in normal and hallux valgus feet: location and surgical implications. Surg Radiol Anat 25:234–240. https://doi.org/10.1007/s00276-003-0112-3
21. Moore NF (2018) Metatarsal fracture management. Orthopaed Trauma 32:428–436. https://doi.org/10.1016/j.mporth.2018.09.008
22. Murlimanju B, Prashanth K, Prabhu LV, Saralaya VV, Pai MM, Rai R (2011) Morphological and topographical anatomy of nutrient foramina in human upper limb long bones and their surgical importance. Rom J Morphol Embryol 52:859–862
23. Nagel A, Fernholz F, Kibele C, Rosenbaum D (2008) Long distance running increases plantar pressures beneath the metatarsal heads: a barefoot walking investigation of 200 marathon runners. Gait Post 27:152–155. https://doi.org/10.1016/j.gaitpost.2006.12.012
24. Patake S, Mysorekar V (1977) Diaphysial nutrient foramina in human metacarpals and metatarsals. J Anat 124:299
25. Petrisor BA, Ekrol I, Court-Brown C (2006) The epidemiology of metatarsal fractures. Foot Ankle Int 27:172–174. https://doi.org/10.1177/107110070602700303
26. Rammelt S, Heineck J, Zwipp H (2004) Metatarsal fractures. Injury 35:SB77–SB86. https://doi.org/10.1016/j.injury.2004.07.016
27. Sandhya K, Singh K (2017) A morphometric study on the nutrient foramen of metatarsal bones in the Jharkhand population. J Dent Med 16:31–34. https://doi.org/10.9790/0853-1606053134
28. Shrestha P, Mehta DK, Shrestha S, Shrestha A (2019) Variations of nutrient foramen of femur and its clinical implications. J Lumbini Med Coll 7:61–64. https://doi.org/10.22502/jlmc.v7i2.270
29. Singh I (1960) Variations in the metatarsal bones. J Anat 94:345
30. Taylor CR (1985) Force development during sustained locomotion: a determinant of gait, speed and metabolic power. J Exp Biol 115:253–262. https://doi.org/10.1242/jeb.115.1.253

Publisher's Note Springer Nature remains neutral with regard to jurisdictional claims in published maps and institutional affiliations.

Springer Nature or its licensor (e.g. a society or other partner) holds exclusive rights to this article under a publishing agreement with the author(s) or other rightsholder(s); author self-archiving of the accepted manuscript version of this article is solely governed by the terms of such publishing agreement and applicable law.

Legal Medicine 68 (2024) 102417

Contents lists available at ScienceDirect

Legal Medicine

journal homepage: www.elsevier.com/locate/legalmed

Estimation of sex using dimensions around the metatarsal diaphyseal nutrient foramen: Application of discriminant function analysis and logistic regression models

Arthur Tsalani Manjatika [a,b], Joshua Gabriel Davimes [a,*], Pedzisai Mazengenya [c,d]

[a] School of Anatomical Sciences, University of the Witwatersrand, Parktown, Johannesburg, South Africa
[b] School of Life Sciences and Allied Health Professions, Anatomy Division, Kamuzu University of Health Sciences, Blantyre, Malawi
[c] College of Medicine, Ajman University, Ajman, United Arab Emirates
[d] Center of Medical and Bio-allied Health Sciences Research, Ajman University, Ajman, United Arab Emirates

ARTICLE INFO

Keywords:
Metatarsal bones
Diaphyseal nutrient foramen
Discriminant function analysis
Logistic regression analysis
Sex estimation
South Africans of European descent

ABSTRACT

Sex estimation equations are population-specific, and a wider use of multiple bones to generate equations will increase the accuracy of sex estimation in forensic settings. The metatarsal bones have been used previously, however the dimensions around the diaphyseal nutrient foramen have not been utilised in sex estimation. The current study aimed to determine the utility of the dimensions around the nutrient foramen of metatarsal bones in estimating sex in the South Africans of European descent (SAED). Five measurements around the nutrient foramen were taken from a total of 876 metatarsal bones (first to fifth) from 186 individual skeletons (99 males, 87 females) obtained from the Raymond A. Dart Modern Skeletal Collection. Measurements subjected to direct and stepwise discriminant function (DFA) and logistic regression (LRA) analyses included total length, distance from proximal end to nutrient foramen, circumference, and mediolateral and dorsoplantar diameters at the level of the nutrient foramen. The original classification accuracies for multivariable functions of the stepwise and direct DFA ranged from 83.1–88.3% to 85.5–88.3%, respectively. The original classification accuracies for multivariable functions of the stepwise and direct LRA ranged from 83.3%–88.7% to 86.2%–88.3%, respectively. The cross-validation classifications showed a drop of 0–2.4% for DFA and 0.2–1.1% for LRA. The width measurements were better predictors of sex than length. The dimensions around the metatarsal bone nutrient foramen exhibit sexual dimorphism in the SAED. The generated DFA and LRA functions produced high average classification accuracies which are useful in sex estimation during forensic human identification.

1. Introduction

Sex estimation from recovered human skeletons is integral to establishing the biological profile of unknown individuals in medico-legal cases [1,2]. Accurate sex estimation is pivotal in establishing the age, stature, and population affinity of skeletal specimens [1]. The development of sex estimation methods involves using metric and non-metric approaches, with metric methods being considered the most reliable due to their reproducibility and reduced reliance on the expertise of the anthropologist [2–4]. The metric method entails taking a series of reproducible measurements that can be validated using different statistical techniques and subjected to different classification analyses, like discriminant function (DFA) and logistic regression (LRA) analyses, to develop sex estimation equations applicable to a specific population group [2]. DFA and LRA are the most commonly used statistical methods for sex estimation in forensic and anthropological contexts [5–8].

Dimensions around the diaphyseal nutrient foramen (NF) of the upper and lower limb long bones have been utilised to generate sex estimation equations yielding high estimation accuracies [1,9–13]. Nutrient foramina are external openings to the nutrient canal on the bone diaphysis that convey blood vessels and nerves [14–16]. South Africa has one of the highest crime rates globally and the identification of murdered victims is challenging due to limited resources and expertise [12]. Most of these victims are found dismembered, burnt, and buried in shallow graves [17]. Positive sex estimation requires the

* Corresponding author at: School of Anatomical Sciences, Faculty of Health Sciences, University of the Witwatersrand, 7 York Road, Parktown, 2193, Johannesburg, South Africa.
E-mail address: Joshua.Davimes@wits.ac.za (J.G. Davimes).

https://doi.org/10.1016/j.legalmed.2024.102417
Received 21 November 2023; Received in revised form 9 January 2024; Accepted 26 January 2024
Available online 28 January 2024
1344-6223/© 2024 Elsevier B.V. All rights reserved.

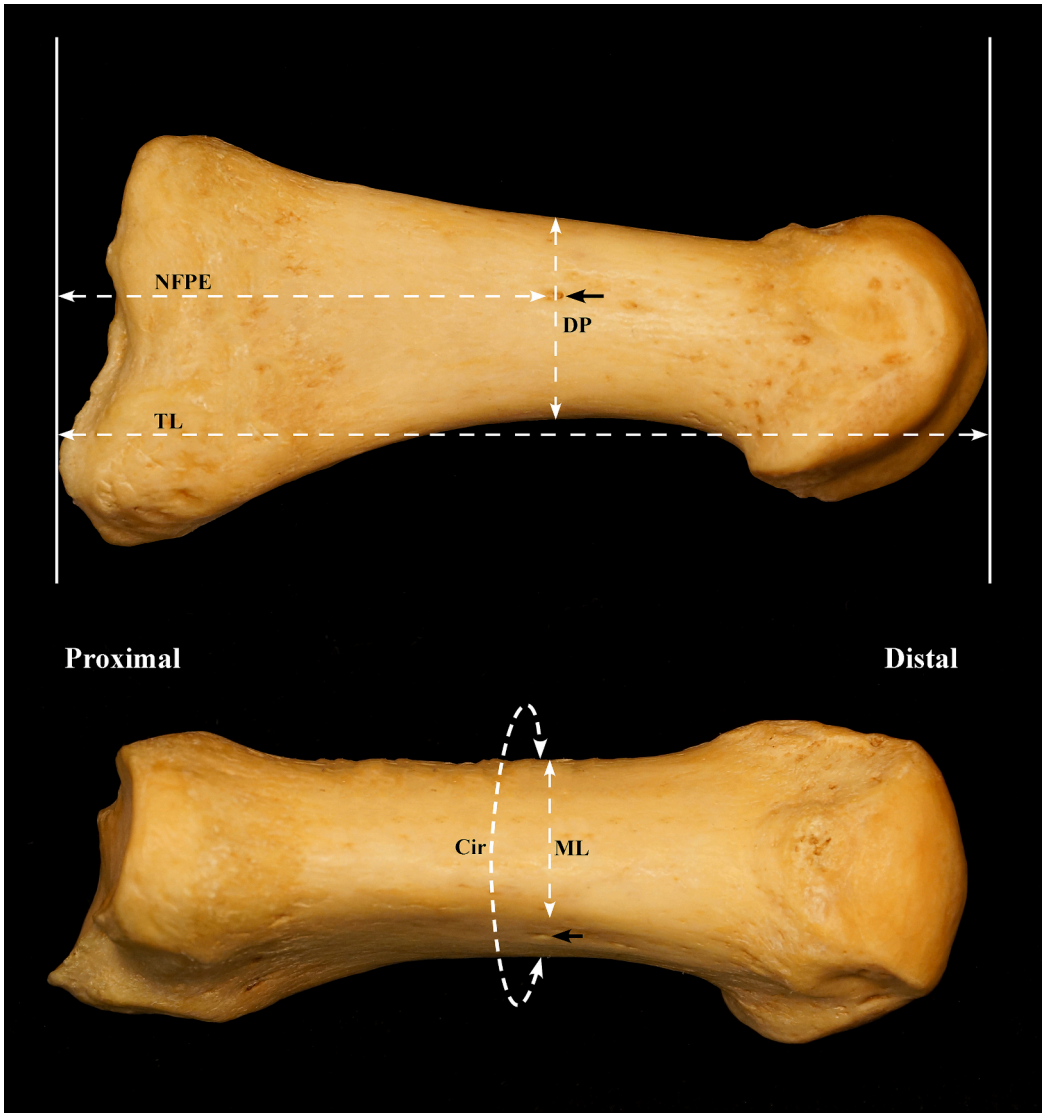


Fig. 1. Photographs of the first metatarsal bones showing the measurements that were taken. The black arrow points at the nutrient foramen. Cir = Circumference, DP = Dorsoplantar diameter, ML = Mediolateral diameter, NFPE = Distance from proximal end to the nutrient foramen, TL = Total length.

presence of all sexually dimorphic bones such as the skull and pelvis [18,19]. In most cases these bones are either missing, fragmented, or found with varying taphonomic alterations such as weathering, fire, or scavenger modifications [1,2,17,20]. This presents an opportunity to develop new standards of estimating sex from other postcranial bones to aid in accurate identification of skeletal specimens [1,2,21]. The metatarsal bones are known to be recovered in large numbers and in a well-preserved state during forensic investigations compared to other long bones [1,2,22].

Previous studies utilised the dimensions around the base, midshaft, head and length of the metatarsal bones in different populations and found them to be sexually dimorphic [2,22–28]; however, none of these studies included the dimensions around the NF. While the dimensions around the metacarpal bone NF were shown to be sexually dimorphic [29], it is unknown whether the same is true for the metatarsal bones in the estimation of sex in the South African populations. To date, no studies have examined the dimensions around the NF of the metatarsal bones to develop sex estimation standards, both globally and within the South African context. The purpose of the current study was to determine the utility of the dimensions around the metatarsal diaphyseal NF in sex estimation using the discriminant function and logistic regression functions/equations in the South Africans of European descent (SAED).

2. Materials and methods

2.1. Study population

The current study utilised a total of 876 left foot metatarsal bones (first to fifth) from 186 individuals (99 males, 87 females) aged 18–65 years (mean age 56.3 ± 10 years). These metatarsal bones were from 20th century South Africans of European descent (SAED) housed in the Raymond A. Dart Modern Skeletal Collection in the School of Anatomical Sciences, University of the Witwatersrand, South Africa [30]. The current study was conducted under the ethical clearance waiver number W-CBP-220504–01 and was covered by the Human Tissue Act (No. 65 of 1983) and the National Health Act (No. 61 of 2003) on the use of human specimens for research and teaching purposes. Metatarsal bones that presented with fractures, gross pathological deformities, malformed deformations, gross evidence of any genetic diseases, any evidence of taphonomic degeneration and any evidence of surgical interventions were excluded from the study. The metatarsal bones that showed absence of a visible NF were also excluded.

Table 1
Descriptive statistics of the measurement parameters.

Bone	Variable	Male			Female			P-Value
		No	Mean (mm)	SD	No	Mean (mm)	SD	
Metatarsal 1	TL	96	67.17	4.62	86	62.41	4.17	<0.0001
	NFPE	96	34.98	7.17	86	31.80	6.69	0.002
	DPNF	96	14.32	1.39	86	13.05	1.62	<0.0001
	MLNF	96	13.87	1.31	86	12.23	1.42	<0.0001
	CNF	96	46.87	3.28	86	41.44	3.72	<0.0001
Metatarsal 2	TL	92	79.56	5.11	85	73.84	4.40	<0.0001
	NFPE	92	35.20	5.52	85	33.00	5.78	0.01
	DPNF	92	9.85	1.22	85	9.14	1.06	<0.0001
	MLNF	92	8.38	1.27	85	7.58	0.97	<0.0001
	CNF	92	30.39	3.34	85	27.47	2.68	<0.0001
Metatarsal 3	TL	93	74.35	4.73	79	68.48	4.35	<0.0001
	NFPE	93	33.13	5.18	79	31.04	5.05	0.009
	DPNF	93	9.42	1.03	79	8.40	0.96	<0.0001
	MLNF	93	7.92	1.12	79	6.73	1.00	<0.0001
	CNF	93	29.74	2.71	79	25.67	2.50	<0.0001
Metatarsal 4	TL	93	72.68	4.95	79	67.13	4.36	<0.0001
	NFPE	93	34.57	4.13	79	31.34	4.08	<0.0001
	DPNF	93	9.97	1.15	79	9.07	1.14	<0.0001
	MLNF	93	7.47	0.96	79	6.58	0.87	<0.0001
	CNF	93	30.33	2.61	79	26.91	2.72	<0.0001
Metatarsal 5	TL	90	74.73	5.79	83	68.47	5.22	<0.0001
	NFPE	90	38.67	4.35	83	35.34	4.32	<0.0001
	DPNF	90	7.88	0.88	83	6.92	0.76	<0.0001
	MLNF	90	11.55	1.30	83	10.35	1.15	<0.0001
	CNF	90	32.89	2.94	83	28.89	2.69	<0.0001

TL = Total length, NFPE = Distance from the proximal end of the bone to the level of nutrient foramina, DPNF = Dorsoplantar diameter at the level of nutrient foramina, MLNF = Mediolateral distance at the level of the nutrient foramina, CNF = Circumference at the level of the nutrient foramina.

2.2. Osteometric measurements around the metatarsal diaphyseal nutrient foramen

A diaphyseal NF was identified macroscopically as a raised margin that surrounds the opening of a groove leading into the foramen on each metatarsal bone. A total of five osteometric measurements (Fig. 1) were taken on each metatarsal bone (MT1–MT5) as described below:

1. Total length (TL) of the bone: This linear distance measurement was taken from the most proximal aspect to the most distal part of the metatarsal bone using a mini-osteometric board (Paleo Tech Concepts, accuracy = 0.02 mm, resolution = 0.01 mm, repeatability = 0.01 mm).
2. Proximal end to nutrient foramen (NFPE): This linear distance measurement was taken from the most proximal aspect of the metatarsal bone to the NF using a digital sliding vernier calliper (Mastercraft^{TM} Africa, accuracy = 0.02 mm, resolution = 0.01 mm, repeatability = 0.01 mm).
3. Circumference at the level of the nutrient foramen (CNF): This circular distance measurement was taken around the diaphysis at the level of the NF of the metatarsal bone using a string and quantified on a vernier calliper scale.
4. Dorso-plantar diameter at the level of the nutrient foramen (DPNF): This linear distance measurement was taken from the dorsal surface to the plantar surface of the metatarsal bone at the level of the NF using a digital sliding vernier calliper.
5. Mediolateral diameter at the nutrient foramen (MLNF): This linear distance measurement was taken from the medial surface to the lateral surface of the metatarsal bone at the level of the NF using a digital sliding vernier calliper.

In addition to the five measurements listed above, the foramina indices (FI) for each metatarsal bone were also calculated using the Hughes' formula: **FI= (NFPE/TL) X 100.** Foramina index (FI) is the percentage of the total length of the bone that is represented by the distance between the proximal end and the NF [31].

2.3. Data management and statistical analysis

The data were managed in Microsoft Excel 365 (Microsoft Corporation) and analysed using IBM® SPSS® version 23 statistical software. Intra and inter-observer error statistics were calculated using the Lin's concordance coefficient of reproducibility [32]. For intra-observer repeatability, the primary observer took five measurements on 200 metatarsal bones from 40 randomly selected individuals (20 males, 20 females) and repeated the exact measurements on the same metatarsal bones two weeks later. The obtained results from the test and re-test measurements were used to calculate the intra-observer error. No significant difference between the two separate measuring occasions was observed (RC = 1.000, 95 %CI for RC = 1.000 lower and upper = 1.000). For inter-observer repeatability, the primary and secondary observers took the same measurements on 100 metatarsal bones from 20 randomly selected individuals (10 males, 10 females) one month apart. There was an almost perfect agreement between the two observers (RC = 0.998, 95 %CI for RC = 0.997 lower and upper 0.998).

Descriptive statistics (mean and standard deviations) were calculated for each measurement per metatarsal bone. The normality of the data was tested using the Kolmogorov-Smirnov test. The distribution of the data was variable, with few measurements being normally distributed across all metatarsal bones. As such, both discriminant function analysis (DFA) and logistic regression analysis (LRA) were considered. The student *t*-test was conducted to determine the significant differences between sex. The direct DFA was performed to develop univariable (each measurement separately) and multivariable equations (combination of measurements for each bone and multiple bones). The stepwise DFA (Wilk's Lambda) was performed to select the combination of measurements that best predict sex. The functions generated were then cross-validated using the "leave-one-out" classification protocol [1,33]. In addition, direct and stepwise binary LRA were performed to develop multivariable equations/functions. Collinearity diagnostics were conducted for the multivariable functions. The presence of significant multicollinearity was confirmed when a Variance Inflation Factor (VIF) value greater than 10 and Tolerance test value less than 0.1 was observed. The variables affected by multicollinearity were then either removed or retained in the functions, depending on their impact on the classification accuracy percentage.

Table 2
Descriptive statistics of the foramina index (FI).

		Male			Female			
	Variable	No	Mean	SD	No	Mean	SD	P-Value
Metatarsal 1	FI	96	51.98	9.48	86	50.93	9.94	0.468
Metatarsal 2	FI	92	44.28	6.56	85	44.62	6.91	0.733
Metatarsal 3	FI	93	44.52	6.10	79	45.27	6.12	0.425
Metatarsal 4	FI	93	47.60	5.02	79	46.70	5.43	0.261
Metatarsal 5	FI	90	51.77	4.45	83	51.61	4.78	0.822

Table 3
Direct discriminant coefficients, constants, and classification accuracies for individual measurements of the metatarsals.

Variable	Unstandardised Coefficient	Constant	Sectioning point	Classification accuracy %					
				Original classification			Cross validation		
				M	F	Average	M	F	Average
MT1TL	0.226	−14.703	−0.030	74	74.4	74.2	74	74.4	74.2
MT1NFPE	0.144	−4.817	−0.013	64.6	53.5	59.3	64.6	53.5	59.3
MT1DPNF	0.664	−9.105	−0.023	74	65.1	69.8	74	65.1	69.8
MT1MLNF	0.734	−9.614	−0.033	79.2	72.1	75.8	79.2	72.1	75.8
MT1CNF	0.286	−12.682	−0.043	87.5	69.8	79.1	87.5	69.8	79.1
MT2TL	0.209	−16.053	−0.024	82.6	76.5	79.7	82.6	76.5	79.7
MT2NFPE	0.177	−6.044	−0.008	67.4	48.2	58.2	67.4	48.2	58.2
MT2DPNF	0.873	−8.298	−0.012	57.6	60	58.8	57.6	60	58.8
MT2MLNF	0.877	−7.012	−0.014	63	62.4	62.7	63	61.2	62.1
MT2CNF	0.329	−9.525	−0.019	69.6	63.5	66.7	69.6	63.5	66.7
MT3TL	0.219	−15.714	−0.053	80.6	74.7	77.9	79.6	74.7	77.3
MT3NFPE	0.195	−6.280	−0.017	68.8	41.8	56.4	68.8	41.8	56.4
MT3DPNF	1.001	−8.962	−0.041	74.2	67.1	70.9	74.2	67.1	70.9
MT3MLNF	0.941	−6.942	−0.046	78.5	77.2	77.9	78.5	77.2	77.9
MT3CNF	0.382	−10.655	−0.063	80.6	77.2	79.1	80.6	77.2	79.1
MT4TL	0.213	−14.959	−0.049	82.8	70.9	77.3	82.8	70.9	77.3
MT4NFPE	0.243	−8.055	−0.032	75.3	57	66.9	75.3	57	66.9
MT4DPNF	0.875	−8.355	−0.032	74.2	55.7	65.7	73.1	55.7	65.1
MT4MLNF	1.091	−7.707	−0.040	73.1	65.8	69.8	73.1	65.8	69.8
MT4CNF	0.376	−10.812	−0.053	78.5	75.9	77.3	78.5	75.9	77.3
MT5TL	0.181	−12.985	−0.023	77.8	72.3	75.1	77.8	72.3	75.1
MT5NFPE	0.231	−8.552	−0.016	68.9	62.7	65.9	68.9	62.7	65.9
MT5DPNF	1.217	−9.030	−0.024	73.3	74.7	74	73.3	74.7	74
MT5MLNF	0.813	−8.917	−0.020	68.9	69.9	69.4	68.9	69.9	69.4
MT5CNF	0.354	−10.970	−0.029	77.8	74.7	76.3	77.8	74.7	76.3

Discriminant function score (DFS) equation = unstandardised coefficient × variable (in millimetres) + constant. DFS greater than the sectioning point indicates male, and DFS less than the sectioning point indicates female.

MT1 = First metatarsal bone, MT2 = Second metatarsal bone, MT3 = Third metatarsal bone, MT 4 = Fourth metatarsal bone, MT 5 = Fifth metatarsal bone TL = Total length, NFPE = Distance from the proximal end of the bone to the level of nutrient foramina, DPNF = Dorsoplantar diameter at the level of nutrient foramina, MLNF = Mediolateral distance at the level of the nutrient foramina, CNF = Circumference at the level of the nutrient foramina, F = Female, M = Male.

3. Results

All the measured parameters showed significant mean differences, with males having higher means than females across all metatarsal bones ($p < 0.05$) (Table 1). The foraminal index (FI) did not show any significant differences between males and females for all metatarsal bones ($p > 0.05$) (Table 2).

Table 3 shows the discriminant function equations generated using individual metatarsal bone measurements. The average classification accuracy rates ranged from 56.4 to 79.7 % (bias 0.4–27 %) for all metatarsal bones. Ten individual metatarsal bone measurements presented with classification rates above 75 %. MT2TL, MT1CNF and MT3CNF presented with the highest classification rates of 79.7 %, 79.1 % and 79.1 % respectively (Table 3).

From the stepwise discriminant function analysis (DFA) for the combination of all metatarsal bone measurements, the average classification accuracy rates ranged from 83.1 to 88.3 % in the original classification and from 81.4 to 88.3 % in the cross-validation (Table 4). A combination of MT1DPNF, MT1MLNF, MT1CNF and MT3CNF produced the highest average classification rate of 88.3 % (function 1, Table 4). The lowest classification rate of 83.1 % was produced by the combination of MT4CNF, MT4MLNF, and MT4NFPE (function 15, Table 4). The highest classification rate for a combination of measurements of a single metatarsal bone was 86.8 % (function 5, Table 4). The drop in the classification accuracy between the original and the cross-validation rates ranged from 0 to 2.4 %. Except for function 6 (Table 4), all the classification accuracy rates were consistently higher for males (84.1–91.4 %) than females (78.5–86.9 %) using the original classification. The MT1CNF exhibited multicollinearity (Tolerance < 0.1, VIF > 10) in functions 1, 2, 3, 5 and 6 (Table 4). Subsequent removal of MT1CNF from the affected predictor functions led to a drop in average classification accuracy rates ranging from 3.5 to 9.3 %, as such MT1CNF was retained.

The functions generated from the direct DFA are presented in a descending order of average classification accuracies (88.3 %–85.5 %) in Table 5. A combination of MT1DPNF, MT1MLNF, MT1CNF and MT3CNF produced the highest average classification rate of 88.3 % (function 1, Table 5). The drop in the classification accuracy between the original and the cross-validation rates ranged from 0 to 1.8 % (Table 5). Except for function 3 (Table 5), all the classification accuracies were consistently higher for males (86–91.4 %) than females (80.3–87.2 %) using the original classification. The MT1CNF exhibited multicollinearity (Tolerance < 0.1, VIF > 10) in functions 1, 2, 3 and 6 (Table 5). Subsequent removal of MT1CNF from the affected predictor

Table 4
Stepwise discriminant function coefficients, constants, and classification rates for a combination of measurements for multiple metatarsals.

Function	Measurement combination	Unstandardised Coefficient	Centroids	Sectioning point	Classification accuracy %					
					Original classification			Cross validation		
					M	F	Average	M	F	Average
1	MT1DPNF	−0.837	F = -1.221	−0.099	91.4	84.6	88.3	91.4	84.6	88.3
	MT1MLNF	−0.594	M = 1.024							
	MT1CNF	0.629								
	MT3CNF	0.196								
	Constant	−14.093								
2	MT1DPNF	−0.992	F = -0.976	−0.043	87.8	86.6	87.2	85.6	86.6	86.0
	MT1MLNF	−0.625	M = 0.890							
	MT1CNF	0.688								
	MT5DPNF	0.288								
	MT5MLNF	0.153								
	Constant	−12.480								
3	MT1DPNF	−0.947	F = -1.166	−0.094	89.2	84.6	87.1	89.2	84.6	87.1
	MT1MLNF	−0.642	M = 0.978							
	MT1CNF	0.641								
	MT4NFPE	0.101								
	MT4CNF	0.175								
	Constant	−15.419								
4	MT3DPNF	−0.361	F = -1.183	−0.078	89.5	83.6	86.8	89.5	83.6	86.8
	MT3CNF	0.294	M = 1.028							
	MT4NFPE	0.101								
	MT4MLNF	0.417								
	MT5MLNF	−0.880								
	MT5CNF	0.424								
	Constant	−14.694								
5	MT1CNF	0.723	F = -0.993		87.5	86	86.8	84.4	84.9	84.6
	MT1MLNF	−0.651	M = 0.890	−0.052						
	MT1TL	0.058								
	MT1DPNF	−0.983								
	Constant	−13.760								
6	MT1DPNF	−0.944	F = -1.015	−0.045	85.9	86.9	86.4	84.8	84.5	84.7
	MT1MLNF	−0.612	M = 0.926							
	MT1CNF	0.687								
	MT2TL	0.074								
	Constant	−15.113								
7	MT3NFPE	0.044	F = -1.011	−0.079	90	81.6	86.1	90	81.6	86.1
	MT3CNF	0.271	M = 0.854							
	MT4NFPE	0.087								
	MT4MLNF	0.453								
	Constant	−15.078								
8	MT3CNF	0.216	F = -1.076	−0.082	89.5	80.8	85.5	88.4	79.5	84.3
	MT4NFPE	0.109	M = 0.913							
	MT4MLNF	0.486								
	MT5DPNF	0.293								
	Constant	−15.219								
9	MT3DPNF	−0.398	F = -1.132	−0.066	87.5	82.9	85.4	85.2	81.6	83.5
	MT3CNF	0.297	M = 1.001							
	MT5NFPE	0.058								
	MT5MLNF	−0.989								
	MT5CNF	0.563								
	Constant	−13.402								
10	MT2TL	0.053	F = -1.029	−0.065	88.5	81.6	85.3	86.2	81.6	84
	MT3CNF	0.212	M = 0.899							
	MT4NFPE	0.099								
	MT4MLNF	0.504								
	Constant	−16.774								
11	MT1CNF	0.182	F = -1.041	−0.075	89.2	79.5	84.8	89.2	79.5	84.8
	MT3CNF	0.231	M = 0.892							
	Constant	−14.475								
12	MT1MLNF	0.367	F = -0.925	−0.066	88.5	78.7	84.0	87.4	78.7	83.3
	MT2MLNF	0.252	M = 0.793							
	MT3MLNF	0.469								
	MT4MLNF	0.395								
	Constant	−13.011								
13	MT4NFPE	0.115	F = -1.034	−0.071	84.1	82.9	83.5	84.1	82.9	83.5
	MT4DPNF	−0.351	M = 0.893							
	MT4CNF	0.337								
	MT5MLNF	−0.715								
	MT5CNF	0.389								
	Constant	−14.355								
14	MT3CNF	0.383	F = -0.945		84.9	81	83.1	84.9	81	83.1
	MT3NFPE	0.091	M = 0.803	−0.071						

(*continued on next page*)

Table 4 (*continued*)

Function	Measurement combination	Unstandardised Coefficient	Centroids	Sectioning point	Classification accuracy %					
					Original classification			Cross validation		
					M	F	Average	M	F	Average
	Constant	−13.602								
15	MT4CNF	0.253	F = -0.926		87.1	78.5	83.1	84.9	77.2	81.4
	MT4MLNF	0.363	M = 0.786	−0.070						
	MT4NFPE	0.162								
	Constant	−15.203								

Discriminant function score (DFS) equation = unstandardised coefficient × variables (in millimetres) + constant. DFS greater than the sectioning point indicates male, and DFS less than the sectioning point indicates female.

MT1 = First metatarsal bone, MT2 = Second metatarsal bone, MT3 = Third metatarsal bone, MT 4 = Fourth metatarsal bone, MT 5 = Fifth metatarsal bone TL = Total length, NFPE = Distance from the proximal end of the bone to the level of nutrient foramina, DPNF = Dorsoplantar diameter at the level of nutrient foramina, MLNF = Mediolateral distance at the level of the nutrient foramina, CNF = Circumference at the level of the nutrient foramina, F = Female, M = Male.

Table 5
Direct discriminant function coefficients, constants, and classification rates for a combination of measurements for multiple metatarsals.

Function	Measurement combination	Unstandardised Coefficient	Centroids	Sectioning point	Classification accuracy %					
					Original classification			Cross validation		
					M	F	Average	M	F	Average
1	MT1CNF	0.629	F = -1.221	−0.099	91.4	84.6	88.3	91.4	84.6	88.3
	MT1DPNF	−0.837	M = 1.024							
	MT1MLNF	−0.594								
	MT3CNF	0.196								
	Constant	−14.093								
2	MT1CNF	0.729	F = -1.070	−0.087	90.3	83.3	87.1	89.2	83.3	86.5
	MT4CNF	0.144	M = 0.897							
	MT1DPNF	−1.014								
	MT1MLNF	−0.715								
	Constant	−13.167								
3	MT1CNF	0.671	F = -1.135	−0.092	86	87.2	86.5	86	87.2	86.5
	MT1DPNF	−0.871	M = 0.952							
	MT1MLNF	−0.604								
	MT3TL	0.080								
	Constant	−15.595								
4	MT3CNF	0.277	F = -0.996	−0.078	91.1	80.3	86.1	88.9	78.9	84.3
	MT3DPNF	−0.127	M = 0.841							
	MT4NFPE	0.117								
	MT4MLNF	0.545								
	Constant	−14.313								
5	MT2CNF	0.033	F = -1.041	−0.065	87.6	83.3	85.6	87.6	82.1	85
	MT1MLNF	0.292	M = 0.912							
	MT3CNF	0.204								
	MT1DPNF	0.114								
	MT2TL	0.061								
	Constant	−16.748	F = -1.067	−0.086	88.2	82.1	85.4	87.1	80.8	84.2
6	MT1DPNF	−0.944	M = 0.895							
	MT1MLNF	−0.663								
	MT1CNF	0.763								
	MT3NFPE	0.007								
	Constant	−12.390								

Discriminant function score (DFS) equation = unstandardised coefficient × variables (in millimetres) + constant. DFS greater than the sectioning point indicates male, and DFS less than the sectioning point indicates female.

MT1 = First metatarsal bone, MT2 = Second metatarsal bone, MT3 = Third metatarsal bone, MT 4 = Fourth metatarsal bone, MT 5 = Fifth metatarsal bone TL = Total length, NFPE = Distance from the proximal end of the bone to the level of nutrient foramina, DPNF = Dorsoplantar diameter at the level of nutrient foramina, MLNF = Mediolateral distance at the level of the nutrient foramina, CNF = Circumference at the level of the nutrient foramina, F = Female, M = Male.

functions led to a drop in average classification accuracy rates ranging from 4.7 to 5.8 %, as such MT1CNF was retained.

From the stepwise logistic regression analysis (LRA) for the combination of all metatarsal measurements, the average classification accuracy rates ranged from 83.3 to 88.7 % in the original classification and from 83.1 to 89.7 % in the cross-validation (Table 6). A combination of MT1DPNF, MT1MLNF, MT1CNF, MT4CNF and MT4NFPE produced the highest average classification accuracy rate of 88.7 % (function 1, Table 6). The lowest classification accuracy rate of 83.1 % was produced by the combination of MT1CNF, and MT3CNF (function 15, Table 6). The highest classification accuracy rates for a combination of measurements of a single metatarsal bone was 86.6 % (function 6, Table 6). The drop in the classification accuracy between the original and the cross-validation classifications ranged from 0.2 to 1.4 %. The classification accuracy between the original and the cross-validations increased for some functions ranging from 0.2 % (function 5, Table 6) to 1.1 % (function 2, Table 6). All the classification accuracies were consistently higher for males (85.6–91.4 %) than females (77.8–87.2 %) using the original classification. The MT1CNF exhibited multicollinearity (Tolerance < 0.1, VIF > 10) in functions 1, 2, 4, 7 and 8 (Table 6). Subsequent removal of MT1CNF from the affected predictor functions led to a drop in average classification accuracy rates ranging from 4.4 to 7.9 %, as such MT1CNF was retained.

Table 7 shows the functions generated from the direct LRA,

Table 6
Stepwise logistic regression coefficients, constants, and classification rates for a combination of measurements for multiple metatarsals.

Function	Measurement combination	Unstandardised Coefficient	Sectioning point	Classification accuracy %					
				Original classification			Cross validation		
				M	F	Average	M	F	Average
1	MT1DPNF	−1.805		90	87.2	88.7	88	86.6	87.3
	MT1MLNF	−1.297	0.50						
	MT1CNF	1.199							
	MT4NFPE	0.242							
	MT4CNF	0.416							
	Constant	−31.033							
2	MT1DPNF	−2.092		91.4	84.6	88.3	93.3	84.8	89.4
	MT1MLNF	−1.643	0.50						
	MT1CNF	1.520							
	MT3CNF	0.413							
	Constant	−28.317							
3	MT3CNF	0.444		89.3	84.9	87.3	87.7	84.6	86.2
	MT4NFPE	0.263	0.50						
	MT4MLNF	1.355							
	Constant	−30.403							
4	MT1DPNF	−1.799		87	86.9	86.9	87.8	87.3	87.6
	MT1MLNF	−1.250	0.50						
	MT1CNF	1.318							
	MT2TL	0.132							
	Constant	−27.319							
5	MT1DPNF	−0.573		88.8	84.6	86.8	90.3	83.3	87
	MT1CNF	0.529	0.50						
	MT3CNF	0.378							
	Constant	−25.866							
6	MT4NFPE	0.291		88.2	84.8	86.6	85.3	86.8	86.0
	MT4CNF	0.608	0.50						
	Constant	−26.845							
7	MT1DPNF	−1.816		87.5	85.2	86.4	88.7	85.7	87.2
	MT1MLNF	−1.203	0.50						
	MT1CNF	1.238							
	MT5CNF	0.250							
	Constant	−21.697							
8	MT1DPNF	−1.910		86.5	83.7	85.2	85.7	86.3	86
	MT1MLNF	−1.311	0.50						
	MT1CNF	1.443							
	Constant	−20.415							
9	MT5MLNF	−1.654		88.4	81.6	85.2	87.1	83.3	85.3
	MT5CNF	0.827	0.50						
	MT4TL	−0.182							
	MT4NFPE	0.412							
	MT4CNF	0.698							
	Constant	−28.125							
10	MT3NFPE	0.128		87.5	81.6	84.8	85.7	84.6	85.2
	MT3CNF	0.559	0.50						
	MT5DPNF	0.741							
	Constant	−24.858							
11	MT1CNF	0.322		86.2	82.7	84.6	86.3	81.3	83.9
	MT3CNF	0.381	0.50						
	MT4NFPE	0.141							
	Constant	−29.339							
12	MT1DPNF	−0.713		85.6	82.9	84.3	87.3	82.9	85.1
	MT1CNF	0.506	0.50						
	MT5CNF	0.285							
	Constant	−21.298							
13	MT1MLNF	0.565							
	MT2MLNF	0.471	0.50	88.1	79.2	84	85.3	82.3	83.8
	MT3MLNF	0.720							
	MT4MLNF	0.690							
	Constant	−21.023							
14	MT3NFPE	0.167		86	81	83.7	85.3	79.1	82.4
	MT3CNF	0.639	0.50						
	Constant	–22.918							
15	MT1CNF	0.308		88.1	77.8	83.3	85.3	80.6	83.1
	MT3CNF	0.404	0.50						
	Constant	−24.704							

Logistic Regression analysis (LRA) model equation = unstandardised coefficient × variables in (in millimetres) + constant. LRA greater than the sectioning point indicates male, and LRA less than the sectioning point indicates female.

MT1 = First metatarsal bone, MT2 = Second metatarsal bone, MT3 = Third metatarsal bone, MT 4 = Fourth metatarsal bone, MT 5 = Fifth metatarsal bone TL = Total length, NFPE = Distance from the proximal end of the bone to the level of nutrient foramina, DPNF = Dorsoplantar diameter at the level of nutrient foramina, MLNF = Mediolateral distance at the level of the nutrient foramina, CNF = Circumference at the level of the nutrient foramina, F = Female, M = Male.

Table 7
Direct logistic regression coefficients, constants, and classification rates for a combination of measurements for multiple metatarsals.

Function	Measurement combination	Unstandardised Coefficient	Sectioning point	Classification accuracy %					
				Original classification			Cross validation		
				M	F	Average	M	F	Average
1	MT1DPNF	−1.909		89.2	87.2	88.3	88.0	86.6	87.3
	MT1MLNF	−1.352	0.50						
	MT1CNF	1.270							
	MT4NFPE	0.221							
	MT4CNF	0.369							
	Constant	−29.944							
2	MT1DPNF	−1.780		87.1	87.2	87.1	90.7	89.4	90.1
	MT1MLNF	−1.342	0.50						
	MT1CNF	1.388							
	MT3TL	0.154							
	Constant	−30.165							
3	MT3CNF	0.407		90	82.9	86.7	87.7	84.6	86.2
	MT4NFPE	0.219	0.50						
	MT4MLNF	1.063							
	Constant	−25.820							
4	MT4NFPE	0.291		88.2	84.8	86.6	85.3	86.8	86
	MT4CNF	0.608	0.50						
	Constant	−26.845							
5	MT1DPNF	−1.983		89.2	83.3	86.5	88	86.6	87.3
	MT1MLNF	−1.483	0.50						
	MT1CNF	1.413							
	MT4CNF	0.250							
	Constant	−22.905							
6	MT1DPNF	0.214		87.6	84.6	86.2	87.5	86.4	87
	MT1MLNF	0.441	0.50						
	MT2CNF	0.090							
	MT2TL	0.143							
	MT3CNF	0.340							
	Constant	−31.536							

Logistic Regression analysis (LRA) model equation = unstandardised coefficient × variables in (in millimetres) + constant. LRA greater than the sectioning point indicates male and LRA less than the sectioning point indicates female.

MT1 = First metatarsal bone, MT2 = Second metatarsal bone, MT3 = Third metatarsal bone, MT 4 = Fourth metatarsal bone, MT 5 = Fifth metatarsal bone TL = Total length, NFPE = Distance from the proximal end of the bone to the level of nutrient foramina, DPNF = Dorsoplantar diameter at the level of nutrient foramina, MLNF = Mediolateral distance at the level of the nutrient foramina, CNF = Circumference at the level of the nutrient foramina, F = Female, M = Male.

presented in a descending order of average classification accuracies (88.3 %–86.2 %). A combination of MT1DPNF, MT1MLNF, MT1CNF, MT4CNF and MT4NFPE produced the highest average classification accuracy rate of 88.7 % (function 1, Table 7). The drop in the classification accuracy between the original and the cross-validation classifications ranged from 0.5 to 1.7 % while increase in classification accuracy ranged from 0.8 to 3 % (Table 7). All the classification accuracies were consistently higher for males (87.1–90 %) than females (80.3–87.2 %) using the original classification. The MT1CNF exhibited multicollinearity (Tolerance < 0.1, VIF > 10) in functions 1, 2 and 5 (Table 7). Subsequent removal of MT1CNF from the affected predictor functions led to a drop in average classification accuracy rates ranging from 4.1 to 5.2 %, as such MT1CNF was retained.

4. Discussion

Accurate estimation of sex of unknown individuals is crucial in both forensic and archaeological settings since it narrows down the process of establishing a biological profile by half [1,11]. The skull and pelvic bones are known sexually dimorphic bones which are utilised in routine forensic investigations [6,18,19,34–36]. However, in certain instances these sexually dimorphic bones are either missing or recovered in varying states of taphonomic alteration, thereby rendering them inapplicable for analysis [2,17]. It is therefore imperative to examine the usefulness of a variety of postcranial structures in sex estimation in order to improve the efficiency of specimen identification in forensic settings. Recently, there has been a surge in the number of studies focussing on the sex estimating potential of various postcranial structures in different populations [2,9,11,29,37–40]. Sex estimation equations are population specific, and equations generated in a particular population cannot be applied to another population. Hence the need to establish population specific standards in various populations. Dimensions around the NF of the long bones have been utilised to generate sex estimation equations in a few studies [e.g., 1, 10, 11] while no studies have investigated the potential of these dimensions on the metatarsal bones. The current study investigated the potential of the dimensions around the NF of the metatarsal bones in sex estimation from the South Africans of European descent (SAED).

The majority of the dimensions around the NF (except the FI) showed sexual dimorphism with males having larger means compared to females (Tables 1 and 2). Similar findings were observed previously in other long bones including the humerus, radius, ulnar, metacarpals, femur, and tibia in the SAED population [1,10–12]. The FI is a calculated variable that relies on the proportions of the NFPE and TL [41] and has been found to be a poor predictor of sex [29].

In the current study, all the classification accuracies of the individual measurements around the NF of the metatarsal bones were found to be below 80 %, which is low compared to a previous study in the same population group that reported classification accuracies greater than 80 % when using individual measurements around the NF of the metacarpal bones [29]. However, the classification accuracies on the individual measurements in the current study are higher than those previously reported in a study that focused on the length of the metatarsal bones only [2]. Notably, most univariable functions in the current study presented a bias (sex-specific differences) of greater than 5 %, suggesting that the univariable functions should be used with caution [42].

Results from the stepwise DFA showed that the combination of measurements around the NF of the first metatarsal bone have the highest correct classification accuracy for sex estimation compared with other individual metatarsal bones. Similar findings were observed in the

Greek population whereby the dimensions from the first metatarsal bone yielded comparatively high sex estimation accuracies [22]. The stepwise LRA, on the other hand, selected the fourth metatarsal bone as the single best predictor of sex.

Previous studies utilizing the dimensions around the base, midshaft, head and length of the metatarsal bones in different populations reported classification accuracies similar to the current study [2,22–25]. In addition, studies in the SAED population using dimensions around the NF of the humerus, radius, ulnar and tibia also produced classification accuracies ranging from 84 to 88 % [1,11]. Generally, classification accuracies greater than 80 % are acceptable in forensic and archaeological settings [43] and a drop of less than 5 % between the original classification and the cross-validation accuracies indicates the validity of the generated functions [11]. In the current study, both the DFA and LRA equations on a combination of measurements produced high classification accuracies greater than 80 % with a drop of 0–2.4 % in the cross-validation.

The DFA and LRA equations in the current study also demonstrated that the combination of the diameter/circular measurements (CNF, DPNF, MLNF) performed better than length measurements (TL and NFPE), similar to that reported in previous studies [9,10,29]. Length measurements are minimally affected by lifetime activities while the diameter and circular measurements are affected by the activity-related factors in different populations. Hence, for correct sex estimation a combination of both width and length measurements is ideal since it factors in both the genetic and physical forces on the bone morphology [24]. In the current study, males were classified with the highest accuracy across all metatarsal bones using the multivariable functions, with a bias between 0.1 % and 10.8 %, similar to other studies [22,44]. Sex-specific accuracies are associated with genetic, hormonal and biomechanical factor differences [42].

It should be noted that only MT1CNF exhibited multicollinearity in most of the generated multivariable function equations that included it in both the DFA and LRA. However, when MT1CNF was removed from the multivariable function equations, the sex estimation classification accuracy rates dropped significantly (range 3.5–9.3 %). This may be due to the fact that the MT1CNF as a single variable has a high sex estimation classification accuracy rate of 79.1 % (Table 3). This finding suggests that MT1CNF is a significant predictor of sex, hence it was retained in the affected multivariable function equations throughout.

Bartholdy et al. [44] suggested that LRA is better than DFA for developing sex estimation equations. Although both methods produce comparable classification accuracies as shown in the current study and also in previous studies [2,5], DFA and LRA possess intrinsic differences that affect their suitability for generating sex estimation equations. LRA provides the probability of group membership with classification values ranging from zero to one, while DFA provides a rigid dichotomous membership classification based on sectioning points [44]. In addition, LRA is a non-parametric analysis that assumes that the multivariable data is not normally distributed, whereas DFA is a parametric analysis that assumes that the multivariable data is normally distributed [33,44]. Given the biological overlaps between sexes within a population, a flexible analysis approach is recommended to account for uncertainties associated with sex estimation equations, particularly in forensic contexts [45]. The assumption of multivariable normality was violated in the present study, suggesting that LRA equations may be more appropriate than DFA equations in the current population.

In conclusion, the dimensions related to the metatarsal bone NF show high sexual dimorphism in the SAED population. A combination of measurements around the NF from different metatarsal bones produced high sex classification rates that are applicable in both medico-legal and archaeological settings particularly for intact or fragmented metatarsal bones. Overall, the study recommends the use of LRA functions on all the non-normally distributed data.

Declaration of competing interest

The authors declare that they have no known competing financial interests or personal relationships that could have appeared to influence the work reported in this paper.

Acknowledgements

The authors would like to thank Dr N. Bacci, Dr B. Billings and Mr M. Mulaudzi for their assistance with access to the Raymond A. Dart Modern Skeletal Collection. The authors also thank Mr T. Kaledzera, Dr N. Bacci and Dr O. Ujaddughe for their statistical advice. The authors also sincerely thank those who donated their bodies to science so that anatomical research could be performed. Results from such research can potentially increase mankind's overall knowledge. Therefore, these donors and their families deserve our highest gratitude.

Funding

The work was supported by the J.J.J Smieszek fellowship (2022, 2023) and the University of the Witwatersrand Faculty research grant (2023).

Ethical approval

The current study was conducted under the ethical clearance waiver number W-CBP-220504-01 and was covered by the Human Tissue Act (No. 65 of 1983) and the National Health Act (No. 61 of 2003) on the use of human specimens for research and teaching purposes.

References

[1] P. Mokoena, B.K. Billings, M.A. Bidmos, P. Mazengenya, Sex estimation using dimensions around the nutrient foramen of the long bones of the arm and forearm in South Africans. Forensic Sci. Int. 278 (2017) e401-404. e405. https://doi.org/10.1016/j.forsciint.2017.06.037.

[2] M. Bidmos, A. Adebesin, P. Mazengenya, O. Olateju, O. Adegboye, Estimation of sex from metatarsals using discriminant function and logistic regression analyses, Aust. J. Forensic Sci. 53 (2021) 543–556, https://doi.org/10.1080/00450618.2019.1711180.

[3] R.W. Mann, D.R. Hunt, S. Lozanoff, Photographic Regional Atlas of Non-Metric Traits and Anatomical Variants in the Human Skeleton, Charles C Thomas Press, Springfield, IL, 2016.

[4] A. Palamenghi, D. Gibelli, D. Mazzarelli, D. De Angelis, C. Sforza, C. Cattaneo, Rumor has it: a narrative review on the use of skeletal non-metric traits and variants for personal identification, Legal Med. 65 (2023) 102316, https://doi.org/10.1016/j.legalmed.2023.102316.

[5] M. Pohar, M. Blas, S. Turk, Comparison of logistic regression and linear discriminant analysis: a simulation study, Metodoloski Zvezki 1 (2004) 143.

[6] P.L. Walker, Sexing skulls using discriminant function analysis of visually assessed traits, Am. J. Phys. Anthropol. 136 (2008) 39–50, https://doi.org/10.1002/ajpa.20776.

[7] D. Charisi, C. Eliopoulos, V. Vanna, C.G. Koilias, S.K. Manolis, Sexual dimorphism of the arm bones in a modern Greek population, J. Forensic Sci. 56 (2011) 10–18, https://doi.org/10.1111/j.1556-4029.2010.01538.x.

[8] E. Nikita, Quantitative sex estimation based on cranial traits using R functions, J. Forensic Sci. 64 (2019) 175–180, https://doi.org/10.1111/1556-4029.13833.

[9] S. Garcia, Is the circumference at the nutrient foramen of the tibia of value to sex determination on human osteological collections? Testing a new method, Int. J. Osteoarchaeol. 22 (2012) 361–365, https://doi.org/10.1002/oa.1202.

[10] G.C. Krüger, E.N. L'Abbé, K.E. Stull, Sex estimation from the long bones of modern South Africans, Int. J. Legal Med. 131 (2017) 275–285, https://doi.org/10.1007/s00414-016-1488-z.

[11] M.D. Fasemore, M.A. Bidmos, P. Mokoena, A. Imam, B.K. Billings, P. Mazengenya, Dimensions around the nutrient foramina of the tibia and fibula in the estimation of sex, Forensic Sci. Int. 287 (222) (2018) e221–e227, https://doi.org/10.1016/j.forsciint.2018.03.015.

[12] P. Mokoena, B.K. Billings, V. Gibbon, M.A. Bidmos, P. Mazengenya, Development of discriminant functions to estimate sex in upper limb bones for mixed ancestry South Africans, Sci. Justice 59 (2019) 660–666, https://doi.org/10.1016/j.scijus.2019.06.007.

[13] M.A. Bidmos, P. Mazengenya, Accuracies of discriminant function equations for sex estimation using long bones of upper extremities, Int. J. Legal Med. 135 (2021) 1095–1102, https://doi.org/10.1007/s00414-020-02458-y.

[14] A.T. Manjatika, P. Mazengenya, J.G. Davimes, Topographical anatomy and clinical implications of the metatarsal diaphyseal nutrient foramina across South African

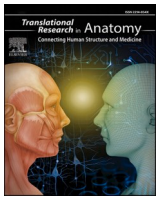
populations, Surg. Radiol. Anat. 45 (2023) 1213–1226, https://doi.org/10.1007/s00276-023-03233-5.
[15] K. Anamika, B. Murlimanju, P. Divya, L.V. Prabhu, V. Saralaya, A.R. Rai, T. Joy, Morphology of nutrient foramina in human metatarsals and their clinical importance, Med. Health 10 (2015) 37–47.
[16] E. Gümüsburun, F. Yücel, Y. Ozkan, Z. Akgün, A study of the nutrient foramina of lower limb long bones, Surg. Radiol. Anat. 16 (1994) 409–412, https://doi.org/10.1007/bf01627662.
[17] M. Steyn, D. Brits, Dismemberment in South Africa: case studies. In: Dismemberments: Elsevier. p (2019) 69-83, https://doi.org/10.1016/B978-0-12-811912-9.00005-8.
[18] P.N. Gonzalez, V. Bernal, S.I. Perez, Geometric morphometric approach to sex estimation of human pelvis, Forensic Sci. Int. 189 (2009) 68–74, https://doi.org/10.1016/j.forsciint.2009.04.012.
[19] M.K. Spradley, R.L. Jantz, Sex estimation in forensic anthropology: skull versus postcranial elements, J. Forensic Sci. 56 (2011) 289–296, https://doi.org/10.1111/j.1556-4029.2010.01635.x.
[20] M. Steyn, Muti murders from South Africa: A case report, Forensic Sci. Int. 151 (2005) 279–287, https://doi.org/10.1016/j.forsciint.2004.05.022.
[21] M. Steyn, M.Y. İşcan, Osteometric variation in the humerus: sexual dimorphism in South Africans, Forensic Sci. Int. 106 (1999) 77–85, https://doi.org/10.1016/S0379-0738(99)00141-3.
[22] C. Mountrakis, C. Eliopoulos, C.G. Koilias, S.K. Manolis, Sex determination using metatarsal osteometrics from the Athens collection, Forensic Sci. Int. 200 (178) (2010) e171–e178, https://doi.org/10.1016/j.forsciint.2010.03.041.
[23] A.G. Robling, D.H. Ubelaker, Sex estimation from the metatarsals, J. Forensic Sci. 42 (1997) 1062–1069.
[24] D.T. Case, A.H. Ross, Sex determination from hand and foot bone lengths, J. Forensic Sci. 52 (2007) 264–270, https://doi.org/10.1111/j.1556-4029.2006.00365.x.
[25] W.M.A. Moneim, R.H.A. Hady, R.M.A. Maaboud, H.M. Fathy, A.M. Hamed, Identification of sex depending on radiological examination of foot and patella, Am. J. Forensic Med. Pathol. 29 (2008) 136–140, https://doi.org/10.1097/PAF.0b013e318173f048.
[26] S. Rodríguez, A. González, A. Simón, M.S. Rodríguez-Calvo, M. Febrero-Bande, C. Cordeiro, J.I. Muñoz-Barús, The use of computerized tomography in determining stature and sex from metatarsal bones, Legal Med. 16 (2014) 252–257, https://doi.org/10.1016/j.legalmed.2014.05.006.
[27] D. Gibelli, P. Poppa, M. Cummaudo, M. Mattia, A. Cappella, D. Mazzarelli, M. Zago, C. Sforza, C. Cattaneo, Sex assessment from the volume of the first metatarsal bone: a comparison of linear and volume measurements, J. Forensic Sci. 62 (2017) 1582–1585, https://doi.org/10.1111/1556-4029.13464.
[28] A.K. Wilbur, The utility of hand and foot bones for the determination of sex and the estimation of stature in a prehistoric population from west-central Illinois, Int. J. Osteoarchaeol. 8 (1998) 180–191.
[29] S. Sallie, M.A. Bidmos, P. Mazengenya, Estimation of sex from the metacarpal dimensions at the nutrient foramen in white South Africans, Aust. J. Forensic Sci. 54 (2022) 533–545, https://doi.org/10.1080/00450618.2020.1805010.
[30] M.R. Dayal, A.D. Kegley, G. Štrkalj, M.A. Bidmos, K.L. Kuykendall, The history and composition of the Raymond A. Dart Collection of human skeletons at the University of the Witwatersrand, Johannesburg, South Africa, Am. J. Phys. Anthropol. 140 (2009) 324–335, https://doi.org/10.1002/ajpa.21072.
[31] H. Hughes, The factors determining the direction of the canal for the nutrient artery in the long bones of mammals and birds, Cells Tissues Organs 15 (1952) 261–280.
[32] I. Lawrence, K. Lin, A concordance correlation coefficient to evaluate reproducibility, Biometrics 45 (1989) 255–268.
[33] T. Ramayah, N.H. Ahmad, H.A. Halim, S.R.M.Z. May-Chiun, Discriminant analysis: An illustrated example, Afr. j, Bus. Manage. 4 (2010) 1654–1667.
[34] Y. Ogawa, K. Imaizumi, S. Miyasaka, M. Yoshino, Discriminant functions for sex estimation of modern Japanese skulls, J. Forensic Legal Med. 20 (2013) 234–238, https://doi.org/10.1016/j.jflm.2012.09.023.
[35] A. Bertsatos, M.E. Chovalopoulou, J. Brůžek, S. Bejdová, Advanced procedures for skull sex estimation using sexually dimorphic morphometric features, Int. J. Legal Med. 134 (2020) 1927–1937, https://doi.org/10.1007/s00414-020-02334-9.
[36] A.R. Klales, Sex estimation using pelvis morphology. In: Sex estimation of the human skeleton: Elsevier. (2020) 75-93, https://doi.org/10.1016/B978-0-12-815767-1.00006-7.
[37] D. Franklin, A. Flavel, A. Kuliukas, A. Cardini, M.K. Marks, C. Oxnard, P. O'Higgins, Estimation of sex from sternal measurements in a Western Australian population, Forensic Sci. Int. 217 (230) (2012) e231–e235, https://doi.org/10.1016/j.forsciint.2011.11.008.
[38] E.F. Kranioti, M.A. Apostol, Sexual dimorphism of the tibia in contemporary Greeks, Italians, and Spanish: forensic implications, Int. J. Legal Med. 129 (2015) 357–363, https://doi.org/10.1111/j.1556-4029.2009.01103.x.
[39] M.K. Moore, E.A. DiGangi, F.P.N. Ruíz, O.J.H. Davila, C.S. Medina, Metric sex estimation from the postcranial skeleton for the Colombian population, Forensic Sci. Int. 262 (286) (2016) e281–e288, https://doi.org/10.1016/j.forsciint.2016.02.018.
[40] M. Hora, V. Sládek, Population specificity of sex estimation from vertebrae. Forensic Sci. Int. 291 (2018) 279. e271-279. e212, https://doi.org/10.1016/j.forsciint.2018.08.015.
[41] G. Pereira, P. Lopes, A. Santos, F. Silveira, Nutrient foramina in the upper and lower limb long bones: morphometric study in bones of Southern Brazilian adults, Int. J. Morphol. 29 (2011) 514–520.
[42] F. Curate, F. Mestre, S.J. Garcia, Sex assessment with the radius in Portuguese skeletal populations (late 19th-early to mid 20th centuries), Legal Med. 48 (2021) 101790, https://doi.org/10.1016/j.legalmed.2020.101790.
[43] W.M. Krogman, M.Y. Isçan, The Human Skeleton in Forensic Medicine, Charles C Thomas, Springfield, IL, 1986, pp. 202–208.
[44] B.P. Bartholdy, E. Sandoval, M.L. Hoogland, S.A. Schrader, Getting rid of dichotomous sex estimations: Why logistic regression should be preferred over discriminant function analysis, J. Forensic Sci. 65 (2020) 1685–1691, https://doi.org/10.1111/1556-4029.14482.
[45] E. Marini, W. Racugno, S.M. Borgognini, S.M. Tarli, Univariate estimates of sexual dimorphism: the effects of intrasexual variability, Am. J. Phys. Anthropol. 109 (1999) 501–508.

Translational Research in Anatomy 37 (2024) 100327

Contents lists available at ScienceDirect

Translational Research in Anatomy

journal homepage: www.elsevier.com/locate/tria



Utility of the metatarsal diaphyseal nutrient foramen in estimating sex in the South African Africans population

Arthur Tsalani Manjatika [a,b], Pedzisai Mazengenya [c,d,e,*], Joshua Gabriel Davimes [a]

[a] School of Anatomical Sciences, University of the Witwatersrand, Parktown, Johannesburg, South Africa
[b] School of Life Sciences and Allied Health Professions, Anatomy Division, Kamuzu University of Health Sciences, Blantyre, Malawi
[c] College of Medicine, Ajman University, Ajman, United Arab Emirates
[d] Center of Medical and Bio-allied Health Sciences Research, Ajman University, Ajman, United Arab Emirates
[e] Faculty of Health Sciences, University of the Witwatersrand, Parktown, Johannesburg, South Africa

ARTICLE INFO

Keywords:
Metatarsal bones
Diaphyseal nutrient foramen
Discriminant function analysis
Logistic regression analysis
Sex estimation
South African Africans

ABSTRACT

Introduction: Sex estimation is challenging in cases where dismembered or non-intact skeletal remains are recovered. Therefore, the development of sex estimation standards using various bones that present with high recovery rates during forensic investigations, like the metatarsal bones, is needed. The usefulness of the dimensions around the metatarsal diaphyseal nutrient foramen in sex estimation has not been assessed in South African Africans (SAA), constituting the majority of the country's population.

Materials and methods: Five measurements around the nutrient foramen were taken from 995 metatarsal bones (first to fifth) from 200 individual skeletons (100 males, 100 females). Measurements subjected to direct and stepwise discriminant function (DFA) and logistic regression (LRA) analyses included the total length, distance from proximal end to nutrient foramen, circumference, and mediolateral and dorsoplantar diameters at the level of the nutrient foramen.

Results: The original classification accuracies for multivariable functions of the stepwise and direct DFA ranged from 75.1 to 80 % and 76–79.5 % respectively. The original classification accuracies for multivariable functions of the stepwise and direct LRA ranged from 76.3% to 79.5 % and 75%–80.5 % respectively. The cross-validation classifications showed a drop of 0–2% for DFA and 0.2–1.9 % for LRA. Overall breadth measurements showed better classification accuracies than length measurements and females were classified with higher accuracy rates than males.

Conclusion: The dimensions around the nutrient foramen of the metatarsal bones show sexual dimorphism in the SAA. The generated DFA and LRA functions produced high average classification accuracies which can be appropriate for use in sex estimation in forensic settings, especially when an isolated foot is recovered.

1. Introduction

Biological sex estimation in forensic analysis is considered simple as the external and internal genitalia can directly suggest the sex of an individual [1]. However, sex estimation from skeletal remains becomes challenging more so in cases where fragmentary and incomplete skeletal remains are recovered. This presents an opportunity to develop new standards of estimating sex to aid in the accurate identification of individuals [2–4]. Previous studies have reported high accuracies for estimating sex from skeletal remains using a variety of cranial and postcranial elements, with the pelvis and skull being the most sexually dimorphic. However, these bones are often missing, decomposed, and or fragmented due to poor preservation, taphonomical alterations, predation, and or dismemberment [3–6]. Recently, there has been a surge in the studies focusing on postcranial elements in various populations, particularly the long bones and their performance in sex estimation equations [4,7–11]. Still, alternative techniques must be developed using other skeletal elements and features to advance the methods of sex estimation in forensic and archaeological settings.

Sex estimation from skeletal remains is crucial in medico-legal settings, as it helps researchers to identify victims of crime from various contexts. These may include recovered mutilated or dismembered body parts, burned remains, and fragmented or intact skeletal remains [9]. There are subjective and objective methods/techniques used to estimate

* Corresponding author. College of Medicine, Ajman University, Ajman, United Arab Emirates.
E-mail address: p.mazengenya@ajman.ac.ae (P. Mazengenya).

https://doi.org/10.1016/j.tria.2024.100327
Received 12 July 2024; Received in revised form 24 July 2024; Accepted 24 July 2024
Available online 26 July 2024
2214-854X/© 2024 Published by Elsevier GmbH. This is an open access article under the CC BY-NC-ND license (http://creativecommons.org/licenses/by-nc-nd/4.0/).

the sex of an individual from skeletal remains. Subjective techniques require having a complete skeleton or access to bones that display typical sexually dimorphic anatomical features, but this scenario is uncommon in forensic cases. In addition, subjective techniques require anthropologists who are highly qualified and experienced to identify precise morphological features that lead to accurate sex estimations [12]. In contrast, objective techniques utilise standardised anatomical landmarks for measurements and employ various statistical models such as discriminant function analysis and logistic regression analysis to develop sex estimation functions/equations [13–16]. Objective techniques are considered ideal for bones that do not present obvious sexual dimorphic traits like most postcranial elements [15,17]. Objective techniques are also useful in sex estimation in cases of commingled remains, like in mass disasters, mass graves or secondary burials [18,19]. While objective techniques are more favourable than subjective techniques, they are population-specific especially for bones that do not exhibit obvious sexually dimorphic traits [20–23]. This necessitates the creation of sex estimation functions/equations for each population group, particularly those most affected by violent crimes and murder, to ensure accurate sex classifications and subsequent positive identification [15].

South Africa has one of the highest crime rates in the world [3,24]. South African Africans, also known as Black South Africans, make up about 80 % of the total South African population, and individuals of this group are most often victims of murder in the country [3,4]. It is, therefore, essential to have a variety of methods for estimating sex in order to improve the establishment of the biological profile of victims during forensic investigations. Previous studies developed metric methods of estimating sex in the South African Africans using anatomical features of various bones like the humerus, radius, ulna [3,25], femur, tibia, fibular [26], calcaneus [22], talus [21], and metatarsals [4]. The dimensions around the nutrient foramina of the upper and lower limb long bones have shown to be useful in estimating sex of individuals in various populations [3,26–30]. Recently, in the South Africans of European descent population, the dimensions around the nutrient foramen of the metatarsal bones demonstrated high sex estimation accuracies [11]. Nutrient foramina are external openings to the nutrient canal on the bone diaphysis that convey blood vessels and nerves [31–33]. Nutrient foramina can be identified macroscopically in almost 100 % of the metatarsal diaphyses, and in cases of multiple nutrient foramina, a dominant one presents as the largest in diameter when compared to the rest [31]. Dimensions around the nutrient foramina can also serve as substitutes for midshaft measurements in cases where fragmentary or broken bones are recovered. During forensic and archaeological settings metatarsal bones have an advantage of being recovered in large quantities and generally in well-preserved states possibly due to their size and numbers compared to other long bones [4,34]. The purpose of the current study was to determine the utility of the dimensions around the metatarsal diaphyseal nutrient foramen in sex estimation using the discriminant function and logistic regression analyses in the South African Africans population.

2. Materials and methods

2.1. Study population

The current study was conducted under the ethical clearance waiver number W-CBP-22050401 obtained from the Faculty of Health Sciences at the University of the Witwatersrand. The study utilised 995 left foot metatarsal bones (first to fifth) from 200 adult individuals (100 males, 100 females) aged 25–65 years (mean age 39.78 ± 10.32 years). The left foot was chosen because it is less likely to be affected by physical activity-related changes since it is the non-dominant side in the majority of the global populations. The metatarsal bones were obtained from the skeletal remains of the 20th century South African Africans (SAA) housed in the Raymond A. Dart Modern Skeletal Collection in the School of Anatomical Sciences at the University of the Witwatersrand in South Africa [35]. The SAA mainly consists of various ethnic tribes including the Pedi, Sotho, Tswana, Ndebele, Zulu, Venda, Xhosa, Swazi and Tsonga. These ethnic groups do not exhibit significant osteometric differences, hence are considered as a homogeneous population group [36,37]. Metatarsal bones showing gross pathologies, deformities, fractures and degradation were excluded from the study. The metatarsal bones without visible nutrient foramen were also excluded.

2.2. Osteometric measurements around the metatarsal diaphyseal nutrient foramen

A diaphyseal nutrient foramen was identified macroscopically as a raised margin that surrounds the opening of a groove leading into the foramen on each metatarsal bone. A total of five osteometric measurements: total length (TL), proximal end to nutrient foramen (NFPE), circumference at the level of the nutrient foramen (CNF), dorsoplantar diameter at the level of the nutrient foramen (DPNF) and mediolateral diameter at the nutrient foramen (MLNF), were taken on each metatarsal bone (MT1–MT5) as previously described by Manjatika et al. [11] and as shown in Fig. 1. In addition, the foramina indices (FI) for each metatarsal bone were also calculated using the Hughes' formula: **FI= (NFPE/TL) X 100.** Foramina index (FI) is the percentage of the total length of the bone that is represented by the distance between the proximal end and the nutrient foramen [38].

2.3. Data management and statistical analysis

The data were managed in Microsoft Excel 365 (Microsoft Corporation) and analysed using IBM® SPSS® version 23 statistical software. Intra and inter-observer error statistics were calculated using the Lin's concordance coefficient of reproducibility [39]. The primary observer took five measurements on 200 metatarsal bones from 40 randomly selected individuals (20 males and 20 females) and repeated this two weeks later to check for intra-observer repeatability. No significant difference between the two separate measuring occasions was observed (RC = 1.000, 95%CI for RC = 1.000 lower and upper = 1.000). For inter-observer repeatability, the primary and secondary observers took the same measurements on 100 metatarsal bones from 20 randomly selected individuals (10 males, 10 females) one month apart. There was an almost perfect agreement between the two observers (RC = 0.998, 95%CI for RC = 0.997 lower and upper 0.998).

Descriptive statistics (mean and standard deviations) were calculated for each measurement on all metatarsal bones. The Kolmogorov-Smirnov tests were used to test the normality of the data. The data showed variable distribution, with only the total length (TL) measurements being normally distributed across all metatarsal bones. Hence, both discriminant function analysis (DFA) and logistic regression analysis (LRA) were utilised. The student t-test and the Mann Whitney *U* test were conducted to determine the significant mean differences between sex depending on the distribution of the data. The direct DFA was performed to develop univariable (individual measurement separately) and multivariable equations (combination of measurements for each bone and multiple bones). The stepwise DFA (Wilk's Lambda) was performed to select the combination of measurements that best estimate sex. The functions generated were then cross-validated using the "leave-one-out" classification protocol as previously described [3,40]. The stepwise and direct binary LRA were also performed to develop multivariable equations/functions. Collinearity diagnostics were conducted, and the presence of significant multicollinearity was confirmed when a Variance Inflation Factor (VIF) value greater than 10 and Tolerance test value less than 0.1 was observed. The variables affected by multicollinearity were then either removed or retained in the functions, depending on their impact on the classification accuracy percentage.

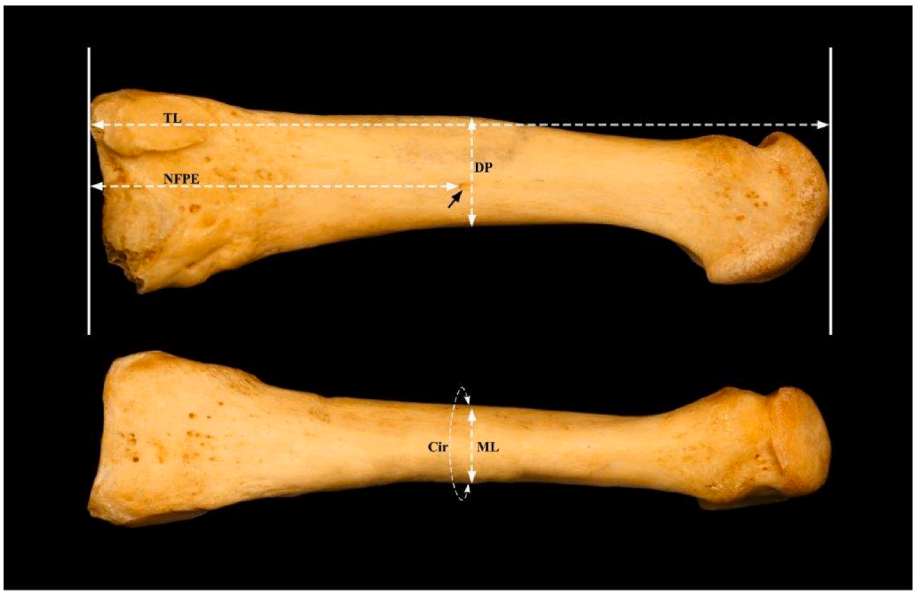


Fig. 1. Photographs of the second metatarsal bones showing the measurements that were taken. The black arrow points at the nutrient foramen. Cir = Circumference, DP = Dorsoplantar diameter, ML = Mediolateral diameter, NFPE = Distance from proximal end to the nutrient foramen, TL = Total length.

3. Results

All the measured parameters showed significant mean differences, with males having higher means than females across all the metatarsal bones ($p < 0.05$) (Table 1). The mean foraminal index (FI) of the fifth metatarsal bone was higher in males than in females ($p = 0.040$) (Table 2).

Table 3 shows the discriminant function equations generated using individual metatarsal bone measurements. The average classification accuracy rates ranged from 53.5 to 75.5 % for all the metatarsal bones. MT1MLNF and MT1CNF presented with the high classification rates of 75 %, and 75.5 % respectively (Table 3).

From the stepwise discriminant function analysis (DFA) of the combination of all the metatarsal bone measurements, the average classification accuracy rates ranged from 75.1 to 80 % in the original classification and from 75.1 to 78.5 % in the cross-validation (Table 4). The drop in the classification accuracy between the original and the cross-validation rates ranged from 0 to 2%. Females were classified with higher accuracy rates (77–84 %) than males (72.6–79 %) throughout using the original classification (Table 4). The MT2CNF exhibited multicollinearity in functions 1 and 2 (Table 4). Removal of MT2CNF from the affected predictor functions led to a drop in the classification

Table 1
Descriptive statistics of the measured parameters.

Bone	Variable	Male			Female			P-Value
		No	Mean	SD	No	Mean	SD	
Metatarsal 1	TL	100	64.67	4.06	100	60.72	3.41	<0.0001
	NFPE	100	34.52	7.00	100	32.07	6.24	0.01
	DPNF	100	13.80	1.84	100	12.58	1.58	<0.0001
	MLNF	100	14.68	1.35	100	13.19	1.37	<0.0001
	CNF	100	47.19	4.01	100	42.52	3.90	<0.0001
Metatarsal 2	TL	100	77.58	4.60	100	72.02	4.04	<0.0001
	NFPE	100	34.42	6.11	100	32.05	5.46	0.004
	DPNF	100	9.85	1.11	100	9.26	1.13	<0.0001
	MLNF	100	8.39	0.98	100	7.63	0.93	<0.0001
	CNF	100	31.07	2.80	100	28.38	2.86	<0.0001
Metatarsal 3	TL	98	72.94	4.46	100	67.83	4.07	<0.0001
	NFPE	98	31.51	5.07	100	29.78	4.25	0.01
	DPNF	98	9.84	1.16	100	9.08	0.95	<0.0001
	MLNF	98	8.08	1.25	100	7.15	1.07	<0.0001
	CNF	98	31.18	3.02	100	27.88	2.45	<0.0001
Metatarsal 4	TL	97	71.31	4.40	100	66.39	4.11	<0.0001
	NFPE	97	33.67	4.90	100	30.32	4.28	<0.0001
	DPNF	97	10.68	1.12	100	9.97	1.06	<0.0001
	MLNF	97	7.59	0.82	100	6.92	0.67	<0.0001
	CNF	97	31.94	3.01	100	29.34	2.45	<0.0001
Metatarsal 5	TL	100	71.58	4.34	100	66.54	4.35	<0.0001
	NFPE	100	37.29	4.00	100	33.77	4.34	<0.0001
	DPNF	100	8.16	1.05	100	7.41	0.76	<0.0001
	MLNF	100	11.36	1.20	100	10.78	1.00	<0.0001
	CNF	100	33.25	2.77	100	30.73	2.42	<0.0001

TL = Total length, NFPE = Distance from the proximal end of the bone to the level of nutrient foramina, DPNF = Dorsoplantar diameter at the level of nutrient foramina, MLNF = Mediolateral distance at the level of the nutrient foramina, CNF= Circumference at the level of the nutrient foramina. All means and SD reported in millimetres.

Table 2
Descriptive statistics of the foramina index (FI).

	Variable	Male			Female			P-Value
		No	Mean	SD	No	Mean	SD	
Metatarsal 1	FI	100	53.38	10.33	100	52.79	9.71	0.676
Metatarsal 2	FI	100	44.29	6.98	100	44.47	6.94	0.857
Metatarsal 3	FI	98	43.23	6.75	100	43.94	5.95	0.434
Metatarsal 4	FI	97	47.16	5.74	100	45.67	5.89	0.074
Metatarsal 5	FI	100	52.09	4.68	100	50.69	5.00	0.040[a]

[a] Represents significant mean differences.

Table 3
Direct discriminant coefficients, constants and classification accuracies for individual measurements of the metatarsals.

Variable	Unstandardised Coefficient	Constant	Sectioning point	Classification accuracy %					
				Original classification			Cross validation		
				M	F	Average	M	F	Average
MT1TL	0.267	−16.727	0.000	66	73	69.5	65	73	69
MT1NFPE	0.151	−5.024	0.000	58	49	53.5	58	49	53.5
MT1DPNF	0.583	−7.694	0.000	60	66	63	60	65	62.5
MT1MLNF	0.737	−10.275	0.000	73	77	75	73	77	75
MT1CNF	0.253	−11.335	0.000	78	73	75.5	78	73	75.5
MT2TL	0.231	−17.273	0.000	74	74	74	74	74	74
MT2NFPE	0.173	−5.734	0.000	56	56	56	56	56	56
MT2DPNF	0.895	−8.550	0.000	56	69	62.5	56	69	62.5
MT2MLNF	1.043	−8.356	0.000	59	71	65	57	71	64
MT2CNF	0.353	−10.503	0.000	71	70	70.5	71	70	70.5
MT3TL	0.235	−16.501	0.006	71.4	68	69.7	71.4	68	69.7
MT3NFPE	0.214	−6.552	0.002	55.1	59	57.1	55.1	59	57.1
MT3DPNF	0.946	−8.944	0.004	59.2	72	65.7	58.2	72	65.2
MT3MLNF	0.859	−6.541	0.004	56.1	75	65.7	56.1	75	65.7
MT3CNF	0.364	−10.758	0.006	69.4	75	72.2	69.4	75	72.2
MT4TL	0.235	−16.175	0.009	69.1	71	70.1	69.1	71	70.1
MT4NFPE	0.218	−6.957	0.006	56.7	64	60.4	56.7	64	60.4
MT4DPNF	0.917	−9.462	0.005	64.9	70	67.5	64.9	70	67.5
MT4MLNF	1.341	−9.717	0.007	57.7	73	65.5	57.7	73	65.5
MT4CNF	0.365	−11.178	0.007	66	70	68	66	70	68
MT5TL	0.230	−15.885	0.000	66	72	69	66	72	69
MT5NFPE	0.239	−8.503	0.000	66	60	63	66	60	63
MT5DPNF	1.094	−8.517	0.000	58	66	62	58	66	62
MT5MLNF	0.906	−10.031	0.000	53	63	58	53	63	58
MT5CNF	0.385	−12.304	0.000	74	61	67.5	74	61	67.5

Discriminant function score (DFS) equation = unstandardised coefficient × variable (in millimetres) + constant. DFS greater than the sectioning point indicates male, and DFS less than the sectioning point indicates female.
MT1 = First metatarsal bone, MT2 = Second metatarsal bone, MT3 = Third metatarsal bone, MT 4 = Fourth metatarsal bone, MT 5 = Fifth metatarsal bone TL = Total length, NFPE = Distance from the proximal end of the bone to the level of nutrient foramina, DPNF = Dorsoplantar diameter at the level of nutrient foramina, MLNF = Mediolateral distance at the level of the nutrient foramina, CNF= Circumference at the level of the nutrient foramina, F= Female, M = Male.

accuracy rates of 5 % in function 1 and 5.5 % in function 2. As such, MT2CNF was retained.

The functions generated from the direct DFA are presented in a descending order of average classification accuracies (79.5%–76 %) in Table 5. The drop in the classification accuracy between the original and the cross-validation rates ranged from 0 to 1.5 %. Females were classified with higher accuracy rates (76–84 %) than males (73–79 %) throughout using the original classification (Table 5). The MT1CNF exhibited multicollinearity in function 5 (Table 5). Removal of MT1CNF from the affected predictor function led to a drop of 3.1 % in classification accuracy rates. As such, MT1CNF was retained.

From the stepwise logistic regression analysis (LRA) of the combination of all the metatarsal measurements, the average classification accuracy rates ranged from 76.3 to 79.5 % in the original classification and from 75.8 to 79.8 % in the cross-validation (Table 6). The drop in the classification accuracy between the original and the cross-validation classifications ranged from 0.2 to 1.9 %. The classification accuracy between the original and the cross-validations increased for some functions ranging from 0.3 to 1%. Functions 3, 5 and 7 classified females with higher accuracy rates than males (Table 6). The MT2CNF exhibited multicollinearity in functions 1 and 2 (Table 6). Removal of MT2CNF from the affected predictor functions led to a drop in the classification accuracy rates of 3 % in function 1 and 6.5 % in function 2. As such, MT2CNF was retained.

Table 7 shows the functions generated from the direct LRA, presented in a descending order of average classification accuracies (80.5–75 %). The drop in the classification accuracy between the original and the cross-validation classifications ranged from 0 to 1.7 % while increases in classification accuracy ranged from 0.2 to 2.9 % (Table 7). Except Function 1, females were classified with higher accuracy rates (76–82 %) than males (72.6–81 %) throughout using the original classification. The MT2CNF exhibited multicollinearity in functions 1 and 3 (Table 7). Removal of MT2CNF from the affected predictor functions led to a drop in the classification accuracy rates of 3.5 % in function 1 and 6.5 % in function 3. Hence, MT2CNF was retained.

4. Discussion

South Africa has high crime statistics in the world, hence, it is crucial to develop sex estimation equations using various skeletal elements in order to positively identify victims [2,24]. Accurately determining the sex of unknown individuals is essential in both forensic and

Table 4
Stepwise discriminant function coefficients, constants, and classification rates for a combination of measurements for multiple metatarsals.

Function	Measurement combination	Unstandardised Coefficient	Centroids	Sectioning point	Classification accuracy %					
					Original classification			Cross validation		
					M	F	Average	M	F	Average
1	MT2TL	0.136	F = −0.849	0.000	76	84	80	75	81	78
	MT2DPNF	−0.900	M = 0.849							
	MT2MLNF	−0.498								
	MT2CNF	0.532								
	MT5MLNF	−0.471								
	MT5CNF	0.273								
	Constant	−16.922								
2	MT2TL	0.167	F = −0.785	0.000	79	79	79	79	78	78.5
	MT2DPNF	−0.923	M = 0.785							
	MT2MLNF	−0.428								
	MT2CNF	0.561								
	Constant	−16.901								
3	MT1CNF	0.094	F = −0.782	0.008	77.6	80	78.8	76.5	79	77.8
	MT3NFPE	0.092	M = 0.798							
	MT3DPNF	−0.363								
	MT3CNF	0.381								
	Constant	−14.861								
4	MT1CNF	0.101	F = −0.775	0.021	74.5	82	78.3	74.5	72	78.3
	MT2TL	0.101	M = 0.816							
	MT3DPNF	−0.350								
	MT3CNF	0.248								
	Constant	−16.091								
5	MT3NFPE	0.129	F = −0.723	0.008	75.5	79	77.3	75.5	79	77.3
	MT3CNF	0.375	M = 0.738							
	Constant	−15.016								
6	MT1CNF	0.147	F = −0.686	0.019	73.5	80	76.8	73.5	80	76.8
	MT3CNF	0.218	M = 0.723							
	Constant	−13.011								
7	MT1MLNF	0.471	F = −0.627	0.017	72.6	80	76.4	70.5	80	75.4
	MT3MLNF	0.304	M = 0.660							
	MT4MLNF	0.436								
	Constant	−12.028								
8	MT1CNF	0.157	F = −0.690	0.011	73.2	77	75.1	73.2	77	75.1
	MT4TL	0.137	M = 0.712							
	Constant	−16.454								

Discriminant function score (DFS) equation = unstandardised coefficient × variables (in millimetres) + constant. DFS greater than the sectioning point indicates male, and DFS less than the sectioning point indicates female.
MT1 = First metatarsal bone, MT2 = Second metatarsal bone, MT3 = Third metatarsal bone, MT 4 = Fourth metatarsal bone, MT 5 = Fifth metatarsal bone TL = Total length, NFPE = Distance from the proximal end of the bone to the level of nutrient foramina, DPNF = Dorsoplantar diameter at the level of nutrient foramina, MLNF = Mediolateral distance at the level of the nutrient foramina, CNF= Circumference at the level of the nutrient foramina, F= Female, M = Male.

archaeological settings as it helps in establishing the age, stature, and population affinity of the unknown individuals [3,25,26,41]. Dimensions around the nutrient foramen of the long bones have been utilised to generate sex estimation equations and have showed acceptably high sex classification accuracies [3,8,11,26,28,29] while no studies have reported on the usefulness of these dimensions on the metatarsal bones in South African Africans.

In the current study, the dimensions around the nutrient foramen (with the exception of the foramina index) showed sexual dimorphism with larger means in males as compared to females (Tables 1 and 2). Similar findings were observed previously in other upper limb long bones including the humerus, radius and ulna, and lower limb long bones like the femur and tibia in the South African Africans population [3,26]. Except the foramina index of the fifth metatarsal bones which exhibited sexual dimorphism, the rest of the foramina indices were found to be poor estimator of sex in the South African Africans population. The foramina index was also a poor estimator of sex in a similar study on the metacarpal and metatarsal bones [8,11].

Previous studies established that the sex estimation equation need to produce classification rates of 80 % and above to be recommended for use in forensic and archaeological settings [8,21,22,42]. Other studies also consider average classification rates between 75 % and 80 % to be useful especially if the drop between original and cross-validated classification rates is less than 5 %, and the bias (sex-specific classification accuracies) is also less than 5 % [26,43,44]. The results in the current study show that the MT1MLNF and MT1CNF are the only individual measurements around the nutrient foramen of the metatarsal bones that produced high sex estimation accuracies (75 % and 75.5 %, respectively) and a bias within a recommended range. Thus, the univariable MT1MLNF and MT1CNF can be recommended for forensic utility. The other individual measurements showed low to moderate sexual dimorphism with average classification accuracies ranging from 53.5 % to 74 %, and these classification accuracies are similar to those previously reported in a study that focused on the length of the metatarsal bones only in the South African Africans population [4].

Results from the stepwise discriminant function analysis (DFA) and logistic regression analysis (LRA) showed that the multivariate analyses of measurements around the nutrient foramen of the second metatarsal bone have the highest correct classification accuracy for sex estimation than from other individual metatarsal bones. This contrast previous findings observed in the Greek and South Africans of European descent populations whereby the dimensions from the first metatarsal bone yielded high sex estimation accuracies compared with the other metatarsal bones [11,34]. Notably, MT1CNF and MT2CNF exhibited multicollinearity in a few of the generated multivariable function equations in both the DFA and LRA. However, when MT1CNF and MT2CNF were removed from the multivariable function equations, the sex estimation classification accuracy rates dropped significantly (range 3–6.5 %). These findings further suggest that MT1CNF and MT2CNF are significant predictors of sex in the current studied population.

Table 5
Direct discriminant function coefficients, constants, and classification rates for a combination of measurements for multiple metatarsals.

Function	Measurement combination	Unstandardised Coefficient	Centroids	Sectioning point	Classification accuracy %					
					Original classification			Cross validation		
					M	F	Average	M	F	Average
1	MT1DPNF	−0.229	F = −0.664	0.000	76	83	79.5	75	83	79
	MT1CNF	0.262	M = 0.664							
	MT2CNF	0.144								
	Constant	−12.993								
2	MT1MLNF	0.515	F = −0.630	0.000	78	79	78.5	78	79	78.5
	MT2CNF	0.182	M = 0.630							
	Constant	−12.595								
3	MT1DPNF	−0.179	F = −0.746	0.000	73	84	78.5	73	82	77.5
	MT1CNF	0.195	M = 0.746							
	MT2TL	0.144								
	Constant	−17.162								
4	MT2TL	0.163	F = −0.764	0.000	75	80	77.5	75	79	77
	MT2DPNF	−0.751	M = 0.764							
	MT2CNF	0.396								
	Constant	−16.759								
5	MT1CNF	0.244	F = −0.709	0.007	73.5	81	77.3	72.4	79	75.8
	MT1DPNF	−0.220	M = 0.723							
	MT1MLNF	−0.081								
	MT3CNF	0.207								
	Constant	−12.991								
6	MT1MLNF	0.357	F = −0.715	0.000	76	77	76.5	76	76	76
	MT2TL	0.162	M = 0.715							
	Constant	−17.054								
7	MT1CNF	0.378	F = −0.617	0.000	76	76	76	74	75	74.5
	MT1DPNF	−0.319	M = 0.617							
	MT1MLNF	−0.094								
	Constant	−11.442								

Discriminant function score (DFS) equation = unstandardised coefficient × variables (in millimetres) + constant. DFS greater than the sectioning point indicates male, and DFS less than the sectioning point indicates female.
MT1 = First metatarsal bone, MT2 = Second metatarsal bone, MT3 = Third metatarsal bone, MT 4 = Fourth metatarsal bone, MT 5 = Fifth metatarsal bone TL = Total length, NFPE = Distance from the proximal end of the bone to the level of nutrient foramina, DPNF = Dorsoplantar diameter at the level of nutrient foramina, MLNF = Mediolateral distance at the level of the nutrient foramina, CNF= Circumference at the level of the nutrient foramina, F= Female, M = Male.

In the current study, the average correct classification accuracy of the combination of multiple metatarsal bone measurements obtained from the stepwise and direct DFA ranged from 75.1 to 80 % and 76–79.5 %, respectively. Similarly, the average correct classification accuracy of the combination of multiple metatarsal bone measurements obtained from the stepwise and direct LRA ranged from 76.3 to 79.5 % and 75–80.5 %, respectively. Thus, the current study supports prior studies that the stepwise DFA and LRA, and the direct DFA and LRA produce relatively similar classification accuracy rates though these statistical methods operate on different normality assumptions [4,13,45,46]. However, LRA equations are more applicable for not normally distributed data than the DFA equations/functions [47]. Except for the total length (TL) of the metatarsal bones, the data in the current study was not normally distributed and this suggests that the LRA equations/functions may be more appropriate than the DFA equations in the current population.

Previous studies utilising the dimensions around the base, midshaft, head and length of the metatarsal bones in different populations reported classification accuracies higher than those in the current study [4,34,48–50]. The classification accuracies in the current study are lower than those reported in the South African Africans utilising the talus and calcaneus which ranged from 80 to 89 % [21,22]. Additionally, studies in the South African Africans population using dimensions around the nutrient foramen of the humerus, radius, and ulna also produced high classification accuracies ranging from 83 to 86 % [3]. A study in the South African Africans population using the dimensions around the nutrient foramen of the tibia however produced classification accuracies ranging from 79 to 82 % [26], relatively similar to the current study. This suggests that the dimensions around the nutrient foramen of the metatarsal bones are weaker estimators of sex than other upper limb and foot bones in the South African Africans populations. Notably, the use of the dimensions around the nutrient foramen of the metacarpals and metatarsals in the South Africans of European descent produced higher sex classification accuracies which ranged from 82 to 94 % [8,11]. Higher sex classification accuracies in one population compared to others while utilising similar measurements around the nutrient foramen of the miniature long bones indicates population-specificity of the sex estimation equations [23].

Sexual dimorphism can be attributed to a combination of genetic and biomechanical factors that are influenced by lifestyle activities [51]. Males and females have distinct hormonal differences that may contribute to the differences in the robustness of bones. Estrogen, for example, is predominant in females and promotes bone resorption and remodelling, which may result in less robust bones. Testosterone, on the other hand, is predominant in males and promotes production of bone cells (osteoblasts) and maintenance of bone density, resulting in more robust bones [52]. Biomechanically, males are considered to have larger body sizes and engage in higher levels of physical activity compared to females [34,49]. This increased activity in males may result in greater stress and load exerted on the bones, leading to increased robustness. Large muscle mass coupled with repeated walking movements increases the stress on weight bearing bones, tendons and arches of the foot leading to continued bone remodelling and subsequent robustness [53,54]. The degree of sexual dimorphism varies between population groups due to intra-population variability [26,55]. The average sex classification accuracies in the current study are low compared to those in the South Africans of European descent utilising the dimensions around the nutrient foramen, suggesting that there is increased intra-population variability in the South African Africans population [11]. The degree of sexual dimorphism in a population is also affected by responses to environmental factors (e.g. physical activities) [55]. In population groups where males and females perform similar physical tasks, like

Table 6
Stepwise logistic regression coefficients, constants, and classification rates for a combination of measurements for multiple metatarsals.

Function	Measurement combination	Unstandardised Coefficient	Sectioning point	Classification accuracy %					
				Original classification			Cross validation		
				M	F	Average	M	F	Average
1	MT1CNF	0.215	0.50	81	78	79.5	81	78.5	79.8
	MT2TL	0.220							
	MT2DPNF	−1.621							
	MT2MLNF	−1.144							
	MT2CNF	0.987							
	Constant	−30.736							
2	MT2TL	0.265	0.50	79	79	79	82.1	72.2	77.3
	MT2DPNF	−1.559							
	MT2MLNF	−0.838							
	MT2CNF	0.970							
	Constant	−26.954							
3	MT2TL	0.250	0.50	77	79	78	79.8	72.2	76.1
	MT2DPNF	−1.063							
	MT2CNF	0.580							
	Constant	−25.686							
4	MT1CNF	0.216	0.50	78	77	77.5	81	75.9	78.5
	MT2TL	0.241							
	Constant	−27.642							
5	MT3NFPE	0.195	0.50	76.5	78	77.3	78	78.5	78.3
	MT3CNF	0.631							
	Constant	−24.556							
6	MT4NFPE	0.145	0.50	77.3	76	76.6	78	74.7	76.4
	MT4CNF	0.328							
	MT5TL	0.126							
	MT5MLNF	−0.947							
	MT5CNF	0.325							
	Constant	−23.255							
7	MT1TL	0.178	0.50	72	81	76.5	76.2	78.5	77.3
	MT1DPNF	−0.326							
	MT1CNF	0.348							
	Constant	−22.442							
8	MT2TL	0.229	0.50	76.5	76	76.3	76.8	74.7	75.8
	MT3CNF	0.362							
	Constant	−27.767							

Logistic Regression analysis (LRA) model equation = unstandardised coefficient × variables in (in millimetres) + constant. LRA greater than the sectioning point indicates male, and LRA less than the sectioning point indicates female.
MT1 = First metatarsal bone, MT2 = Second metatarsal bone, MT3 = Third metatarsal bone, MT 4 = Fourth metatarsal bone, MT 5 = Fifth metatarsal bone TL = Total length, NFPE = Distance from the proximal end of the bone to the level of nutrient foramina, DPNF = Dorsoplantar diameter at the level of nutrient foramina, MLNF = Mediolateral distance at the level of the nutrient foramina, CNF= Circumference at the level of the nutrient foramina, F= Female, M = Male.

agricultural and industrialised activities, sexually dimorphic traits may not be very distinct, and this may result in low (below 75 %) or moderate to high (75–80 %) sex classification accuracies [54–57]. Notably, females were more accurately classified than males in the current study with a bias between 0 % and 11 %. The moderate to high sex classification accuracies in the current study suggests that South African Africans females in the period studied were engaged in similar occupations to males like agriculture and long distance travelling, resulting in bone robustness relatively similar to that of males.

The current study shows that the combination of the breadth measurements (CNF, DPNF, MLNF) showed higher sex estimation accuracy rates than the combination of the length measurements (TL and NFPE) in most of the DFA and LRA equations. This finding is consistent with previous studies [8,11,27,28]. Breadth measurements are more susceptible to the influence of lifestyle activities and environmental factors compared to length measurements which appear more affected by genetic factors [49]. In the current study, a combination of the breadth and length measurements as shown in function 1, Table 4 and function 1, Table 7 produced high sex estimation accuracy rates. Hence, it is advisable to utilise both breadth and length measurements for South African Africans individuals to correctly estimate sex, since it factors in both the genetic and physical forces on bone morphology.

5. Study limitations

The main limitation of the equations generated in the current study is that some functions were affected by significant multicollinearity, thereby limiting their applicability to a general population. The data was also not normally distributed, and this may add bias to the current findings especially those derived from the DFA functions. It is therefore critical to generate population-specific sex estimating functions to comprehensively validate the utility of the dimensions around the metatarsal diaphyseal nutrient foramina.

6. Conclusion

The dimensions around the nutrient foramen of the metatarsal bones show sexual dimorphism in the South African Africans population. A combination of measurements around the nutrient foramen from different metatarsal bones produced sex classification rates of 75–80.5 % which are lower than those using other foot bones and upper limb bones in the same population. The current study suggests that the dimensions around the nutrient foramen of the metatarsal bones can be used with caution in the South African Africans, especially when the foot is the only recovered body part in forensic and archaeological settings.

Table 7
Direct logistic regression coefficients, constants, and classification rates for a combination of measurements for multiple metatarsals.

Function	Measurement combination	Unstandardised Coefficient	Sectioning point	Classification accuracy %					
				Original classification			Cross validation		
				M	F	Average	M	F	Average
1	MT1MLNF	0.484	0.50	81	80	80.5	82.1	78.5	80.4
	MT2TL	0.225							
	MT2DPNF	−1.480							
	MT2MLNF	−0.998							
	MT2CNF	0.929							
	Constant	−28.965							
2	MT1DPNF	−0.279	0.50	77	82	79.5	79.8	78.5	79.1
	MT1CNF	0.355							
	MT2CNF	0.204							
	Constant	−18.286							
3	MT2TL	0.265	0.50	79	79	79	82.1	72.2	77.3
	MT2DPNF	−1.559							
	MT2MLNF	−0.838							
	MT2CNF	0.970							
	Constant	−26.954							
4	MT1DPNF	−0.289	0.50	76	82	79	78.6	79.7	79.1
	MT1CNF	0.318							
	MT2TL	0.239							
	Constant	−28.300							
5	MT1DPNF	−0.275	0.50	76.5	79	77.8	79.3	79.7	79.5
	MT1CNF	0.309							
	MT3CNF	0.370							
	Constant	−21.078							
6	MT1MLNF	0.254	0.50	75	80	77.5	82.1	78.5	80.4
	MT1CNF	0.185							
	MT2CNF	0.215							
	Constant	−18.174							
7	MT1DPNF	−0.335	0.50	77	76	76.5	81	73.4	77.3
	MT1CNF	0.425							
	Constant	−14.629							
8	MT1MLNF	0.626	0.50	72.6	80	76.4	73.8	74.7	74.2
	MT3MLNF	0.413							
	MT4MLNF	0.596							
	Constant	−16.205							
9	MT5TL	0.201	0.50	74	76	75	78.6	73.4	76.1
	MT5MLNF	−0.925							
	MT5CNF	0.526							
	Constant	−20.458							

Logistic Regression analysis (LRA) model equation = unstandardised coefficient × variables in (in millimetres) + constant. LRA greater than the sectioning point indicates male and LRA less than the sectioning point indicates female.
MT1 = First metatarsal bone, MT2 = Second metatarsal bone, MT3 = Third metatarsal bone, MT 4 = Fourth metatarsal bone, MT 5 = Fifth metatarsal bone TL = Total length, NFPE = Distance from the proximal end of the bone to the level of nutrient foramina, DPNF = Dorsoplantar diameter at the level of nutrient foramina, MLNF = Mediolateral distance at the level of the nutrient foramina, CNF= Circumference at the level of the nutrient foramina, F= Female, M = Male.

Ethical approval

The current study was conducted under the ethical clearance waiver number W-CBP-220504-01 and was covered by the Human Tissue Act (No. 65 of 1983) and the National Health Act (No. 61 of 2003) on the use of human specimens for research and teaching purposes.

Ethics statement

The current study was conducted under the ethical clearance waiver number **W-CBP-22050401** obtained from the Faculty of Health Sciences at the University of the Witwatersrand.

Funding statement

This study was undertaken with funding from the Smieszek fellowship (2022, 2023) and the University of the Witwatersrand Faculty research grant (2023) awarded to A.T. Manjatika.

Manuscript submission checklist

1 All authors contributed to the article. We declare that this work is not being considered by any other journal and no use of generative AI was employed during the preparation of this manuscript.

CRediT authorship contribution statement

Arthur Tsalani Manjatika: Data curation, Formal analysis, Funding acquisition, Investigation, Methodology, Writing – original draft, Writing – review & editing. **Pedzisai Mazengenya:** Conceptualization, Data curation, Formal analysis, Investigation, Methodology, Project administration, Supervision, Validation, Writing – original draft, Writing – review & editing. **Joshua Gabriel Davimes:** Conceptualization, Data curation, Formal analysis, Investigation, Supervision, Validation, Writing – original draft, Writing – review & editing.

Declaration of competing interest

The authors declare the following financial interests/personal relationships which may be considered as potential competing interests: Arthur Tsalani Manjatika reports financial support was provided by

Smieszek fellowship. If there are other authors, they declare that they have no known competing financial interests or personal relationships that could have appeared to influence the work reported in this paper.

Acknowledgements

The authors would like to thank Dr N. Bacci, Dr B. Billings and Mr M. Mulaudzi for their assistance with access to the Raymond A. Dart Modern Skeletal Collection. The authors also sincerely thank those who donated their bodies to science so that anatomical research could be performed. Results from such research can potentially increase mankind's overall knowledge. Therefore, these donors and their families deserve our highest gratitude.

References

[1] T. Kanchan, K. Krishan, Anthropometry of hand in sex determination of dismembered remains- a review of literature, J. Forensic Leg. Med. 18 (2011) 14–17, https://doi.org/10.1016/j.jflm.2010.11.013.
[2] M. Steyn, M.Y. İşcan, Osteometric variation in the humerus: sexual dimorphism in South Africans, Forensic Sci. Int. 106 (1999) 77–85, https://doi.org/10.1016/S0379-0738(99)00141-3.
[3] P. Mokoena, B.K. Billings, M.A. Bidmos, P. Mazengenya, Sex estimation using dimensions around the nutrient foramen of the long bones of the arm and forearm in South Africans, Forensic Sci. Int. 278 (2017) e401–e404. e405, https://doi.org/10.1016/j.forsciint.2017.06.037.
[4] M. Bidmos, A. Adebesin, P. Mazengenya, O. Olateju, O. Adegboye, Estimation of sex from metatarsals using discriminant function and logistic regression analyses, Aust. J. Forensic Sci. 53 (2021) 543–556, https://doi.org/10.1080/00450618.2019.1711180.
[5] M. Steyn, Muti murders from South Africa: a case report, Forensic Sci. Int. 151 (2005) 279–287. https://doi:10.1016/j.forsciint.2004.05.022.
[6] M. Steyn, D. Brits, Dismemberment in South Africa: case studies, in: Dismemberments, Elsevier, 2019, pp. 69–83, https://doi.org/10.1016/B978-0-12-811912-9.00005-8.
[7] T.R. Peckmann, S. Scott, S. Meek, P. Mahakkanukrauh, Sex estimation from scapula in a contemporary Thai population: applications for forensic anthropology, Sci. Justice 57 (2017) 270–275, https://doi.org/10.1016/j.scijus.2017.02.005.
[8] S. Sallie, M.A. Bidmos, P. Mazengenya, Estimation of sex from the metacarpal dimensions at the nutrient foramen in white South Africans, Aust. J. Forensic Sci. 54 (2022) 533–545, https://doi.org/10.1080/00450618.2020.1805010.
[9] C. Kiskira, C. Eliopoulos, V. Vanna, S.K. Manolis, Biometric sex assessment from the femur and tibia in a modern Greek population, Leg. Med. 59 (2022) 102126, https://doi.org/10.1016/j.legalmed.2022.102126.
[10] L. Nogueira, F. Santos, F. Castier, S. Knecht, C. Bernardi, V. Alunni, Sex assessment using the radius bone in a French sample when applying various statistical models, Int. J. Leg. Med. 137 (2023) 925–934, https://doi.org/10.1007/s00414-023-02981-8.
[11] A.T. Manjatika, J.G. Davimes, P. Mazengenya, Estimation of sex using dimensions around the metatarsal diaphyseal nutrient foramen: application of discriminant function analysis and logistic regression models, Leg. Med. (2024) 102417, https://doi.org/10.1016/j.legalmed.2024.102417.
[12] T.L. Rogers, A visual method of determining the sex of skeletal remains using the distal humerus, J. Forensic Sci. 44 (1999) 57–60, https://doi.org/10.1520/JFS14411J.
[13] M. Pohar, M. Blas, S. Turk, Comparison of logistic regression and linear discriminant analysis: a simulation study, Metodoloski zvezki 1 (2004) 143.
[14] P.L. Walker, Sexing skulls using discriminant function analysis of visually assessed traits, Am. J. Phys. Anthropol. 136 (2008) 39–50. https://doi:10.1002/ajpa.20776.
[15] D. Charisi, C. Eliopoulos, V. Vanna, C.G. Koilias, S.K. Manolis, Sexual dimorphism of the arm bones in a modern Greek population, J. Forensic Sci. 56 (2011) 10–18. https://doi:10.1111/j.1556-4029.2010.01538.x.
[16] E. Nikita, Quantitative sex estimation based on cranial traits using R functions, J. Forensic Sci. 64 (2019) 175–180. https://doi:10.1111/1556-4029.13833.
[17] M.K. Spradley, R.L. Jantz, Sex estimation in forensic anthropology: skull versus postcranial elements, J. Forensic Sci. 56 (2011) 289–296. https://doi:10.1111/j.1556-4029.2010.01635.x.
[18] I. Anastopoulou, F.A. Karakostis, K. Moraitis, A reliable regression-based approach for reassociating human skeletal elements of the lower limbs from commingled assemblages, J. Forensic Sci. 64 (2019) 502–506, https://doi.org/10.1111/1556-4029.13884.
[19] I. Anastopoulou, F.A. Karakostis, C. Eliopoulos, K. Moraitis, Development of regression equations to reassociate upperlimb bones from commingled contexts, Forensic Sci. Int. 315 (2020) 110439, https://doi.org/10.1016/j.forsciint.2020.110439.
[20] M.Y. Isçan, M. Steyn, Craniometric determination of population affinity in SouthAfricans, Int. J. Leg. Med. 112 (1999) 91–97.
[21] M. Bidmos, M. Dayal, Further evidence to show population specificity of discriminant function equations for sex determination using the talus of South African Blacks, J. Forensic Sci. 49 (6) (2004) JFS2003431.
[22] M. Bidmos, S.A. Asala, Sexual dimorphism of the calcaneus of South African Blacks, J. Forensic Sci. 49 (3) (2004) JFS2003254, https://doi.org/10.1520/JFS2003254.
[23] L. Indra, W. Vach, J. Desideri, M. Besse, S.L. Pichler, Testing the validity of population-specific sex estimation equations: an evaluation based on talus and patella measurements, Sci. Justice 61 (5) (2021) 555–563, https://doi.org/10.1016/j.scijus.2021.06.011.
[24] E.N. L'Abbé, M. Steyn, The establishment and advancement of forensic anthropology in South Africa, in: A Companion to Forensic Anthropoplogy, A John Wiley & Sons Ltd, Publication, 2012, pp. 626–638, https://doi.org/10.1002/9781118255377.ch30.
[25] P. Maass, L.J. Friedling, Sex and ancestry variation in ulna morphology in an adult South African cadaveric sample, Transl. Res. Anat 36 (2024) 100306, https://doi.org/10.1016/j.tria.2024.100306.
[26] M.D. Fasemore, M.A. Bidmos, P. Mokoena, A. Imam, B.K. Billings, P. Mazengenya, Dimensions around the nutrient foramina of the tibia and fibula in the estimation of sex, Forensic Sci. Int. 287 (2018) 222. e221–e227, https://doi.org/10.1016/j.forsciint.2018.03.015.
[27] S. Garcia, Is the circumference at the nutrient foramen of the tibia of value to sex determination on human osteological collections? Testing a new method, Int. J. Osteoarchaeol. 22 (2012) 361–365. https://doi:10.1002/oa.1202.
[28] G.C. Krüger, E.N. L'Abbé, K.E. Stull, Sex estimation from the long bones of modern South Africans, Int. J. Leg. Med. 131 (2017) 275–285. https://doi:10.1007/s00414-016-1488-z.
[29] P. Mokoena, B.K. Billings, V. Gibbon, M.A. Bidmos, P. Mazengenya, Development of discriminant functions to estimate sex in upper limb bones for mixed ancestry South Africans, Sci. Justice 59 (2019) 660–666, https://doi.org/10.1016/j.scijus.2019.06.007.
[30] M.A. Bidmos, P. Mazengenya, Accuracies of discriminant function equations for sex estimation using long bones of upper extremities, Int. J. Leg. Med. 135 (2021) 1095–1102, https://doi.org/10.1007/s00414-020-02458-y.
[31] A.T. Manjatika, P. Mazengenya, J.G. Davimes, Topographical anatomy and clinical implications of the metatarsal diaphyseal nutrient foramina across South African populations, Surg. Radiol. Anat. 45 (2023) 1213–1226, https://doi.org/10.1007/s00276-023-03233-5.
[32] K. Anamika, B. Murlimanju, P. Divya, L.V. Prabhu, V. Saralaya, A.R. Rai, T. Joy, Morphology of nutrient foramina in human metatarsals and their clinical importance, Med. Health 10 (2015) 37–47.
[33] E. Gümüsburun, F. Yücel, Y. Ozkan, Z. Akgün, A study of the nutrient foramina of lower limb long bones, Surg. Radiol. Anat. 16 (1994) 409–412, https://doi.org/10.1007/bf01627662.
[34] C. Mountrakis, C. Eliopoulos, C.G. Koilias, S.K. Manolis, Sex determination using metatarsal osteometrics from the Athens collection, Forensic Sci. Int. 200 (2010) 178. e171–e178. https://doi:10.1016/j.forsciint.2010.03.041.
[35] M.R. Dayal, A.D. Kegley, G. Štrkalj, M.A. Bidmos, K.L. Kuykendall, The history and composition of the Raymond A. Dart collection of human skeletons at the university of the Witwatersrand, johannesburg, South Africa, Am. J. Phys. Anthropol. 140 (2009) 324–335. https://doi:10.1002/ajpa.21072.
[36] H. De Villiers, Sexual dimorphism of the skull of the South African Bantu-speaking Negro, South Afr. J. Sci. 64 (1968) 118–124.
[37] J.K. Lundy, Selected Aspects of Metrical and Morphological Infracranial Skeletal Variation in the South African Negro, University of the Witwatersrand, Johannesburg, 1985, p. 3140.
[38] H. Hughes, The factors determining the direction of the canal for the nutrient artery in the long bones of mammals and birds, Cells Tissues Organs 15 (1952) 261–280, https://doi.org/10.1159/000140748.
[39] I. Lawrence, K. Lin, A concordance correlation coefficient to evaluate reproducibility, Biometrics 45 (1989) 255–268, https://doi.org/10.2307/2532051.
[40] T. Ramayah, N.H. Ahmad, H.A. Halim, S.R.M.Z. May-Chiun, Discriminant analysis: an illustrated example, Afr. J. Bus. Manag. 4 (2010) 1654–1667, https://doi.org/10.5897/AJBM.9000211.
[41] O.M. Ujaddughe, J. Haberfeld, M.A. Bidmos, O.I. Olateju, Cranial measurements obtained by three-dimensional computed tomography technique in the estimation of sex of contemporary Black South Africans, Forensic Imaging 37 (2024) 200585, https://doi.org/10.1016/j.fri.2024.200585.
[42] W.M. Krogman, M.Y. Isçan, The Human Skeleton in Forensic Medicine, Charles C Thomas, Springfield, IL, 1986, pp. 202–208.
[43] F. Curate, I. Alves, T. Rodrigues, S.J. Garcia, Assigned sex estimation with the clavicle and scapular: a study in a Portuguese reference sample, Med. Sci. Law 64 (1) (2024) 15–22, https://doi.org/10.1177/00258024231174822.
[44] F. Curate, F. Mestre, S.J. Garcia, Sex assessment with the radius in Portuguese skeletal populations (late 19th-early to mid 20th centuries), Leg. Med. 48 (2021) 101790, https://doi.org/10.1016/j.legalmed.2020.101790.
[45] S.J. Press, S. Wilson, Choosing between logistic regression and discriminant analysis, J. Am. Stat. Assoc. 73 (1978) 699–705, https://doi.org/10.2307/2286261.
[46] G.A. Morgan, J.J. Vaske, J.A. Gliner, R.J. Harmon, Logistic regression and discriminant analysis: use and interpretation, J. Am. Acad. Child Adolesc. Psychiatry 42 (2003) 994–997. https://doi:10.1097/01.CHI.0000046896.27264.0F.
[47] B.P. Bartholdy, E. Sandoval, M.L. Hoogland, S.A. Schrader, Getting rid of dichotomous sex estimations: why logistic regression should be preferred over discriminant function analysis, J. Forensic Sci. 65 (2020) 1685–1691. https://doi:10.1111/1556-4029.14482.
[48] A.G. Robling, D.H. Ubelaker, Sex estimation from the metatarsals, J. Forensic Sci. 42 (1997) 1062–1069, https://doi.org/10.1520/JFS14261J.

[49] D.T. Case, A.H. Ross, Sex determination from hand and foot bone lengths, J. Forensic Sci. 52 (2007) 264–270. https://doi:10.1111/j.1556-4029.2006.00365.x.
[50] W.M.A. Moneim, R.H.A. Hady, R.M.A. Maaboud, H.M. Fathy, A.M. Hamed, Identification of sex depending on radiological examination of foot and patella, Am. J. Forensic Med. Pathol 29 (2008) 136–140. https://doi:10.1097/PAF.0b013e318173f048.
[51] M.Y. Işçan, M. Steyn, The Human Skeleton in Forensic Medicine, vol. 15, Charles C. Thomas, Springfield, IL, 1986, pp. 143–150.
[52] M. Tarnopolsky, R.N. Cortright, Hormonal differences between males and females, in: Gender Differences in Metabolism, CRC Press, 2020, pp. 15–35.
[53] C.B. Ruff, Morphological adaptation to climate in modern and fossil hominids, Am. J. Phys. Anthropol. 37 (1994) 65–107, https://doi.org/10.1002/ajpa.1330370605.
[54] C.B. Ruff, Mechanical determinant of bone form: insights from skeletal remains, J. Musculoskelet. Neuronal Interact. 5 (2005) 202–212.
[55] D.W. Frayer, M.H. Wolpoff, Sexual dimorphism, Annu. Rev. Anthropol. 14 (1985) 429–473, https://doi.org/10.1146/annurev.an.14.100185.002241.
[56] C. Ruff, Sexual dimorphism in human lower limb bone structure: relationship to subsistence strategy and sexual division of labor, J. Hum. Evol. 16 (1987) 391–416, https://doi.org/10.1016/0047-2484(87)90069-8.
[57] R.M. Malina, B.B. Little, Physical activity: the present in the context of the past, Am. J. Hum. Biol. 20 (2008) 373–391. https://doi:10.1002/ajhb.20772.



Taylor & Francis
Taylor & Francis Group

Australian Journal of Forensic Sciences

ISSN: (Print) (Online) Journal homepage: www.tandfonline.com/journals/tajf20

Application of discriminant function analysis and logistic regression models to estimate sex using the dimensions around the metatarsal diaphyseal nutrient foramen in the South Africans of Mixed ancestry

Arthur Tsalani Manjatika, Joshua Gabriel Davimes & Pedzisai Mazengenya

To cite this article: Arthur Tsalani Manjatika, Joshua Gabriel Davimes & Pedzisai Mazengenya (26 Aug 2024): Application of discriminant function analysis and logistic regression models to estimate sex using the dimensions around the metatarsal diaphyseal nutrient foramen in the South Africans of Mixed ancestry, Australian Journal of Forensic Sciences, DOI: 10.1080/00450618.2024.2394419

To link to this article: https://doi.org/10.1080/00450618.2024.2394419

© 2024 The Author(s). Published by Informa UK Limited, trading as Taylor & Francis Group.

Published online: 26 Aug 2024.

Submit your article to this journal

View related articles

View Crossmark data

Full Terms & Conditions of access and use can be found at
https://www.tandfonline.com/action/journalInformation?journalCode=tajf20

AUSTRALIAN JOURNAL OF FORENSIC SCIENCES
https://doi.org/10.1080/00450618.2024.2394419

Taylor & Francis
Taylor & Francis Group

OPEN ACCESS Check for updates

Application of discriminant function analysis and logistic regression models to estimate sex using the dimensions around the metatarsal diaphyseal nutrient foramen in the South Africans of Mixed ancestry

Arthur Tsalani Manjatika [a,b], Joshua Gabriel Davimes [a] and Pedzisai Mazengenya [c,d,e]

[a]School of Anatomical Sciences, University of the Witwatersrand, Johannesburg, South Africa; [b]School of Life Sciences and Allied Health Professions, Anatomy Division, Kamuzu University of Health Sciences, Blantyre, Malawi; [c]College of Medicine, Ajman University, Ajman, United Arab Emirates; [d]Center of Medical and Bio-Allied Health Sciences Research, Ajman University, Ajman, United Arab Emirates; [e]Faculty of Health Sciences, University of the Witwatersrand, Johannesburg, South Africa

ABSTRACT

The development of sex estimation standards, especially in locations with high murder case loads like South Africa, is important to aid in establishing the biological profile of victims. There is a lack of information on the utility of the measurements around the metatarsal diaphyseal nutrient foramina (NF) in sex estimation in South Africans of Mixed ancestry (SAMA). Five measurements around the NF were taken from a total of 248 metatarsals (first to fifth) from 28 males and 23 females of SAMA population. Measurements subjected to direct and stepwise discriminant function (DFA) and logistic regression (LRA) analyses included total length, distance from proximal end to NF, circumference, and mediolateral and dorsoplantar diameters at the level of the NF. The univariable functions produced 60.8–80% accuracy rates. The original classification accuracies for the stepwise and direct DFA multivariable functions ranged from 75.5–80% and 75–81.3%, respectively. The original classification accuracies for the stepwise and direct LRA multivariable functions ranged from 75.5%–80% and 75%–83.7%, respectively. The cross-validation classifications showed a drop of 0–4% for DFA and 0.7–5.4% for LRA. The multivariable DFA and LRA functions produced high average classification accuracies appropriate for use in forensic settings.

ARTICLE HISTORY
Received 8 May 2024
Accepted 5 August 2024

KEYWORDS
Metatarsal; diaphyseal nutrient foramina; discriminant function analysis; logistic regression analysis; sex estimation; South Africans of Mixed ancestry

1. Introduction

Sex estimation in forensic or archaeological settings involves the estimation of the biological sex of an unknown individual using skeletal or any other biological markers. Accurate sex estimation from the skeletal remains requires the presence of known sexually dimorphic cranial and postcranial elements, such as the skull and pelvis[1]. It is widely recognized that these bones/skeletal elements are rarely recovered in an intact

CONTACT Joshua Gabriel Davimes Joshua.Davimes@wits.ac.za

© 2024 The Author(s). Published by Informa UK Limited, trading as Taylor & Francis Group.
This is an Open Access article distributed under the terms of the Creative Commons Attribution-NonCommercial-NoDerivatives License (http://creativecommons.org/licenses/by-nc-nd/4.0/), which permits non-commercial re-use, distribution, and reproduction in any medium, provided the original work is properly cited, and is not altered, transformed, or built upon in any way. The terms on which this article has been published allow the posting of the Accepted Manuscript in a repository by the author(s) or with their consent.

and well-preserved state in forensic and archaeological settings. This makes the process of estimating the sex of an unknown individual challenging[2,3]. As a result, there is a need to identify other bones that are likely to be recovered in large quantities and are well-preserved to aid in sex estimation. Several studies have explored the use of other postcranial elements for possible use in sex estimation, in case the skull and the pelvis are not recovered or are damaged, including the upper limb long bones[4–8], lower limb long bones[9–11] and also irregular bones of the skeletons[12–14].

The metatarsal bones (first to fifth) are long bones of the feet. Due to their smaller sizes and large numbers, they are known to have a high recovery rate in forensic settings[15,16]. While the feet may be subject to scavenging or removal in certain circumstances, they are important elements for sex estimation in cases of commingling or recovery of an isolated foot. The dimensions around the metatarsal head, midshaft, base, and total length have been utilized in sex estimation in various populations[15–22]. Recently, the dimensions around the metatarsal diaphyseal nutrient foramina (NF) showed high sex estimation accuracy rates acceptable in forensic settings in the South Africans of European descent (SAED) commonly known as the White South Africans[23]. The NF are macroscopically distinct external openings to the nutrient canal on the diaphysis of the bone that convey blood (nutrient) vessels and nerves[24–26]. The dimensions around the diaphyseal NF are also known to be useful in estimating sex with high estimation accuracies in the upper and lower limb long bones[3,8,27–31].

The South Africans of Mixed ancestry (SAMA, also known as Coloured South Africans) are the second largest population group in South Africa (about 8.2%), and they are the largest population group in the Western Cape (about 42.1%) and Northern Cape (about 41.6%) provinces[32]. This population group is also disproportionately affected by high homicide and other crime rates[33]. The identification of murdered victims from recovered skeletal remains is challenging in South Africa due to limited resources and expertise[30]. Studies have been instituted to develop sex estimation standards applicable to the South Africans of Mixed ancestry populations by utilizing the skull and a variety of postcranial elements including the clavicle, scapula, humerus, radius, ulnar, sacrum, ilium, femur, tibia and fibular bones[28,30,34]. Information is however lacking on the utility of the dimensions of the metatarsal nutrient foramina for sex estimation in the South Africans of Mixed ancestry population. Developing sex estimation standards from a variety of bones is vital in situations where sexually dimorphic bones are missing in both archaeological and forensic settings. The aim of the current study was to determine the usefulness of the measurements around the metatarsal diaphyseal nutrient foramina in estimating sex using the discriminant function and logistic regression models in the South Africans of Mixed ancestry populations.

2. Materials and methods

2.1. Study population

The current study examined 255 left foot dry metatarsal bones (first to fifth) from 51 individuals (28 males, 23 females) aged 20–65 years (mean age 39.3 ± 12.5 years). These metatarsal bones were obtained from South Africans of Mixed ancestry (SAMA) from the 20th century housed in the Raymond A. Dart Modern Skeletal Collection in the School of Anatomical Sciences, University of the Witwatersrand, South Africa[35]. The SAMA are a self-

Table 1. Descriptive statistics of the measured parameters in the South Africans of Mixed ancestry population.

		Male			Female			
Bone	Variable	No	Mean (mm)	SD	No	Mean (mm)	SD	*P*-Value
Metatarsal 1	TL	27	62.04	4.69	23	57.72	4.43	0.002
	NFPE	27	31.41	6.88	23	31.26	6.39	0.934
	DPNF	27	13.85	1.82	23	11.94	1.07	<0.0001
	MLNF	27	14.04	1.56	23	12.52	1.47	0.001
	CNF	27	46.82	4.69	23	41.00	3.41	<0.0001
Metatarsal 2	TL	26	74.46	4.81	23	68.87	4.20	<0.0001
	NFPE	26	31.38	4.81	23	28.35	4.50	0.028
	DPNF	26	9.94	1.25	23	9.33	1.38	0.112
	MLNF	26	7.98	1.22	23	7.46	1.01	0.117
	CNF	26	30.23	3.69	23	28.44	3.72	0.097
Metatarsal 3	TL	26	70.27	4.69	23	64.77	4.05	<0.0001
	NFPE	26	30.54	3.75	23	27.61	5.12	0.026
	DPNF	26	9.74	1.39	23	9.10	0.87	0.063
	MLNF	26	7.38	0.91	23	6.64	0.57	0.002
	CNF	26	29.62	3.54	23	27.61	2.04	0.021
Metatarsal 4	TL	28	68.37	4.54	23	63.17	3.95	<0.0001
	NFPE	28	32.24	4.47	23	29.63	3.58	0.028
	DPNF	28	10.03	1.21	23	9.47	0.48	0.040
	MLNF	28	7.16	0.93	23	6.59	0.77	0.022
	CNF	28	29.89	3.13	23	27.78	1.86	0.006
Metatarsal 5	TL	26	68.09	5.14	23	63.88	5.56	0.008
	NFPE	26	35.37	3.89	23	32.12	4.41	0.009
	DPNF	26	7.58	0.88	23	7.07	0.69	0.030
	MLNF	26	10.93	1.55	23	10.10	0.95	0.030
	CNF	26	32.00	3.31	23	29.26	2.40	0.002

TL = Total length, NFPE = Distance from the proximal end of the bone to the level of nutrient foramina, DPNF = Dorsoplantar diameter at the level of nutrient foramina, MLNF = Mediolateral distance at the level of the nutrient foramina, CNF = Circumference at the level of the nutrient foramina.

identified group whose genetic heritage is contributed from South African Africans (or black South Africans), South Africans of European descent (or white South Africans) and South Africans of Asian origin[28]. The current study was conducted under the ethical clearance waiver number W-CBP-220504-01 and was covered by the Human Tissue Act (No. 65 of 1983) and the National Health Act (No. 61 of 2003) on the use of human specimens for research and teaching purposes. Macroscopically, the NF were identifiable in over 99.2% of the metatarsal diaphyses originally investigated, with indistinguishable NF occurring mainly on the third metatarsal bone. The main/primary nutrient foramen was identified using a 28-gauge hypodermic needle in cases where multiple foramina were present[24]. Metatarsal bones with fractures, gross pathological deformities, physical malformations, gross genetic diseases, taphonomic degeneration and surgical interventions were excluded from the study. The metatarsal bones without visible nutrient foramina were also excluded. Seven (7) metatarsal bones from different males were removed following the exclusion criteria, and 248 metatarsal bones from 51 individuals (28 males and 23 females) were utilized in the study, as shown in Table 1.

2.2. Osteometric measurements around the metatarsal diaphyseal nutrient foramen

A diaphyseal nutrient foramen was identified macroscopically as a raised margin that surrounds the opening of a groove leading into the foramen on each metatarsal bone.

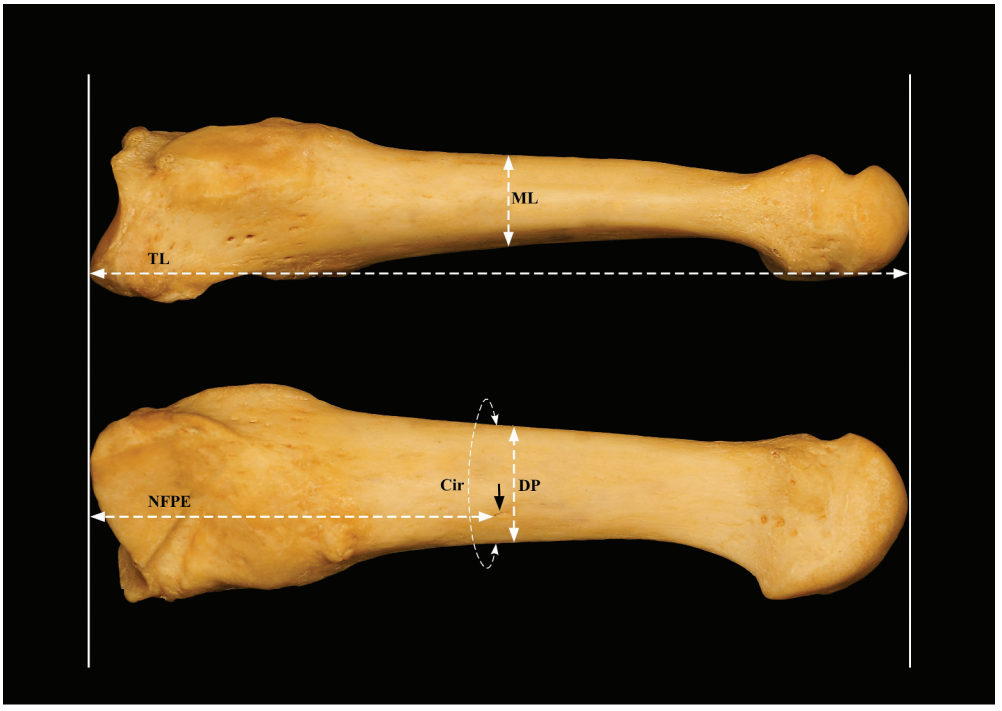


Figure 1. Photographs of the fourth metatarsal bones showing the measurements that were utilized in the study. The short black arrow indicates the nutrient foramen. Cir = Circumference, DP = Dorsoplantar diameter, ML = Mediolateral diameter, NFPE = Distance from proximal end to the nutrient foramen, TL = Total length.

Five metatarsal osteometric measurements as previously described[23] were taken on each metatarsal bone (MT1-MT5) as shown below and illustrated in Figure 1.

(1) Total length (TL) of the bone: This linear distance measurement was taken from the most proximal aspect to the most distal part of the metatarsal using a mini-osteometric board (Palaeo Tech Concepts, accuracy = 0.02 mm, resolution = 0.01 mm, repeatability = 0.01 mm).
(2) Proximal end to nutrient foramen (NFPE): This linear distance measurement was taken from the most proximal aspect of the metatarsal bone to the nutrient foramen using a digital sliding vernier calliper (Mastercraft^{TM} Africa, accuracy = 0.02 mm, resolution = 0.01 mm, repeatability = 0.01 mm).
(3) Circumference at the level of the nutrient foramen (CNF): This circular distance measurement was taken around the diaphysis at the level of the nutrient foramen using a standard cotton string (Archies Hardware RSA, diameter = 1 mm) and quantified on a Vernier calliper scale.
(4) Dorso-plantar diameter at the level of the nutrient foramen (DPNF): This linear distance measurement was taken from the dorsal surface to the plantar surface of the metatarsal bones at the level of the nutrient foramen using a digital sliding vernier calliper.

(5) Mediolateral diameter at the nutrient foramen (MLNF): This linear distance measurement was taken from the medial surface to the lateral surface of the metatarsal bones at the level of the nutrient foramen using a digital sliding vernier calliper.

The foramina indices (FI) for each metatarsal bone were also calculated using the Hughes' formula:

$$FI = (NFPE/TL) \times 100$$

Foramina index (FI) is the percentage of the total length of the bone that is represented by the distance between the proximal end and the nutrient foramen[36].

2.3. Data management and statistical analysis

The data were managed in Microsoft Excel 365 (Microsoft Corporation) and analysed using IBM® SPSS® version 23 statistical software (IBM Corp., Armonk, NY, USA). Intra and inter-observer error statistics were calculated using the Lin's concordance coefficient of reproducibility[37]. For intra-observer repeatability, the primary observer took five measurements on 50 metatarsal bones from 10 randomly selected individuals (5 males, 5 females) and repeated the exact measurements on the same metatarsal bones 2 weeks later to calculate the intra-observer error. No significant difference between the two separate measuring occasions was observed (RC = 1.000, 95%CI for RC = 1.000 lower and upper = 1.000). The primary and secondary observers took the same measurements on 50 metatarsal bones from 10 randomly selected individuals (5 males, 5 females) one month apart for inter-observer repeatability. An almost perfect agreement between the two observers was found (RC = 0.997, 95%CI for RC = 0.997 lower and upper 0.998).

Descriptive statistics (mean and standard deviations) were calculated for each measurement per metatarsal bone. The normality of the data was tested using the Kolmogorov-Smirnov tests. The distribution of the data was variable, with few measurements being normally distributed across all metatarsal bones. As such, both discriminant function analysis (DFA) and logistic regression analysis (LRA) were considered. The student t-test or non-parametric equivalent test was conducted to determine the differences between sex. The direct DFA was performed to develop univariable (each measurement separately) and multivariable equations (combination of measurements for each bone and multiple bones). The stepwise DFA (Wilk's Lambda) was performed to select the combination of measurements that best estimate sex. The functions generated were then cross-validated using the 'leave-one-out' classification protocol[3,38]. The direct and stepwise binary LRA were performed to develop multivariable equations/functions. Collinearity diagnostics were conducted for the multivariable functions. The presence of significant multicollinearity was confirmed when a variance inflation factor (VIF) value greater than 10 and the tolerance test value less than 0.1 was observed. The variables affected by multicollinearity were then either removed or retained in the functions, depending on their impact on the average classification accuracy percentage.

3. Results

The measured parameters showed significant mean differences, with males having higher means than females across most metatarsal bones ($p < 0.05$) (Table 1). MT1NFPE, MT2DPNF, MT2MLNF, MT2CNF and MT3DPNF did not show significant mean differences between sexes ($p > 0.05$). The foraminal index (FI) did not show any significant differences between males and females for all metatarsal bones ($p > 0.05$) (Table 2).

Table 3 shows the discriminant function equations generated using individual metatarsal bone measurements. The average classification accuracy rates ranged from 60.8 to 80%, while bias (or sex-specific classification difference) ranged from 1.5 to 24.7% for all metatarsal bones. MT1CNF presented with 80% and MT1DPNF presented with 76%

Table 2. Descriptive statistics of the foramina index (FI) in the South Africans of Mixed ancestry population.

		Male			Female			
	Variable	No	Mean (mm)	SD	No	Mean (mm)	SD	*P*-Value
Metatarsal 1	FI	27	50.56	10.02	23	53.95	9.14	0.220
Metatarsal 2	FI	26	42.23	6.46	23	41.36	7.29	0.659
Metatarsal 3	FI	26	43.61	5.88	23	42.48	6.52	0.529
Metatarsal 4	FI	28	47.18	5.97	23	46.89	4.69	0.853
Metatarsal 5	FI	26	51.98	4.62	23	50.26	5.21	0.226

Table 3. Direct discriminant function coefficients, constants and classification accuracies for individual measurements of the metatarsals.

				Classification accuracy %					
				Original classification			Cross validation		
Variable	Unstandardised Coefficient	Constant	Sectioning point	M	F	Average	M	F	Average
MT1TL	0.219	−13.126	−0.038	66.7	65.2	66	66.7	65.2	66
MT1DPNF	0.658	−8.527	−0.050	70.4	82.6	76	63	82.6	72
MT1MLNF	0.659	−8.788	−0.040	74.1	69.6	72	74.1	69.6	72
MT1CNF	0.241	−10.627	−0.056	74.1	87	80	74.1	87	80
MT2TL	0.220	−15.838	−0.038	61.5	69.6	65.3	61.5	69.6	65.3
MT2NFPE	0.214	−6.424	−0.020	73.1	52.2	63.3	73.1	52.2	63.3
MT3TL	0.227	−15.376	−0.039	65.4	73.9	69.4	65.4	73.9	69.4
MT3NFPE	0.225	−6.560	−0.020	76.9	56.5	67.3	76.9	52.2	65.3
MT3MLNF	1.298	−9.126	−0.030	65.4	73.9	69.4	65.4	73.9	69.4
MT3CNF	0.340	−9.760	−0.021	57.7	78.3	67.3	57.7	78.3	67.3
MT4TL	0.233	−15.400	−0.060	75	65.2	70.6	75	65.2	70.6
MT4NFPE	0.244	−7.586	−0.032	64.3	56.5	60.8	60.7	56.5	58.8
MT4DPNF	1.050	−10.261	−0.029	67.9	56.5	62.7	67.9	52.2	60.8
MT4MLNF	1.159	−8.005	−0.033	71.4	60.9	66.7	71.4	60.9	66.7
MT4CNF	0.379	−10.977	−0.039	60.7	73.9	66.7	60.7	73.9	66.7
MT5TL	0.187	−12.382	−0.024	76.9	56.5	67.3	73.1	56.5	65.3
MT5NFPE	0.241	−8.164	−0.024	69.2	56.5	63.3	69.2	56.5	63.3
MT5DPNF	1.261	−9.261	−0.020	73.1	56.5	65.3	73.1	56.5	65.3
MT5MLNF	0.767	−8.086	−0.020	73.1	56.5	65.3	69.2	56.5	63.3
MT5CNF	0.343	−10.523	−0.029	69.2	78.3	73.5	69.2	78.3	73.5

Discriminant function score (DFS) equation = unstandardized coefficient × variable (in millimetres) + constant. DFS greater than the sectioning point indicates male, and DFS less than the sectioning point indicates female.

MT1 = First metatarsal bone, MT2 = Second metatarsal bone, MT3 = Third metatarsal bone, MT 4 = Fourth metatarsal bone, MT 5 = Fifth metatarsal bone TL = Total length, NFPE = Distance from the proximal end of the bone to the level of nutrient foramina, DPNF = Dorsoplantar diameter at the level of nutrient foramina, MLNF = Mediolateral distance at the level of the nutrient foramina, CNF = Circumference at the level of the nutrient foramina, F = Female, M = Male.

average classification rates, and the other individual metatarsal bone measurements presented with average classification rates below 75%.

The stepwise discriminant function analysis (DFA) for the combination of all metatarsal bone measurements produced two functions as shown in Table 4, with the average classification accuracy rates of 80% and 75.5% in function 1 and function 2, respectively. All the classification accuracies were higher for females than males with a bias ranging from 5.2 to 12.9% using the original classification. The functions were not affected by multicollinearity (tolerance >0.1, VIF < 10).

The functions generated from the direct DFA are presented in a descending order of average classification accuracies (81.3–75%) in Table 5. A combination of MT1CNF and MT5NFPE produced the highest average classification rate of 81.3% (function 1, Table 5). Except for function 4, the drop in the average classification accuracy between the original and the cross-validation rates ranged from 0 to 4% (Table 5). Except for function 7 (Table 5), all the classification accuracies were consistently higher for females than males with a bias ranging from 2.1 to 12.9% using the original classification. The MT5CNF exhibited multicollinearity (tolerance <0.1, VIF > 10) in function 3 (Table 5). Subsequent removal of MT5CNF from the affected predictor function led to a drop in average classification accuracy rate of 8.2%, as such MT5CNF was retained.

From the stepwise logistic regression analysis (LRA) for the combination of all metatarsal bone measurements, the average classification accuracy rates ranged from 75.5 to 80% in the original classification and from 72.7 to 81.1% in the cross-validation (Table 6). The drop in the average classification accuracy between the original and the cross-validation classifications ranged from 2.8 to 3.4% while the increase in average classification accuracy was 1.1% (Table 6). All the classification accuracies were higher for females than males with a bias ranging from 5.2 to 13% using the original classification. The functions were not affected by multicollinearity (tolerance >0.1, VIF < 10).

Table 7 shows the functions generated from the direct LRA, presented in a descending order of average classification accuracies (83.7–75%). A combination of MT5DPNF, MT5MLNF, MT5CNF and MT5NFPE produced the highest average classification accuracy rate of 83.7% (function 1, Table 7). The drop in the average classification accuracy between the original and the cross-validation classifications ranged from 0.7 to 5.4% while increase in average classification accuracy ranged from 1.3 to 1.7% (Table 7). The

Table 4. Stepwise discriminant function coefficients, constants, and classification rates for a combination of measurements for multiple metatarsals.

					Classification accuracy %					
					Original classification			Cross validation		
Function	Measurement combination	Unstandardised Coefficient	Centroids	Sectioning point	M	F	Average	M	F	Average
1	MT1CNF	0.268	F = −0.664	0.000	74.1	87	80	74.1	87	80
	Constant	−11.649	*M* = 0.664							
2	MT5NFPE	0.157	F = −0.657	−0.038	73.1	78.3	75.5	73.1	78.3	75.5
	MT5CNF	0.265	*M* = 0.581							
	Constant	−13.474								

Discriminant function score (DFS) equation = unstandardized coefficient × variables (in millimetres) + constant. DFS greater than the sectioning point indicates male, and DFS less than the sectioning point indicates female.

MT1 = First metatarsal bone, MT 5 = Fifth metatarsal bone, NFPE = Distance from the proximal end of the bone to the level of nutrient foramina, CNF = Circumference at the level of the nutrient foramina, F = Female, M = Male.

Table 5. Direct discriminant function coefficients, constants, and classification rates for a combination of measurements for multiple metatarsals.

					Classification accuracy %					
					Original classification			Cross validation		
Function	Measure-ment combination	Unstand-ardised Coefficient	Centroids	Sectioning point	M	F	Average	M	F	Average
1	MT1CNF	0.209	F = −0.769	−0.031	76	87	81.3	76	87	81.3
	MT5NFPE	0.087	*M* = 0.707							
	Constant	−12.131								
2	MT1MLNF	0.302	F = −0.751	−0.056	74.1	87	80	66.7	87	76
	MT1DPNF	0.488	*M* = 0.640							
	Constant	−10.353								
3	MT5DPNF	−1.686	F = −0.805	−0.047	76.9	82.6	79.6	76.9	82.6	79.6
	MT5MLNF	−1.099	*M* = 0.712							
	MT5CNF	0.997								
	MT5NFPE	0.172								
	Constant	−12.473								
4	MT1DPNF	0.395	F = 0.771	−0.057	74.1	82.6	78	70.4	73.9	72
	MT4TL	0.095	*M* = 0.657							
	MT4NFPE	0.036								
	MT4CNF	0.041								
	Constant	−13.683								
5	MT1DPNF	0.405	F = −0.735	−0.030	72	82.6	77.1	68	82.6	75
	MT2TL	0.131	*M* = 0.676							
	Constant	−14.589								
6	MT1DPNF	0.444	F=−0.749	−0.056	70.4	82.6	76	63	82.6	72
	MT4NFPE	0.090	*M* = 0.638							
	MT4CNF	0.141								
	Constant	−12.640								
7	MT3NFPE	0.069	F = −0.629	−0.026	76	73.9	75	76	69.6	72.9
	MT5NFPE	0.057	*M* = 0.578							
	MT4TL	0.166								
	Constant	−14.828								

Discriminant function score (DFS) equation = unstandardized coefficient × variables (in millimetres) + constant. DFS greater than the sectioning point indicates male, and DFS less than the sectioning point indicates female.

MT1 = First metatarsal bone, MT2 = Second metatarsal bone, MT3 = Third metatarsal bone, MT 4 = Fourth metatarsal bone, MT 5 = Fifth metatarsal bone TL = Total length, NFPE = Distance from the proximal end of the bone to the level of nutrient foramina, DPNF = Dorsoplantar diameter at the level of nutrient foramina, MLNF = Mediolateral distance at the level of the nutrient foramina, CNF = Circumference at the level of the nutrient foramina, F = Female, M = Male.

classification accuracies were higher for females than males in most functions with a bias ranging from 0.5 to 10.4% using the original classification. The MT5CNF exhibited multi-collinearity (tolerance <0.1, VIF > 10) in functions 1 and 3 (Table 7). Subsequent removal of MT5CNF from the affected predictor functions led to a drop in average classification accuracy rates ranging from 12.3 to 14.3%, as such MT5CNF was retained.

4. Discussion

The development of sex estimation standards is important as accurate sex estimation enables the establishment of other biological profile markers such as age, stature and population affinity in forensic and archaeological settings. Recently, the dimensions around the metatarsal diaphyseal nutrient foramen have been shown to be useful in estimating sex in other South African populations[23]. This further necessitates a need to determine the utility of these measurements in other populations, especially those which are disproportionately affected by high murder rates, like the South Africans of Mixed

Table 6. Stepwise logistic regression coefficients, constants, and classification rates for a combination of measurements for multiple metatarsals.

				Classification accuracy %					
				Original classification			Cross validation		
Function	Measurement combination	Unstandardised Coefficient	Sectioning point	M	F	Average	M	F	Average
1	MT1CNF	0.368	0.50	74.1	87	80	88	73.7	81.1
	Constant	−15.838							
2	MT1DPNF	0.945	0.50	69.6	82.6	76.1	76	68.4	72.7
	Constant	−11.952							
3	MT5NFPE	0.206	0.50	73.1	78.3	75.5	72	73.7	72.7
	MT5CNF	0.374							
	Constant	−18.224							

Logistic Regression analysis (LRA) model equation = unstandardized coefficient × variables in (in millimetres) + constant. LRA greater than the sectioning point indicates male, and LRA less than the sectioning point indicates female.

MT1 = First metatarsal bone, MT 5 = Fifth metatarsal bone NFPE = Distance from the proximal end of the bone to the level of nutrient foramina, DPNF = Dorsoplantar diameter at the level of nutrient foramina, CNF = Circumference at the level of the nutrient foramina, F = Female, M = Male.

ancestry, where such reports are lacking. Moreover, sexual dimorphism is usually population specific and sex estimation equations in one population group may not be accurate when applied to a different population group[31]. Recently, Manjatika et al.[23] generated sex estimation equations using the dimensions around the metatarsal diaphyseal nutrient foramina, but some variables in their equations were affected by multicollinearity, making them less applicable to other populations. It is therefore imperative to develop sex estimation standards from individual population groups for successful individualization in both forensic and archaeological settings. The current study aimed to assess the utility of the dimensions around the metatarsal diaphyseal nutrient foramina in sex estimation and to develop functions for estimating sex in South Africans of Mixed ancestry.

In the current study, most of the dimensions (Table 1) around the NF exhibited sexual dimorphism with males having larger means compared to females, similar to previous studies on the dimensions around the NF in the upper and lower limb in different South African populations[3,28–30]. However, the MT1NFPE, MT2DPNF, MT2MLNF, MT2CNF and MT3DPNF did not show significant mean differences between sexes in the current study and this contradicts previous reports in the South Africans of European descent where all measured parameters around the NF showed significant sexual dimorphism[23]. The FI which is a calculated value from dimensions around the nutrient foramen showed no significant difference between the males and females across all the metatarsal bones in the current study, similar to previous studies[8,23].

It is widely known that average classification rates of 80% and above, with a drop of less than 5% between the original and cross-validated classifications, are considered good classification accuracies and are appropriate for sex estimation in forensic and archaeological settings[29,39]. Other authors also recommend that average classification accuracy rates within 75–80% may be used with caution to substantiate other sexually dimorphic bones[16]. In the current study, the MT1CNF presented with an average classification rate of 80%, making it a univariable function that can be of forensic utility in estimating sex. However, in the previous study on the South Africans of European descent population, the MT2TL was the univariable function with the highest average classification accuracy of 79.1%[23]. This difference may be attributable to population variation and specificity. Most

Table 7. Direct logistic regression coefficients, constants, and classification rates for a combination of measurements for multiple metatarsals.

				Classification accuracy %					
				Original classification			Cross validation		
Function	Measurement combination	Unstandardized Coefficient	Sectioning point	M	F	Average	M	F	Average
1	MT5DPNF	−2.147	0.50	84.6	82.6	83.7	84	78.9	81.8
	MT5MLNF	−1.640							
	MT5CNF	1.442							
	MT5NFPE	0.224							
	Constant	−18.488							
2	MT1CNF	0.334	0.50	80	87	83.3	79.2	84.2	81.4
	MT5NFPE	0.153							
	Constant	−19.554							
3	MT5DPNF	−1.572	0.50	80.8	78.3	79.6	80	68.4	75
	MT5MLNF	−1.824							
	MT5CNF	1.412							
	Constant	−12.351							
4	MT1DPNF	0.651	0.50	76	82.6	79.2	73.9	73.7	73.8
	MT2TL	0.196							
	Constant	−22.170							
5	MT1DPNF	0.746	0.50	77.8	78.3	78	80	73.7	77.3
	MT4NFPE	0.125							
	MT4CNF	0.217							
	Constant	−19.409							
6	MT1MLNF	0.408	0.50	77.8	78.3	78	80	68.4	75
	MT1DPNF	0.815							
	Constant	−15.615							
7	MT1DPNF	0.673	0.50	74.1	78.3	76	80	73.7	77.3
	MT4TL	0.127							
	MT4NFPE	0.062							
	MT4CNF	0.088							
	Constant	−21.184							
8	MT1MLNF	0.345	0.50	80	69.6	75	83.3	68.4	76.7
	MT5TL	0.013							
	MT5CNF	0.282							
	Constant	−13.955							
9	MT3NFPE	0.077	0.50	76	73.9	75	79.2	63.2	72.1
	MT5NFPE	0.067							
	MT4TL	0.205							
	Constant	−17.865							

Logistic Regression analysis (LRA) model equation = unstandardized coefficient × variables in (in millimetres) + constant. LRA greater than the sectioning point indicates male and LRA less than the sectioning point indicates female.

MT1 = First metatarsal bone, MT2 = Second metatarsal bone, MT3 = Third metatarsal bone, MT 4 = Fourth metatarsal bone, MT 5 = Fifth metatarsal bone TL= Total length, NFPE = Distance from the proximal end of the bone to the level of nutrient foramina, DPNF = Dorsoplantar diameter at the level of nutrient foramina, MLNF = Mediolateral distance at the level of the nutrient foramina, CNF = Circumference at the level of the nutrient foramina, F = Female, M = Male.

of the univariable functions in the current study presented with average classification accuracy rates below 75%, similar to previous reports on various bones in the South Africans of Mixed ancestry population[28,40]. Noteworthy, the univariable bias (sex-specific differences) was high, implying that these functions should be used cautiously in generating sex estimation equations[41].

Results from the stepwise DFA and LRA in the current study produced average classification accuracies lower than those reported in the South Africans of European descent population utilizing similar dimensions around the metatarsal NF[23]. The first metatarsal bone produced the highest average classification accuracies, similar to previous reports in the Greek and South Africans of European

descent populations[15,23]. Notably, the MT1CNF has the highest average classification accuracy rates in both stepwise DFA and LRA functions. This contradicts previous reports that multivariable functions are always better predictors than univariable functions[28].

The direct DFA and LRA functions in the current study produced high average classification accuracy rates that can be appropriate for use in forensic and archaeological settings, similar to the previous study utilizing dimensions around the NF of the upper limb bones[30]. The current average classification rates are also comparable to those previously reported in the South Africans of Mixed ancestry using different cranial and postcranial bones[28,40,42,43]. The drop in classification accuracy between the original and cross-validation also falls within the appropriate range and this indicates good validity of the generated functions[29]. Most of the multivariable functions in the current study classified females with higher accuracy than males with a bias between 0.5% and 12.9%. This was in contrast to the South Africans of European descent populations where males were classified with higher accuracy rates than females[23]. Differences in bias within and between population groups may be due to genetic, biomechanical and hormone-related factors[41].

In the current study, the MT5CNF exhibited multicollinearity in some of the direct DFA and LRA functions. However, subsequent removal of the MT5CNF from the affected functions led to a significant drop (8.2–14.3%) in the sex estimation classification accuracy rates. Similar trends were also reported in the South Africans of European descent populations when MT1CNF was removed from the affected functions[23]. Given that circumference measurements (e.g. CNF) are considered better estimators of sex in most of the intact or fragmentary bones[27,44,45], the MT5CNF was retained in the generated functions.

Other authors have demonstrated that DFA and LRA yield comparable results, although the two statistical approaches use different assumptions[16,23,46]. The DFA is ideally used when the data is normally distributed, while the LRA is used when the data is not normally distributed[47]. In the current study, some variables were normally distributed while other variables were not normally distributed, necessitating the need to utilize both DFA and LRA in generating the sex estimation equations. The direct LRA average classification accuracy rates performed better than the direct DFA functions. However, the stepwise DFA and LRA functions produced similar results, possibly because the DFA focuses on the linear combination of variables that best classify sexes even when the assumption of normality is violated[47]. The data in the current study was non-parametric overall, making the use of LRA equations more appropriate than the DFA equations for the South Africans of Mixed ancestry population.

The current study poses some limitations that may limit the generalizability and utility of the derived equations to a larger population. Firstly, the sample size was limited, and the data distribution was not normally distributed, which may add bias to the findings. Significant multicollinearity was also present, limiting the utility of some of the generated functions. Thus, the generated functions may be appropriate for use in South Africans of Mixed ancestry populations, however, further population-specific studies are required to comprehensively validate the use of metatarsal diaphyseal nutrient foramina.

In conclusion, the current study has shown that the dimensions related to the metatarsal NF exhibit sexual dimorphism in South Africans of Mixed ancestry. Both univariable and multivariable DFA and LRA functions produced sex classification accuracy rates that can be recommended for use in South Africans of Mixed ancestry. This is especially the case for when the foot is the only body part recovered, to further substantiate other recovered dimorphic bones, or when comingling is present in both forensic or archaeological settings.

Highlights

- Sex estimation using measurements around metatarsal nutrient foramen (NF).
- Univariable DFA classification accuracy ranged from 60.8 to 80%.
- Classificationaccuracies for multivariable DFA ranged from 75 to 81.3%.
- Classification accuracies for multivariable LRA ranged from 75 to 83.7%.
- The measurements around metatarsal NF are appropriate for sex estimation in SAMA.

Acknowledgments

The authors would like to thank Dr N. Bacci, Dr B. Billings and Mr M. Mulaudzi for their assistance with access to the Raymond A. Dart Modern Skeletal Collection. The authors also sincerely thank those who donated their bodies to science so that anatomical research could be performed. Results from such research can potentially increase mankind's overall knowledge. Therefore, these donors and their families deserve our highest gratitude.

Disclosure statement

No potential conflict of interest was reported by the author(s).

Funding

This study was undertaken with funding from the Smieszek fellowship (2022, 2023) and the University of the Witwaters and Faculty Research grant (2023) awarded to ATM.

Author contributions

ATM: Project development, data collection, data analysis, manuscript writing. JGD: Project development, manuscript writing. PM: Project development, manuscript writing. All authors have read and approved the final manuscript.

ORCID

Arthur Tsalani Manjatika http://orcid.org/0000-0003-0867-7123
Joshua Gabriel Davimes http://orcid.org/0000-0001-9808-5249
Pedzisai Mazengenya http://orcid.org/0000-0003-4733-1563

Data availability statement

The data that support the findings of this study are available from the corresponding author upon reasonable request.

References

1. Steyn M, Patriquin M. Osteometric sex determination from the pelvis-does population specificity matter? Forensic Sci Int. 2009;191(1–3):e1131–e1135. doi:10.1016/j.forsciint.2009.07.009.
2. Steyn M. Muti murders form South Africa: a case report. Forensic Sci Int. 2005;151(2–3):279–287. doi:10.1016/j.forsciint.2004.05.022.
3. Mokoena P, Billings BK, Bidmos MA, Mazengenya P. Sex estimation using dimensions around the nutrient foramen of the long bones of the arm and forearm in South Africans. Forensic Sci Int. 2017;278:e4041–e4045. doi:10.1016/j.forsciint.2017.06.037.
4. Dabbs GR, Moore-Jansen PH. A method for estimating sex using metric analysis of the scapula. J Forensic Sci. 2010;55(1):149–152. doi:10.1111/j.1556-4029.2009.01232.x.
5. Bozdag M, Er A, Kranioti E, Basa CD, Oztop B, Kacmaz E, Moghaddam N, Ekizoglu O, Grabherr S. Sex estimation in a modern Turkish population using the clavicle: a computed tomography study. Aust J Forensic Sci. 2022;54(2):187–198. doi:10.1080/00450618.2020.1781255.
6. Curate F, Alves I, Rodrigues T, Garcia SJ. Assigned sex estimation with the clavicle and scapula: a study in a Portuguese reference sample. Med Sci Law. 2023;64(1):15–22. doi:10.1177/00258024231174822.
7. Nogueira L, Santos F, Castier F, Knecht S, Bernardi C, Alunni V. Sex assessment using the radius bone in a French sample when applying various statistical models. Int J Legal Med. 2023;137(3):925–934. doi:10.1007/s00414-023-02981-8.
8. Sallie S, Bidmos MA, Mazengenya P. Estimation of sex from the metacarpal dimensions at the nutrient foramen in white South Africans. Aust J Forensic Sci. 2022;54(4):533–545. doi:10.1080/00450618.2020.1805010.
9. Kiskira C, Eliopoulos C, Vanna V, Manolis SK. Biometric sex assessment from the femur and tibia in a modern Greek population. Legal Med. 2022;59:102126. doi:10.1016/j.legalmed.2022.102126.
10. Steyn M, İşcan MY. Sex determination from the femur and tibia in South African whites. Forensic Sci Int. 1997;90(1–2):111–119. doi:10.1016/S0379-0738(97)00156-4.
11. King CA, İşcan MY, Loth SR. Metric and comparative analysis of sexual dimorphism in the Thai femur. J Forensic Sci. 1998;43(5):954–958. doi:10.1520/JFS14340J.
12. Bidmos MA, Asala SA. Discriminant function sexing of the calcaneus of the South African whites. J Forensic Sci. 2003;48(6):JFS2003104. doi:10.1520/JFS2003104.
13. Bidmos MA, Dayal MR. Sex determination from the talus of South African whites by discriminant function analysis. Am J Forensic Med Pathol. 2003;24(4):322–328. doi:10.1097/01.paf.0000098507.78553.4a.
14. Gualdi-Russo E. Sex determination from the talus and calcaneus measurements. Forensic Sci Int. 2007;171(2–3):151–156. doi:10.1016/j.forsciint.2006.10.014.
15. Mountrakis C, Eliopoulos C, Koilias CG, Manolis SK. Sex determination using metatarsal osteometrics from the athens collection. Forensic Sci Int. 2010;200(1–3):e1781–e1787. doi:10.1016/j.forsciint.2010.03.041.
16. Bidmos M, Adebesin A, Mazengenya P, Olateju O, Adegboye O. Estimation of sex from metatarsals using discriminant function and logistic regression analyses. Aust J Forensic Sci. 2021;53(5):543–556. doi:10.1080/00450618.2019.1711180.
17. Robling AG, Ubelaker DH. Sex estimation from the metatarsals. J Forensic Sci. 1997;42(6):1062–1069. doi:10.1520/JFS14261J.

18. Case DT, Ross AH. Sex determination from hand and foot bone lengths. J Forensic Sci. 2007;52 (2):264–270. doi:10.1111/j.1556-4029.2006.00365.x.
19. Moneim WMA, Hady RHA, Maaboud RMA, Fathy HM, Hamed AM. Identification of sex depending on radiological examination of foot and patella. Am J Forensic Med Pathol. 2008;29(2):136–140. doi:10.1097/PAF.0b013e318173f048.
20. Rodríguez S, González A, Simón A, Rodríguez-Calvo MS, Febrero-Bande M, Cordeiro C, Muñoz-Barús JI. The use of computerized tomography in determining stature and sex from metatarsal bones. Legal Med. 2014;16(5):252–257. doi:10.1016/j.legalmed.2014.05.006.
21. Gibelli D, Poppa P, Cummaudo M, Mattia M, Cappella A, Mazzarelli D, Zago M, Sforza C, Cattaneo C. Sex assessment from the volume of the first metatarsal bone: a comparison of linear and volume measurements. J Forensic Sci. 2017;62(6):1582–1585. doi:10.1111/1556-4029.13464.
22. Wilbur AK. The utility of hand and foot bones for the determination of sex and the estimation of stature in a prehistoric population from west-central Illinois. Int J Osteoarchaeol. 1998;8 (3):180–191. doi:10.1002/(SICI)1099-1212(199805/06)8:3<180::AID-OA421>3.0.CO;2-D.
23. Manjatika AT, Davimes JG, Mazengenya P. Estimation of sex using dimensions around the metatarsal diaphyseal nutrient foramen: application of discriminant function analysis and logistic regression models. Legal Med. 2024;68:102417. doi:10.1016/j.legalmed.2024.102417.
24. Manjatika A, Mazengenya P, Davimes J. Topographical anatomy and clinical implications of the metatarsal diaphyseal nutrient foramina across South African populations. Surg Radiol Anat. 2023;45(10):1213–1226. doi:10.1007/s00276-023-03233-5.
25. Anamika K, Murlimanju B, Divya P, Prabhu LV, Saralaya V, Rai AR, Joy T. Morphology of nutrient foramina in human metatarsals and their clinical importance. Med Health. 2015;10 (1):37–47.
26. Gümüsburun E, Yücel F, Ozkan Y, Akgün Z. A study of the nutrient foramina of lower limb long bones. Surg Radiol Anat. 1994;16(4):409–412. doi:10.1007/bf01627662.
27. Garcia S. Is the circumference at the nutrient foramen of the tibia of value to sex determination on human osteological collections? Testing a new method. Int J Osteoarchaeol. 2012;22 (3):361–365. doi:10.1002/oa.1202.
28. Krüger GC, L'Abbé EN, Stull KE. Sex estimation from the long bones of modern South Africans. Int J Legal Med. 2017;131(1):275–285. doi:10.1007/s00414-016-1488-z.
29. Fasemore MD, Bidmos MA, Mokoena P, Imam A, Billings BK, Mazengenya P. Dimensions around the nutrient foramina of the tibia and fibula in the estimation of sex. Forensic Sci Int. 2018;287:e2221–e2227. doi:10.1016/j.forsciint.2018.03.015.
30. Mokoena P, Billings BK, Gibbon V, Bidmos MA, Mazengenya P. Development of discriminant functions to estimate sex in upper limb bones for mixed ancestry South Africans. Sci Justice. 2019;59(6):660–666. doi:10.1016/j.scijus.2019.06.007.
31. Bidmos MA, Mazengenya P. Accuracies of discriminant function equations for sex estimation using long bones of upper extremities. Int J Legal Med. 2021;135(3):1095–1102. doi:10.1007/s00414-020-02458-y.
32. South-Africa Census. 2022. Census 2022 statistical release. https://census.statssa.gov.za/assets/documents/2022/P03014Census2022StatisticalRelease.pdf.
33. Silber G, Geffen N. Race, class and violent crime in South Africa: dispelling the'huntley thesis'. SA Crime Q. 2009;2009(30):35–43.
34. L'Abbé EN, Steyn M. The establishment and advancement of forensic anthropology in South Africa. In: Dirkmaat DC, editor. A companion to forensic anthropology. Oxford: Blackwell Publishing Ltd; 2012. p. 626–638.
35. Dayal MR, Kegley AD, Štrkalj G, Bidmos MA, Kuykendall KL. The history and composition of the Raymond A. Dart collection of human skeletons at the University of the Witwatersrand, Johannesburg, South Africa. Am J Phys Anthropol. 2009;140(2):324–335. doi:10.1002/ajpa.21072.
36. Hughes H. The factors determining the direction of the canal for the nutrient artery in the long bones of mammals and birds. Cells Tissues Organs. 1952;15(3):261–280. doi:10.1159/000140748.

37. Lawrence I, Lin K. A concordance correlation coefficient to evaluate reproducibility. Biometrics. 1989;45(1):255–268. doi:10.2307/2532051.
38. Ramayah T, Ahmad NH, Halim HA, May-Chiun SRMZ. Discriminant analysis: an illustrated example. Afr J Bus Manag. 2010;4(9):1654–1667.
39. Krogman WM, İşcan MY. The human skeleton in forensic medicine. Springfield (IL): Charles C Thomas; 1986. p. 202–208.
40. Abdellatif A. 2019. Sexual dimorphism by measuring the mesiodistal width of the permanent maxillary and mandibular canine in a sample of the South African population in the Northern suburb of Cape Town. https://etd.uwc.ac.za.
41. Curate F, Mestre F, Garcia SJ. Sex assessment with the radius in Portuguese skeletal populations (late 19th–early to mid 20th centuries). Legal Med. 2021;48:101790. doi:10.1016/j.legalmed.2020.101790.
42. Liebenberg L, Krüger GC, L'Abbé EN, Stull KE. Postcraniometric sex and ancestry estimation in South Africa: a validation study. Int J Legal Med. 2019;133(1):289–296. doi:10.1007/s00414-018-1865-x.
43. Shakoane GP, Dussault MC, L'Abbé EN. Estimating sex among South African groups using the dentition. Forensic Sci Int Rep. 2021;4:100233. doi:10.1016/j.fsir.2021.100233.
44. Safont S, Malgosa A, Subirà ME. Sex assessment on the basis of long bone circumference. Am J Phys Anthropol. 2000;113(3):317–328. doi:10.1002/1096-8644(200011)113:3<317::AID-AJPA4>3.0.CO;2-J.
45. Black TK III. A new method for assessing the sex of fragmentary skeletal remains: femoral shaft circumference. Am J Phys Anthropol. 1978;48(2):227–231. doi:10.1002/ajpa.1330480217.
46. Pohar M, Blas M, Turk S. Comparison of logistic regression and linear discriminant analysis: a simulation study. Metodoloski Zvezki. 2004;1(1):143. doi:10.51936/ayrt6204.
47. Bartholdy BP, Sandoval E, Hoogland ML, Schrader SA. Getting rid of dichotomous sex estimations: why logistic regression should be preferred over discriminant function analysis. J Forensic Sci. 2020;65(5):1685–1691. doi:10.1111/1556-4029.14482.

Chapter 6: Submitted to the Journal of Biomechanics as:

Title: Age-related trabecular morphologic changes around the metatarsal diaphyseal nutrient foramina: implications for risk of fracture assessment

Running title: Trabecular structure around the metatarsal diaphyseal nutrient foramen

Arthur Tsalani Manjatika[a,b], Erin Frances Hutchinson[a], Pedzisai Mazengenya[c,d,e*], Joshua Gabriel Davimes[a]

[a] School of Anatomical Sciences, University of the Witwatersrand, Parktown, Johannesburg, South Africa

[b] School of Life Sciences and Allied Health Professions, Anatomy Division, Kamuzu University of Health Sciences, Blantyre, Malawi

[c] College of Medicine, Ajman University, Ajman, United Arab Emirates

[d] Center of Medical and Bio-allied Health Sciences Research, Ajman University, Ajman, United Arab Emirates

[e] Faculty of Health Sciences, University of the Witwatersrand, Parktown, Johannesburg, South Africa

***Correspondence to**: Dr Pedzisai Mazengenya, College of Medicine, Ajman University, Ajman, United Arab Emirates Tel: +971551848743; Email: p.mazengenya@ajman.ac.ae
ORCID:

ATM: 0000-0003-0867-7123

EFH: 0000-0002-1797-1140

PM: 0000-0003-4733-1563

JGD: 0000-0001-9808-5249

ABSTRACT

Metatarsal fractures are common, with a high incidence rate in the first and fifth metatarsals (MT). The trabecular bone quality is a good predictor for the risk of fracture development. The nutrient foramen (NF) is potentially weak, and the role of the trabecular structure around the NF in fracture development is unclear. This study examined the trabecular structure around the NF of the first and fifth MT bones across different ages of the three South African population groups. Eighty-eight dry MTs from the left and right sides, aged 0-40 years, of known sex and population affinity, were scanned using µCT to examine ontogeny and population-related variabilities of the trabecular morphology including the bone volume fraction (BV/TV), bone surface volume (BS/BV), trabecular thickness (TbTh), trabecular number (TbN) and trabecular spacing (TbSp), and the local bone density. There were no sex, side, or population differences. In both MTs, the BV/TV, TbTh, and local bone density measures peaked between 21-30 years of age and then decreased thereafter and were highest at the NF level compared to the proximal and distal regions *($p<0.0001$)*. The BS/BV, TbN, and TbSp were lowest at the NF level *($p<0.0001$)*. The fifth MT medial surface showed the most variation in trabecular parameters *($p<0.0001$)*, while the first MT showed no surface variations *($p>0.05$)*. Knowledge of the ontogenetic, sex, and population variability of the trabecular architecture may help understand bone fragility, fracture development patterns and fracture management in different individuals.

Keywords

Age-related changes; Diaphyseal nutrient foramen; Metatarsal bones; Micro-computed tomography; Trabecular bone structure; South African populations.

1. Introduction

Metatarsal fractures are common in the first five decades of life and account for up to 35% of all foot injuries in adults and about 61% in children, leading to pain and disability when not appropriately managed (Buddecke et al., 2010; Moore, 2018; Sarpong et al., 2018). The incidence of the metatarsal fractures varies depending on the metatarsal bone involved. The fifth metatarsal bone is the most frequently fractured, with 40-70% incidence rates, followed by the first metatarsal bone, with 5-19% incidence rates (Moore, 2018; Zwitser and Breederveld, 2010). Fractures to the first and fifth metatarsals are debilitating as these bones support the longitudinal arches of the foot and ensure normal gait patterns (Moore, 2018; Petrisor et al., 2006; Zwitser and Breederveld, 2010). As such, their detailed histomorphology is essential to understand the fracture patterns, mechanisms and subsequent fracture management.

The fracture sites vary along the length of the metatarsal bone diaphysis, with some occurring at the proximal, middle or distal segments (Cakir et al., 2011; Dameron Jr, 1975; Moore, 2018; Sarpong et al., 2018). Fractures may also occur at the level of the diaphyseal nutrient foramen (Craig et al., 2003). Nutrient foramina are external openings to the nutrient canal that carry nutrient vessels and nerves to the bone (Götzen et al., 2003; Kothapalli, 2018; Manjatika et al., 2023; Mazengenya and Billings, 2016; Xue et al., 2016). The nutrient foramen and the area around it may present as a potentially weak area along the diaphysis for fracture development (Craig et al., 2003; Götzen et al., 2003; Mazengenya and Fasemore, 2015), but this requires further investigation. A previous study limited their focus to the cortical bone around nutrient foramina of the equine metacarpals to understand bone quality and the risk of fracture development (Götzen et al., 2003). However, the trabecular bone was not examined, probably because the diaphysis contains more cortical bone than the trabecular bone (Götzen et al., 2003). Thus, the trabecular morphology around the nutrient foramen is yet to be investigated. Clinically, the trabecular bone morphology is a good predictor of bone quality and fragility and may help in predicting the risk of fracture development due to its higher environmental plasticity compared to the cortical bone (Komza, 2017; Stock and Pfeiffer, 2001). The quality of trabecular bone also determines the success or failure of bone implants during fracture management (Cheal et al., 1987; Drago, 1992; Puleo and Nanci, 1999).

Previous studies showed that ontogenetic or age-related changes in the trabecular bone manifest differently in various sites along the length of the bone diaphysis, making some sites more prone to fractures than others (Gosman and Ketcham, 2009; Oftadeh et al., 2015; Parkinson and Fazzalari, 2012; Raichlen et al., 2015; Ryan and Krovitz, 2006). The ontogenetic changes of the trabecular bone morphology around the nutrient foramen of long bones, however, remain elusive. Trabecular parameters that are indicators/predictors of bone quality and the risk of fracture development include bone volume density, bone surface volume, trabecular thickness, trabecular number, trabecular spacing and trabecular interconnectedness (Gosman and Ketcham, 2009; Kivell, 2016). Assessing these trabecular parameters can help predict an individual's risk of bone fragility and subsequent fracture development (Agarwal et al., 2004; Komza, 2017; Stock and Pfeiffer, 2001). Micro-computed tomography (µCT) scanning provides a detailed analysis of the trabecular morphological parameters and has been utilised in various evolutionary (Komza, 2017; Saers et al., 2016; Tsegai et al., 2018; Zeininger et al., 2016) and clinical studies (Hutchinson et al., 2017; Ocak et al., 2022). The current study examined the trabecular morphology around the nutrient foramen of the first and fifth metatarsal bones across different age and sex groups from the 20th century populations of South Africa, including the South African Africans, South Africans of Mixed Ancestry, and South Africans of European descent individuals. Knowledge of the ontogenetic, sex and population variability of the trabecular architecture may help understand bone fragility and susceptibility to high risk of fracture development in individuals of various ages, sexes, and population affinity.

2. Materials and Methods

2.1 Study population

The current cross-sectional study utilised the dry metatarsal bones from 20th-century individuals from the Raymond A. Dart Collection of Modern Human Skeletons housed in the School of Anatomical Sciences at the University of the Witwatersrand, South Africa. The study was conducted under the ethical clearance waiver number W-CBP-220504-01 obtained from the Faculty of Health Sciences, University of the Witwatersrand. The study utilised a total of 88 metatarsal bones from both the left and right sides (44 first and 44 fifth) from 38 skeletons of known population affinity, age and sex (table 1). The metatarsal bones were obtained from individuals aged between 0-40 years old. The age group was selected because of the significant growth morphological changes and the varying rates of metatarsal fractures previously observed particularly in this age group (Moore, 2018; Sarpong et al., 2018). The metatarsal bones were age-matched and grouped at 10-year intervals across the three population groups, as shown in Table 1. Metatarsal bones that presented with fractures, pathological and malformed deformities, gross evidence of any genetic diseases and any evidence of surgical interventions were excluded from the study. The cause of death and previous medical and occupational history of the cadaveric specimens were not recorded in the Raymond A. Dart Collection of Modern Human Skeletons catalogue (Dayal et al., 2009); hence, the non-evident macroscopic genetic diseases and occupational history were not exclusion factors.

The South African population comprises of the four population groups classified based on their descent (South Africa Statistics, 2022). The South African Africans (SAA), also known as Black South Africans, mainly consist of various ethnic tribes, including the Pedi, Sotho, Tswana, Ndebele, Zulu, Venda, Xhosa, Swazi and Tsonga. These ethnic groups are believed to exhibit similar genetic traits and are collectively considered homogeneous (De Villiers, 1968; Gonzalez-Santos et al., 2015; Lundy, 1985). The South Africans of European descent (SAED), also known as White South Africans, are distinct homogeneous White South African-born individuals who derive mainly from the admixture through intermarriages of the colonial immigrants from European countries, including the Netherlands, Germany, Britain, Portugal, Greece, Italy, Dutch and France (Bank, 1997; Kriger, 1996; Patriquin et al., 2003; Preston-Whyte, 1982; Steyn and İşcan, 1997). The South Africans of Mixed ancestry (SAMA), also known as Coloured South Africans, are a self-identified and diverse group

whose genetic heritage is contributed from SAA, SAED and some contributions from South Africans of Asian descent (Adhikari, 2005; Krüger et al., 2017; L'Abbé et al., 2011; Patterson et al., 2010; Stull et al., 2014).

Table 1: Sample distribution of the metatarsal bones across different age and population groups

Sex	0-10 year		11-20 year		21-30 year		31-40 year		Total
(side)	M (R/L)	F (R/L)	M (R/L)	F (R/L)	M (R/L)	F (R/L)	M (R/L)	F (R/L)	M+F
MT1									
SAA	2 (1/1)	2 (1/1)	2 (1/1)	2 (1/1)	2 (1/1)	2 (1/1)	2 (1/1)	2 (1/1)	16
SAED	4 (2/2)	-	3 (2/1)	1 (0/1)	1 (1/0)	3 (3/0)	2 (1/1)	2 (1/1)	16
SAMA	-	-	2 (1/1)	2 (1/1)	-	4 (1/3)	3 (1/2)	1 (0/1)	12
Total	6 (3/3)	2 (1/1)	7 (4/3)	5 (2/3)	3 (2/1)	9 (5/4)	7 (3/4)	5 (2/3)	44
MT5									
SAA	2 (1/1)	2 (1/1)	2 (1/1)	2 (1/1)	2 (1/1)	2 (1/1)	2 (1/1)	2 (1/1)	16
SAED	4 (2/2)	-	3 (2/1)	1 (0/1)	1 (/0)	3 (3/0)	2 (1/1)	2 (1/1)	16
SAMA	-	-	2 (1/1)	2 (1/1)	-	4 (1/3)	3 (1/2)	1 (0/1)	12
Total	6 (3/3)	2 (1/1)	7 (4/3)	5 (2/3)	3 (2/1)	9 (5/4)	7 (3/4)	5 (2/3)	44

Abbreviations: Mt= Metatarsal bone; SAA= South African Africans; SAED= South Africans of European descent; SAMA= South Africans of Mixed ancestry; M= Male; F= Female; R= Right side, L= Left side.

2.2 Acquisition of µCT scans for trabecular morphology

The metatarsal bones were scanned using a Nikon XTH 225L micro-focus computed tomography (µCT) X-ray unit (Nikon Metrology, Leuven, Belgium) located at the MIXRAD laboratory at the Nuclear Energy Corporation of South Africa (NECSA), Pelindaba. Four metatarsal bones (2 first and 2 fifth) were scanned at a time and these were secured in a vertical orientation (proximal end pointing upwards) in a florist (oasis foam) block. A plastic density reference peg was utilised due to its uniform material composition and this was embedded in the florist foam during scanning. The mounted metatarsal bones were then placed on a rotating sample manipulator that facilitates 360 degrees scanning. The scanning was done at an acceleration voltage of 100KV, 100mA, 100 µA, using a 0.5mm thick aluminium filter to approximate a homogeneous x-ray beam spectrum by removing lower energy photons. The images were reconstructed as 3000 x 3000 16-bit single Tiff image stacks from 1000 projections with two frames averaging. The projections were sent to the Nikon CT pros software version XT4.4.3 (Nikon Metrology, Leuven, Belgium), in which volume files were created.

2.3 Trabecular morphometric analysis

The volume files were imported into VG studio Max V3.2.3 software (Volume Graphics GmbH, Heidelberg, Germany) for morphological analysis. Bone surface determination analysis was done following a standardised orientation. Three fiducial landmarks were created using three tuberosities on the plantar surface of the base and head of the first metatarsal bone and three tuberosities on the medial surface of the base and head of the fifth metatarsal bone to create anatomical reference planes (Komza, 2017; Saers et al., 2019). All the metatarsal bones were then aligned to these reference points. Three-dimensional disks of 1mm thickness were taken from the transverse slices from a total of five set points. Three set points were around each nutrient foramen: 1mm above the nutrient foramen (ANF), 1mm at the nutrient foramen (NF) and 1mm below the nutrient foramen (BNF) in order to determine the trabecular bone quality around the nearest regions to the NF. Additionally, transverse slices from two control points (proximal and distal ends of the diaphysis just before the epiphysis) were taken. These control points were selected because they transmit mechanical load/forces from the joints to the diaphysis and are common fracture sites (Sarpong et al., 2018). Four regions of interest (ROI) of the diameter (2-3mm) were selected on the medial, lateral, dorsal and plantar surfaces of each transverse slide at each of the five set points of the bone. The trabecular morphometric parameters and the local bone density in each ROI were quantified using the µCT analyser and the formula used previously by other authors to achieve consistency in the analysis of the trabecular morphometric parameters (Da Silva et al., 2014; Silva et al., 2011). The trabecular morphometric parameters analysed included the bone volume fraction (BV/TV), bone material surface to bone material volume (BS/BV), trabecular thickness (TbTh), trabecular number (TbN), and trabecular spacing (TbSp). In addition, the volumetric local bone density (Gray value analysis) was also quantified to determine qualitative bone strength.

1. Bone volume fraction (BV/TV): represents the proportion of bone volume (BV) to the total volume (TV) of the region of interest. It is calculated as *BV/TV* and measured in %.
2. Bone material surface-to-material volume (BS/BV): the amount of bone mineral present on the bone surface (BS) per unit of bone volume (BV). It is calculated as *BS/BV* and measured in mm^-1.
3. Trabecular thickness (TbTh): the thickness of the trabeculae in the selected region of interest of the bone. It is calculated as *2 /* (*BS/BV)* and measured in mm.

4. Trabecular number (TbN): the number of trabeculae within a selected region of interest of the bone. It is calculated as (*BV/TV*) / *TbTh* and measured in mm^-1.
5. Trabecular spacing (TbSp): the distance between trabeculae in the selected region of interest of the bone. It is calculated as *(1 / TbN) – TbTh* and measured in mm.
6. Local bone density is the relative measure of the volumetric bone density on the selected region of interest in relation to the whole bone. It is measured in gray value or Hounsfield units (HU) (Da Silva et al., 2014; Silva et al., 2011).

2.4 Data Analysis

The data were managed in Microsoft Excel Office 365 (Microsoft Corporation) and analysed with IBM® SPSS® version 23 (IBM Corp., Armonk, NY, USA). The normality of the continuous data for each variable was determined using the Shapiro-Wilk test and histograms. The data was not normally distributed for most variables, as such, the continuous data were presented as medians and interquartile ranges. Sex and side of the body differences on the trabecular parameters were analysed only in the pooled sample of adult individuals in the 21-30 and 31-40 years groups, owing to small and uneven sample sizes within each age group (Table 1). The Mann-Whitney U test was used to test for significant differences between sex and sides of the body with regards to the trabecular parameters for the non-parametric data within each population group, while the independent sample student t-test was used to test for significant differences between sex and sides of the body with regards to the trabecular parameters for the parametric data. Since there were no significant differences between the sex or side of the body with regards to the trabecular parameters ($p>0.05$), the subsequent analysis of the ontogenetic variations of the trabecular architecture utilised both the pooled sex and side of the body samples while the analysis at the different levels and surfaces of the first and fifth metatarsal bones utilised the pooled age, sex and side of the body samples. For the normally distributed variables, the one-way analysis of variance (ANOVA) was used to test for the significant mean differences on trabecular parameters across age groups and different levels of bone across the three population groups. For the non-parametric variables, the Kruskal-Wallis test was used to test for the significant median differences on trabecular parameters across age groups and different levels of bone across the three population groups. Tukey's post hoc test was used to determine the specific significant differences observed. A significance level of $p \leq 0.05$ was used for all comparisons.

3. Results

3.1 Ontogenetic variability of the trabecular bone morphology at different levels and surfaces of the first and fifth metatarsal bones across populations in pooled sex and sides of the body

The age-matched medians and interquartile ranges comparisons of each trabecular morphologic parameter ((bone volume fraction (BV/TV), bone surface to bone volume (BS/BV), trabecular thickness (TbTh), trabecular number (TbN) and trabecular spacing (TbSp)) at different levels and surfaces of the first and fifth metatarsal bones across populations in the 0-10-year group are presented in Table 2. On the first metatarsal bones, statistically significant population differences for the trabecular structure parameters were only found at the proximal diaphysis and the nutrient foramen (NF) levels *($p \leq 0.05$)* (Table 2). At the proximal diaphysis level and on the lateral surface of the first metatarsal bone, the TbSp was higher in the South African Africans (SAA) when compared to the South Africans of European descent (SAED) *($p \leq 0.05$).* At the NF level and on the plantar surface of the first metatarsal bone, TbN was higher while the TbSp was lower in the SAED when compared to the SAA group *($p \leq 0.05$).* On the fifth metatarsal bones, statistically significant population differences for all trabecular structure parameters were only found at the proximal diaphysis and the below nutrient foramen (BNF) regions *($p \leq 0.05$).* At the proximal diaphysis level and on the medial surface of the fifth metatarsal bone, the BS/BV, TbN and TbSp were higher while the BV/TV and TbTh were lower in the SAED than the SAA *($p \leq 0.05$).* At the BNF level of the fifth metatarsal bone on both the lateral and dorsal surfaces, the BS/BV, TbN and TbSp were higher while the BV/TV and TbTh were lower in the SAED than the SAA *($p \leq 0.05$)* (Table 2).

The age-matched medians and interquartile ranges comparisons of each trabecular morphologic parameter at different levels and surfaces of the first and fifth metatarsal bones across populations in the 11-20-year group are presented in Table 3. On the first metatarsal bones, there were no statistically significant population differences for all trabecular structure parameters (BV/TV, BS/BV, TbTh, TbN, and TbSp) ($p>0.05$). On the fifth metatarsal bones, statistically significant population differences for the trabecular structure parameters were only found at the proximal diaphysis, NF, and BNF levels *($p\leq0.05$)*. At the proximal diaphysis and BNF levels of the fifth metatarsal bone on the dorsal surface, the BS/BV, TbN and TbSp were higher while the BV/TV and TbTh were lower in the SAA than the South Africans of Mixed ancestry (SAMA) *($p\leq0.05$)*. At the NF level of the fifth metatarsal bone on the medial surface, the BS/BV and TbN were higher while the TbTh was lower in the SAA than the SAMA *($p\leq0.05$)* (Table 3).

The age-matched medians and interquartile ranges comparisons of each trabecular morphologic parameter at different levels and surfaces of the first and fifth metatarsal bones across populations in the 21-30-year group are presented in Table 4. On the first metatarsal bones, statistically significant population differences for the trabecular structure parameters were only found at the BNF region *($p\leq0.05$)* (Table 4). At the BNF of the first metatarsal bone and on the lateral surface, the BS/BV and TbN were higher while the TbTh was lower in the SAA than the SAMA *($p\leq0.05$)*. On the fifth metatarsal bones, statistically significant differences were only observed at the proximal diaphysis, above the NF (ANF) and distal diaphysis levels *($p\leq0.05$)*. At the proximal diaphysis of the fifth metatarsal bone, the BS/BV and TbN were higher while the BV/TV and TbTh were lower in the SAA than the SAED on the dorsal surface *($p\leq0.05$)* (Table 4). At the ANF and distal diaphysis of the fifth metatarsal bone, the BS/BV and TbN were higher while the BV/TV and TbTh were lower in the SAA than the SAMA on the medial and plantar surfaces *($p\leq0.05$)* (Table 4).

The age-matched medians and interquartile ranges comparisons of each trabecular morphologic parameter at different levels and surfaces of the first and fifth metatarsal bones across populations in the 31-40-year group are presented in Table 5. On the first metatarsal bones, statistically significant population differences for the trabecular structure parameters were only found at the NF region *($p\leq0.05$)* (Table 5). At the NF of the first metatarsal bone and on the lateral surface, the TbN was higher in the SAED than the SAA *($p\leq0.05$)*. At the NF of the first metatarsal bone and on the dorsal surface, the BV/TV was higher in the SAA

than the SAMA *(p≤0.05)*. On the fifth metatarsal bones, statistically significant population differences for the trabecular structure parameters were only found at the ANF region *(p≤0.05)* (Table 5). At the ANF of the fifth metatarsal bone, the BS/BV and TbN were higher while the BV/TV and TbTh were lower in the SAMA than the SAA on the dorsal surface *(p≤0.05)* (Table 5).

Table 2: Age matched comparisons of trabecular structure parameters on different surfaces of the bone across population groups in the 0-10-year group

First metatarsal bone															
Level of bone		Proximal Diaphysis			Above Nutrient Foramina			Nutrient foramina			Below Nutrient Foramina			Distal Diaphysis		
Surface	Trabecular	SAA	SAED	SAMA	SAA	SAED	SAMA	SAA	SAED	SAMA	SAA	SAED	SAMA	SAA	SAED	SAMA
Lateral	BV/TV	0.70±0.15	0.85±0.15		0.904±0.231	0.86±0.15		0.792±0.389	0.85±0.05		0.731±0.412	0.82±0.26		0.541±0.272	0.77±0.34	
	BS/BV	3.28±1.71	2.59±2.57		1.0±2.41	2.68±1.14		1.74±2.92	2.55±0.79		2.82±3.63	2.98±0.8		5.22±3.44	3.27±4.81	
	TbTh	0.61±0.49	0.77±0.68		2.37±3.15	0.75±0.35		1.53±3.22	0.79±0.25		0.88±1.69	0.67±0.25		0.39±0.34	0.62±3.05	
	TbN	1.15±0.4	1.1±0.89		0.46±0.81	1.15±0.34		0.57±0.8	1.07±0.34		0.84±0.89	1.02±0.49		1.32±0.98	1.25±1.22	
	TbSp	**0.26±0.05**	**0.13±0.07**		0.18±0.33	0.14±0.13		0.24±0.42	0.13±0.07		0.24±0.32	0.19±0.42		0.41±0.57	0.19±0.12	
Dorsal	BV/TV	0.59±0.37	0.82±0.1		0.818±0.178	0.83±0.12		0.816±0.141	0.86±0.06		0.834±0.235	0.84±0.08		0.81±0.256	0.88±0.13	
	BS/BV	4.55±4.46	3.91±2.55		2.05±1.84	3.36±2.54		1.86±0.82	2.39±1.64		1.62±2.26	2.96±1.32		1.89±2.16	2.02±1.08	
	TbTh	0.48±1.08	0.52±0.56		1.01±1.91	0.6±2.36		1.13±0.49	0.88±0.72		1.24±1.71	0.68±0.34		1.19±1.34	1.01±0.52	
	TbN	1.22±0.95	1.6±0.9		0.84±0.64	1.39±1.04		0.77±0.44	1.01±0.66		0.68±0.72	1.25±0.46		0.77±0.61	0.89±0.34	
	TbSp	0.31±0.23	0.12±0.08		0.2±0.17	0.11±0.04		0.25±0.43	0.15±0.05		0.2±0.2	0.14±0.04		0.25±0.3	0.14±0.01	

Medial	BV/TV	0.71±0.48	0.74±0.25	0.89±0.23	0.83±0.12	0.914±0.162	0.81±0.16	0.880±0.035	0.87±0.13	0.757±0.246	0.61±0.25
	BS/BV	2.89±4.95	3.76±4.87	1.28±0.92	2.94±2.71	1.15±0.85	3.32±3.33	1.53±1.3	2.35±3.04	2.48±1.7	4.54±3.98
	TbTh	0.81±1.18	0.57±1.27	1.7±1.28	0.77±1.0	1.76±2.05	0.69±1.11	1.42±1.28	0.97±1.85	0.81±0.4	0.49±0.43
	TbN	0.95±0.7	1.39±1.43	0.52±0.35	1.2±1.0	0.49±0.39	1.31±1.14	0.67±0.57	1.01±1.17	1.01±0.31	1.39±0.86
	TbSp	0.28±0.29	0.16±0.15	0.26±0.42	0.13±0.05	0.13±0.4	0.15±0	0.17±0.16	0.13±0.04	0.28±0.22	0.28±0.19
Plantar	BV/TV	0.69±0.42	0.78±0.29	0.843±0.109	0.81±0.21	0.892±0.276	0.77±0.14	0.820±0.257	0.85±0.09	0.78±0.206	0.69±0.15
	BS/BV	3.48±7.34	4.88±5.8	1.62±0.79	3.71±5.33	1.55±1.38	3.57±3.23	1.79±0.94	2.83±2.83	2.45±1.64	4.57±2.41
	TbTh	0.58±0.47	0.42±3.75	1.24±0.51	0.56±1.6	1.32±1.16	0.63±0.52	1.17±0.6	0.79±0.95	0.83±0.57	0.44±0.29
	TbN	1.19±0.76	1.89±1.72	0.68±0.23	1.5±1.74	**0.7±0.31**	**1.44±1.11**	0.7±0.18	1.19±1.1	0.94±0.37	1.51±0.75
	TbSp	0.26±0.19	0.12±0.04	0.23±0.08	0.12±0.03	**0.18±0.32**	**0.12±0.13**	0.23±0.33	0.13±0.04	0.23±0.13	0.21±0.15

Fifth metatarsal bone															
	Proximal Diaphysis			Above Nutrient Foramina			Nutrient foramina			Below Nutrient Foramina			Distal Diaphysis		
	SAA	SAED	SAMA	SAA	SAED	SAMA	SAA	SAED	SAMA	SAA	SAED	SAMA	SAA	SAED	SAMA

Lateral	BV/TV	0.91±0.05	0.81±0.2	0.96±0.08	0.73±0.17	0.92±0.06	0.82±0.2	**0.97±0.05**	**0.76±0.11**	0.61±0.28	0.74±0.16
	BS/BV	1.95±1.08	3.84±4.13	0.86±1.25	3.81±3.85	1.24±1.45	3.22±3.56	**0.87±1.17**	**3.5±2.69**	4.74±3.43	4.43±4.22
	TbTh	1.02±0.45	0.64±0.66	2.5±2.0	0.55±1.27	1.74±2.18	0.74±0.67	**2.68±2.68**	**0.60±0.36**	0.43±0.72	0.46±0.49
	TbN	0.89±0.44	1.49±1.26	0.41±0.52	1.39±1.32	0.57±0.63	1.29±1.09	**0.42±0.53**	**1.37±0.86**	1.32±0.86	1.63±1.26
	TbSp	0.11±0.03	0.13±0.04	0.11±0.05	0.15±0.11	0.13±0.09	0.14±0.06	**0.08±0.01**	**0.14±0.07**	0.27±0.15	0.14±0.04
Dorsal	BV/TV	0.87±0.17	0.77±0.12	0.90±0.11	0.92±0.15	0.93±0.1	0.80±0.18	**0.93±0.09**	**0.79±0.09**	0.57±0.07	0.75±0.38
	BS/BV	2.01±2.2	4.19±2.04	1.42±1.6	1.54±2.88	1.72±1.6	3.47±3.89	**1.3±1.14**	**3.68±2.18**	5.32±1.42	5.19±7.37
	TbTh	1.0±1.47	0.49±0.3	1.46±4.0	1.47±1.71	1.19±1.12	0.59±3.08	**1.57±1.09**	**0.55±0.27**	0.38±0.1	0.47±0.73
	TbN	0.87±0.78	1.6±0.66	0.64±0.67	0.7±1.11	0.8±0.64	1.39±1.42	**0.60±0.45**	**1.46±0.66**	1.6±0.28	1.75±1.49
	TbSp	0.15±0.08	0.12±0.08	0.14±0.08	0.10±0.05	0.11±0.0 60	0.13±0.06	**0.12±0.06**	**0.14±0.01**	0.27±0.07	0.14±0.11
Medial	BV/TV	**0.97±0.06**	**0.85±0.03**	0.96±0.04	0.93±0.18	0.96±0.13	0.92±0.19	0.97±0.09	0.91±0.19	0.95±0.06	0.89±0.15
	BS/BV	**0.77±1.03**	**2.59±0.89**	0.78±0.76	1.42±3.36	0.78±1.3	1.62±3.81	0.63±1.07	1.53±3.49	1.32±0.62	2.58±2.37
	TbTh	**2.63±1.67**	**0.78±0.23**	2.58±2.54	2.64±5.3	2.65±3.54	1.59±3.2	3.27±5.19	2.16±4.12	1.58±0.83	0.83±1.15

	TbN	**0.37±0.44**	**1.11±0.34**	0.37±0.34	0.64±1.31	0.37±0.51	0.74±1.39	0.31±0.46	0.67±1.32	0.6±0.28	1.14±0.86
	TbSp	**0.09±0.03**	**0.13±0.02**	0.1±0.04	0.09±0.06	0.11±0.12	0.11±0.04	0.09±0.07	0.11±0.05	0.12±0.1	0.09±0.05
Plantar	BV/TV	0.81±0.17	0.71±0.27	0.91±0.26	0.85±0.16	0.89±0.11	0.88±0.36	0.84±0.18	0.76±0.14	0.76±0.37	0.82±0.16
	BS/BV	2.62±1.19	5.44±2.79	1.53±1.83	3.12±3.22	1.37±1.18	2.62±4	1.87±2.24	4.23±2.22	2.79±3.63	3.0±2.09
	TbTh	0.76±0.33	0.37±0.31	1.32±1.23	0.71±0.93	1.46±1.24	0.81±3.44	1.09±9.47	0.47±0.58	0.73±1.35	0.67±1.17
	TbN	1.02±0.44	1.73±0.69	0.69±0.45	1.31±1.06	0.61±0.44	1.14±1.03	0.78±0.86	1.6±0.71	1.05±0.73	1.16±0.87
	TbSp	0.17±0.19	0.15±0.15	0.16±0.24	0.13±0.05	0.18±0.09	0.10±0.19	0.16±0.13	0.15±0.04	0.24±0.2	0.15±0.11

Note: Values are medians±interquartile range, measured in millimeters. SAA=South African Africans, SAED=South Africans of European descent, SAMA=South Africans of Mixed Ancestry, BB/TV=Bone volume fraction, BS/BV=Bone surface volume, TbTh=Trabecular thickness, TbN=Trabecular number, TbSp=Trabecular spacing. The highlighted areas in **Bold** represent statistically significant differences $p<0.05$.

Table 3: Age matched comparisons of trabecular structure parameters on different surfaces of the bone across population groups in the 11-20-year group

First metatarsal bone																
Level of bone		Proximal Diaphysis			Above Nutrient Foramina			Nutrient foramina			Below Nutrient Foramina			Distal Diaphysis		
Surface	Trabecular	SAA	SAED	SAMA	SAA	SAED	SAMA	SAA	SAED	SAMA	SAA	SAED	SAMA	SAA	SAED	SAMA
Lateral	BV/TV	0.89±0.13	0.79±0.57	0.97±0.5	0.9±0.29	0.97±0.38	0.92±0.21	0.91±0.34	0.95±0.32	0.90±0.17	0.9±0.46	0.95±0.27	0.74±0.5	0.74±0.45	0.69±0.53	0.57±0.35
	BS/BV	1.3±0.79	3.58±7.35	0.61±5.69	1.11±2.08	0.77±4.42	0.72±1.32	1.04±2.2	1.14±3.21	0.94±1.21	0.97±4.2	0.97±2.8	2.98±5.04	2.59±6.53	3.33±4.77	5.09±4.3
	TbTh	1.55±1.89	0.62±1.51	3.39±3.3	1.94±1.74	5.29±9.08	6.37±9.84	2.59±3.77	4.19±6.94	2.61±11.97	3.09±8.53	2.27±3.86	1.77±8.0	0.77±2.13	1.05±1.79	0.42±0.49
	TbN	0.56±0.3	0.96±1.06	0.29±0.78	0.49±0.53	0.37±1.13	0.28±0.54	0.45±0.58	0.52±0.97	0.4±0.48	0.41±0.92	0.46±0.85	0.78±1.22	0.95±1.05	0.79±0.88	1.33±0.6
	TbSp	0.18±0.18	0.17±0.58	0.11±0.36	0.2±0.28	0.11±0.23	0.16±0.35	0.19±0.34	0.11±0.2	0.20±0.23	0.21±0.33	0.14±0.16	0.25±0.29	0.28±0.2	0.29±0.39	0.28±0.19
Dorsal	BV/TV	0.81±0.23	0.76±0.69	0.92±0.35	0.88±0.27	0.86±0.35	0.94±0.32	0.86±0.32	0.84±0.38	0.94±0.36	0.94±0.27	0.85±0.44	0.93±0.35	0.76±0.41	0.68±0.46	0.81±0.29
	BS/BV	2.4±2.42	3.46±11.77	1.57±2.66	1.53±2.5	2.47±3.93	0.97±2.79	1.2±1.87	2.53±4.74	0.90±2.87	0.91±2.03	2.16±4.98	1.01±2.72	2.86±3.52	2.93±5.42	1.56±1.87
	TbTh	0.94±2.24	0.86±3.71	1.54±1.39	1.34±3.47	1.26±4.72	2.25±3.01	1.91±2.48	2.39±8.89	2.59±3.27	2.29±3.99	1.8±3.71	2.0±7.01	0.88±1.97	1.11±1.7	1.28±1.16
	TbN	0.94±0.79	0.92±1.19	0.61±0.54	0.67±0.75	0.88±1.26	0.45±0.73	0.5±0.49	0.85±1.46	0.42±0.7	0.43±0.6	0.84±1.14	0.47±0.71	0.95±0.83	0.85±0.92	0.63±0.46
	TbSp	0.19±0.12	0.20±0.49	0.17±0.3	0.19±0.18	0.14±0.2	0.13±0.22	0.25±0.34	0.15±0.15	0.31±0.5	0.16±0.21	0.16±0.22	0.14±0.31	0.22±0.28	0.38±0.18	0.27±0.3

Medial	BV/TV	0.81±0.14	0.54±0.67	0.86±0.46	0.92±0.38	0.90±0.35	0.90±0.4	0.94±0.43	0.96±0.33	0.83±0.46	0.95±0.53	0.87±0.47	0.8±0.54	0.66±0.43	0.56±0.33	0.50±0.27
	BS/BV	2.64±0.7	6.39±13.88	1.63±4.47	1.12±3.93	2.15±4.03	1.32±4.21	0.76±5.16	0.79±3.61	1.77±6.14	0.58±7.45	1.11±3.63	2.91±7.02	4.38±5.25	3.9±3.32	6.6±5.14
	TbTh	0.76±0.27	0.39±1.35	1.29±1.58	1.89±4.93	1.81±1 0.76	1.53±5.27	2.78±2.96	3.34±1 1.13	1.84±4.01	3.44±9.83	1.81±2.54	1.71±4.46	0.46±0.37	0.51±0.26	0.30±0.47
	TbN	1.03±0.21	1.0±1.1	0.70±0.65	0.51±0.91	0.8±1.33	0.59±0.97	0.36±0.97	0.37±1.04	0.67±1.32	0.28±1.02	0.49±0.65	0.96±1.43	1.36±0.29	1.04±0.27	1.63±0.77
	TbSp	0.17±0.12	0.30±0.73	0.19±0.32	0.16±0.2	0.11±0.19	0.17±0.24	0.16±0.22	0.10±0.19	0.22±0.2	0.18±0.28	0.33±0.48	0.16±0.27	0.24±0.3	0.43±0.36	0.33±0.08
Plantar	BV/TV	0.7±0.44	0.72±0.56	0.84±0.57	0.93±0.06	0.76±0.56	0.89±0.49	0.86±0.50	0.93±0.21	0.85±0.39	0.97±0.46	0.88±0.37	0.95	0.71±0.4	0.45±0.45	0.76±0.3
	BS/BV	3.14±7.77	4.03±9.87	1.86±10.71	1.3±0.74	2.79±5.45	1.39±2.53	1.02±4.13	1.68±2.84	1.95±2.09	0.54±4.55	1.56±3.15	0.56	2.69±3.5	4.14±3.89	2.65±1.85
	TbTh	0.65±0.81	0.54±0.5	1.08±1.64	1.55±1.12	4.15±7.61	1.49±3.45	2.99±6.34	2.06±5.49	1.15±2	5.02±10.31	1.72±4.48	3.6	0.75±1.86	0.53±0.62	0.81±0.61
	TbN	1.07±1.17	1.18±0.42	0.79±0.96	0.6±0.31	0.59±1.3	0.61±0.67	0.41±0.77	0.75±1.05	0.66±0.55	0.26±0.89	0.67±0.79	0.27	0.96±0.66	0.99±0.64	0.87±0.33
	TbSp	0.22±0.22	0.19±0.49	0.21±0.32	0.16±0.07	0.22±0.41	0.18±0.25	0.3±0.43	0.11±0.11	0.19±0.45	0.12±0.34	0.18±0.24	0.17	0.3±0.28	0.35±0.25	0.25±0.27

Fifth metatarsal bone

	Proximal Diaphysis			Above Nutrient Foramina			Nutrient foramina			Below Nutrient Foramina			Distal Diaphysis		
	SAA	SAED	SAMA	SAA	SAED	SAMA	SAA	SAED	SAMA	SAA	SAED	SAMA	SAA	SAED	SAMA

Lateral	BV/TV	0.95±0.25	0.92±0.19	0.98±0.05	0.96±0.08	0.98±0.1	0.99±0.15	0.95±0.08	0.88±0.24	0.98±0.2	0.94±0.11	0.88±0.3	0.98±0.1	0.55±0.64	0.76±0.32	0.78±0.49
	BS/BV	0.8±2.42	1.32±4.05	0.58±1.28	0.77±1.47	0.74±1.91	0.18±1.79	0.69±0.74	1.57±4	0.42±1.51	0.89±1.26	2.39±4.92	0.29±1.76	4.98±12.81	3.96±4.37	3.81±7.6
	TbTh	2.61±3.07	1.52±4.99	3.99±4.45	2.61±4.3	2.78±8.06	11.79±26.99	3.15±12.53	3.51±11.5	4.76±4.4	2.27±2.12	3.28±8.74	7.21±7.61	0.40±1.55	0.58±1.17	0.54±0.41
	TbN	0.38±0.75	0.61±1.43	0.28±0.59	0.37±0.63	0.36±0.82	0.09±0.72	0.32±0.33	0.62±1.48	0.21±0.52	0.42±0.5	0.93±1.66	0.14±0.76	1.3±0.72	1.24±1.22	1.50±0.44
	TbSp	0.16±0.17	0.14±0.05	0.08±0.02	0.12±0.22	0.09±0.05	0.11±0.08	0.14±0.14	0.11±0.11	0.11±0.2	0.17±0.07	0.11±0.1	0.10±0.09	0.33±0.46	0.21±0.17	0.16±0.31
Dorsal	BV/TV	**0.68±0.35**	0.87±0.3	**0.93±0.04**	0.84±0.15	0.84±0.28	0.98±0.14	0.88±0.17	0.83±0.35	0.95±0.14	**0.89±0.14**	0.81±0.36	**0.98±0.02**	0.53±0.42	0.79±0.27	0.80±0.46
	BS/BV	**3.83±4.94**	2.56±5.74	**1.25±0.63**	2.05±0.58	2.93±4.83	0.50±1.61	1.79±1.17	2.49±5.43	0.88±1.61	**2.01±1.22**	2.61±5.84	**0.39±0.55**	6.08±5.19	3.28±4.81	2.44±7.83
	TbTh	**0.57±0.58**	1.05±2.83	**1.6±2.21**	0.98±0.29	1.66±4.38	3.99±4.73	1.12±1.06	2.17±4.69	2.31±5.14	**1.04±0.9**	2.36±4.19	**5.09±4.16**	0.33±0.42	0.86±2.11	0.99±2.32
	TbN	**1.26±0.6**	1.07±1.73	**0.58±0.29**	0.84±0.25	1.07±1.62	0.25±0.63	0.79±0.35	0.89±1.62	0.42±0.64	**0.82±0.46**	0.87±1.73	**0.19±0.26**	1.46±0.45	1.19±1.43	0.95±1.5
	TbSp	**0.26±0.15**	0.12±0.05	**0.13±0.02**	0.17±0.21	0.13±0.09	0.08±0.11	0.16±0.15	0.15±0.12	0.12±0.11	**0.15±0.13**	0.13±0.16	**0.09±0.06**	0.3±0.29	0.19±0.06	0.21±0.15
Medial	BV/TV	0.87±0.1	0.95±0.09	0.97±0.04	0.92±0.1	0.92±0.13	0.97±0.03	0.98±0.04	0.98±0.04	0.99±0.01	0.97±0.02	0.95±0.15	0.99±0.02	0.78±0.34	0.86±0.24	0.98±0.06
	BS/BV	1.18±1.18	1.13±1.91	0.59±0.7	0.94±1.22	1.21±2.76	0.28±0.24	**0.33±0.6**	0.58±1.04	**0.17±0.1**	0.53±0.35	1.04±2.62	0.39±0.55	2.14±2.64	3.1±2.75	0.48±0.87
	TbTh	1.76±1.27	2.75±9.36	3.42±8.8	2.16±22.5	2.96±7.06	8.63±7.72	**6.3±6.18**	6.0±9.25	**11.91±10.38**	4.06±2.45	4.53±7.51	8.57±27.84	1.16±2.81	0.65±3.72	4.22±3.7

	TbN	0.52± 0.46	0.53±0. 85	0.29±0. 33	0.43± 0.53	0.53±1. 16	0.13±0. 11	**0.16±0. 28**	0.28±0. 49	**0.08±0. 05**	0.26±0. 16	0.48± 1.07	0.13±0. 17	0.77±0. 71	1.23±1. 09	0.23± 0.38
	TbSp	0.22± 0.14	0.09±0. 02	0.11±0. 05	0.18± 0.08	0.11±0. 06	0.19±0. 13	0.11±0. 03	0.09±0. 03	0.11±0. 04	0.11±0. 09	0.09± 0.07	0.10±0. 04	0.27±0. 25	0.12±0. 15	0.12± 0.04
Plant ar	BV/T V	0.83± 0.36	0.86±0. 25	0.96±0. 07	0.98± 0.04	0.85±0. 37	0.97±0. 05	0.94±0. 06	0.89±0. 26	0.91±0. 29	0.94±0. 14	0.85± 0.41	0.99±0. 04	0.74±0. 44	0.83±0. 6	0.78± 0.26
	BS/BV	1.7±2. 9	2.42±3. 73	0.82±1. 25	0.45± 0.23	2.63±4. 74	0.69±0. 74	0.7±0.4 3	2.3±4.2	1.26±1. 67	0.83±1. 09	2.5±4. 57	0.19±0. 67	2.82±4. 71	3.22±1 1.41	2.68± 3.87
	TbTh	1.28± 1.99	1.3±4.3 7	2.43±4. 72	4.46± 2.48	2.2±5.9 4	3.28±6. 97	2.89±3. 47	3.43±6. 05	2.05±5. 94	2.55±2. 05	3.23± 5.98	11.55±1 5.49	0.71±2. 35	1.14±5. 43	0.78± 0.97
	TbN	0.68± 0.69	0.9±1.3 9	0.40±0. 55	0.22± 0.1	0.88±1. 49	0.33±0. 34	0.32±0. 19	0.84±1. 61	0.50±0. 59	0.39±0. 39	0.74± 1.42	0.10±0. 31	1.03±0. 98	1.06±1. 7	1.03± 0.96
	TbSp	0.24± 0.26	0.15±0. 12	0.10±0. 03	0.1±0. 11	0.12±0. 18	0.10±0. 07	0.17±0. 11	0.11±0. 08	0.15±0. 35	0.15±0. 12	0.13± 0.23	0.13±0. 04	0.25±0. 27	0.16±0. 27	0.21± 0.05

Note: Values are medians±interquartile range, measured in millimeters. SAA=South African Africans, SAED=South Africans of European descent, SAMA=South Africans of Mixed Ancestry, BB/TV=Bone volume fraction, BS/BV=Bone surface volume, TbTh=Trabecular thickness, TbN=Trabecular number, TbSp=Trabecular spacing. The highlighted areas in **Bold** represent statistically significant differences $p<0.05$.

Table 4: Age matched comparisons of trabecular structure parameters on different surfaces of the bone across population groups in the 21-30-year group

First metatarsal bone																
Level of bone		Proximal Diaphysis			Above Nutrient Foramina			Nutrient foramina			Below Nutrient Foramina			Distal Diaphysis		
Surface	Trabecular	SAA	SAED	SAMA	SAA	SAED	SAMA	SAA	SAED	SAMA	SAA	SAED	SAMA	SAA	SAED	SAMA
Lateral	BV/TV	0.87±0.08	0.94±0.07	0.91±0.07	0.98±0.03	0.99±0.02	0.99±0.02	0.99±0.04	0.98±0.02	0.99±0.08	0.97±0.09	0.99±0.01	0.98±0.01	0.84±0.21	0.91±0.11	0.95±0.05
	BS/BV	1.43±0.37	0.95±0.73	1.3±0.62	0.45±0.54	0.24±0.35	0.24±0.3	0.39±0.28	0.38±0.4	0.16±0.79	**0.65±0.64**	0.27±0.14	**0.3±0.2**	1.41±1.73	1.12±1.32	0.64±0.68
	TbTh	1.4±0.29	2.11±2.62	1.55±0.82	5.06±5.07	8.38±5.07	8.27±7.32	5.54±4.8	5.32±6.87	12.28±9.92	**3.38±2.81**	7.47±2.74	**6.76±8.58**	1.8±2.22	1.84±2.35	3.21±3.4
	TbN	0.64±0.15	0.47±0.4	0.57±0.3	0.22±0.26	0.12±0.17	0.12±0.15	0.19±0.14	0.19±0.19	0.08±0.35	**0.3±0.29**	0.13±0.07	**0.15±0.1**	0.56±0.59	0.51±0.52	0.30±0.3
	TbSp	0.18±0.13	0.14±0.05	0.14±0.11	0.09±0.04	0.09±0.01	0.10±0.06	0.08±0.12	0.10±0.09	0.12±0.11	0.09±0.22	0.09±0.05	0.11±0.05	0.23±0.18	0.17±0.08	0.15±0.08
Dorsal	BV/TV	0.92±0.17	0.87±0.37	0.87±0.18	0.89±0.15	0.95±0.17	0.94±0.07	0.94±0.15	0.95±0.05	0.97±0.13	0.90±0.18	0.97±0.05	0.93±0.07	0.85±0.25	0.88±0.08	0.88±0.18
	BS/BV	0.93±1.87	1.95±4.38	1.67±2.69	1.3±0.78	0.87±1.96	1.15±1.2	0.89±1.4	0.80±0.99	0.65±1.44	0.94±1.15	0.45±0.76	0.94±1.09	2.14±1.58	1.24±0.41	1.51±1.29
	TbTh	2.18±1.77	1.33±3.54	1.57±3.44	1.55±2.16	4.07±6.06	1.78±5.63	2.47±5.46	2.65±4.12	3.32±3.79	2.52±5.1	4.55±6.47	2.25±7.75	0.95±1.27	1.62±0.65	1.33±1.69
	TbN	0.43±0.66	0.81±1.17	0.69±1.02	0.54±0.36	0.4±0.76	0.53±0.55	0.41±0.56	0.38±0.45	0.31±0.57	0.41±0.43	0.22±0.35	0.43±0.5	0.83±0.46	0.53±0.16	0.66±0.42
	TbSp	0.16±0.16	0.15±0.2	0.14±0.1	0.17±0.26	0.14±0.11	0.09±0.08	0.14±0.14	0.11±0.06	0.11±0.1	0.2±0.25	0.12±0.04	0.14±0.14	0.17±0.22	0.21±0.14	0.20±0.16

Medial	BV/TV	0.93±0.08	0.86±0.06	0.90±0.12	0.93±0.12	0.97±0.14	0.96±0.02	0.93±0.12	0.91±0.08	0.94±0.04	0.9±0.22	0.95±0.07	0.96±0.09	0.63±0.20	0.79±0.13	0.76±0.29
	BS/BV	1.22±0.73	1.96±1.18	1.8±1.43	0.92±1.15	0.53±1.99	0.86±0.49	1.11±1.23	1.16±1.36	0.91±0.21	1.6±2.33	0.84±0.98	0.74±0.94	4.41±2.06	2.81±2.73	2.46±3.4
	TbTh	1.7±0.93	1.04±0.54	1.12±5.39	2.64±2.94	3.79±3.09	2.38±1.71	2.19±3.5	1.74±2.68	2.19±0.62	2.01±5.5	2.44±3.81	2.8±5.47	0.45±0.2	0.71±0.42	0.82±0.7
	TbN	0.56±0.28	0.85±0.45	0.79±0.6	0.42±0.46	0.26±0.78	0.41±0.23	0.5±0.51	0.53±0.59	0.43±0.09	0.64±0.9	0.40±0.43	0.35±0.41	1.42±0.37	1.11±0.74	0.95±0.8
	TbSp	0.13±0.07	0.14±0.05	0.12±0.09	0.15±0.13	0.11±0.07	0.11±0.05	0.13±0.11	0.13±0.11	0.14±0.06	0.13±0.15	0.12±0.07	0.12±0.09	0.23±0.15	0.19±0.02	0.20±2.18
Plantar	BV/TV	0.93±0.04	0.86±0.21	0.91±0.19	0.95±0.11	0.97±0.04	0.97±0.08	0.94±0.1	0.97±0.06	0.93±0.13	0.91±0.17	0.98±0.03	0.97±0.03	0.92±0.24	0.86±0.12	0.86±0.07
	BS/BV	1.13±0.14	2.31±3.93	1.52±3.47	0.77±1.31	0.47±0.28	0.58±1.22	0.89±1.6	0.57±0.63	1.00±1.59	0.85±1.4	0.35±0.38	0.57±0.54	1.54±1	1.79±0.63	1.19±1.76
	TbTh	1.77±0.22	1.62±3.58	1.39±2.31	2.69±2.08	4.22±1.61	3.54±4.9	2.46±4.75	3.81±3.78	2.19±8.72	2.67±2.68	5.83±5.95	3.61±10.1	1.38±1.08	1.12±0.51	1.7±1.29
	TbN	0.52±0.07	0.92±1.44	0.69±1.22	0.36±0.53	0.23±0.13	0.28±0.53	0.42±0.68	0.28±0.28	0.46±0.66	0.36±0.56	0.17±0.18	0.27±0.26	0.61±0.33	0.76±0.18	0.51±0.71
	TbSp	0.14±0.08	0.13±0.03	0.13±0.05	0.13±0.09	0.13±0.1	0.14±0.07	0.13±0.09	0.13±0.11	0.15±0.1	0.13±0.3	0.14±0.06	0.12±0.04	0.12±0.32	0.18±0.13	0.23±0.21

Fifth metatarsal bone

		Proximal Diaphysis			Above Nutrient Foramina			Nutrient foramina			Below Nutrient Foramina			Distal Diaphysis		
		SAA	SAED	SAMA	SAA	SAED	SAMA	SAA	SAED	SAMA	SAA	SAED	SAMA	SAA	SAED	SAMA
Lateral	BV/TV	0.92±0.12	0.97±0.06	0.92±0.08	0.98±0.04	0.99±0.0	0.98±0.06	0.98±0.11	0.99±0.01	0.95±0.21	0.95±0.09	0.97±0.04	0.93±0.11	0.71±0.24	0.90±0.3	0.93±0.08

	BS/BV	1.23±1.66	0.47±0.67	1.41±1.22	0.31±0.47	0.18±0.08	0.60±1.13	0.51±1.18	0.3±0.32	0.72±3.45	0.79±1.36	0.49±0.59	1.11±1.41	3.83±2.26	1.35±3.03	1.31±1.28
	TbTh	1.65±8.26	4.28±6.53	1.49±3.71	6.78±7.75	11.24±5.01	3.95±11.38	4.07±6.56	6.67±6.77	3.12±7.11	2.92±5.27	5.29±14.5	2.43±5.49	0.54±0.39	1.74±5.16	1.54±0.99
	TbN	0.57±0.69	0.23±0.3	0.64±0.52	0.15±0.22	0.08±0.04	0.29±0.52	0.25±0.49	0.15±0.16	0.34±1.23	0.37±0.58	0.24±0.28	0.50±0.6	1.31±0.44	0.59±0.93	0.61±0.5
	TbSp	0.14±0.09	0.12±0.07	0.15±0.11	0.11±0.1	0.09±0.02	0.08±0.03	0.10±0.11	0.09±0.05	0.14±0.15	0.15±0.09	0.12±0.04	0.13±0.09	0.2±0.14	0.15±0.21	0.11±0.04
Dorsal	BV/TV	**0.88±0.05**	**0.96±0.03**	0.91±0.1	0.91±0.14	0.98±0.19	0.95±0.03	0.97±0.12	0.93±0.16	0.96±0.22	0.94±0.1	0.98±0.15	0.95±0.14	0.94±0.05	0.76±0.21	0.81±0.16
	BS/BV	**1.49±0.43**	**0.93±0.7**	1.67±1.26	1.42±1.52	0.55±1.62	0.99±0.31	0.84±1.06	1.31±1.59	0.87±2.17	0.85±1.05	0.67±2.5	1.11±0.96	1.49±0.86	3.89±2.71	3.06±2.75
	TbTh	**1.35±0.37**	**2.2±2.6**	1.2±1.54	1.64±4.12	4.66±5.6	2.02±0.99	2.38±4.32	1.72±2.79	2.85±10.85	3.54±4.25	3.19±3.64	1.84±2.53	1.37±1.29	0.51±0.88	0.70±0.94
	TbN	**0.67±0.17**	**0.44±0.32**	0.74±0.54	0.63±0.62	0.27±0.59	0.47±0.14	0.41±0.43	0.61±0.6	0.41±0.77	0.39±0.45	0.33±0.97	0.53±0.36	0.68±0.4	1.35±0.98	1.17±1.11
	TbSp	0.17±0.1	0.10±0.01	0.11±0.10	0.13±0.13	0.07±0.18	0.10±0.06	0.09±0.13	0.11±0.13	0.10±0.17	0.12±0.11	0.07±0.08	0.10±0.18	0.13±0.07	0.17±0.12	0.12±0.16
Medial	BV/TV	0.92±0.06	0.96±0.03	0.95±0.03	**0.94±0.1**	0.99±0.02	**0.99±0.01**	0.98±0.04	0.99±0.01	0.99±0.01	0.99±0.02	0.99±0.01	0.98±0.01	0.93±0.06	0.95±0.06	0.93±0.06
	BS/BV	0.84±1.39	0.93±0.7	0.90±0.48	**0.46±0.82**	0.26±0.32	**0.20±0.1**	0.6±0.32	0.29±0.12	0.11±0.18	0.28±0.09	0.31±0.25	0.35±0.07	**1.01±0.4**	0.93±0.57	**1.36±1.13**
	TbTh	2.89±3.75	3.7±2.54	2.22±0.83	**4.96±5.04**	7.67±6.97	**10.08±4.8**	3.35±3.29	6.9±3.61	18.29±14.59	7.22±2.35	6.62±4.78	5.78±1.21	**2.02±0.73**	2.16±0.93	**1.56±1.42**
	TbN	0.38±0.59	0.26±0.1	0.43±0.21	**0.21±0.35**	0.13±0.15	**0.10±0.05**	0.29±0.15	0.14±0.06	0.06±0.09	0.14±0.04	0.15±0.12	0.53±0.36	**0.48±0.14**	0.44±0.24	**0.62±0.49**

	TbSp	0.24±0.15	0.16±0.08	0.12±0.02	0.15±0.27	0.08±0.05	0.12±0.05	0.12±0.1	0.09±0.04	0.12±0.05	0.08±0.09	0.07±0.03	0.10±0.04	0.15±0.08	0.11±0.07	0.12±0.03
Plantar	BV/TV	0.84±0.12	0.95±0.04	0.74±0.41	**0.97±0.05**	0.98±0.01	**0.98±0.28**	0.95±0.06	0.98±0.02	0.98±0.02	0.95±0.08	0.98±0.01	0.97±0.27	**0.85±0.2**	0.89±0.11	**0.93±0.04**
	BS/BV	1.62±2.04	0.87±0.64	3.37±4.14	**0.66±1.1**	0.49±0.45	**0.40±3.72**	1.01±0.67	0.41±0.46	0.46±0.24	0.77±1.19	0.46±0.44	0.61±3.97	**2.51±2.8**	1.59±1.59	**1.15±0.47**
	TbTh	1.25±0.83	2.55±1.79	0.70±2.44	**3.4±4.81**	4.38±5.57	**5.03±4.27**	2.02±2.74	4.95±4.88	4.36±2.5	2.82±3.37	4.36±4.71	3.33±3.4	**0.80±0.62**	1.26±2.11	**1.76±0.62**
	TbN	0.67±0.7	0.41±0.3	1.12±0.94	**0.32±0.5**	0.24±0.22	**0.20±1.09**	0.48±0.29	0.2±0.22	0.06±0.09	0.36±0.53	0.23±0.21	0.29±1.19	**1.06±0.72**	0.69±0.65	**0.54±0.2**
	TbSp	0.19±0.1	0.11±0.08	0.21±0.23	0.08±0.04	0.07±0.02	0.10±0.14	0.1±0.09	0.10±0.04	0.10±0.06	0.09±0.13	0.08±0.02	0.12±0.11	0.15±0.06	0.13±0.09	0.14±0.05

Note: Values are medians±interquartile range, measured in millimeters. SAA=South African Africans, SAED=South Africans of European descent, SAMA=South Africans of Mixed Ancestry, BB/TV=Bone volume fraction, BS/BV=Bone surface volume, TbTh=Trabecular thickness, TbN=Trabecular number, TbSp=Trabecular spacing. The highlighted areas in **Bold** represent statistically significant differences *p<0.05*.

Table 5: Age matched comparisons of trabecular structure parameters on different surfaces of the bone across population groups in the 31-40-year group

First metatarsal bone																
Level of bone		Proximal Diaphysis			Above Nutrient Foramina			Nutrient foramina			Below Nutrient Foramina			Distal Diaphysis		
Surface	Trabecular	SAA	SAED	SAMA	SAA	SAED	SAMA	SAA	SAED	SAMA	SAA	SAED	SAMA	SAA	SAED	SAMA
Lateral	BV/TV	0.91±0.24	0.95±0.12	0.75±0.27	0.98±0.02	0.98±0.02	0.88±0.28	0.99±0.01	0.99±0.02	0.92±0.22	0.99±0.01	0.96±0.06	0.97±0.26	0.86±0.11	0.92±0.14	0.64±0.52
	BS/BV	1.26±1.46	1.23±1.64	3.31±2.1	0.46±0.23	0.41±0.47	2.21±3.59	0.37±0.26	0.24±0.43	1.24±3.26	0.37±0.13	0.49±0.54	0.62±3.33	1.56±1.57	1.29±1.29	4.43±6.92
	TbTh	1.6±1.07	2.21±3.04	0.60±2.23	4.35±3.89	5.2±8.88	1.27±5.9	5.61±6.38	8.3±10.18	1.81±7.01	5.41±2.21	4.10±7.6	3.25±4.73	1.28±1.3	1.63±3.93	0.51±0.9
	TbN	0.57±0.36	0.58±0.68	1.12±0.83	0.22±0.11	0.2±0.23	0.91±1.22	0.18±0.13	0.12±0.21	0.57±1.13	0.18±0.06	0.24±0.24	0.3±1.05	0.67±0.62	0.59±0.51	1.3±0.85
	TbSp	0.16±0.23	0.09±0.07	0.20±0.191	0.08±0.06	0.10±0.03	0.15±0.16	**0.08±0.02**	**0.10±0.01**	0.16±0.11	0.08±0.04	0.14±0.16	0.12±0.16	0.15±0.12	0.13±0.13	0.25±0.27
Dorsal	BV/TV	0.82±0.18	0.90±0.14	0.86±0.65	0.98±0.04	0.93±0.12	0.82±0.33	**0.96±0.06**	0.94±0.23	**0.84±0.21**	0.96±0.03	0.88±0.18	0.78±0.27	0.84±0.3	0.77±0.14	0.79±0.37
	BS/BV	2.11±2.05	1.8±3.07	2.63±6.01	0.42±0.39	1.0±2.65	1.72±3.98	0.75±0.76	0.85±4.46	2.46±3.58	0.69±0.31	1.51±3.29	2.51±3.48	2.05±3.65	3.0±1.71	2.3±4.38
	TbTh	1.03±0.92	1.33±2.54	0.96±3.35	4.77±3.32	2.01±3.36	1.96±2.88	2.89±8.32	2.35±5.26	1.34±1.79	2.94±1.88	1.33±8.68	0.88±4.11	1.82±4.36	0.67±0.59	1.11±2.16
	TbN	0.79±0.72	0.8±1.21	0.96±1.15	0.21±0.18	0.47±1.1	0.60±1.23	0.36±0.35	0.40±1.52	0.85±1.29	0.33±0.14	0.67±1.24	0.93±1.13	0.78±1.16	1.16±0.53	0.86±1.07
	TbSp	0.2±0.18	0.11±0.07	0.13±0.33	0.09±0.08	0.10±0.11	0.15±0.27	0.11±0.17	0.13±0.07	0.26±0.12	0.11±0.05	0.15±0.09	0.19±0.17	0.17±0.13	0.25±0.11	0.24±0.16

Medial	BV/TV	0.88±0.16	0.82±0.17	0.79±0.25	0.98±0.07	0.95±0.06	0.87±0.14	0.99±0.03	0.91±0.21	0.84±0.32	0.98±0.03	0.97±0.28	0.85±0.26	0.57±0.31	0.66±0.07	0.46±0.37
	BS/BV	1.91±1.29	3.52±2.1	2.34±1.16	0.52±1.12	0.94±1.16	1.81±1.36	0.33±0.41	1.65±1.85	1.57±3.62	0.46±0.48	0.82±3.04	2.24±4.21	5.23±3.66	4.21±1.53	8.98±6.93
	TbTh	1.06±0.62	0.59±0.5	0.88±0.45	3.92±2.91	2.25±2.7	1.11±2.94	6.14±6.83	1.35±2.12	1.5±2.85	4.44±2.7	2.99±6.82	0.96±2.3	0.39±0.22	0.48±0.19	0.23±0.28
	TbN	0.85±0.36	1.3±0.7	0.89±0.23	0.25±0.48	0.45±0.52	0.75±0.6	0.16±0.2	0.66±0.74	0.62±1.06	0.22±0.22	0.40±0.95	0.95±1.26	1.69±0.45	1.41±0.5	1.86±0.61
	TbSp	0.14±0.13	0.15±0.1	0.25±0.25	0.1±0.04	0.95±1.260.10±0.05	0.15±0.14	0.09±0.03	0.14±0.24	0.16±0.26	0.09±0.04	0.08±0.16	0.18±0.07	0.27±0.22	0.23±0.11	0.27±0.18
Plantar	BV/TV	0.78±0.14	0.81±0.2	0.68±0.52	0.96±0.1	0.92±0.14	0.87±0.4	0.97±0.09	0.92±0.08	0.93±0.16	0.98±0.1	0.96±0.04	0.93±0.36	0.93±0.26	0.73±0.22	0.76±0.44
	BS/BV	4.09±2.01	3.19±2.35	4.01±7.06	0.77±1.61	1.51±2.6	1.98±2.8	0.64±1.17	1.11±1.28	1.06±2.47	0.57±0.71	0.91±0.92	1.41±3.53	1.08±2.58	2.55±2.69	3.58±4.41
	TbTh	0.49±0.2	0.64±0.92	0.66±1.01	2.62±5.05	2.1±11.07	1.36±2.12	3.16±3.97	2.38±2.69	1.93±4.53	3.88±3.54	2.27±2.52	1.58±1.74	1.86±2.13	0.86±0.86	0.57±1.5
	TbN	1.6±0.42	1.17±0.83	0.95±1.4	0.37±0.68	0.68±1.08	0.67±0.78	0.31±0.5	0.5±0.56	0.49±0.94	0.28±0.29	0.43±0.42	0.65±0.7	0.5±0.73	0.9±0.74	1.18±0.96
	TbSp	0.14±0.05	0.15±0.14	0.19±0.4	0.1±0.07	0.11±0.04	0.16±0.38	0.09±0.08	0.13±0.09	0.14±0.05	0.09±0.16	0.08±0.04	0.15±0.27	0.15±0.15	0.26±0.15	0.20±0.31

Fifth metatarsal bone

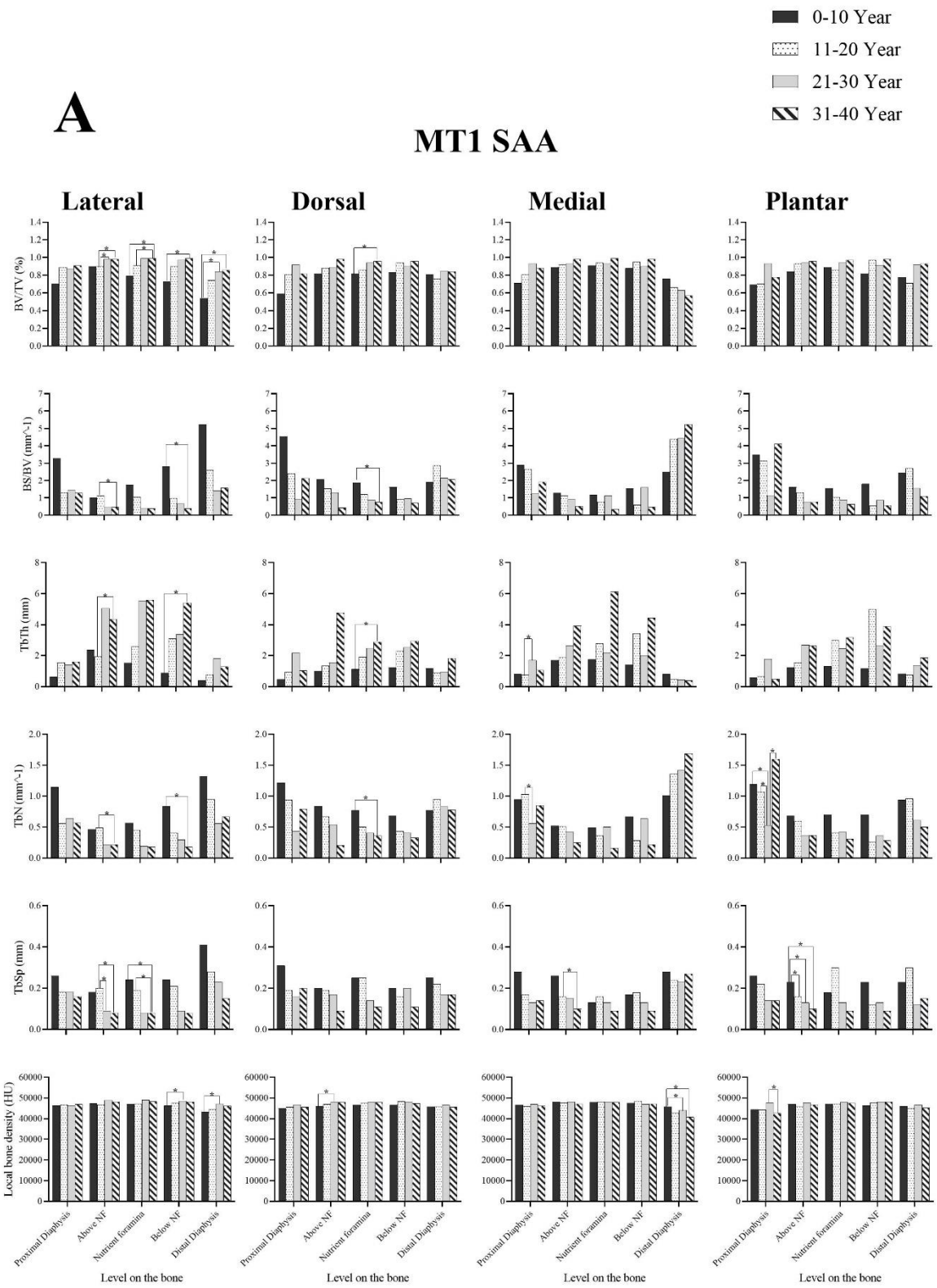
Proximal Diaphysis			Above Nutrient Foramina			Nutrient foramina			Below Nutrient Foramina			Distal Diaphysis		
SAA	SAED	SAMA	SAA	SAED	SAMA	SAA	SAED	SAMA	SAA	SAED	SAMA	SAA	SAED	SAMA

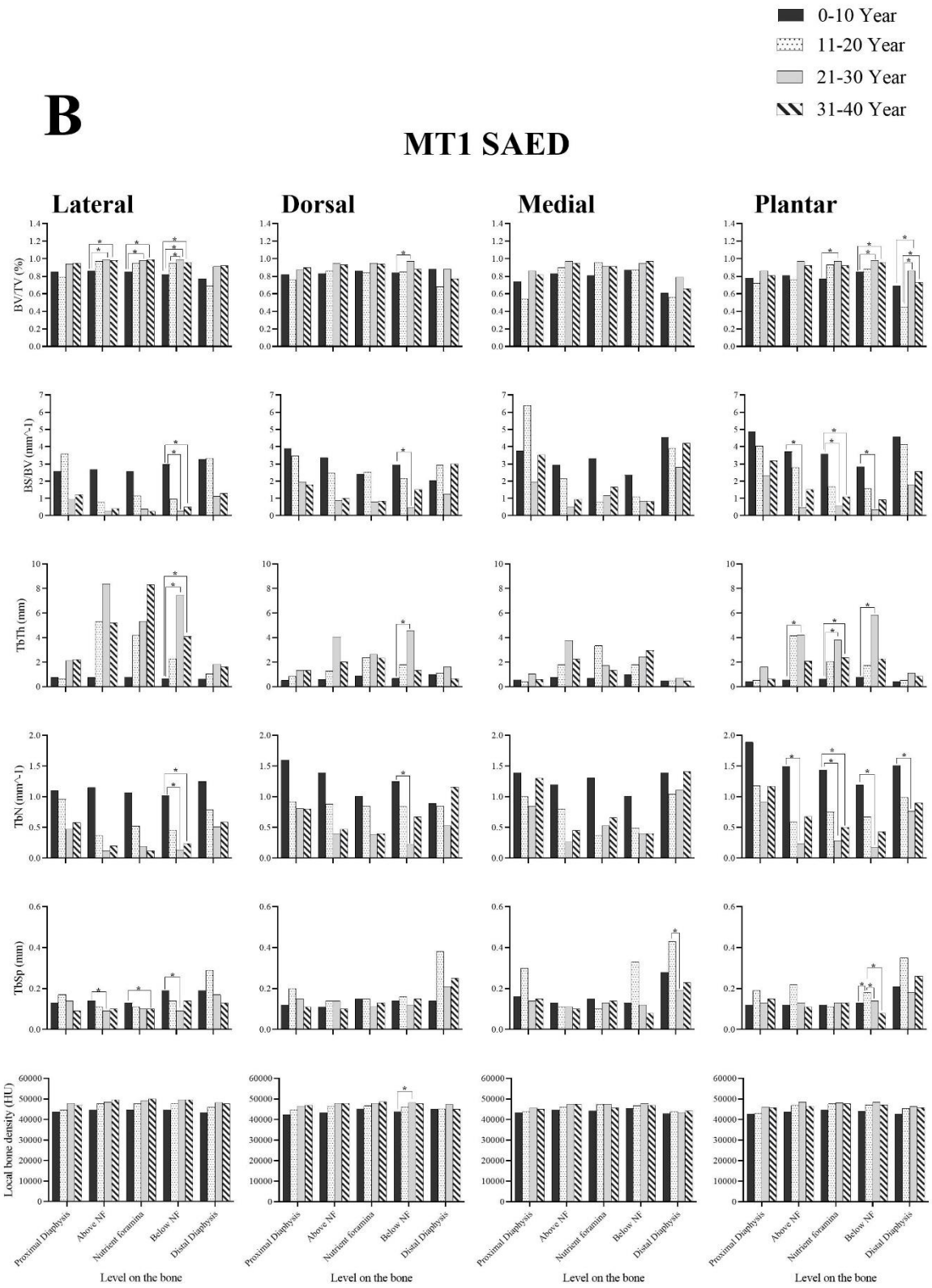
Lateral	BV/TV	0.92±0.06	0.98±0.03	0.94±0.1	0.98±0.03	0.99±0.04	0.95±0.06	0.97±0.04	0.98±0.13	0.96±0.07	0.98±0.03	0.98±0.06	0.90±0.16	0.89±0.13	0.84±0.37	0.87±0.15
	BS/BV	1.41±0.97	0.40±0.46	1.05±1.27	0.42±0.57	0.25±1.1	0.92±1.02	0.6±0.65	0.44±1.39	0.88±0.98	0.42±0.53	0.32±1.18	1.07±1.65	1.87±0.59	2.71±3.55	2.94±3.93
	TbTh	1.42±1.79	4.95±3.32	2.01±1.57	5.98±8.85	8.09±7.79	2.48±10.54	3.36±6.49	4.73±4.9	2.27±2.18	5.2±5.42	6.45±7.4	1.91±1.76	1.09±0.32	1.05±1.29	1.09±1.73
	TbN	0.65±0.41	0.2±0.22	0.49±0.51	0.20±0.27	0.12±0.52	0.43±0.47	0.29±0.3	0.21±0.55	0.42±0.42	0.20±0.25	0.16±0.53	0.48±0.59	0.84±0.15	0.91±0.94	1.22±1.47
	TbSp	0.12±0.02	0.10±0.03	0.14±0.07	0.08±0.04	0.08±0.03	0.13±0.03	0.11±0.03	0.10±0.1	0.11±0.04	0.09±0.03	0.11±0.07	0.17±0.16	0.13±0.13	0.14±0.23	0.12±0.05
Dorsal	BV/TV	0.93±0.1	0.95±0.21	0.83±0.45	**0.98±0.01**	0.95±0.09	**0.83±0.34**	0.98±0.07	0.92±0.1	0.87±0.27	0.97±0.03	0.96±0.11	0.92±0.23	0.78±0.21	0.82±0.18	0.88±0.11
	BS/BV	1.34±2.0	1.34±3.49	2.19±6.72	**0.63±0.35**	1.37±1.12	**2.50±3.94**	0.41±0.88	1.85±1.54	2.31±4.06	0.79±0.34	0.88±2.48	1.73±2.97	3.0±2.64	2.71±2.97	2.3±1.24
	TbTh	1.73±2.16	1.84±2.12	0.93±0.85	**3.18±1.46**	1.46±2.09	**1.06±1.57**	4.83±2.82	1.08±6.16	1.4±2.59	2.57±1.26	2.34±3.41	1.26±2.16	0.70±0.65	0.74±0.53	0.88±0.38
	TbN	0.61±0.84	0.63±1.19	0.92±0.76	**0.31±0.17**	0.65±0.47	**0.96±1.03**	0.20±0.38	0.83±0.71	0.95±1.33	0.38±0.16	0.42±1.03	0.80±0.95	1.15±0.7	1.1±0.76	1.01±0.38
	TbSp	0.1±0.07	0.09±0.07	0.19±0.23	0.07±0.01	0.07±0.06	0.16±0.16	0.08±0.08	0.09±0.07	0.12±0.1	0.09±0.04	0.09±0.05	0.10±0.11	0.19±0.09	0.18±0.04	0.12±0.07
Medial	BV/TV	0.96±0.14	0.96±0.02	0.96±0.05	0.96±0.09	0.98±0.02	0.99	0.99±0.04	0.99±0.02	0.97±0.07	0.99±0.02	0.98±0.01	0.98±0.02	0.97±0.08	0.94±0.07	0.97±0.02
	BS/BV	0.7±1.33	0.72±0.26	0.90±0.36	0.76±1.07	0.41±0.26	0.21±0.16	0.29±0.57	0.26±0.34	0.66±0.86	0.31±0.3	0.35±0.17	0.36±0.54	0.79±1.07	1.32±1.39	0.73±0.58
	TbTh	3.02±2.86	2.78±0.92	2.24±0.75	3.98±8.66	4.86±3.34	9.96±11.98	7.51±7.22	8.38±13.76	3.92±6.18	6.71±4.52	5.75±3.5	5.58±5.02	2.6±2.38	1.56±2.87	2.95±2.84

	TbN	0.33±0.51	0.35±0.12	0.43±0.14	0.35±0.49	0.2±0.12	0.10±0.08	0.14±0.26	0.13±0.16	0.31±0.4	0.15±0.14	0.17±0.08	0.18±0.26	0.39±0.45	0.62±0.61	0.35±0.27
	TbSp	0.13±0.12	0.11±0.05	0.11±0.07	0.09±0.11	0.08±0.05	0.08±0.04	0.08±0.07	0.07±0.03	0.09±0.1	0.08±0.03	0.10±0.04	0.08±0.03	0.08±0.06	0.09±0.03	0.08±0.02
Plantar	BV/TV	0.94±0.21	0.93±0.06	0.93±0.29	0.98±0.03	0.99±0.02	0.95±0.13	0.98±0.01	0.98±0.01	0.95±0.23	0.99±0.03	0.99±0.01	0.98±0.03	0.97±0.26	0.96±0.08	0.91±0.31
	BS/BV	0.86±2.12	1.33±0.64	1.44±2.84	0.41±0.49	0.43±0.43	0.83±1.78	0.5±0.1	0.40±0.24	1.06±2.94	0.44±0.18	0.41±0.3	0.52±0.96	0.85±4.39	0.99±0.81	1.48±4.77
	TbTh	2.52±3.86	1.52±0.88	1.51±1.7	4.93±4.42	5.61±5.99	2.67±5.14	4.0±0.99	4.99±2.41	2.45±3.38	4.57±1.41	4.97±3.4	4.02±4.16	2.35±2.12	2.05±1.87	1.82±2.35
	TbN	0.40±0.73	0.62±0.28	0.66±0.75	0.2±0.23	0.21±0.21	0.39±0.73	0.24±0.05	0.2±0.11	0.50±1.0	0.22±0.08	0.2±0.14	0.25±0.45	0.41±1.31	0.48±0.34	0.66±1.34
	TbSp	0.14±0.13	0.11±0.08	0.12±0.17	0.08±0.05	0.07±0.02	0.13±0.09	0.08±0.03	0.08±0.04	0.11±0.12	0.06±0.07	0.06±0.02	0.07±0.03	0.08±0.09	0.11±0.11	0.14±0.09

Note: Values are medians±interquartile range, measured in millimeters. SAA=South African Africans, SAED=South Africans of European descent, SAMA=South Africans of Mixed Ancestry, BB/TV=Bone volume fraction, BS/BV=Bone surface volume, TbTh=Trabecular thickness, TbN=Trabecular number, TbSp=Trabecular spacing. The highlighted areas in **Bold** represent statistically significant differences $p<0.05$.

Generally, in all the population groups and all surfaces and levels of the first and fifth metatarsal bones, the BV/TV and TbTh gradually increased from the 0-10-year group, peaked in the 21-30-year group and then decreased in the 31-40-year group. The BS/BV, TbN and TbSp gradually decreased from the 0-10-year group and reached the lowest values in the 21-30-year group and then increased in the 31-40-year group. On the first metatarsal bone, ontogenetic differences of the trabecular structures were more evident on the lateral surface in the SAA (Fig. 1A), SAED (Fig. 1B), and SAMA (Fig. 1C), compared to other surfaces (i.e. dorsal, medial, and plantar). On the fifth metatarsal bone, ontogenetic differences of the trabecular structure were more evident on the medial surface in the SAA (Fig. 2A), SAED (Fig. 2B), and SAMA (Fig. 2C), compared to other surfaces (i.e. lateral, dorsal, and plantar).


A
MT1 SAA
0-10 Year
11-20 Year
21-30 Year
31-40 Year
Lateral
Dorsal
Medial
Plantar
BV/TV (%)
BS/BV (mm^-1)
TbTh (mm)
TbN (mm^-1)
TbSp (mm)
Local bone density (HU)
Proximal Diaphysis
Above NF
Nutrient foramina
Below NF
Distal Diaphysis
Level on the bone


B
MT1 SAED
0-10 Year
11-20 Year
21-30 Year
31-40 Year
Lateral
Dorsal
Medial
Plantar
BV/TV (%)
BS/BV (mm^-1)
TbTh (mm)
TbN (mm^-1)
TbSp (mm)
Local bone density (HU)
Proximal Diaphysis
Above NF
Nutrient foramina
Below NF
Distal Diaphysis
Level on the bone

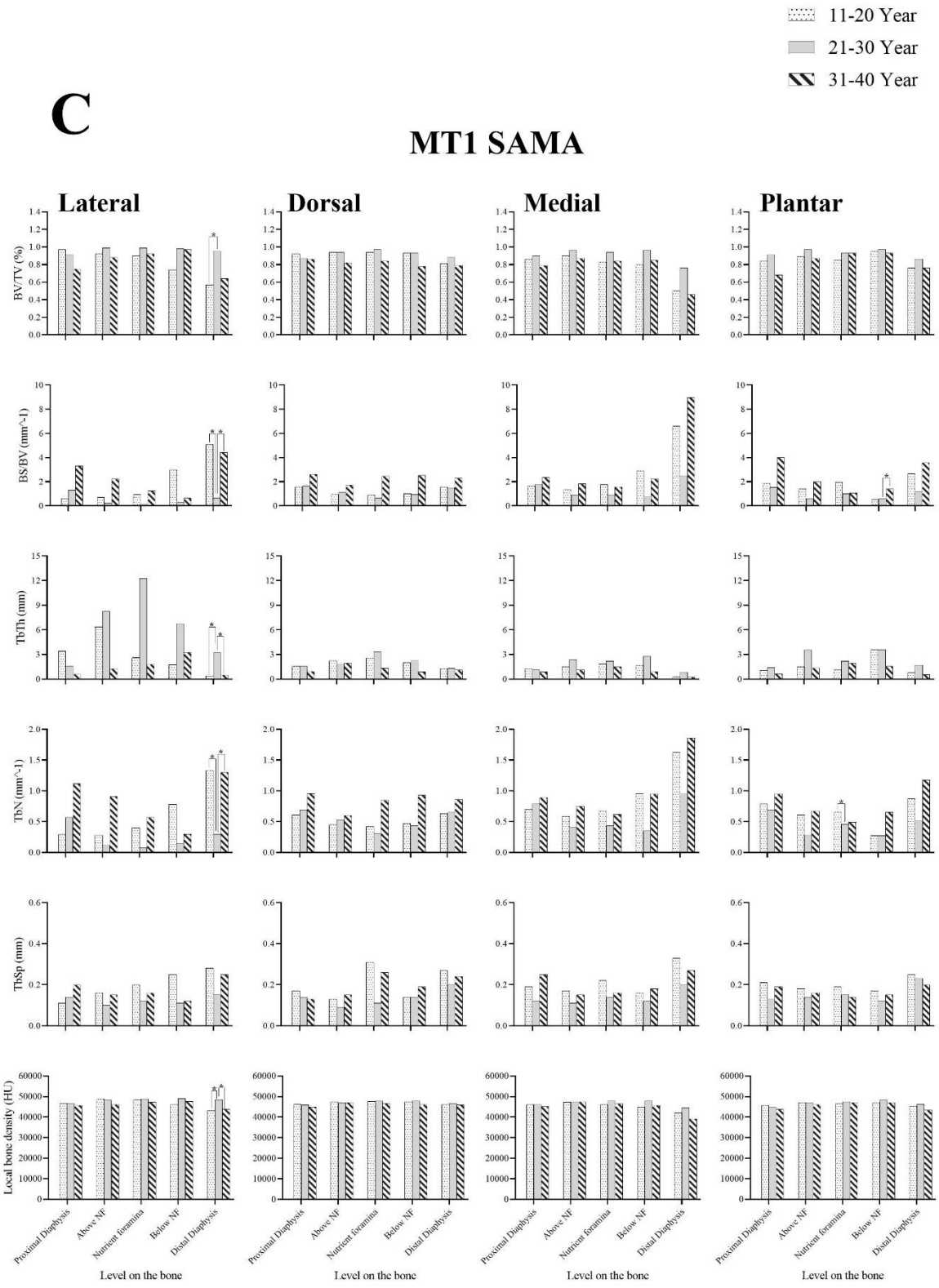
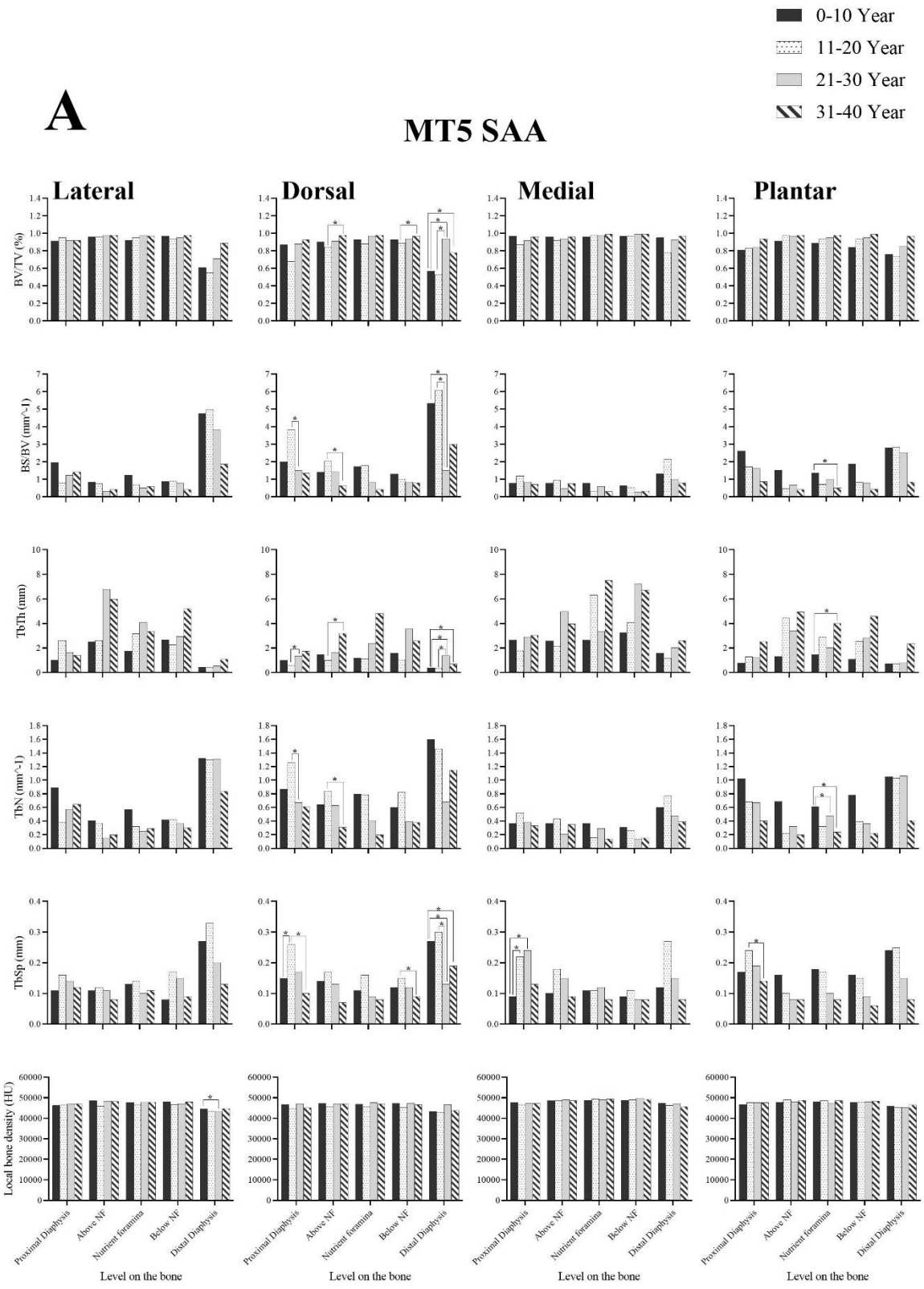
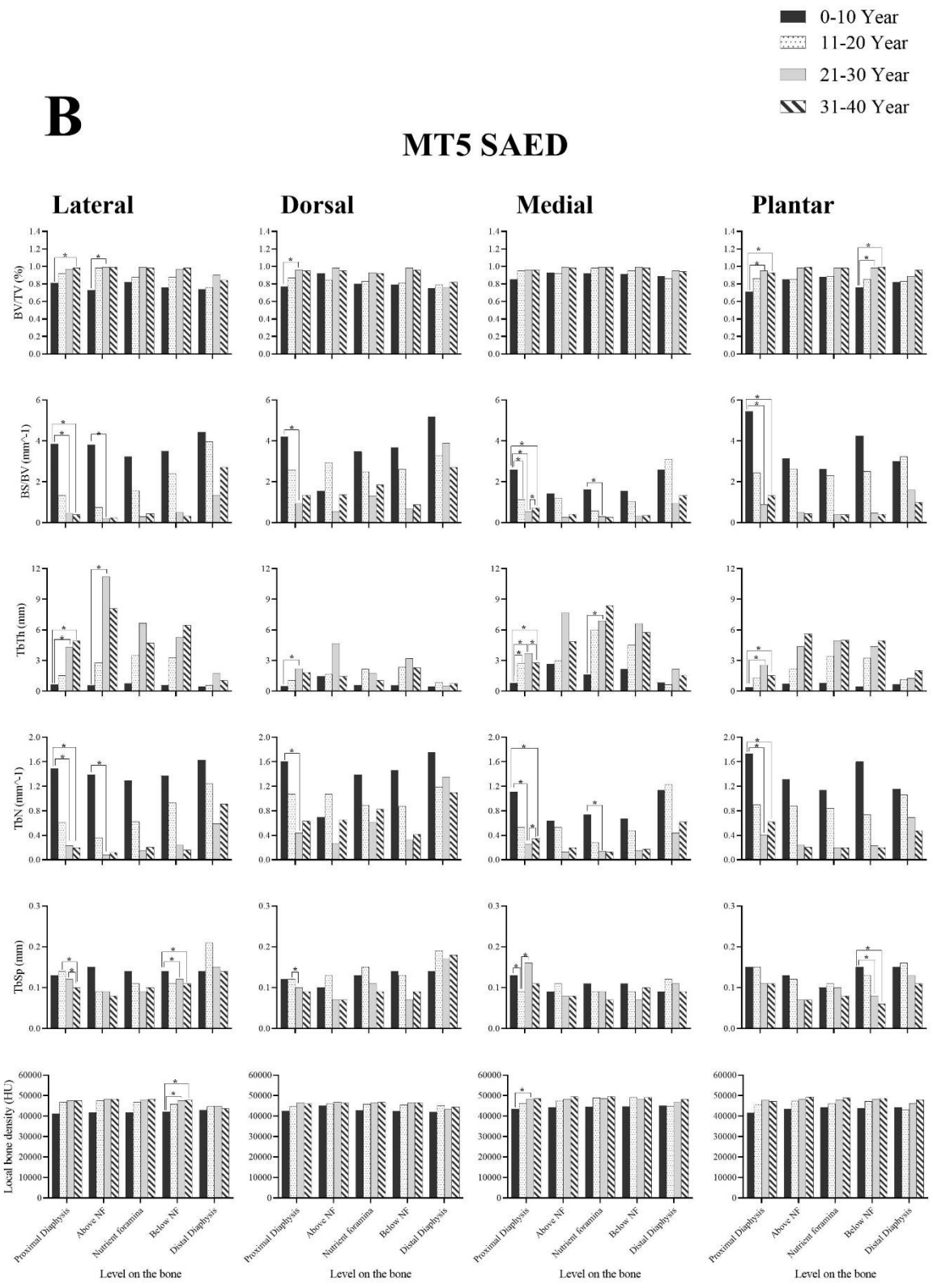


Figure 1: A plate of graphs showing age-related trabecular structural changes at different levels and surfaces of the first metatarsal bone in the **A**. SAA (South African Africans), **B.** SAED (South Africans of European descent) and **C.** SAMA (South Africans of Mixed Ancestry) populations. Bars indicate median trabecular values. MT1= First metatarsal bone,

BV/TV= Bone volume fraction, BS/BV= Bone surface volume, TbTh=Trabecular thickness, TbN=Trabecular number, TbSp= Trabecular spacing, mm= millimetres, %= Percentage, *= Significant median differences $p \leq 0.05$, HU= Hounsfield units.




B
MT5 SAED
0-10 Year
11-20 Year
21-30 Year
31-40 Year
Lateral
Dorsal
Medial
Plantar
BV/TV (%)
BS/BV (mm^-1)
TbTh (mm)
TbN (mm^-1)
TbSp (mm)
Local bone density (HU)
Proximal Diaphysis
Above NF
Nutrient foramina
Below NF
Distal Diaphysis
Level on the bone

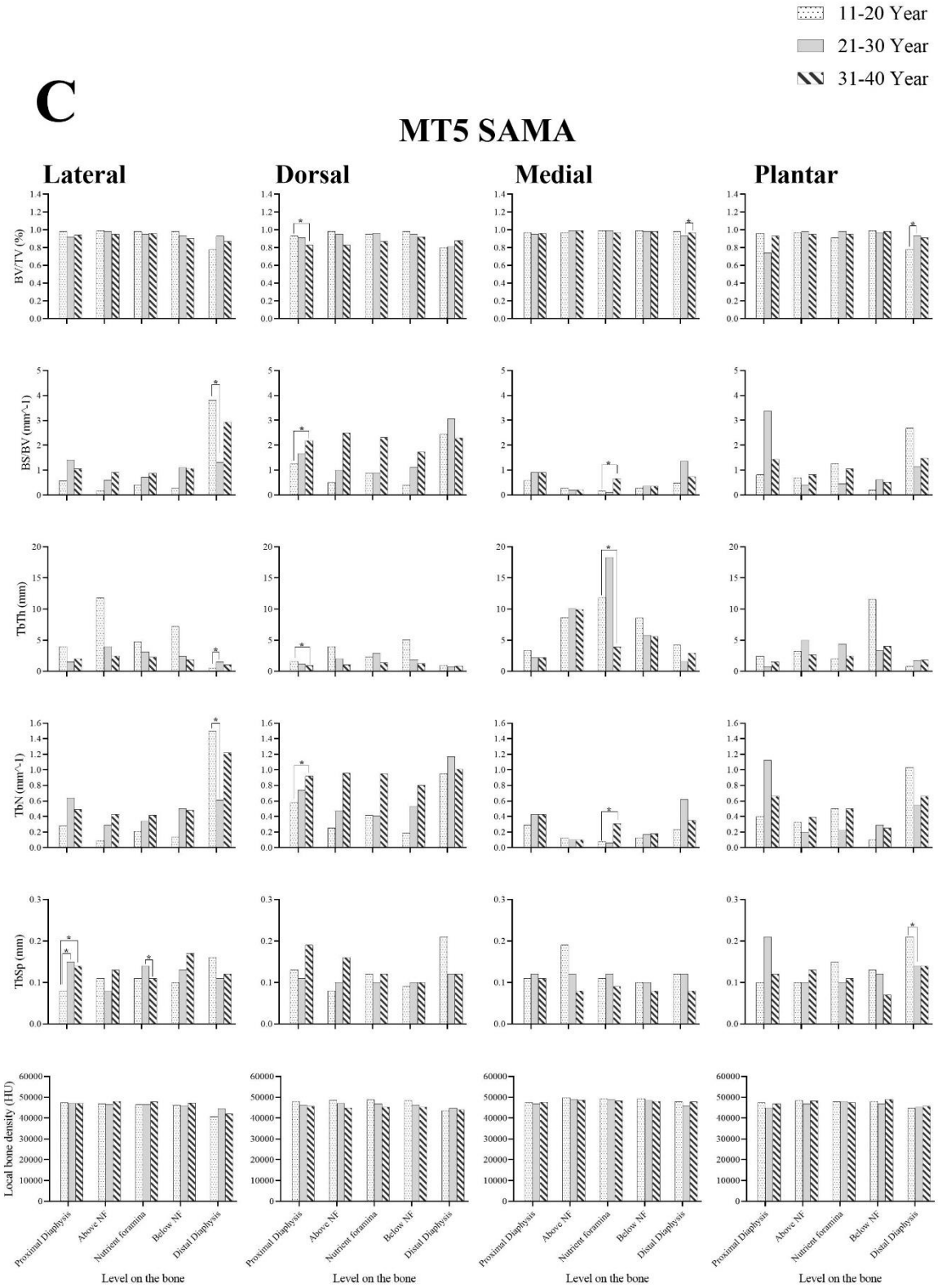
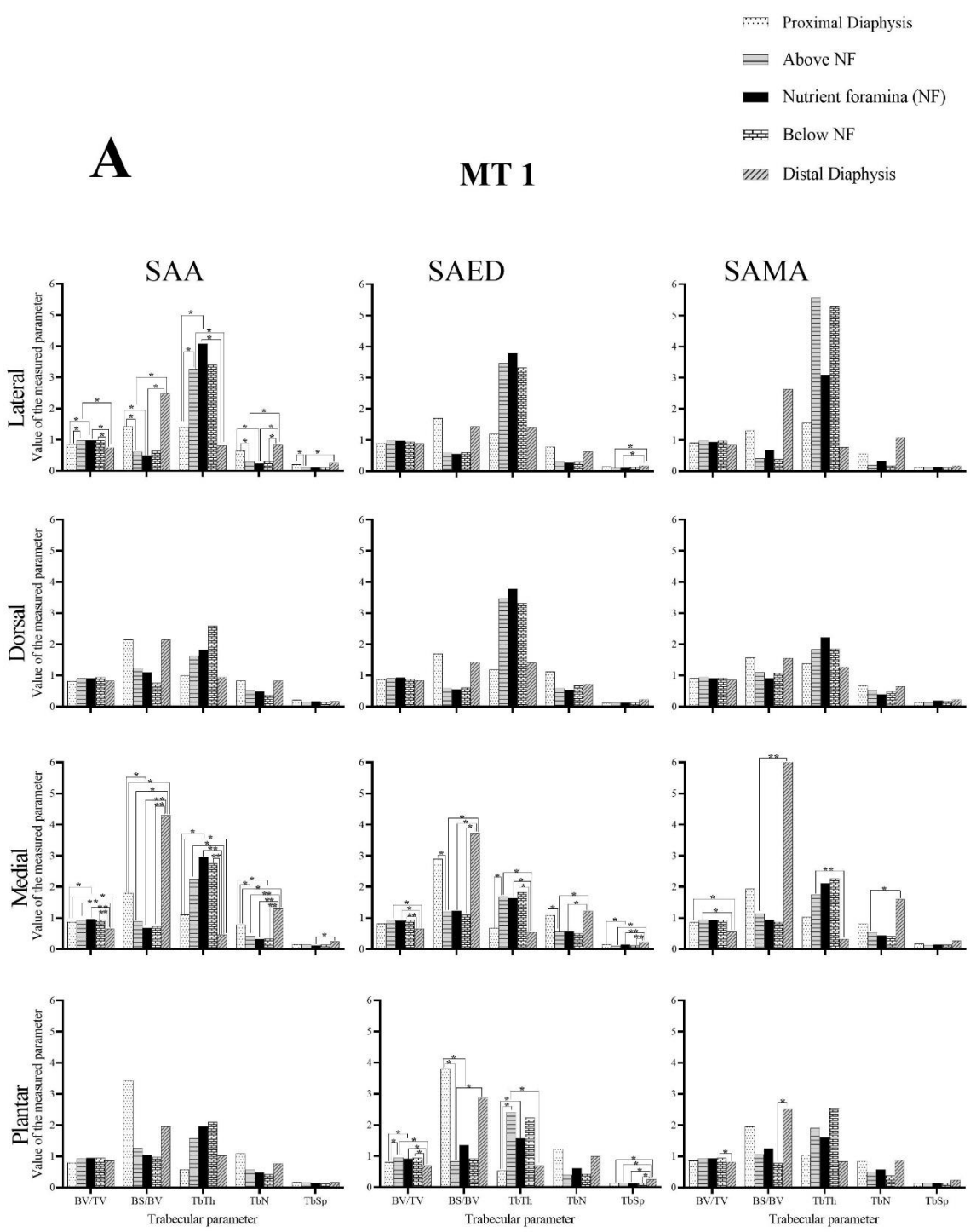


Figure 2: A plate of graphs showing age-related trabecular structural changes at different levels and surfaces of the fifth metatarsal bone in the **A**. SAA (South African Africans), **B.** SAED (South Africans of European descent) and **C.** SAMA (South Africans of Mixed

Ancestry) populations. Bars indicate median trabecular values. MT5= Fifth metatarsal bone, BV/TV= Bone volume fraction, BS/BV= Bone surface volume, TbTh=Trabecular thickness, TbN=Trabecular number, TbSp= Trabecular spacing, mm= millimetres, %= Percentage, *= Significant median differences $p \leq 0.05$, HU= Hounsfield units.

3.2 Variability in trabecular morphological parameters in the first and fifth metatarsals in pooled population, sex, and age groups

The BV/TV and TbTh increased from the proximal diaphysis to the nutrient foramen (NF) level and then decreased to the distal diaphysis in all three populations across all age groups *($p \leq 0.05$)*. The BS/BV, TbN, and TbSp decreased from the proximal diaphysis towards the NF and then increased towards the distal diaphysis. The ANF, NF, and BNF showed significantly higher BV/TV and TbTh but lower BS/BV, TbN, and TbSp than the proximal and distal diaphyses levels *($p \leq 0.05$)* for both the first (Fig. 3A) and fifth (Fig. 3B) metatarsal bones. There were no statistically significant median differences for all the trabecular morphologic parameters (BV/TV, BS/BV, TbTh, TbN and TbSp) at the ANF, NF, and BNF levels *($p > 0.05$).*


A
MT 1
Proximal Diaphysis
Above NF
Nutrient foramina (NF)
Below NF
Distal Diaphysis
SAA
SAED
SAMA
Lateral
Dorsal
Medial
Plantar
Value of the measured parameter
BV/TV
BS/BV
TbTh
TbN
TbSp
Trabecular parameter

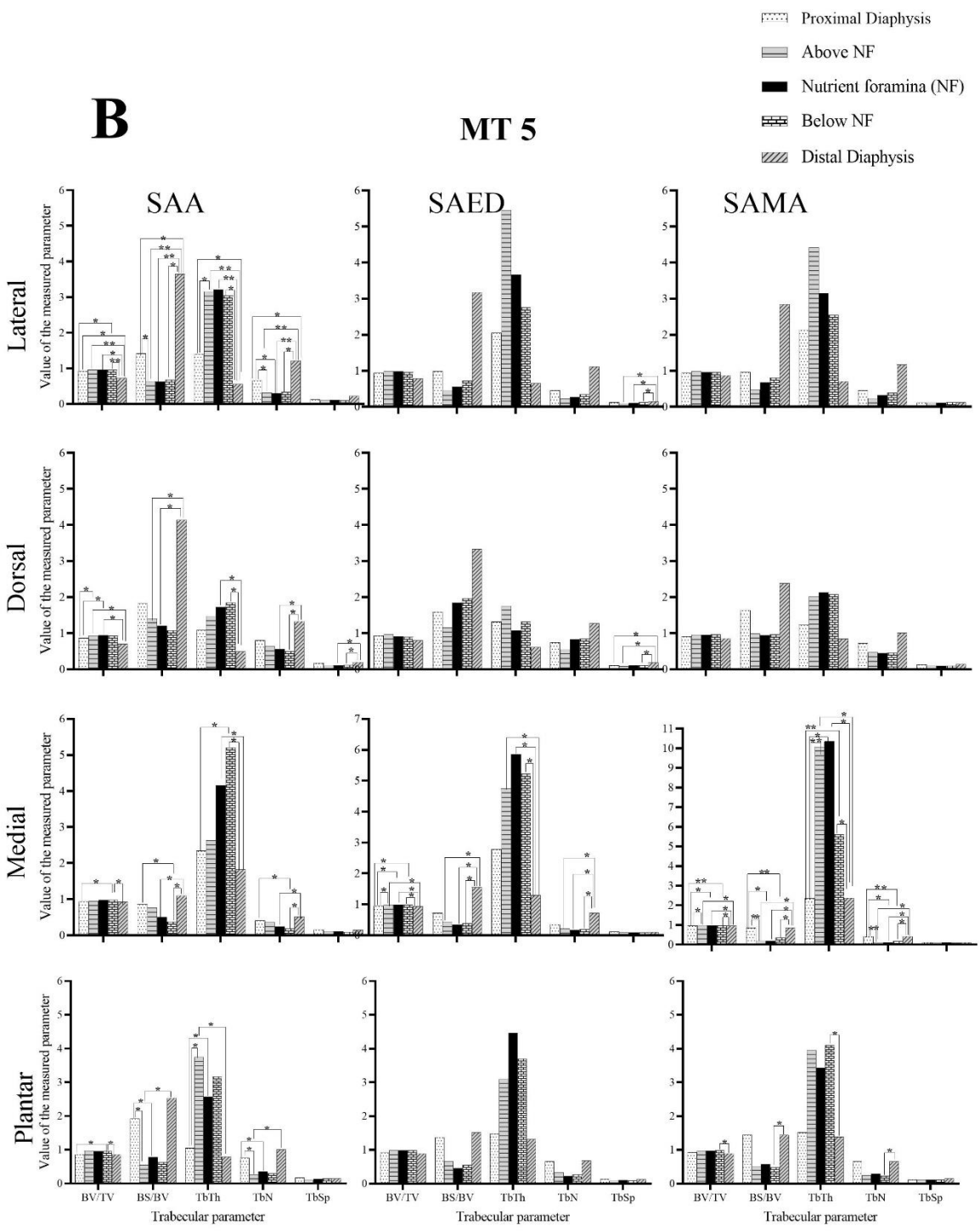


Figure 3: A plate of graphs showing trabecular quality at different levels of the metatarsal bones within each population group in pooled age groups. **A.** First metatarsal bone. **B.** Fifth metatarsal bone. Bars indicate median trabecular values. MT1= First metatarsal bone, BV/TV= Bone volume fraction, BS/BV= Bone surface volume, TbTh= Trabecular thickness, TbN= Trabecular number, TbSp= Trabecular spacing, SAA= South African Africans,

SAED= South Africans of European descent, SAMA= South Africans of Mixed ancestry, *= Significant median differences $p \leq 0.05$, **= Significant median differences $p < 0.0001$.

3.3. Variations of trabecular morphological parameters on the first and fifth metatarsal bone surfaces in pooled population, sex, and age groups

The median comparisons of each trabecular morphologic parameter at the different levels and surfaces of the first and fifth metatarsal bones are presented in Figure 4. On all the first metatarsals utilised, the nutrient foramen was located on the lateral surface of the bone. On the first metatarsal bones, statistically significant differences in the trabecular morphologic parameters and the bone surfaces were only found at the proximal and distal diaphyses regions *($p \leq 0.05$).* At the distal diaphysis level of the first metatarsal bone, the medial surface had statistically significant higher BS/BV and TbN than the lateral *($p < 0.0001$),* dorsal *($p < 0.0001$),* and plantar *($p < 0.0001$)* surfaces. At the distal diaphysis level of the first metatarsal bone, the medial surface had statistically significant lower BV/TV and TbTh than the lateral *($p < 0.0001$),* dorsal *($p < 0.0001$)* and plantar *($p < 0.0001$)* surfaces. At the proximal diaphysis level of the first metatarsal bone, the lateral surface had significantly higher BV/TV but lower BS/BV than the plantar surface *($p < 0.0001$).* On all the fifth metatarsals scanned, the nutrient foramen was located on the medial surface of the bone. The medial surface of the fifth metatarsal had statistically significant higher BV/TV and TbTh but lower BS/BV, TbN, and TbSp than the lateral *($p < 0.0001$),* dorsal *($p < 0.0001$)* and plantar *($p < 0.0001$)* surfaces at all levels of the bone (ANF, NF, BNF, proximal, and distal diaphyses) (Fig. 4).

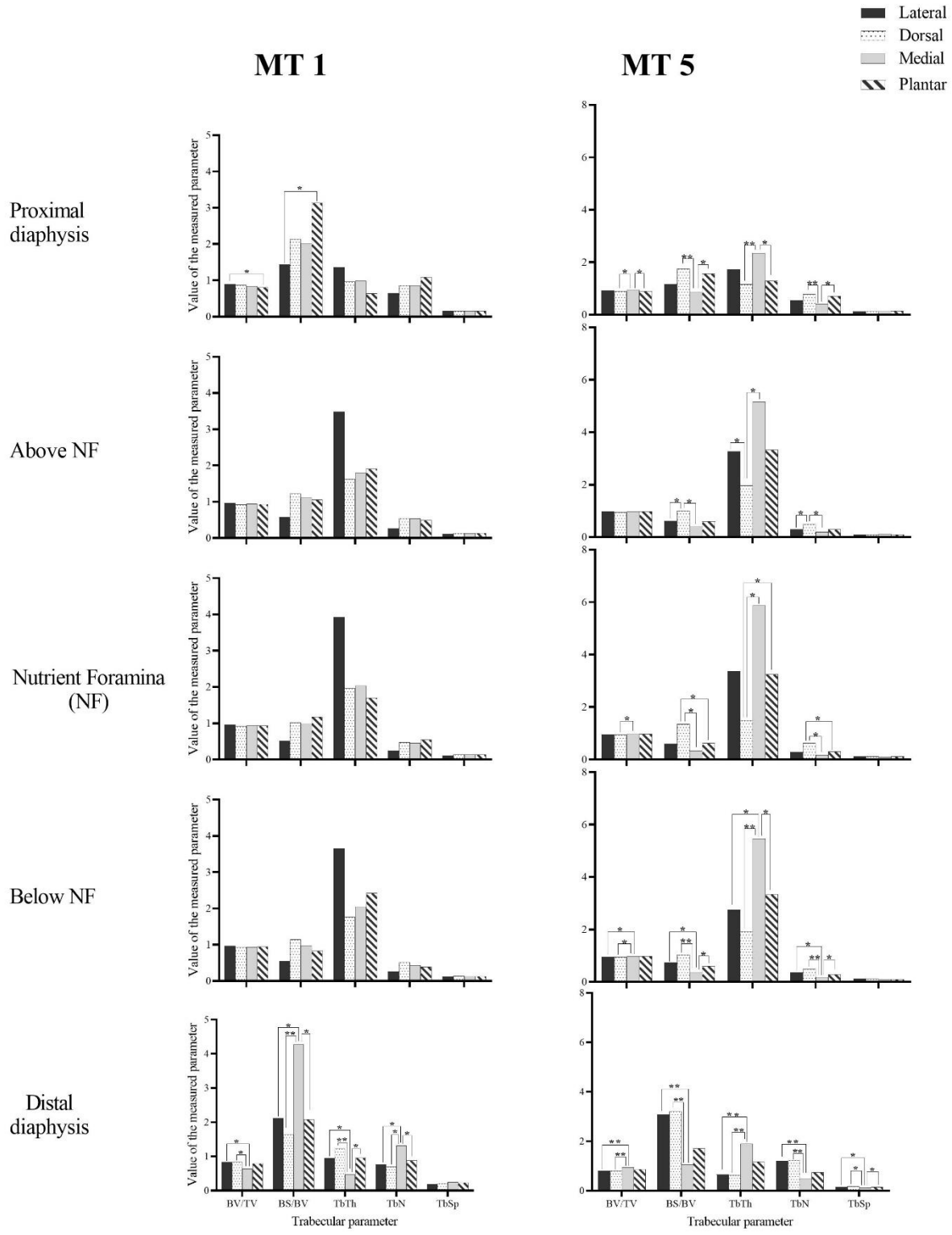
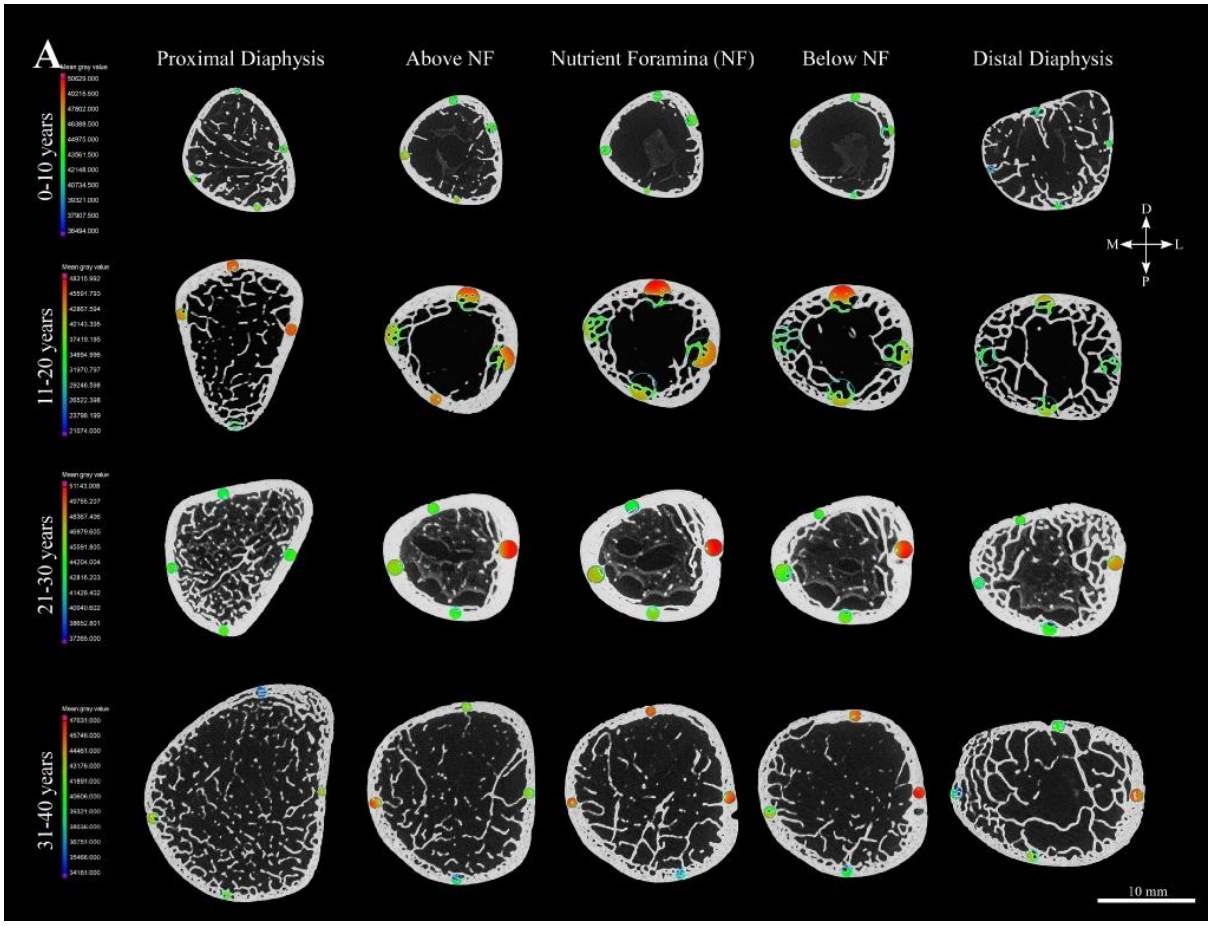


Figure 4: A plate of graphs showing variations of trabecular bone quality on the first and fifth metatarsal bone surfaces in a pooled population and age group. Bars indicate median trabecular values. MT1= First metatarsal bone, MT5= Fifth metatarsal bone, BV/TV= Bone volume fraction, BS/BV= Bone surface volume, TbTh= Trabecular thickness, TbN=

Trabecular number, TbSp= Trabecular spacing. *= Significant median differences $p \leq 0.05$, **= Significant median differences $p < 0.0001$.

3.4 Variations in the volumetric local bone density distribution in the first and fifth metatarsal bones

The cross-section of segmented μCT and colour maps of the distribution of local bone density on the first and fifth metatarsal bones are shown in Figures 5A and 5B, respectively. The local bone density showed no statistically significant ontogenetic differences at all levels and on all surfaces of the first and fifth metatarsal bones *(p>0.05)* but gradually increased from the 0-10-year group, peaked in the 21-30-year group and then decreased in the 31-40-year group in the pooled populations. In a pooled population, sex, and age sample, the local bone density increased from the proximal diaphysis towards the NF level and then decreased towards the distal diaphysis level in both the first and fifth metatarsal bones. The surfaces of the proximal and distal diaphyses level of the first metatarsal bone showed statistically significant differences in the local bone density *(p≤0.05)*. At the distal diaphysis level of the first metatarsal, the local bone density was lower on the medial surface compared to the dorsal *(p≤0.05)* and plantar *(p≤0.05)* surfaces. At the proximal diaphysis level, the local bone density was lower on the plantar surface compared to the lateral surface *(p≤0.05)*. On the fifth metatarsal bone, there were statistically significant differences in local bone density across all levels except on the proximal diaphysis level. At the ANF, NF, BNF, and distal diaphysis levels, the local bone density was higher on the medial surface compared to the dorsal *(p<0.0001)* and lateral *(p<0.0001)* surfaces, and the local bone density on the plantar surface was higher than the dorsal *(p≤0.05)* surface. Generally, the local bone density was higher on the surfaces where the nutrient foramen was located (lateral on the first metatarsal and medial on the fifth metatarsal) in the pooled population, sex and age groups compared to the other surfaces.


A
Proximal Diaphysis
Above NF
Nutrient Foramina (NF)
Below NF
Distal Diaphysis
0-10 years
11-20 years
21-30 years
31-40 years
D
M
L
P
10 mm

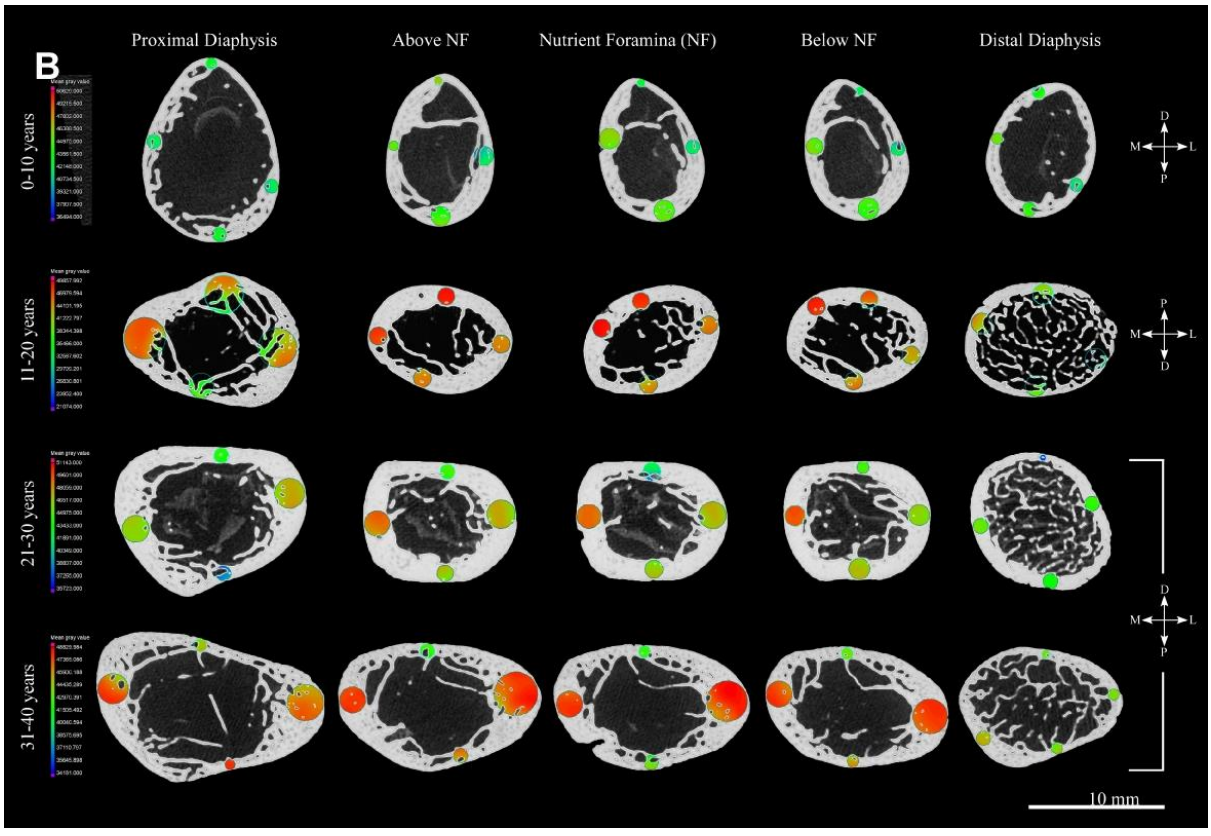

B
Proximal Diaphysis
Above NF
Nutrient Foramina (NF)
Below NF
Distal Diaphysis
0-10 years
11-20 years
21-30 years
31-40 years
D
M
L
P
10 mm

Figure 5: A plate of µCT photographs showing local bone densities (colour maps) of the trabeculated bone at different levels of the metatarsal bones across different age groups. **A.** First metatarsal bone and the nutrient foramen is located on the lateral surface. **B.** Fifth metatarsal bone and the nutrient foramen is located on the medial surface. A higher mean gray value (reddish colour) indicates more dense areas, and a low mean gray value (blueish colour) indicates less dense areas. M= Medial surface, L= Lateral surface, D= Dorsal surface, P= Plantar surface.

4. Discussion

The current study determined the nature of the trabecular structure around the level of the nutrient foramen in order to understand the age-related changes, population-specific differences and the trabecular bone quality on different levels of the diaphyses of the first and fifth metatarsal bones. Knowledge of the internal bone architecture provides valuable information about bone quality and fragility (Agarwal et al., 2004). Trabecular architecture informs about the risk of fracture development and bone-implant integration in clinical settings. Trabecular morphologic parameters including the bone volume fraction (BV/TV), trabecular thickness (TbTh), bone surface volume (BS/BV), trabecular number (TbN) and trabecular spacing (TbSp), can be assessed individually, but combining them can provide a comprehensive understanding of trabecular bone quality and fragility (Banse, 2002). In healthy children and adult bones, high trabecular bone quality is associated with a greater BV/TV and thicker (high TbTh), compact (less TbN and TbSp), and dense (high volumetric local bone density) trabeculae (Klintström et al., 2014; Ocak et al., 2022; Saers et al., 2016). Individuals and regions of the bone with high trabecular bone quality are less prone to fractures than individuals with low trabecular bone quality (Han et al., 2012; Link et al., 1999; Ocak et al., 2022).

The trabecular morphology of bones is influenced by age, sex, genetics, population affinity, diet, health, environment, and climatic conditions (Agarwal, 2021; Ruff, 1987, 1994, 2005). In the current study, the different levels assessed across both metatarsal bones showed ontogenetic changes, with the region around the NF level showing significant changes. The NF level and the area around it receive adequate amounts of blood from the nutrient arteries (Nagel, 1993). The high blood supply to this region renders it metabolically active and responsive to age and environmental-related factors (Marenzana and Arnett, 2013; Trueta, 1974). In the current study, the 0-10 and 11-20-year-old groups showed higher BS/BV, TbN, and TbSp but lower BS/BV, TbTh, and volumetric local bone density compared to the 21-30 and 31-40-year-old groups, demonstrating that children have lower trabecular bone quality than adults. The low trabecular bone quality in children are usually exposed to higher-risk physical activities like jumping and climbing trees during play, possibly explaining the high incidence of metatarsal fractures observed in children compared to adults (Moore, 2018).

The ontogenetic differences observed may potentially be attributable to variations in the stages of bone development, mineralisation processes, growth rates, nutrition, and physical

activity (Carter et al., 1996). The 0-10-year group showed high BS/BV, TbN and TbSp but low TbTh and BV/TV in the current study indicating early stages of bone formation. The 11-20-year group is associated with rapid bone growth that coincides with the adolescent growth spurt, leading to increased bone density and quality compared to the 0-10-year group (Cunningham et al., 2016). In the current study, the 21-30-year group exhibits the highest trabecular bone quality due to the higher BV/TV, TbTh, and volumetric local bone density but lower BS/BV, TbN, and TbSp compared to the other age groups. The bones in the 21-30-year period are still resilient with a balance of bone formation and resorption processes (Chan and Duque, 2002; Patton et al., 2019). In the 21-30-year group, individuals are more physically active and participate in competitive sporting activities which leads to increased bone quality (McKay et al., 2011). The 31-40-year period is marked by reduced osteoblast differentiation, increased osteoclast activity, hormonal deprivation, and reduced physical activities, all of which can reduce bone quality (Chan and Duque, 2002; Jain and Vokes, 2019; Patton et al., 2019). Oftadeh et al. (2015) reported that the peak bone strength of the vertebra and tibia bones is achieved in the 30-40 and 40-50 years, respectively. These findings indicate that different bones reach peak development and maturity at different times, suggesting that the risk of fracture development varies with age and anatomical bone location.

In the present study, there were no statistically significant sex differences in the trabecular morphologic parameters examined and these findings are similar to other studies (Saers et al., 2016; Tsegai et al., 2018). The absence of significant sex differences in the current study may be attributed to the role played by the metatarsal bones in weight-bearing and ambulation, which are universal physical activities for both sexes (Al-Munajjed et al., 2016; Ruff, 1987). Population-specific differences in the trabecular microarchitecture on different bones have been reported previously in various populations including South Africans (Cauley, 2011; Cole et al., 2015; Saers et al., 2016; Schnitzler et al., 1990). For instance, black South Africans were associated with greater trabecular thickness of the iliac bone than White South Africans in the modern populations (Schnitzler et al., 1990). In addition, trabecular microarchitecture of the lower limb bones was found to demonstrate secular changes, whereby the hunter-gatherer populations showed significant bones loss, higher bone volume fraction and thicker and fewer trabeculae but the agriculturists and the most recent modern populations showed lower bone volume fraction, thinner and more trabecular (Chirchir et al., 2015; Saers et al., 2016, 2019). The observed trabecular differences from these studies are

attributed to the changes in the environment, climate, nutrition and lifestyle (Chirchir et al., 2015, 2017; Ruff, 1994, 2015; Stock, 2006). However, the current study indicated negligible differences in the trabecular bone morphologic parameters across the three population groups. A similar study on the iliac bones of the South African populations reported minimum variations (Schnitzler et al., 1990), suggesting that bone microarchitecture may be more responsive to environmental factors than genetic factors. In addition, the modern South African populations in the current study may have been exposed to similar nutritional standards and climatic conditions that led to absent and or minimum variations in the trabecular microarchitecture.

The current findings show that the distal diaphysis, followed by the proximal diaphysis, are the weakest areas of the first and fifth metatarsal diaphysis compared to the areas around the level of the NF when using all trabecular bone quality and fragility predictors (BV/TV, BS/BV, TbTh, TbN, TbSp) and the volumetric local bone density. It may be suggested that the proximal and distal diaphyses levels of the metatarsal bones are more prone to fracturing when compared to the areas around the NF, especially when these areas are subjected to similar compression and bending forces. Thus, results from the current study indicates that the proximal diaphysis is weaker than middle diaphysis further supporting the observation that the majority (80%) of the fifth metatarsal fractures are located on the proximal portion of the diaphysis (Moore, 2018; Rammelt et al., 2004; Singer et al., 2008; Zwitser and Breederveld, 2010). In contrast, several studies postulated that the region of the NF is weak due to the foramen piercing the cortical and trabecular bone thereby weakening the bone structural integrity (Campos et al., 1987; Gümüsburun et al., 1994; Kizilkanat et al., 2007; Manjatika et al., 2023). The high trabecular bone quality around the NF could be due to increased vascularisation through the nutrient artery (Nagel, 1993). Increased vascularisation stimulates bone growth and remodelling and subsequently contributes to increased trabecular bone quality in the NF region (Gümüsburun et al., 1994; Murlimanju et al., 2011; Pereira et al., 2011). Craig et al. (2003) observed stress fracture patterns around the NF of the tibia and postulated that the areas around the NF may naturally be weak. However, the current study has shown that the area around the NF has high trabecular bone quality, and stress fractures around the NF as reported by Craig et al. (2003), could possibly be due to the mechanism of injury i.e., direct trauma or rotational stress applied to a weakened bone due to other underlying conditions like osteoporosis. Topographically, the NF is located in the middle third of the metatarsal diaphysis (Kothapalli, 2018; Manjatika et al., 2023). In long bones, the

middle diaphysis has greater cortical thickness and resists bending and compression forces more compared to the proximal and distal diaphysis making the middle diaphysis less prone to fracturing (Kontulainen et al., 2008; Popp et al., 2012).

In the current study, all the surfaces of the first metatarsal bone diaphysis exhibited similar trabecular morphologic parameters at all levels of the bone except at the distal diaphysis. The first metatarsal bone is more mobile and adapts to weight distribution changes (e.g. compression, tension and shear forces) during walking (Al-Munajjed et al., 2016; Kristen et al., 2005). The mobility of the first metatarsal bone facilitates uniform distribution of the load on its surfaces resulting in similar trabecular bone development on its surfaces. On the fifth metatarsal bone, however, the medial surface of the diaphysis showed high trabecular bone quality throughout the length of the bone. The medial surface of the fifth metatarsal is an attachment site of the fourth dorsal and third plantar interosseus muscles (Hirasaki and Oishi, 2018; Kalin and Hirsch, 1987), which exert tensional forces on this surface during adduction and abduction of the metatarsals, hence the marked development of the trabecular bone quality and fragility indicators compared to other none muscle attachment surfaces.

The NF was located on the lateral surface of the first metatarsal and the medial surface of the fifth metatarsal bone (Manjatika et al., 2023). The volumetric local bone density colour maps also show that the lateral surface of the first metatarsal bone is denser than the other surfaces. Similarly, the colour maps of the fifth metatarsal bones show that the medial surface is denser than the other surfaces. The observed high densities on the surfaces around the NF could be due to the high vascularization of the area. Developmentally, the NF forms at the site where the bone is developing and growing, and these areas have increased cellular activity, which may lead to high volumetric local bone density (Brookes and Revell, 2012).

The current study presents some limitations. Firstly, the study utilised dry cadaveric metatarsal bones, and the chemical composition, specifically the water and mineral content of dry bones, is different from that of wet bones of living individuals. Thus, the values of the trabecular morphometric parameters (i.e. BV/TV, BS/BV, TbTh, TbN, and TbSp) may be higher or lower than those in living individuals. Additionally, the low sample sizes in the current study may not allow generalizability of the findings to the large populations and a large-sized sample study is recommended to confirm the current findings.

5. Conclusion

The current study has shown that the first and fifth metatarsal bones reach peak trabecular bone quality in the 21-30-year age group and very minor population differences exist depending on the level of the bone. Results also demonstrated for the first time that the areas around and at the level of the nutrient foramen have high trabecular bone quality compared to other parts of the diaphysis. This study has provided a new understanding of the ontogenetic, level and surface of the bone, and population-related changes of the trabecular morphology around the diaphysis of the first and fifth metatarsal bones. The implications of these findings may help to understand the fracture development patterns in different age groups at different levels of the metatarsal bones.

Acknowledgements

The authors would like to thank Dr N. Bacci, Dr B. Billings and Mr M. Mulaudzi for their assistance with access to the Raymond A. Dart Modern Skeletal Collection. The authors thank Dr L. Bam and Mr J. Hoffmann from NESCA for their assistance with µCT scanning. The authors also sincerely thank those who donated their bodies to science so that anatomical research could be performed. Results from such research can potentially increase mankind's overall knowledge. Therefore, these donors and their families deserve our highest gratitude.

Funding

This study was funded by the Smieszek fellowship (2022, 2023) and the University of the Witwatersrand Faculty research grant (2023) awarded to A.T. Manjatika.

Declaration of competing interest

There are no conflicts of interest regarding the publication of this paper.

Ethical approval: The current study was conducted under the ethical clearance waiver number W-CBP-220504-01 and was covered by the Human Tissue Act (No. 65 of 1983) and the National Health Act (No. 61 of 2003) on the use of human specimens for research and teaching purposes.

Author contributions: ATM: Project development, data collection, data analysis, manuscript writing. EFH: Manuscript review. PM: Project development, manuscript review. JGD: Project development, manuscript review. All authors have read and approved the final manuscript.

References

Adhikari, M., 2005. Contending approaches to coloured identity and the history of the coloured people of South Africa. Hist. Compass, 3 (1), 1-16.

Agarwal, S.C., 2021. What is normal bone health? A bioarchaeological perspective on meaningful measures and interpretations of bone strength, loss, and aging. Am. J. Hum. Biol. 33 (5), e23647. https://doi.org/10.1002/ajhb.23647.

Agarwal, S.C., Dumitriu, M., Tomlinson, G.A., Grynpas, M.D., 2004. Medieval trabecular bone architecture: the influence of age, sex, and lifestyle. Am. J. Phys. Anthropol. 124 (1), 33-44. https://doi.org/10.1002/ajpa.10335.

Al-Munajjed, A.A., Bischoff, J.E., Dharia, M.A., Telfer, S., Woodburn, J., Carbes, S., 2016. Metatarsal loading during gait—a musculoskeletal analysis. J. Biomech. Eng. 138 (3), 034503. https://doi.org/10.1115/1.4032413.

Bank, A., 1997 The great debate and the origins of South African historiography. J. Afr. Hist. 38 (2), 261-281. https://doi.org/10.1017/S0021853797006993.

Banse, X., 2002. When density fails to predict bone strength. Doctoral dissertation, UCL-Université Catholique de Louvain.

Brookes, M., Revell, W.J., 2012. Blood supply of bone: scientific aspects. Springer Science & Business Media.

Buddecke, D.E., Polk, M.A., Barp, E.A., 2010. Metatarsal fractures. Clin. Podiatr. Med. Surg. 27 (4), 601-624. https://doi.org/10.1016/j.cpm.2010.07.001.

Cakir, H., Van Vliet-Koppert, S., Van Lieshout, E., De Vries, M., Van Der Elst, M., Schepers, T., 2011. Demographics and outcome of metatarsal fractures. Arch. Orthop. Trauma Surg. 131, 241-245. https://doi.org/10.1007/s00402-010-1164-6.

Campos, F.F., Pellico, L.G., Alias, M.G., Fernandez-Valencia, R., 1987. A study of the nutrient foramina in human long bones. Surg. Radiol. Anat. 9 (3), 251-255. https://doi.org/10.1007/bf02109636.

Carter, D., Van der Meulen, M., Beaupre, G., 1996. Mechanical factors in bone growth and development. Bone. 18 (1), S5-S10.

Cauley, J.A., 2011. Defining ethnic and racial differences in osteoporosis and fragility fractures. Clin. Orthop. Relat. Res. 469 (7), 1891-1899. https://doi.org/10.1007/s11999-011-1863-5.

Chan, G.K., Duque, G., 2002. Age-related bone loss: old bone, new facts'. Gerontology, 48 (2), 62-71.

Cheal, E., Snyder, B., Nunamaker, D., Hayes, W., 1987. Trabecular bone remodeling around smooth and porous implants in an equine patellar model. J. Biomech. 20, 1121-1134. https://doi.org/10.1016/0021-9290(87)90029-7.

Chirchir, H., Kivell, T.L., Ruff, C.B., Hublin, J.-J., Carlson, K.J., Zipfel, B., Richmond, B.G., 2015. Recent origin of low trabecular bone density in modern humans. Proc. Natl. Acad. Sci. 112 (2), 366-371. https://doi.org/10.1073/pnas.1411696112.

Chirchir, H., Ruff, C.B., Junno, J.A., Potts, R., 2017. Low trabecular bone density in recent sedentary modern humans. Am. J. Phys. Anthropol. 162 (3), 550-560. https://doi.org/10.1002/ajpa.23138.

Cole, T.J., Rousham, E.K., Hawley, N.L., Cameron, N., Norris, S.A., Pettifor, J.M., 2015. Ethnic and sex differences in skeletal maturation among the birth to twenty cohort in South Africa', Arch. Dis. child. 100 (2), 138-143. https://doi.org/10.1136/archdischild-2014-306399.

Craig, J.G., Widman, D., van Holsbeeck, M., (2003. Longitudinal stress fracture: patterns of edema and the importance of the nutrient foramen. Skeletal Radiol. 32 (1), 22-27. https://doi.org/10.1007/s00256-002-0597-6.

Cunningham, C., Scheuer, L.. Black, S., 2016. Developmental juvenile osteology. Academic press.

Da Silva, A.M.H., Alves, J.M., da Silva, O.L., da Silva Junior, N.F., 2014. Two and three-dimensional morphometric analysis of trabecular bone using X-ray microtomography

(μCT). Braz. J. Biomed. Eng. 30 (2), 93-101. http://dx.doi.org/10.1590/rbeb.2014.011.

Dameron Jr, T.B., 1975. Fractures and anatomical variations of the proximal portion of the fifth metatarsal. J. Bone Joint Surg. 57 (6), 788-792.

Dayal, M.R., Kegley, A.D., Štrkalj, G., Bidmos, M.A., Kuykendall, K.L., 2009. The history and composition of the Raymond A. Dart Collection of human skeletons at the University of the Witwatersrand, Johannesburg, South Africa. Am. J. Phsy. Anthropol. 140 (2), 324-335. https://doi.org/10.1002/ajpa.21072.

De Villiers, H., 1968. Sexual dimorphism of the skull of the South African Bantu-speaking Negro. S. Afr. J. Sci. 64 (2), 118-124.

Drago, C.J., 1992. Rates of osseointegration of dental implants with regard to anatomical location. J. Prosthodont. 1 (1), 29-31. https://doi.org/10.1111/j.1532-849X.1992.tb00423.x.

Gonzalez-Santos, M., Montinaro, F., Oosthuizen, O., Oosthuizen, E., Busby, G. B., Anagnostou, P., Destro-Bisol, G., Pascali, V., Capelli, C., 2015. Genome-wide SNP analysis of southern African populations provides new insights into the dispersal of Bantu-speaking groups. Genome Biol. Evol. 7 (9), 2560-2568. https://doi.org/10.1093/gbe/evv164.

Gosman, J.H., Ketcham, R.A., 2009. Patterns in ontogeny of human trabecular bone from SunWatch village in the Prehistoric Ohio valley: General features of microarchitectural change. Am. J. Phys. Anthropol. 138 (3), 318-332. https://doi.org/10.1002/ajpa.20931.

Götzen, N., Cross, A.R., Ifju, P.G., Rapoff, A.J., 2003. Understanding stress concentration about a nutrient foramen. J. Biomech. 36 (10), 1511-1521. https://doi.org/10.1016/S0021-9290(03)00130-1.

Gümüsburun, E., Yücel, F., Ozkan, Y., Akgün, Z., 1994. A study of the nutrient foramina of lower limb long bones. Surg. Radiol. Anat. 16 (4), 409-412. https://doi.org/10.1007/bf01627662.

Han, K.-J., Kim, J., Chung, N.-S., Lee, H., Lee, Y., 2012. Trabecular microstructure of the human lunate in Kienböck's disease. J. Hand Surg. 37 (4), 336-341. https://doi.org/10.1177/1753193411422337.

Hirasaki, E., Oishi, M., 2018. Arrangement of foot interosseous muscles in African great apes. Am. J. Phys. Anthropol. 167 (4), 924-929. https://doi.org/10.1002/ajpa.23685.

Hutchinson, E.F., Farella, M., Hoffman, J., Kramer, B., 2017. Variations in bone density across the body of the immature human mandible. J. Anat. 230 (5), 679-688. https://doi.org/10.1111/joa.12591.

Jain, R.K., Vokes, T., 2019. Physical activity as measured by accelerometer in NHANES 2005–2006 is associated with better bone density and trabecular bone score in older adults. Arch. Osteoporos. 14, 1-7. https://doi.org/10.1007/s11657-019-0583-4.

Kalin, P.J., Hirsch, B.E., 1987. The origins and function of the interosseous muscles of the foot. J. Anat. 152, 83-91.

Kivell, T.L., 2016. A review of trabecular bone functional adaptation: what have we learned from trabecular analyses in extant hominoids and what can we apply to fossils? J. Anat. 228 (4), 569-594. https://doi.org/10.1111/joa.12446.

Kizilkanat, E., Boyan, N., Ozsahin, E.T., Soames, R., Oguz, O., 2007. Location, number and clinical significance of nutrient foramina in human long bones. Ann. Anat. 189 (1), 87-95. https://doi.org/10.1016/j.aanat.2006.07.004.

Klintström, E., Smedby, Ö., Klintström, B., Brismar, T., Moreno, R., 2014. Trabecular bone histomorphometric measurements and contrast-to-noise ratio in CBCT. Dentomaxillofac. Radiol. 43 (8), 20140196. http://dx.doi.org/10.1259/dmfr.20140196.

Komza, K., 2017. A unique form of locomotion in Swartkrans hominins: An analysis of the trabecular structure of the first metatarsal. Masters dissertation, University of Kent.

Kontulainen, S., Johnston, J., Liu, D., Leung, C., Oxland, T., McKay, H., 2008. Strength indices from pQCT imaging predict up to 85% of variance in bone failure properties at tibial epiphysis and diaphysis. J. Musculoskelet. Neuronal Interact. 8 (4), 401-9.

Kothapalli, J., 2018. Nutrient foramina architecture in metacarpal and metatarsal bones. Int. J. Anat. Res. 6 (4.2), 5848-52. https://dx.doi.org/10.16965/ijar.2018.359.

Kriger, R.S., 1996. Afrikaans: recollection, redefmition, restitution introduction. Matatu. 15 (1), 3-11.

Kristen, K.H., Berger, K., Berger, C., Kampla, W., Anzböck, W., Weitzel, S., 2005. The first metatarsal bone under loading conditions: a finite element analysis. Foot Ankle Clin. 10 (1), 1-14. https://doi.org/10.1016/j.fcl.2004.11.003.

Krüger, G.C., L'Abbé, E.N., Stull, K.E., 2017. Sex estimation from the long bones of modern South Africans. Int. J. Legal Med. 131 (1), 275-285. https://doi.org/10.1007/s00414-016-1488-z.

L'Abbé, E.N., Van Rooyen, C., Nawrocki, S.P., Becker, P.J., 2011. An evaluation of non-metric cranial traits used to estimate ancestry in a South African sample. Forensic Sci. Int. 209 (1-3), 195. e1-195. e7. https://doi.org/10.1016/j.forsciint.2011.04.002.

Link, T., Majumdar, S., Grampp, S., Guglielmi, G., Van Kuijk, C., Imhof, H., Glueer, C., Adams, J., 1999. Imaging of trabecular bone structure in osteoporosis. Eur. Radiol. 9, 1781-1788.

Lundy, J.K., 1985. Selected aspects of metrical and morphological infracranial skeletal variation in the South African Negro. Doctoral dissertation, University of the Witwatersrand, Johannesburg.

Manjatika, A.T, Mazengenya, P., Davimes, J., 2023. Topographical anatomy and clinical implications of the metatarsal diaphyseal nutrient foramina across South African populations. Surg. Radiol. Anat. 45, 1213-1226. https://doi.org/10.1007/s00276-023-03233-5.

Marenzana, M., Arnett, T.R., 2013. The key role of the blood supply to bone. Bone Res. 1 (1), 203-215. https://doi.org/10.4248/BR201303001.

Mazengenya, P., Billings, B., 2016. Topographic and morphometric features of the nutrient foramina of the fibula in the South African mixed-ancestry population group and their surgical relevance. Eur. J. Anat. 20 (4), 329-336.

Mazengenya, P, Fasemore, M.D., 2015. Morphometric studies of the nutrient foramen in lower limb long bones of adult black and white South Africans. Eur. J. Anat. 19 (2), 155-163.

McKay, H., Liu, D., Egeli, D., Boyd, S., Burrows, M., 2011. Physical activity positively predicts bone architecture and bone strength in adolescent males and females. Acta Paediatr. 100 (1), 97-101. https://doi.org/10.1111/j.1651-2227.2010.01995.x.

Moore, N.F., 2018. Metatarsal fracture management', Orthop. Trauma, 32 (6), 428-436. https://doi.org/10.1016/j.mporth.2018.09.008.

Murlimanju, B., Prashanth, K., Prabhu, L.V., Saralaya, V.V., Pai, M.M., Rai, R., 2011. Morphological and topographical anatomy of nutrient foramina in human upper limb long bones and their surgical importance. Rom. J. Morphol. Embryol. 52 (3), 859-862.

Nagel, A., 1993. The clinical significance of the nutrient artery', Orthop. Rev. 22 (5), 557-561.

Ocak, H., Çelik, H.H., Ocak, M., Geneci, F., 2022. Evaluation of trabecular structure of hamate using micro-computed tomography. Int. J. Exp. Clin. Anat. 16 (2), 62-68. https://doi.org/10.2399/ana.22.2210175.

Oftadeh, R., Perez-Viloria, M., Villa-Camacho, J.C., Vaziri, A., Nazarian, A., 2015. Biomechanics and mechanobiology of trabecular bone: a review. J. Biomech. Eng. 137 (1), 010802. https://doi.org/10.1115%2F1.4029176.

Parkinson, I.H., Fazzalari, N.L., 2012. Characterisation of trabecular bone structure', in Skeletal aging and osteoporosis: biomechanics and mechanobiology. Springer. 31-51.

Patriquin, M. L., Loth, S., Steyn, M., 2003. Sexually dimorphic pelvic morphology in South African whites and blacks. Homo. 53 (3), 255-262.

Patterson, N., Petersen, D.C., van der Ross, R.E., Sudoyo, H., Glashoff, R.H., Marzuki, S., Reich, D., Hayes, V.M., 2010. Genetic structure of a unique admixed population: implications for medical research. Hum. Mol. Genet. 19 (3), 411-419. https://doi.org/10.1093/hmg/ddp505.

Patton, D.M., Bigelow, E.M., Schlecht, S.H., Kohn, D.H., Bredbenner, T.L., Jepsen, K.J., 2019. The relationship between whole bone stiffness and strength is age and sex dependent. J. Biomech. 83, 125-133. https://doi.org/10.1016/j.jbiomech.2018.11.030.

Pereira, G., Lopes, P., Santos, A., Silveira, F., 2011. Nutrient foramina in the upper and lower limb long bones: morphometric study in bones of Southern Brazilian adults. Int. J. Morphol. 29 (2), 514-20.

Petrisor, B.A., Ekrol, I., Court-Brown, C., 2006. The epidemiology of metatarsal fractures. Foot Ankle Int. 27 (3), 172-174.

Popp, A.W., Windolf, M., Senn, C., Tami, A., Richards, R.G., Brianza, S., Schiuma, D., 2012. Prediction of bone strength at the distal tibia by HR-pQCT and DXA. Bone, 50 (1), 296-300. https://doi.org/10.1016/j.bone.2011.10.033.

Preston-Whyte, E., 1982. Are white South Africans afraid to trace their ancestors?', Theoria. 21-38.

Puleo, D., Nanci, A., 1999. Understanding and controlling the bone–implant interface. Biomaterials. 20 (23-24), 2311-2321. https://doi.org/10.1016/S0142-9612(99)00160-X.

Raichlen, D.A., Gordon, A.D., Foster, A.D., Webber, J.T., Sukhdeo, S.M., Scott, R.S., Gosman, J.H., Ryan, T.M., 2015. An ontogenetic framework linking locomotion and trabecular bone architecture with applications for reconstructing hominin life history. J. Hum. Evol. 81, 1-12. https://doi.org/10.1016/j.jhevol.2015.01.003.

Rammelt, S., Heineck, J., Zwipp, H., 2004. Metatarsal fractures. Injury, 35, 77-86. https://doi.org/10.1016/j.injury.2004.07.016.

Ruff, C., 1987. Sexual dimorphism in human lower limb bone structure: relationship to subsistence strategy and sexual division of labor. J. Hum. Evol. 16 (5), 391-416. https://doi.org/10.1016/0047-2484(87)90069-8.

Ruff, C., 1994. Morphological adaptation to climate in modern and fossil hominids. Am. J Phys. Anthropol. 37 (19), 65-107.

Ruff, C., 2005. Mechanical determinants of bone form: insights from skeletal remains. J. Musculoskelet. Neuronal Interact. 5 (3), 202-212.

Ruff, C., Holt, B., Niskanen, M., Sladek, V., Berner, M., Garofalo, E., Garvin, H. M., Hora, M., Junno, J.A., Schuplerova, E., 2015. Gradual decline in mobility with the adoption of food production in Europe. Proc. Natl. Acad. Sci. 112 (23), 7147-7152. https://doi.org/10.1073/pnas.1502932112.

Ryan, T.M., Krovitz, G.E., 2006. Trabecular bone ontogeny in the human proximal femur. J. Hum. Evol. 51 (6), 591-602. https://doi.org/10.1016/j.jhevol.2006.06.004.

Saers, J.P., Cazorla-Bak, Y., Shaw, C.N., Stock, J.T., Ryan, T.M., 2016. Trabecular bone structural variation throughout the human lower limb. J. Hum. Evol. 97, 97-108. https://doi.org/10.1016/j.jhevol.2016.05.012.

Saers, J.P., Ryan, T.M., Stock, J.T., 2019. Trabecular bone functional adaptation and sexual dimorphism in the human foot. Am. J. Phys. Anthropol. 168 (1), 154-169. https://doi.org/10.1002/ajpa.23732.

Sarpong, N.O., Swindell, H.W., Trupia, E.P., Vosseller, J.T., 2018. Metatarsal fractures. Foot Ankle Orthop. 3 (3), 2473011418775094. https://doi.org/10.1177/2473011418775094.

Schnitzler, C., Pettifor, J., Mesquita, J., Bird, M., Schnaid, E., Smyth, A., 1990. Histomorphometry of iliac crest bone in 346 normal black and white South African adults. Bone Miner. 10 (3), 183-199. https://doi.org/10.1016/0169-6009(90)90261-D.

Silva, A., Alves, J., Da Silva, O., Junior, N.S., Gazziro, M., Pereira, J., Lasso, P., Vaz, C., Pereira, C., Leiva, T., 2011. Microstructural assessment of cancellous bone using 3D microtomography. J. Phys. 313 (1), 012008. https://doi.org/10.1088/1742-6596/313/1/012008.

Singer, G., Cichocki, M., Schalamon, J., Eberl, R., Höllwarth, M.E., 2008. A study of metatarsal fractures in children. J. Bone Joint Surg. 90 (4), 772-776. https://doi.org/10.2106/JBJS.G.00547.

South-Africa, Statistics., .2022. Census 2022 statistical release. Available at: https://census.statssa.gov.za/assets/documents/2022/P03014_Census_2022_Statistical_Release.pdf (Accessed: 18 March 2024).

Steyn, M., İşcan, M.Y., 1997. Sex determination from the femur and tibia in South African whites. Forensic Sci. Int. 90 (1-2), 111-119. https://doi.org/10.1016/S0379-0738(97)00156-4.

Stock J., 2006. Hunter-gatherer postcranial robusticity relative to patterns of mobility, climatic adaptation, and selection for tissue economy. Am. J. Phys. Anthropol. 131 (2), 194-204. https://doi.org/10.1002/ajpa.20398.

Stock, J., Pfeiffer, S., 2001. Linking structural variability in long bone diaphyses to habitual behaviors: foragers from the southern African later stone age and the Andaman Islands. Am. J. Phys. Anthropol. 115 (4), 337-348. https://doi.org/10.1002/ajpa.1090.

Stull, K.E., Kenyhercz, M.W., L'Abbé, E.N., 2014. Ancestry estimation in South Africa using craniometrics and geometric morphometrics. Forensic Sci. Int. 245, 206. e1-206. e7. https://doi.org/10.1016/j.forsciint.2014.10.021.

Trueta, J., 1974. Blood supply and the rate of healing of tibial fractures. Clin. Orthop. Relat. Res. 105, 11-26.

Tsegai, Z.J., Skinner, M.M., Pahr, D.H., Hublin, J.J., Kivell, T.L., 2018. Ontogeny and variability of trabecular bone in the chimpanzee humerus, femur and tibia. Am. J. Phys. Anthropol. 167 (4), 713-736. https://doi.org/10.1002/ajpa.23696.

Xue, Z., Ding, H., Hu, C., Xu, H., An, Z., 2016. An anatomical study of the nutrient foramina of the human humeral diaphysis. Med. Sci. Monit. 22, 1637-1645. https://doi.org/10.12659%2FMSM.898361.

Zeininger, A., Patel, B. A., Zipfel, B., Carlson, K.J., 2016. Trabecular architecture in the StW 352 fossil hominin calcaneus. J. Hum. Evol. 97, 145-158. https://doi.org/10.1016/j.jhevol.2016.05.009.

Zwitser, E., Breederveld, R., 2010. Fractures of the fifth metatarsal; diagnosis and treatment. Injury. 41 (6), 555-562. https://doi.org/10.1016/j.injury.2009.05.035.

Chapter 7: Submitted to the Journal of Human Evolution as

Title: Morpho-functional adaptations of the trabecular microarchitecture around the metatarsal diaphyseal nutrient foramen of 19th and 20th century individuals

Running title: Metatarsal trabecular morphologic variations between the 19th and 20th century individuals

Arthur Tsalani Manjatika[a,b], Erin Frances Hutchinson[a], Joshua Gabriel Davimes[a*], Pedzisai Mazengenya[c,d,e]

[a] School of Anatomical Sciences, University of the Witwatersrand, Parktown, Johannesburg, South Africa

[b] School of Life Sciences and Allied Health Professions, Anatomy Division, Kamuzu University of Health Sciences, Blantyre, Malawi

[c] College of Medicine, Ajman University, Ajman, United Arab Emirates

[d] Center of Medical and Bio-allied Health Sciences Research, Ajman University, Ajman, United Arab Emirates

[e] Faculty of Health Sciences, University of the Witwatersrand, Parktown, Johannesburg, South Africa

***Correspondence to**: Dr Joshua Gabriel Davimes, School of Anatomical Sciences, University of the Witwatersrand, South Africa; Tel: +27117171337; Email: Joshua.Davimes@wits.ac.za

ORCID:

ATM: 0000-0003-0867-7123

EFH: 0000-0002-1797-1140

PM: 0000-0003-4733-1563

JGD: 0000-0001-9808-5249

ABSTRACT

Trabecular structural differences between past and modern populations with different inferred locomotory behaviours have been studied. However, trabecular structural variations within contemporary populations, like those of the 19th (inferred variably unshod) and 20th (inferred shod) centuries, are unclear. This study examined the trabecular microarchitecture around the nutrient foramen (NF) of the first and fifth metatarsals (MT) in 19th and 20th century South African African (SAA) population samples. Sixty-four dry MTs, aged 18-65 years were µCT scanned to examine the bone volume fraction (BV/TV), bone surface volume (BS/BV), trabecular thickness (TbTh), trabecular number (TbN) and trabecular spacing (TbSp). There were no differences between sex, side or population samples. On the first MTs, the BS/BV, TbN and TbSp gradually increased while the BV/TV and TbTh gradually decreased from 18-29 to 50-65 years in both the population samples. The fifth MT exhibited ontogenetic variations between the population samples. In the 19th SAA, the BV/TV and TbTh were highest while the BS/BV, TbN and TbSp were lowest in the 30-49 year group. These trends were observed in the 18-29 year groups of the 20th SAA. In both population samples and MTs, the BV/TV and TbTh were higher, while the BS/BV, TbN and TbSp were lower around the NF than at the proximal and distal diaphyses *($p<0.0001$)*. The fifth MT medial surface showed most variation in trabecular parameters *($p<0.0001$)* while the first MT showed no surface variations *($p>0.05$)*. The two sampled populations exhibited similar trabecular microarchitecture groups despite having different inferred locomotor behaviours. The current study showed that the first and fifth MT exhibit the highest trabecular bone quality around the NF for all age and population samples examined. Trabecular microarchitectural variations over time may aid in understanding the degree of bone quality loss in individuals with different habitual locomotory behaviours.

Keywords

Metatarsal bones; Diaphyseal nutrient foramen; Trabecular bone morphology; South African populations; Inferred locomotory behaviour; Trabecular bone quality indicators; Modern/contemporary populations; Historical populations.

1. Introduction

Bones are dynamic tissues that continuously undergo growth and remodelling throughout life (Agarwal, 2021). Bone remodelling is a well-regulated process between osteoclast and osteocyte activities that replace old bone tissue with new in order to maintain bone integrity and normal functioning (Hill, 1998; Bartl et al., 2017). An imbalance between osteoclast and osteocyte activities during the bone remodelling process leads to conditions like osteoporosis and pathological fractures (Bartl et al., 2017; Yang et al., 2020). Osteoporosis results when bone resorption supersedes bone formation leading to weaker and brittle bones (Yang et al., 2020). Osteoporosis is a global health concern that is often neglected, especially in older individuals since it predisposes them to a high risk of fracture development (Paruk et al., 2017; Paruk et al., 2021; Ward et al., 2024). To understand the patterns and prevalence of bone fragility, previous studies examined bone mass and quality from past and modern populations from diverse settings (Pfeiffer and Lazenby, 1994; Agarwal and Grynpas, 1996; Saers et al., 2016; Saers et al., 2019). The bone quality morphology includes the architectural arrangement of the trabecular and cortical bones. The trabecular bone has a higher remodelling rate compared to the cortical bone (Ryan and Krovitz, 2006; Barak et al., 2011; Ryan and Shaw, 2012; Agarwal, 2021), making the trabecular bone important in studying the effect of different factors that affect the remodelling processes such as age, genetics, sex, nutrition, and mechanical loading, in particular, habitual locomotory behaviours (Stock and Pfeiffer, 2001; Ruff et al., 2006; Ryan and Shaw, 2015; Komza, 2017).

Ontogenetic trabecular structural changes have been demonstrated in the lumbar vertebra and metacarpals of both historical and modern humans from different population groups (Vogel et al., 1990; Kneissel et al., 1997; Brickley and Howell, 1999; Agarwal et al., 2004), but the majority of them had methodological limitations due to imprecise age classification of skeletal remains in various skeletal collections (Pfeiffer and Lazenby, 1994; Agarwal, 2012). Recent studies have described the trabecular structural variations on different segments of the lower limb bones from archaeological population groups exhibiting different habitual locomotory behaviours (Scherf et al., 2013; Saers et al., 2016; Saers et al., 2019). Frequently studied archaeological population groups included hunter-gatherers/foragers, pastoralists and agriculturists who lived between 1300 and 10000 years ago (Chirchir et al., 2015; Ryan and Shaw, 2015; Chirchir et al., 2017). These studies demonstrated human skeletal evolutionary secular changes marked by significantly decreased trabecular bone quality from the hunter-gatherers to the agriculturists (Ruff et al., 2015; Ryan and Shaw, 2015; Saers et al., 2016;

Saers et al., 2019). These trabecular structural differences have been attributed to different lifestyles, technology and improved terrain in modern years which influenced changes in locomotory behaviours over time (Zipfel, 2004; Zipfel and Berger, 2007; Chirchir et al., 2015; Ryan and Shaw, 2015). The common pitfall from these previous studies is that they compared individuals from different geographical locations such as the United States of America versus Eastern Africa (Saers et al., 2016; Saers et al., 2019). Such comparisons make it difficult to exclude the confounding effects of environment, diet and genetic factors on trabecular morphology (Ruff et al., 1993; Wallace et al., 2013). It is therefore imperative to examine trabecular morphologic variations overtime from populations with similar genetic composition that occupied the same geographic location but exhibiting different locomotory behaviours in order to minimise the effect of environmental and climatic variables.

The trabecular structural variations within recent modern human populations or contemporary populations, like those of the 19th century and 20th century, have not been fully explored and are poorly understood. It is unclear whether the trabecular structure of the 19th century and 20th century individuals exhibits secular trends. Locomotory behaviours such as shod and unshod walking affect the adaptation of the trabecular bone (Stock and Pfeiffer, 2001; Zipfel, 2004; Altman and Davis, 2012; Komza, 2017). Shod walking implies that an individual uses some form of footwear while unshod walking implies that an individual habitually walks barefooted (Altman and Davis, 2012; Willems et al., 2017). It is believed that footwear or shod walking was invented about 25000 years ago, however, there have been different cultural practices regarding footwear use, with some populations using and or not using footwear on a daily basis (Willens et al., 2017). For instance, habitual unshod walking is considered healthier for the growth of strong foot bones and muscles than habitual shod walking which is considered to restrict foot mobility and, in some instances, causing foot pathologies (Zipfel and Berger 2007). In South Africa, the locomotory behaviours of the 19th century and 20th century South African Africans (SAA), also known as Black South Africans, can be considered different due to different forms of habitual footwear. There is inadequate evidence to classify the 19th century SAA individuals as entirely unshod or barefooted, but there may be certain periods in their life time when they were habitually unshod, particularly during childhood but later had access to some form of shoes during adulthood, probably not on daily basis (Zipfel and Berger, 2007). In the 19th century, the most common type of footwear in some tropical and subtropical African countries like South Africa was slippers or flip flops for protective functions (Kadambande et al., 2006; Onywera et al., 2006). This type

of footwear is flat and allows for the normal function of the longitudinal arches of the foot, similar to that of unshod walking. In comparison, the majority of modern footwear in the 20th century have built-in heel and longitudinal arch supports hence the transmission of locomotory forces through the metatarsal bones may differ from that of flat shoes or slippers (Kadambande et al., 2006). Based on this concept, it may be inferred that the 19th century SAA individuals were habitually variably unshod, while the 20th century SAA individuals were shod.

During unshod walking, there is high mechanical loading on the metatarsal bones that support the medial and lateral longitudinal arches of the foot compared to shod walking (Nagel et al., 2008; Altman and Davis, 2012; Chirchir et al., 2015; Willems et al., 2017; Tommy, 2018). The first and fifth metatarsal bones support the medial and lateral longitudinal arches of the foot, respectively, and these bones account for the majority of metatarsal fractures (Petrisor et al., 2006; Zwitser and Breederveld, 2010; Moore, 2018). Metatarsal fractures are debilitating as they lead to loss of mobility and low quality of life (Moore, 2018). The common anatomical sites for fractures in the long bones (e.g., metatarsal bones) include the proximal and distal diaphyses and the level of nutrient foramina (Craig et al., 2003; Petrisor et al., 2006; Cakir et al., 2011)

Nutrient foramina are external openings to the nutrient canal that carries nutrient vessels and nerves to the bone (Götzen et al., 2003; Xue et al., 2016; Kothapalli, 2018; Manjatika et al., 2023). The level of the nutrient foramen is prone to fracture development, possibly due to its midshaft topographical location and the nutrient canal weakening the cortical bone as it courses through the diaphysis (Craig et al., 2003; Götzen et al., 2003; Xue et al., 2016; Kothapalli, 2018; Manjatika et al., 2023). The morpho-functional adaptations of the trabecular morphology around the diaphyseal nutrient foramen of the metatarsal bones are unclear, particularly in bones subjected to different locomotory behaviours. Most studies have examined the trabecular microarchitecture of the base and head of the metatarsal bones and less on the diaphysis (Komza, 2017; Hagihara and Nara, 2018; Saers et al., 2019). Given that the response of the trabecular bone to the mechanical loading is anatomical site-dependent (Eckstein et al., 2007; Saers et al., 2016), it is important to determine the trabecular morphological changes on multiple anatomical sites along the diaphysis in order to determine the degree of bone fragility and risk of fracture development. Important trabecular morphologic parameters that are important for the understanding of the trabecular bone quality, fragility and functional adaptability are bone volume fraction, bone surface volume,

trabecular thickness, trabecular number, trabecular spacing, and interconnectedness (Stock and Pfeiffer, 2001; Gosman and Ketcham, 2009; Kivell, 2016). The current study aimed to examine the trabecular morphologic parameters of the first and fifth metatarsal bones in different age groups of the 19th and 20th-century South African Africans (SAA) with a particular focus on the region around the diaphyseal nutrient foramen. Examining the trabecular structure at different anatomical sites may help understand the structural changes along the entire diaphysis of the bone and potentially identify high-risk anatomical sites for fracture development.

2. Materials and Methods

2.1 Study population

The study was conducted under the ethical clearance waiver number W-CBP-220504-01 obtained from the Faculty of Health Sciences, University of the Witwatersrand. The study utilised 64 dry metatarsal bones (32 first and 32 fifth) of both sexes and sides of the body obtained from 32 skeletons of 19th and 20th century South African Africans (Black South Africans) housed in the Raymond A. Dart Collection of Modern Human Skeletons in the School of Anatomical Sciences, University of the Witwatersrand, South Africa. The skeletons were of known population, date of birth, age at death and sex and these details were obtained from the Raymond A. Dart Collection of Modern Human Skeletons catalogue. The 19th century individuals are those whose date of birth was recorded as from 1800-1899AD, while 20th century individuals' date of birth span from 1900-1999AD in the Raymond A. Dart Collection of Modern Human Skeletons catalogue (Dayal et al., 2009). The South African Africans were chosen as their habitual locomotory behaviours can be predicted considering the demographical and life style changes over the past centuries (Paruk et al., 2017). The metatarsal bones of the 19th century and 20th century individuals were age-matched and categorised into three adult age groups: early adulthood (18-29), middle adulthood (30-49) and old (50-65), as shown in Table 1. This age-grouping criteria was previously described by Agarwal et al. (2004) to represent three streams of adulthood. The current study excluded metatarsal bones with pathological and malformed deformities and fractures, gross evidence of any genetic and metabolic diseases and any evidence of surgical interventions. Since the cause of death and previous medical and occupational history of the cadaveric specimens were not recorded in the Raymond A. Dart Collection of Modern Human Skeletons catalogue, the non-evident macroscopic genetic diseases and occupational history were not exclusion factors.

Table 1: Sample distribution of the metatarsal bones across different age and population groups

Age group		18-29 Years		30-49 Years		50-65 Years		Total
SAA Population	Locomotor behaviour	M (R/L)	F (R/L)	M (R/L)	F (R/L)	M (R/L)	F (R/L)	
MT1								
19th century	Variably Unshod	3 (2/1)	-	2 (2/0)	4 (3/1)	3 (0/3)	3 (2/1)	15
20th century	Shod	3 (1/2)	2 (1/1)	4 (3/1)	2 (2/0)	4 (1/3)	2 (1/1)	17
Total		6 (3/3)	2 (1/1)	6 (5/1)	6 (5/1)	7 (1/6)	5 (3/2)	32
MT5								
19th century	Variably Unshod	3 (2/1)	-	2 (2/0)	4 (3/1)	3 (0/3)	3 (2/1)	15
20th century	Shod	3 (1/2)	2 (1/1)	4 (3/1)	2 (2/0)	4 (1/3)	2 (1/1)	17
Total		6 (3/3)	2 (1/1)	6 (5/1)	6 (5/1)	7 (1/6)	5 (3/2)	32

Abbreviations: Mt= Metatarsal bone; SAA= South African Africans; M= Male; F= Female; R= Right side, L= Left side.

2.2 Acquisition of µCT scans for trabecular morphology

The step-by-step procedure to obtain and analyse the µCT scans followed the methodology previously described (Zipfel, 2004; Komza, 2017). The metatarsal bones were scanned using a Nikon XTH 225L micro-focus computed tomography (CT) X-ray unit (Nikon Metrology, Leuven, Belgium) located at the MIXRAD laboratory at the Nuclear Energy Corporation of South Africa (NECSA), Pelindaba. Four metatarsal bones (2 first and 2 fifth) were scanned at a time and these were secured in a vertical orientation (proximal end pointing upwards) in a florist (oasis foam) block. A plastic density reference peg was used owing to its uniform material composition, and it was embedded in the florist foam during scanning. The mounted metatarsal bones were then placed on a rotating sample manipulator that facilitates 360-degree scanning. The scanning was done at an acceleration voltage of 100KV, 100mA, 100 µA, using a 0.5mm thick aluminium filter to approximate a homogeneous x-ray beam spectrum by removing lower energy photons. The images were reconstructed as 3000 x 3000 16-bit single Tiff image stacks from 1000 projections with two frames averaging. The projections were sent to the Nikon CT pros software version XT4.4.3 (Nikon Metrology, Leuven, Belgium), in which volume files were created.

2.3 Trabecular morphometric analysis

The volume files were imported into VG studio Max V3.2.3 (Volume Graphics GmbH, Heidelberg, Germany) for morphological analysis. Bone surface determination analysis was done following a standardised orientation. Three fiducial landmarks were created using three tuberosities on the plantar surface of the base and head of the first metatarsal bone and three tuberosities on the medial surface of the base and head of the fifth metatarsal bone to create anatomical reference planes (Komza, 2017; Saers et al., 2019). All the metatarsal bones were then aligned to these reference points. Three-dimensional disks of 1mm thick were taken from the transverse slices at three set points around each nutrient foramen: 1mm above the nutrient foramen (ANF), 1mm at the nutrient foramina (NF) and 1mm below the nutrient foramen (BNF) in order to determine any degree of trabecular bone weakening. Additionally, transverse slices from two control points (proximal and distal ends of the diaphysis) were taken, thus a total of five reference points were used. These control points were selected because they are common metatarsal fracture sites (Sarpong et al., 2018), and they also transmit mechanical load/forces from the joints to the diaphysis during walking. Four regions of interest (ROI) of the diameter (2-3mm) were selected on the medial, lateral, dorsal and plantar surfaces of each transverse slide at each level of the bone, as shown in Fig 1. The trabecular morphometric parameters and the local bone density in each ROI were quantified using the µCT analyser and the formula used previously by other authors (Silva et al., 2011; Da Silva et al., 2014). The trabecular morphometric parameters analysed included the bone volume fraction (BV/TV), bone material surface to bone material volume (BS/BV), trabecular thickness (TbTh), trabecular number (TbN), and trabecular spacing (TbSp). In addition, the volumetric local bone density (Gray value analysis) was also quantified to determine qualitative bone strength.

Bone volume fraction (BV/TV): represents the proportion of bone volume (BV) to the total volume (TV) of the region of interest. It is calculated as *BV/TV* and measured in %. Bone material surface-to-material volume (BS/BV): the amount of bone mineral present on the bone surface (BS) per unit of bone volume (BV). It is calculated as *BS/BV* and measured in mm^-1. Trabecular thickness (TbTh): the thickness of the trabeculae in the selected region of interest of the bone. It is calculated as *2 / (BS/BV)* and measured in mm. Trabecular number (TbN): the number of trabeculae within a selected region of interest of the bone. It is calculated as *(BV/TV) / TbTh* and measured in mm^-1. Trabecular spacing (TbSp): the distance between trabeculae in the selected region of interest of the bone. It is calculated as *(1*

/ TbN) – TbTh and measured in mm. Local bone density is the relative measure of the volumetric bone density on the selected region of interest in relation to the whole bone. It is measured in gray value or Hounsfield units (HU) (Silva et al., 2011; Da Silva et al., 2014).

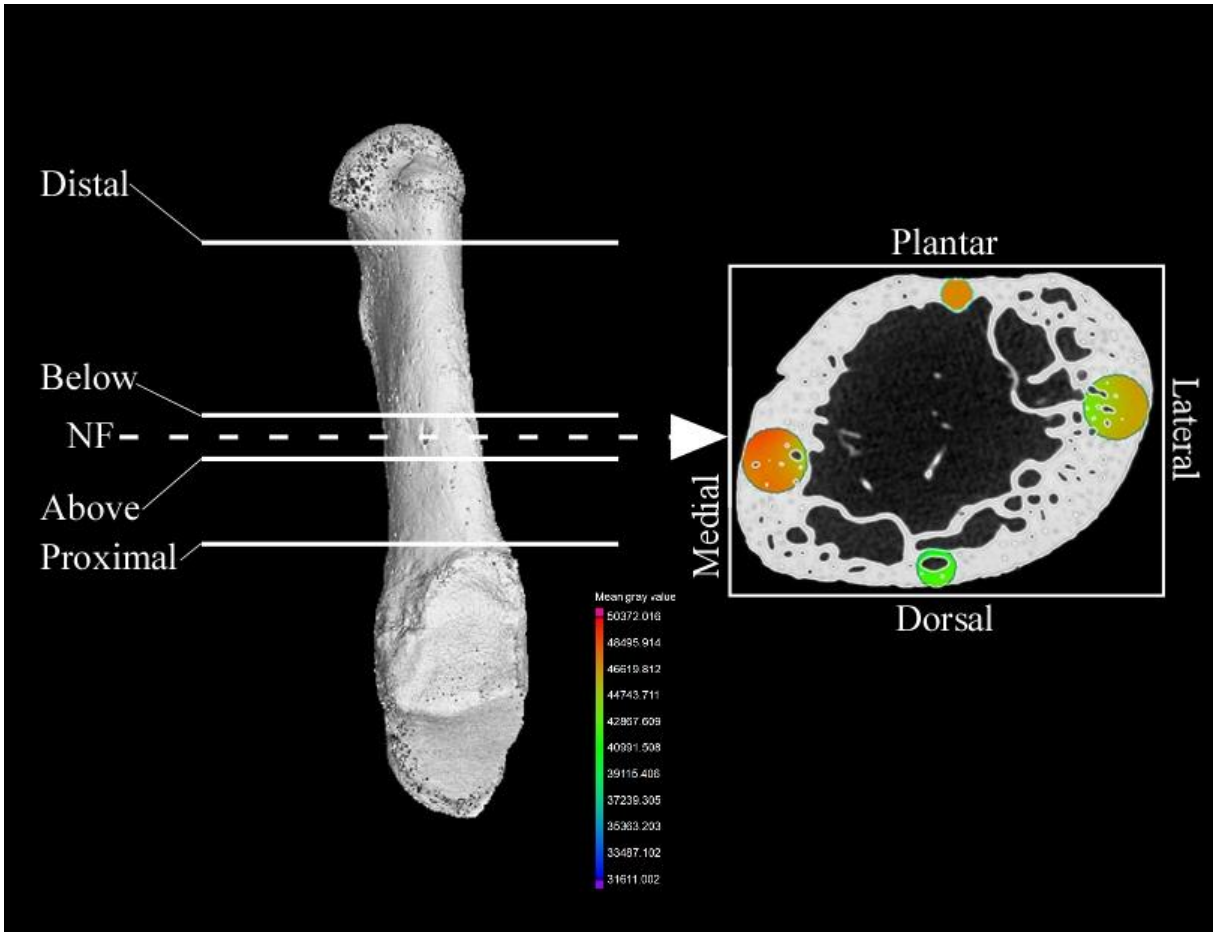


Figure 1: A µCT photograph of the fifth metatarsal bone showing the medial surface and the levels of the bone where the transverse slices were taken. The dashed lines pass through the nutrient foramen level, and the arrowhead points at the insert box, showing the selected regions of interest on each surface of the bone. The coloured circled areas represent different regions of interest of the trabeculated bone with different local bone densities. NF= Nutrient foramina, Above= the area above the nutrient foramina, Below= the area below the nutrient foramina.

2.4 Data Analysis

The data were managed in Microsoft Excel Office 365 (Microsoft Corporation) and analysed with IBM® SPSS® version 23 (IBM Corp., Armonk, NY, USA). The Shapiro-Wilk test and histograms were used to determine the normality of the data. The data for most variables were not normally distributed. Hence, the data were presented as medians and interquartile ranges. Sex and side of the body differences on trabecular structure parameters were only analysed in the pooled sample of all age groups owing to the small and uneven sample sizes within each age group (Table 1). The independent sample student t-test was used to test for statistically significant differences in the trabecular morphologic parameters between sides of the body and sexes for the parametric data while the Mann-Whitney U test was used to test for statistically significant differences in the trabecular morphologic parameters between sides of the body and sexes for the non-parametric data within each population sample. The independent sample student t-test and the Mann-Whitney U tests were also used for two group comparisons between the 19th and 20th century population samples, i.e., 18-29 year group comparison between the 19th and 20th century SAA). Since there were no significant differences between the sex or side of the body with regards to the trabecular morphologic parameters ($p>0.05$), the subsequent analysis of the ontogenetic variations of the trabecular architecture utilised both the pooled sex and side of the body samples while the analysis at the different levels and surfaces of the first and fifth metatarsal bones utilised the pooled age, sex and side of the body samples within each population sample. The one-way analysis of variance (ANOVA) was used to test for significant mean differences in trabecular morphologic parameters across age groups and different levels and surfaces of the bone for the normally distributed data (i.e., age comparisons (18-29 versus 30-49 versus 50-65 years) within each population sample). The Kruskal-Wallis test was used to test for significant median differences in trabecular morphologic parameters across age groups and different levels and surfaces of the bone for the non-parametric data within each population sample. Tukey's (a post hoc for multiple variable comparisons) test was applied to determine which pairs of groups/variables differed significantly. A $p\leq0.05$ was used to infer statistically significant differences for all comparisons.

3. Results

3.1 Ontogenetic variability of the trabecular bone morphology at different levels and surfaces of the first and fifth metatarsal bones in a pooled sex and sides of the body between the study population samples

The age-matched medians and interquartile ranges comparisons of each trabecular morphologic parameter ((bone volume fraction (BV/TV), bone surface to bone volume (BS/BV), trabecular thickness (TbTh), trabecular number (TbN) and trabecular spacing (TbSp)) at different levels and surfaces of the first and fifth metatarsal bones between the two populations in the 18-29 year group are presented in Table 2. On both the first metatarsal and fifth metatarsal bones, there were no statistically significant population sample differences for all trabecular morphologic parameters examined (BV/TV, BS/BV, TbTh, TbN, and TbSp) ($p>0.05$).

The age-matched medians and interquartile ranges comparisons of each trabecular morphologic parameter at different levels and surfaces of the first and fifth metatarsal bones between the two populations in the 30-49 year group are presented in Table 3. On the first metatarsal bone, there were no statistically significant population differences for all the trabecular morphologic parameters examined (BV/TV, BS/BV, TbTh, TbN and TbSp) ($p>0.05$). On the fifth metatarsal bones, statistically significant population differences for the trabecular morphologic parameters were only found at the proximal diaphysis on the dorsal surface, where the TbN was significantly higher in the 20th century SAA than 19th century SAA *($p\leq0.05$)*.

The age-matched medians and interquartile ranges comparisons of each trabecular morphologic parameter at different levels and surfaces of the first and fifth metatarsal bones between the two populations in the 50-65 year group are presented in Table 4. On both the first metatarsal and fifth metatarsal bones, there were no statistically significant population differences for all trabecular morphologic parameters examined (BV/TV, BS/BV, TbTh, TbN, and TbSp) ($p>0.05$).

Table 2: Age matched comparisons of trabecular morphologic parameters on different surfaces of the metatarsal bone across the 19th century and 20th century population groups in the 18-29 year group

First metatarsal bone											
Level of bone		Proximal Diaphysis		Above Nutrient Foramen		Nutrient Foramen		Below Nutrient Foramen		Distal Diaphysis	
Surface	Trabecular Parameter	19th century	20th century	19th century	20th century	19th century	20th century	19th century	20th century	19th century	20th century
Lateral	BV/TV	0.81	0.93±0.11	0.99	0.98±0.02	0.98	0.98±0.03	0.99	0.91±0.13	0.93	0.77±0.17
	BS/BV	2.67	1.1±1.32	0.39	0.43±0.34	0.37	0.38±0.49	0.39	1.21±1.17	1.19	2.71±2.19
	TbTh	0.75	1.81±1.27	5.08	4.67±2.89	5.47	5.27±5.21	5.17	1.65±3.46	1.68	0.74±0.59
	TbN	1.08	0.53±0.51	0.19	0.21±0.16	0.18	0.19±0.23	0.19	0.54±0.46	0.53	1.1±0.55
	TbSp	0.17	0.15±0.08	0.07	0.09±0.06	0.07	0.09±0.04	0.07	0.16±0.13	0.12	0.24±0.11
Dorsal	BV/TV	0.90	0.92±0.13	0.98	0.97±0.05	0.98	0.97±0.04	0.96	0.89±0.16	0.87	0.82±0.16
	BS/BV	1.63	1.49±2.31	0.68	0.55±0.4	0.38	0.62±0.58	0.64	1.1±1.09	1.55	1.78±1.79
	TbTh	1.22	1.35±2.93	2.95	3.64±3.68	5.32	3.23±4.12	3.12	1.82±2.99	1.29	1.12±1.8
	TbN	0.77	0.69±0.85	0.33	0.27±0.18	0.18	0.30±0.27	0.31	0.49±0.4	0.68	0.72±0.63
	TbSp	0.16	0.13±0.06	0.07	0.10±0.11	0.10	0.11±0.06	0.13	0.23±0.2	0.19	0.18±0.1
Medial	BV/TV	0.81	0.83±0.2	0.98	0.97±0.11	0.99	0.95±0.2	0.95	0.91±0.29	0.55	0.50±0.26
	BS/BV	3.68	2.35±2.48	0.55	0.49±1.72	0.44	0.94±2.6	0.74	1.09±3.71	7.62	6.46±4.0
	TbTh	0.54	0.85±2.95	3.65	4.07±4.75	4.54	2.13±5.81	2.72	1.84±4.41	0.26	0.31±0.4
	TbN	1.40	0.98±0.82	0.27	0.24±0.7	0.22	0.45±0.97	0.35	0.50±1.15	2.07	1.58±0.63
	TbSp	0.12	0.17±0.19	0.08	0.12±0.04	0.09	0.15±0.09	0.13	0.20±0.09	0.22	0.29±0.09
Plantar	BV/TV	0.66	0.89±0.08	0.98	0.98±0.02	0.95	0.98±0.05	0.98	0.98±0.12	0.88	0.82±0.22
	BS/BV	6.06	2.04±1.24	0.51	0.37±0.19	0.87	0.53±0.68	0.55	0.64±1.55	2.97	2.88±2.46
	TbTh	0.33	0.98±0.78	3.95	5.45±1.81	2.28	3.76±4.44	3.62	3.11±5.13	0.67	0.69±1.58

	TbN	1.85	0.89±0.47	0.25	0.18±0.09	0.42	0.26±0.3	0.27	0.31±0.59	1.28	1.06±0.8
	TbSp	0.17	0.14±0.04	0.08	0.08±0.06	0.12	0.12±0.08	0.07	0.13±0.09	0.11	0.19±0.12

Fifth metatarsal bone

		Proximal Diaphysis		Above Nutrient Foramen		Nutrient Foramen		Below Nutrient Foramen		Distal Diaphysis	
	Trabecular Parameter	19th century	20th century	19th century	20th century	19th century	20th century	19th century	20th century	19th century	20th century
Lateral	BV/TV	0.86	0.97±0.04	0.96	0.98±0.03	0.96	0.98±0.03	0.96	0.98±0.04	0.83	0.72±0.6
	BS/BV	2.02	0.64±0.74	0.61	0.39±0.64	0.54	0.47±0.5	0.27	0.40±0.88	2.02	4.31±11.91
	TbTh	0.99	3.12±4.29	3.26	5.09±5.72	3.7	4.21±4.45	7.3	4.97±6.19	0.99	0.46±2.17
	TbN	0.89	0.31±0.34	0.28	0.19±0.3	0.26	0.23±0.23	0.14	0.20±0.41	0.83	1.55±1.86
	TbSp	0.16	0.10±0.03	0.11	0.15±0.07	0.14	0.11±0.02	0.14	0.09±0.04	0.21	0.18±0.19
Dorsal	BV/TV	0.88	0.95±0.11	0.89	0.97±0.09	0.90	0.97±0.02	0.93	0.96±0.09	0.71	0.80±0.22
	BS/BV	2.14	1.04±1.53	1.76	0.55±1.2	1.27	0.61±0.58	1.15	0.89±1.19	4.64	3.86±3.76
	TbTh	0.94	1.92±2.5	1.13	3.64±2.63	1.57	3.28±2.17	1.74	2.25±1.95	0.43	0.52±0.7
	TbN	0.94	0.49±0.63	0.64	0.27±0.49	0.55	0.29±0.27	0.53	0.43±0.5	1.64	1.55±1.08
	TbSp	0.13	0.11±0.07	0.13	0.11±0.07	0.12	0.12±0.06	0.14	0.10±0.08	0.18	0.13±0.07
Medial	BV/TV	0.92	0.98±0.1	0.99	0.98±0.02	0.95	0.98±0.04	0.96	0.98±0.02	0.94	0.96±0.07
	BS/BV	1.12	0.51±0.93	0.34	0.27±0.37	0.21	0.39±0.43	0.39	0.34±0.28	1.07	0.86±1.2
	TbTh	1.78	3.94±5.58	5.85	7.41±6.9	9.50	5.08±8.61	5.07	5.82±6.8	1.86	2.32±2.52
	TbN	0.52	0.25±0.4	0.17	0.13±0.18	0.10	0.19±0.2	0.19	0.17±0.13	0.51	0.42±0.52
	TbSp	0.18	0.10±0.12	0.07	0.11±0.05	0.11	0.09±0.11	0.16	0.10±0.03	0.11	0.11±0.07
Plantar	BV/TV	0.72	0.90±0.15	0.94	0.97±0.12	0.94	0.91±0.12	0.94	0.98±0.03	0.91	0.91±0.13
	BS/BV	2.99	2.04±1.67	0.73	0.62±1.66	0.86	1.18±1.64	0.57	0.46±0.47	1.14	1.43±1.93
	TbTh	0.67	0.98±1.68	2.72	3.24±4.02	2.32	1.69±2.74	3.52	4.32±3.46	1.76	1.40±1.94
	TbN	1.25	0.89±0.63	0.35	0.30±0.69	0.42	0.54±0.67	0.28	0.23±0.22	0.51	0.64±0.78

TbSp	0.22	0.11±0.1	0.14	0.10±0.07	0.11	0.14±0.08	0.15	0.08±0.05	0.14	0.09±0.1

Note: Values are medians±interquartile range, measured in millimetres. SAA=South African Africans, BV/TV=Bone volume fraction, BS/BV=Bone surface volume, TbTh=Trabecular thickness, TbN=Trabecular number, TbSp=Trabecular spacing.

Table 3: Age matched comparisons of trabecular morphologic parameters on different surfaces of the metatarsal bone across 19th century and 20th century population groups in the 30-49 year group

First metatarsal bone											
Level of bone		Proximal Diaphysis		Above Nutrient Foramen		Nutrient Foramen		Below Nutrient Foramen		Distal Diaphysis	
Surface	Trabecular Parameter	19th century	20th century	19th century	20th century	19th century	20th century	19th century	20th century	19th century	20th century
Lateral	BV/TV	0.90±0.07	0.95±0.18	0.99±0.02	0.97±0.02	0.98±0.02	0.98±0.05	0.98±0.03	0.97±0.05	0.82±0.17	0.83±0.32
	BS/BV	1.59±1.71	0.99±3.01	0.42±0.32	0.63±0.54	0.51±0.18	0.45±0.92	0.48±0.55	0.55±0.84	1.51±1.98	2.55±3.58
	TbTh	1.30±1.32	2.02±2.39	4.76±3.47	3.25±2.97	3.97±2.74	4.45±3.66	4.31±4.16	3.8±3.33	1.40±1.12	0.80±2.86
	TbN	0.71±0.71	0.47±1.08	0.21±0.15	0.30±0.26	0.25±0.09	0.22±0.42	0.23±0.25	0.27±0.37	0.63±0.71	1.06±1.03
	TbSp	0.12±0.04	0.11±0.05	0.08±0.04	0.10±0.05	0.07±0.05	0.10±0.02	0.10±0.02	0.09±0.03	0.21±0.16	0.16±0.11
Dorsal	BV/TV	0.92±0.1	0.91±0.12	0.98±0.02	0.96±0.06	0.98	0.94±0.13	0.97±0.1	0.97±0.17	0.97±0.13	0.79±0.31
	BS/BV	1.39±1.68	1.50±1.95	0.48±0.42	0.74±1.22	0.47±0.17	0.97±2.09	0.53±1.09	0.71±2.56	0.68±0.98	2.34±3.71
	TbTh	1.72±2.46	1.34±1.64	4.24±5.22	3.19±4.31	4.27±1.45	2.06±4.59	3.83±4.38	2.83±6.77	2.93±2.77	1.16±2.83
	TbN	0.63±0.69	0.65±0.82	0.23±0.2	0.35±0.56	0.23±0.08	0.46±0.84	0.26±0.46	0.34±1.02	0.33±0.38	0.84±1.16
	TbSp	0.12±0.06	0.12±0.09	0.09±0.02	0.10±0.05	0.10±0.03	0.09±0.1	0.10±0.09	0.10±0.09	0.11±0.16	0.22±0.25
Medial	BV/TV	0.96±0.08	0.85±0.23	0.98±0.05	0.97±0.06	0.98±0.07	0.96±0.12	0.98±0.25	0.97±0.29	0.53±0.33	0.72±0.63
	BS/BV	1.0±0.65	2.51±3.71	0.40±0.61	0.93±1.43	0.48±0.73	0.87±2.13	0.65±3.13	0.69±4.27	6.57±4.63	4.1±9.02
	TbTh	2.0±1.28	0.88±1.67	5.15±7.13	2.16±3.81	4.35±4.53	2.38±3.61	3.15±6.17	3.01±4.39	0.30±0.24	0.58±1.5
	TbN	0.48±0.23	1.05±1.18	0.19±0.28	0.45±0.64	0.24±0.32	0.42±0.86	0.31±1.11	0.33±1.27	1.56±0.5	1.18±1.2
	TbSp	0.09±0.1	0.15±0.07	0.09±0.09	0.08±0.05	0.10±0.09	0.08±0.06	0.08±0.14	0.09±0.15	0.27±0.24	0.20±0.29
Plantar	BV/TV	0.92±0.14	0.86±0.31	0.98±0.03	0.96±0.06	0.97±0.08	0.94±0.11	0.94±0.18	0.96±0.1	0.84±0.3	0.91±0.26
	BS/BV	1.37±2.29	2.95±5.23	0.43±0.52	0.83±1.12	0.47±0.8	1.18±1.37	1.33±2.12	0.90±1.21	2.27±2.43	1.69±2.69
	TbTh	1.47±1.15	0.85±1.83	4.71±5.4	2.42±2.44	4.51±5.53	2.09±2.98	1.98±6.11	2.46±3.03	0.90±1.32	1.18±1.55

	TbN	0.64±0.63	1.22±1.5	0.21±0.25	0.40±0.49	0.23±0.32	0.55±0.57	0.62±0.83	0.41±0.55	0.87±0.73	0.77±0.8
	TbSp	0.12±0.09	0.12±0.08	0.09±0.07	0.09±0.06	0.11±0.09	0.14±0.09	0.11±0.11	0.10±0.1	0.15±0.25	0.12±0.13

Fifth metatarsal bone

		Proximal Diaphysis		Above Nutrient Foramen		Nutrient Foramen		Below Nutrient Foramen		Distal Diaphysis	
	Trabecular Parameter	19th century	20th century	19th century	20th century	19th century	20th century	19th century	20th century	19th century	20th century
Lateral	BV/TV	0.98±0.02	0.97±0.08	0.98±0.01	0.97±0.07	0.98±0.04	0.97±0.09	0.96±0.03	0.95±0.07	0.77±0.26	0.79±0.25
	BS/BV	0.34±0.33	0.48±1.39	0.31±0.3	0.58±1.48	0.43±0.78	0.62±1.83	0.83±0.89	0.81±1.45	3.32±3.16	2.88±3.61
	TbTh	5.93±5.97	4.65±6.96	6.51±3.78	4.02±7.15	4.78±12.03	3.25±8.0	2.60±6.26	2.51±3.2	0.63±0.87	0.70±0.8
	TbN	0.17±0.16	0.24±0.62	0.15±0.15	0.28±0.65	0.21±0.37	0.30±0.82	0.40±0.42	0.38±0.64	1.17±0.84	1.2±1.05
	TbSp	0.11±0.05	0.12±0.06	0.10±0.05	0.08±0.04	0.08±0.03	0.09±0.04	0.09±0.04	0.11±0.05	0.16±0.14	0.16±0.13
Dorsal	BV/TV	0.96±0.07	0.91±0.15	0.97±0.08	0.89±0.29	0.97±0.03	0.86±0.17	0.97±0.04	0.92±0.12	0.80±0.32	0.77±0.14
	BS/BV	0.67±0.76	1.73±2.66	0.70±0.84	2.04±4.85	0.59±0.18	2.3±2.49	0.63±0.52	1.93±3.09	3.11±3.73	3.43±2.94
	TbTh	3.0±2.07	1.16±0.91	2.95±3.1	1.38±3.5	3.41±0.66	0.96±2.01	3.15±1.98	1.04±2.34	0.64±0.64	0.59±0.45
	TbN	**0.32±0.32**	**0.79±0.85**	0.34±0.37	0.86±1.6	0.29±0.08	0.97±0.87	0.31±0.23	0.89±1.25	1.28±0.70	1.39±0.72
	TbSp	0.13±0.07	0.11±0.09	0.09±0.09	0.11±0.1	0.10±0.05	0.14±0.08	0.10±0.05	0.09±0.04	0.18±0.16	0.19±0.14
Medial	BV/TV	0.97±0.03	0.94±0.11	0.99±0.01	0.97±0.05	0.99±0.01	0.96±0.06	0.99±0.02	0.98±0.07	0.95±0.03	0.92±0.08
	BS/BV	0.56±0.32	1.42±1.56	0.25±0.14	0.70±0.68	0.23±0.16	0.66±1.1	0.31±0.21	0.56±1.35	0.88±0.47	1.69±0.6
	TbTh	3.56±3.16	1.43±3.18	7.89±3.08	2.86±3.48	8.98±5.84	3.47±8.67	5.7±8.11	3.6±5.65	2.3±1.18	1.18±0.77
	TbN	0.27±0.15	0.67±0.63	0.13±0.07	0.34±0.31	0.12±0.08	0.32±0.51	0.15±0.1	0.27±0.59	0.42±0.22	0.78±0.22
	TbSp	0.09±0.06	0.10±0.07	0.10±0.05	0.09±0.07	0.11±0.05	0.09±0.04	0.08±0.03	0.08±0.04	0.13±0.07	0.11±0.06
Plantar	BV/TV	0.95±0.3	0.81±0.26	0.98±0.05	0.94±0.08	0.98±0.02	0.98±0.08	0.98±0.02	0.97±0.07	0.93±0.08	0.93±0.15
	BS/BV	0.82±1.7	2.49±4.46	0.37±0.54	1.19±1.44	0.41±0.22	0.61±1.45	0.47±0.28	0.70±1.46	1.33±1.28	1.45±2.96
	TbTh	2.43±1.92	0.85±1.03	5.34±3.61	1.69±2.12	4.93±2.03	3.32±3.52	4.31±2.57	2.98±3.05	1.56±1.14	1.53±2.65
	TbN	0.39±0.44	0.97±1.16	0.18±0.23	0.56±0.61	0.20±0.1	0.30±0.64	0.23±0.13	0.34±0.64	0.62±0.51	0.67±1.16

TbSp	0.14±0.37	0.13±0.16	0.08±0.09	0.11±0.05	0.09±0.03	0.08±0.05	0.08±0.04	0.08±0.03	0.12±0.03	0.10±0.03

Note: Values are medians±interquartile range, measured in millimetres. SAA=South African Africans, BV/TV=Bone volume fraction, BS/BV=Bone surface volume, TbTh=Trabecular thickness, TbN=Trabecular number, TbSp=Trabecular spacing. The highlighted areas in **bold** represent statistically significant differences $p<0.05$.

Table 4: Age matched comparisons of trabecular morphologic parameters on different surfaces of the metatarsal bone across 19th century and 20th century population groups in the 50-65 year group

First metatarsal bone											
Level of bone		Proximal Diaphysis		Above Nutrient Foramen		Nutrient Foramen		Below Nutrient Foramen		Distal Diaphysis	
Surface	Trabecular Parameter	19th century	20th century	19th century	20th century	19th century	20th century	19th century	20th century	19th century	20th century
Lateral	BV/TV	0.93±0.06	0.88±0.17	0.96±0.03	0.98±0.05	0.96±0.03	0.95±0.07	0.93±0.05	0.94±0.03	0.73±0.37	0.85±0.24
	BS/BV	1.61±0.84	1.97±2.53	0.88±0.78	0.63±1.47	1.12±0.72	0.59±1.37	1.46±1.07	1.02±0.49	3.23±6.37	2.01±3.66
	TbTh	1.24±0.57	1.07±2.25	2.29±2.54	3.24±5.69	1.79±2.13	3.45±6.47	1.37±1.06	1.97±0.95	0.63±0.79	1.02±1.8
	TbN	0.75±0.33	0.86±0.92	0.42±0.36	0.31±0.66	0.54±0.33	0.28±0.61	0.68±0.46	0.47±0.24	1.22±0.98	0.85±1.03
	TbSp	0.08±0.04	0.14±0.05	0.08±0.02	0.09±0.04	0.09±0.05	0.14±0.07	0.10±0.03	0.14±0.09	0.26±0.17	0.14±0.15
Dorsal	BV/TV	0.87±0.12	0.93±0.1	0.92±0.16	0.95±0.07	0.94±0.07	0.92±0.08	0.95±0.08	0.94±0.09	0.90±0.14	0.74±0.21
	BS/BV	2.34±1.72	1.59±1.89	1.46±1.54	1.12±1.1	0.84±1.54	1.30±1.54	0.93±0.81	1.23±0.94	1.72±1.28	2.37±2.24
	TbTh	0.85±1.33	1.32±3.44	1.43±3.29	1.86±4.18	2.42±2.86	1.55±5.78	2.16±1.71	1.68±2.52	1.22±0.98	0.85±0.95
	TbN	0.98±0.67	0.73±0.66	0.64±0.66	0.51±0.51	0.39±0.68	0.58±0.70	0.44±0.33	0.55±0.4	0.75±0.47	0.98±0.69
	TbSp	0.12±0.06	0.12±0.04	0.10±0.08	0.09±0.04	0.09±0.08	0.09±0.08	0.11±0.09	0.10±0.1	0.13±0.1	0.26±0.23
Medial	BV/TV	0.89±0.07	0.87±0.12	0.95±0.07	0.93±0.11	0.94±0.21	0.95±0.18	0.93±0.24	0.84±0.18	0.73±0.46	0.60±0.39
	BS/BV	2.13±1.46	2.16±2.06	1.03±1.11	1.2±1.08	1.28±2.36	1.40±1.49	1.18±3.92	1.79±2.13	3.57±6.08	4.45±6.76
	TbTh	0.94±0.89	0.95±1.34	1.97±3.76	1.67±2.66	1.65±2.06	1.44±3.84	1.70±1.54	1.16±1.56	0.56±0.42	0.45±0.4
	TbN	0.94±0.53	0.92±0.8	0.49±0.49	0.56±0.43	0.60±0.77	0.66±0.55	0.55±0.81	0.75±0.72	1.33±0.36	1.44±0.61
	TbSp	0.12±0.03	0.13±0.08	0.11±0.04	0.12±0.09	0.14±0.1	0.09±0.19	0.15±0.12	0.17±0.14	0.22±0.3	0.34±0.2
Plantar	BV/TV	0.79±0.08	0.87±0.11	0.95±0.05	0.95±0.07	0.95±0.16	0.92±0.12	0.94±0.1	0.96±0.1	0.88±0.39	0.60±0.21
	BS/BV	3.53±0.76	2.13±2.0	1.12±1.03	1.07±0.8	1.16±1.41	1.33±1.83	1.19±1.65	1.18±1.16	2.64±3.89	4.16±1.64
	TbTh	0.57±0.11	1.01±1.03	1.79±1.79	1.96±1.5	1.77±2.5	1.73±2.39	1.73±1.41	1.70±2.86	0.83±1.58	0.48±0.39

	TbN	1.39±0.21	0.92±0.75	0.53±0.44	0.51±0.33	0.55±0.6	0.60±0.73	0.56±0.62	0.56±0.48	0.83±1.02	1.28±0.5
	TbSp	0.14±0.05	0.12±0.05	0.09±0.07	0.13±0.12	0.10±0.04	0.13±0.08	0.10±0.11	0.10±0.11	0.17±0.29	0.30±0.17

Fifth metatarsal bone

		Proximal Diaphysis		Above Nutrient Foramen		Nutrient Foramen		Below Nutrient Foramen		Distal Diaphysis	
	Trabecular Parameter	19th century	20th century	19th century	20th century	19th century	20th century	19th century	20th century	19th century	20th century
Lateral	BV/TV	0.97±0.02	0.93±0.06	0.98±0.02	0.97±0.04	0.98±0.03	0.95±0.05	0.96±0.04	0.95±0.06	0.92±0.13	0.77±0.2
	BS/BV	0.40±0.21	1.17±1.41	0.52±0.39	0.72±1.08	0.46±0.61	0.97±0.62	0.68±0.81	1.03±0.8	1.63±0.82	3.93±2.65
	TbTh	4.95±1.92	1.71±2.17	3.95±4.37	3.04±6.07	4.59±7.49	2.07±1.44	2.94±4.3	2.01±1.74	1.23±0.61	0.52±0.51
	TbN	0.20±0.1	0.54±0.61	0.25±0.19	0.35±0.5	0.22±0.29	0.46±0.27	0.33±0.37	0.48±0.36	0.73±0.28	1.44±0.84
	TbSp	0.14±0.08	0.11±0.02	0.09±0.03	0.08±0.1	0.10±0.06	0.10±0.05	0.11±0.03	0.12±0.07	0.11±0.15	0.14±0.09
Dorsal	BV/TV	0.89±0.19	0.85±0.29	0.94±0.24	0.94±0.08	0.98±0.1	0.92±0.11	0.90±0.17	0.88±0.15	0.81±0.19	0.83±0.11
	BS/BV	1.91±2.76	3.38±3.12	1.06±2.78	1.44±0.77	0.56±1.26	1.65±2.32	1.68±2.37	1.77±2.09	3.31±2.69	3.39±2.04
	TbTh	1.09±1.24	0.59±0.44	1.89±2.77	1.41±0.83	3.59±2.74	1.21±1.24	1.29±2.31	1.29±1.18	0.61±0.79	0.59±0.38
	TbN	0.85±0.79	1.4±1.0	0.50±0.86	0.65±0.33	0.27±0.52	0.76±0.88	0.75±0.81	0.77±0.76	1.25±0.98	1.42±0.63
	TbSp	0.11±0.11	0.09±0.13	0.15±0.12	0.09±0.05	0.09±0.08	0.10±0.06	0.13±0.07	0.14±0.08	0.15±0.14	0.12±0.05
Medial	BV/TV	0.96±0.05	0.92±0.21	0.97±0.02	0.97±0.08	0.98±0.02	0.98±0.12	0.99±0.04	0.97±0.07	0.92±0.16	0.93±0.06
	BS/BV	0.78±0.63	1.32±3.9	0.50±0.47	0.51±0.82	0.39±0.65	0.38±0.91	0.38±0.94	0.70±0.77	1.86±2.67	1.67±1.2
	TbTh	2.59±2.73	1.81±2.82	4.03±2.84	3.94±3.09	5.17±6.78	5.24±4.61	5.3±5.86	2.86±3.14	1.08±3.44	1.2±0.69
	TbN	0.36±0.3	0.60±1.28	0.24±0.22	0.25±0.34	0.19±0.31	0.19±0.38	0.19±0.43	0.34±0.33	0.86±1.02	0.77±0.47
	TbSp	0.10±0.12	0.12±0.08	0.11±0.04	0.09±0.1	0.09±0.04	0.10±0.13	0.07±0.05	0.09±0.08	0.09±0.07	0.10±0.05
Plantar	BV/TV	0.93±0.13	0.89±0.08	0.95±0.1	0.96±0.12	0.94±0.11	0.95±0.08	0.97±0.1	0.96±0.08	0.92±0.38	0.83±0.24
	BS/BV	1.45±1.84	2.16±1.29	1.44±1.93	1.01±1.73	1.1±1.82	1.27±1.02	0.59±2.14	1.09±1.06	2.03±4.1	2.41±2.48
	TbTh	1.45±1.78	0.93±0.54	1.69±2.55	1.98±2.39	1.95±3.31	1.58±1.34	3.39±3.32	1.85±1.23	1.09±1.45	0.91±1.12
	TbN	0.67±0.69	0.98±0.48	0.67±0.8	0.49±0.68	0.52±0.72	0.60±0.4	0.29±0.92	0.52±0.39	0.93±0.91	0.96±0.73

TbSp	0.10±0.09	0.13±0.05	0.08±0.04	0.11±0.06	0.10±0.11	0.09±0.06	0.09±0.03	0.08±0.05	0.10±0.21	0.15±0.17

Note: Values are medians±interquartile range, measured in millimetres. SAA=South African Africans, BV/TV=Bone volume fraction, BS/BV=Bone surface volume, TbTh=Trabecular thickness, TbN=Trabecular number, TbSp=Trabecular spacing.

In both populations, all the diaphyseal surfaces and levels of the first metatarsal bones showed a gradual increase in the BS/BV, TbN, and TbSp from 18-29 year group to 50-65 year group while the BV/TV and TbTh gradually decreased from 18-29 year group to 50-65 year group. Statistically significant ontogenetic differences on the trabecular morphologic parameters were observed at the ANF level on the plantar surface ($p>0.05$) in both the 19th century (Fig. 2) and the 20th century population groups (Fig. 3).

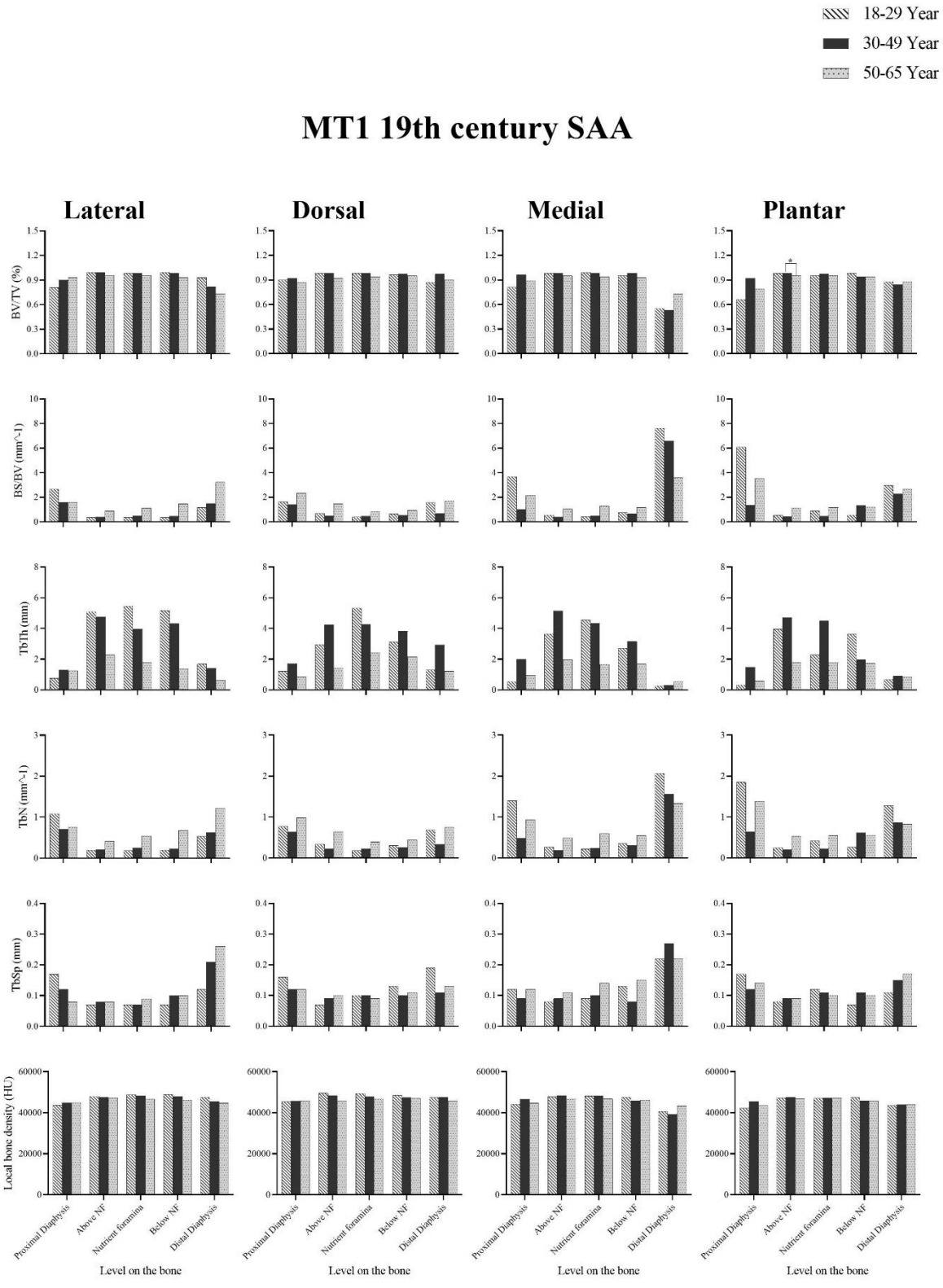


Figure 2: A plate of graphs showing age-related trabecular structural changes at different levels and surfaces of the first metatarsal bone in the 19th century SAA population. Bars indicate median trabecular values. MT1= First metatarsal bone, BV/TV= Bone volume fraction, BS/BV= Bone surface volume, TbTh=Trabecular thickness, TbN=Trabecular

number, TbSp= Trabecular spacing, SAA= South African Africans, mm= millimetres, %= Percentage, *= Significant median differences $p \leq 0.05$, HU= Hounsfield units.

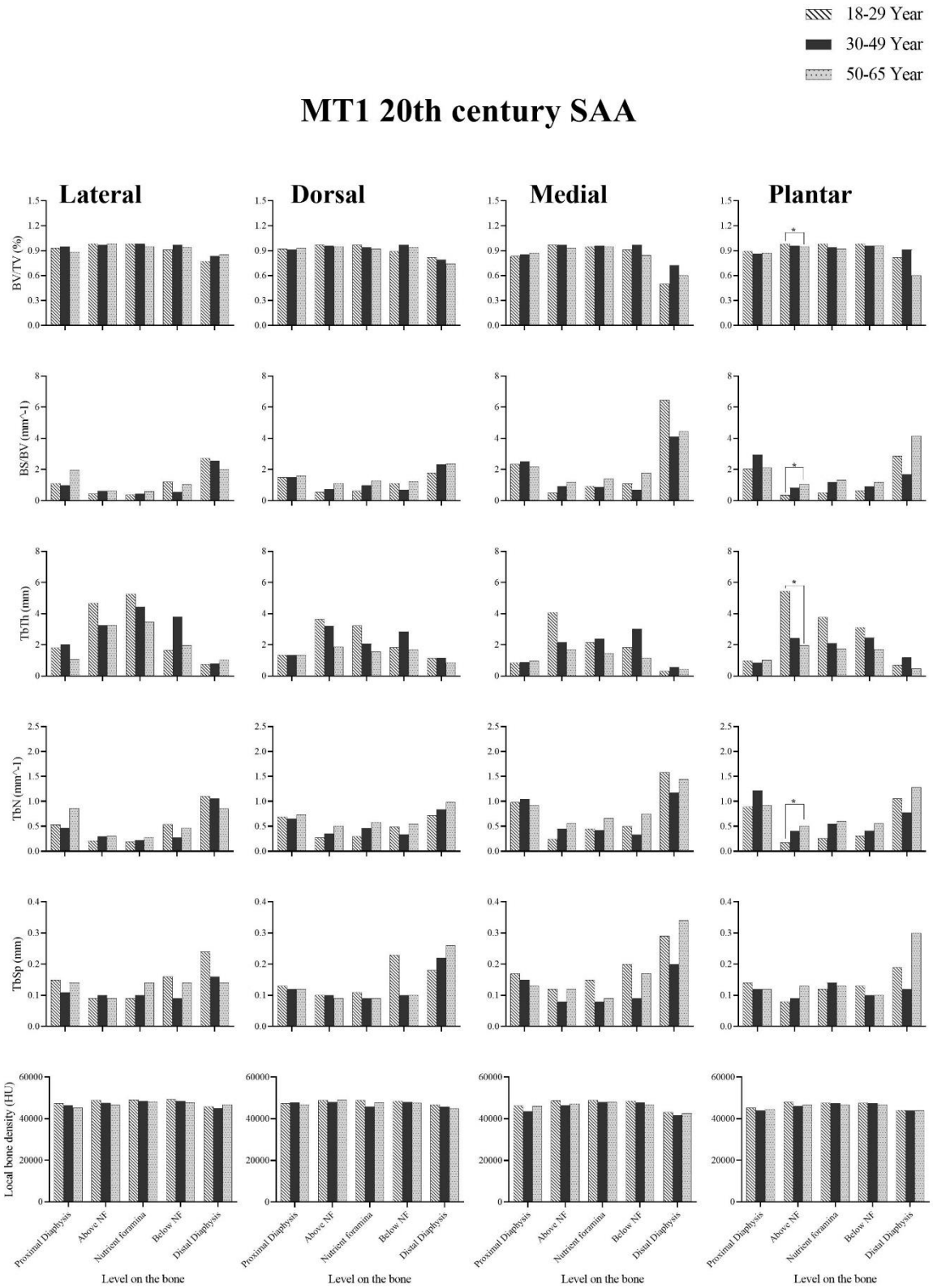


Figure 3: A plate of graphs showing age-related trabecular structural changes at different levels and surfaces of the first metatarsal bone in the 20th century SAA population. Bars indicate median trabecular values. MT1= First metatarsal bone, BV/TV= Bone volume fraction, BS/BV= Bone surface volume, TbTh= Trabecular thickness, TbN= Trabecular number, TbSp= Trabecular spacing, SAA= South African Africans, mm= millimetres, %= Percentage, *= Significant median differences $p \leq 0.05$, HU=Hounsfield units.

On the fifth metatarsal bone, the trabecular morphologic parameters exhibited variant ontogenetic patterns between the 19th century and 20th century SAA population groups. In the 19th century SAA, the BV/TV and TbTh increased from the 18-29 year group to the 30-49 year group and decreased to the 50-65 year group. The BS/BV, TbN and TbSp decreased from the 18-29 year group to the 30-49 year group and then increased to the 50-65 year group. There were no statistically significant ontogenetic trabecular morphologic differences at all levels and surfaces of the fifth metatarsal in the 19th century populations ($p>0.05$) (Fig. 4).

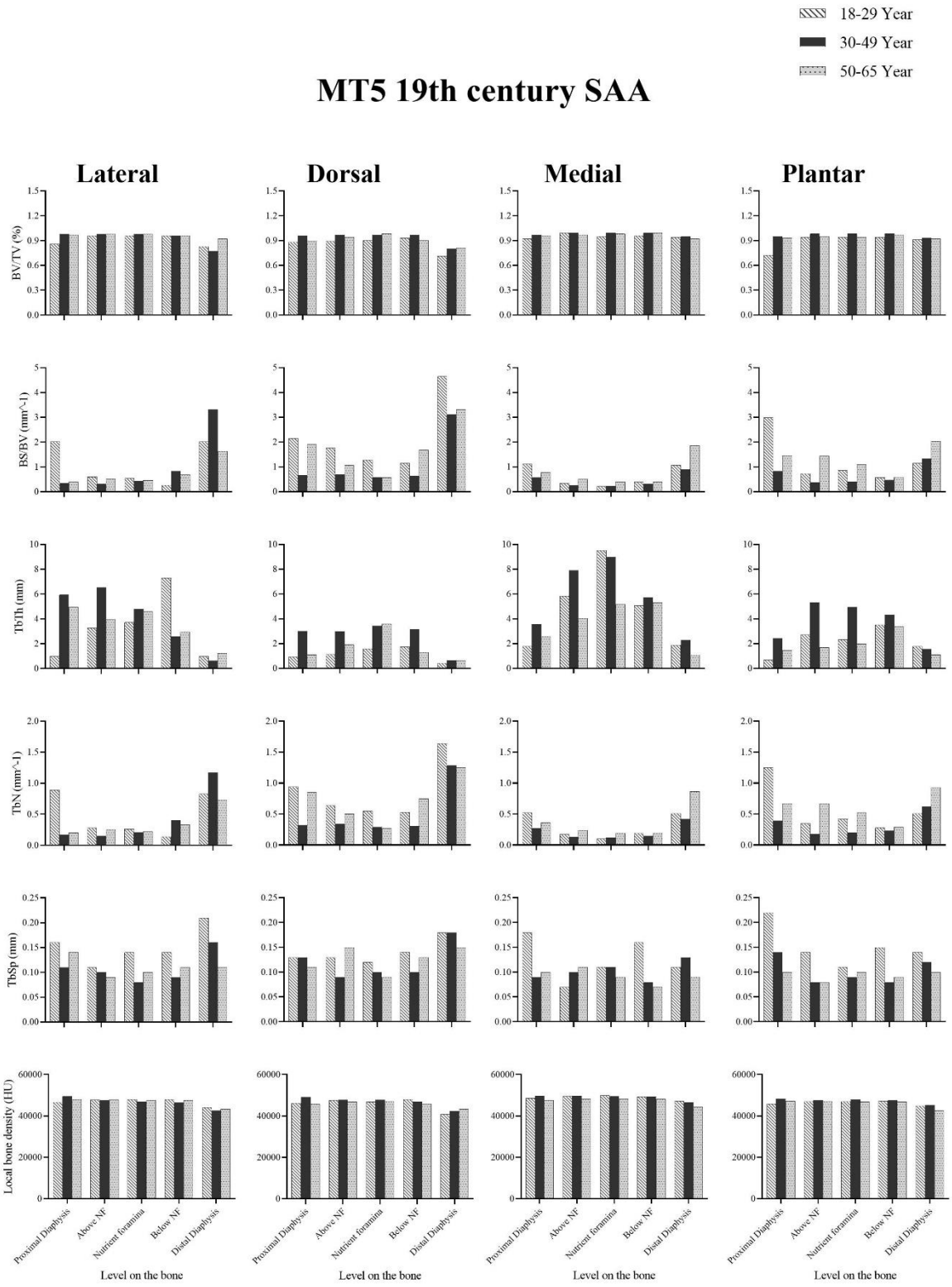


Figure 4: A plate of graphs showing age-related trabecular structural changes at different levels and surfaces of the fifth metatarsal bone in the 19th century SAA population. Bars indicate median trabecular values. MT5= Fifth metatarsal bone, BV/TV= Bone volume fraction, BS/BV= Bone surface volume, TbTh= Trabecular thickness, TbN= Trabecular

number, TbSp= Trabecular spacing, SAA= South African Africans, mm= millimetres, %= Percentage, HU=Hounsfield units.

In the 20th century SAA, the BS/BV, TbN, and TbSp gradually increased from 18-29 year group to 50-65 year group while the BV/TV and TbTh gradually decreased from 18-29 year group to 50-65 year group (Fig. 5). Significant ontogenetic trabecular differences were only observed at the NF on the dorsal surface where the BS/BV and TbN were significantly higher in the 30-49 year group than in the 18-29 year group *($p \leq 0.05$)*, (Fig. 5).

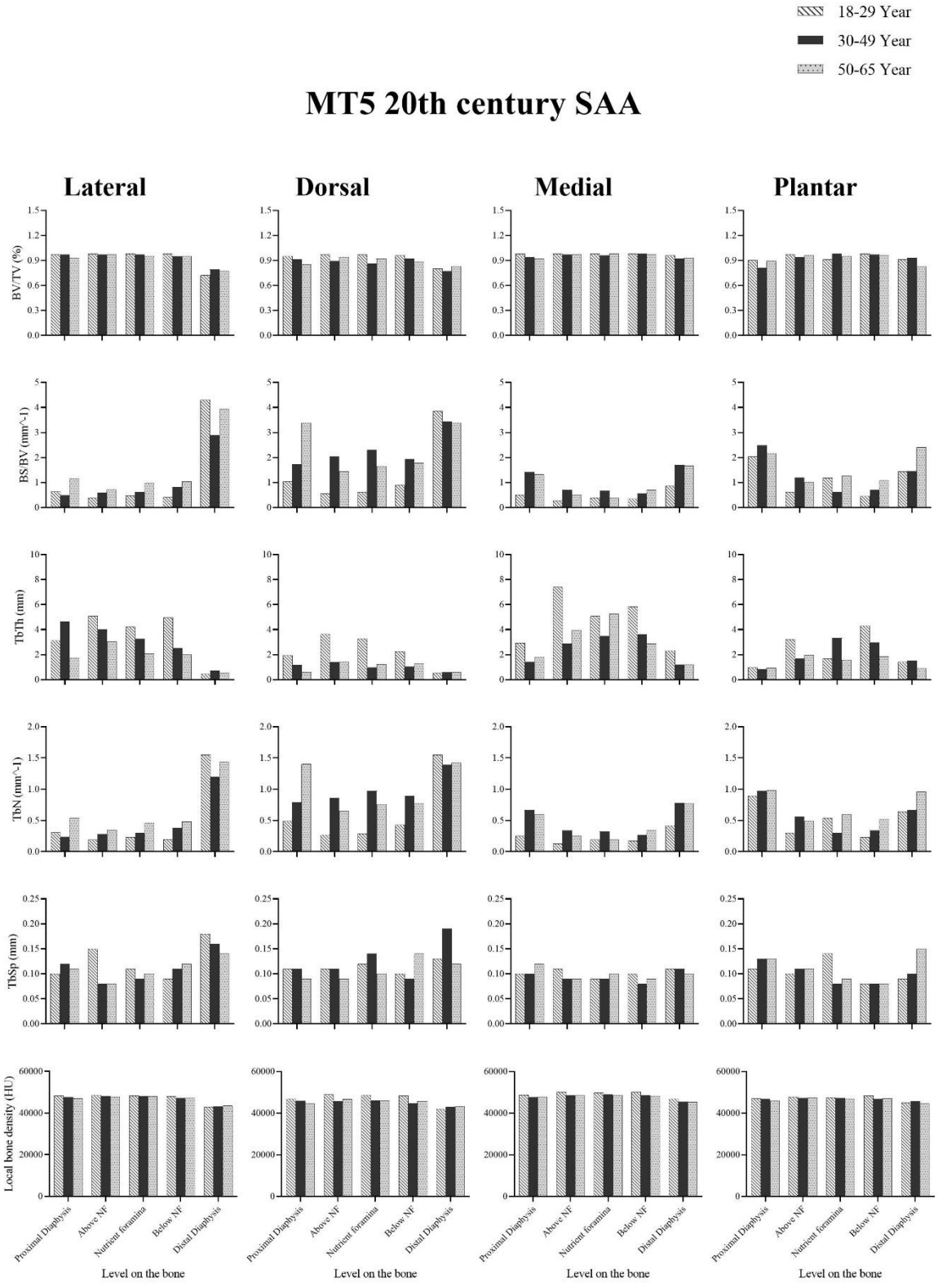


Figure 5: A plate of graphs showing age-related trabecular structural changes at different levels and surfaces of the fifth metatarsal bone in the 20th century SAA population. Bars indicate median trabecular values. MT5= Fifth metatarsal bone, BV/TV= Bone volume

fraction, BS/BV= Bone surface volume, TbTh= Trabecular thickness, TbN= Trabecular number, TbSp= Trabecular spacing, SAA= South African Africans, mm= millimetres, %= Percentage, HU=Hounsfield units.

3.2 Variability in the trabecular morphological parameters along the diaphysis of the first and fifth metatarsal bones in the pooled population, sex, and age sample

The BV/TV and TbTh increased *($p<0.0001$)* from the proximal diaphysis to the nutrient foramen (NF) level and then decreased to the distal diaphysis in both the 19th century and the 20th century populations. The BS/BV, TbN and TbSp decreased *($p<0.0001$)* from the proximal diaphysis towards the NF level and then increased towards the distal diaphysis (Figs. 6 and 7). The ANF, NF, and BNF levels showed significantly higher BV/TV and TbTh but lower BS/BV, TbN and TbSp when compared to the proximal and distal diaphyses levels *($p<0.0001$)* on both the first (Fig. 6) and fifth (Fig. 7) metatarsal bones. There were no statistically significant differences for all the trabecular morphologic parameters (BV/TV, BS/BV, TbTh, TbN and TbSp) at the ANF, NF, and BNF levels *($p>0.05$)* between the study populations.

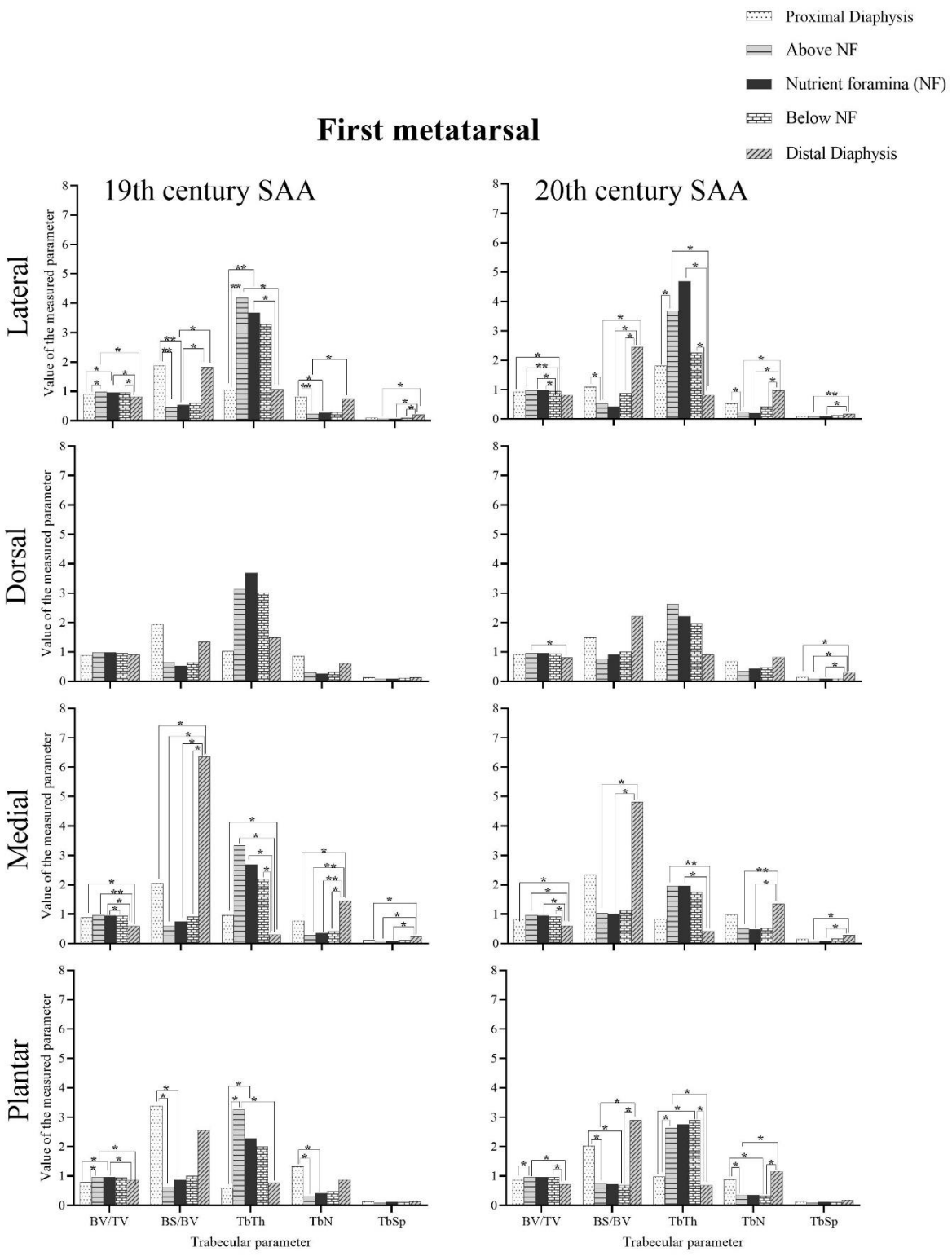


Figure 6: A plate of graphs showing trabecular bone quality indicators at different levels of the first metatarsal bone within the 19th century and 20th century population groups in pooled age groups. Bars indicate median trabecular values. BV/TV= Bone volume fraction, BS/BV= Bone surface volume, TbTh= Trabecular thickness, TbN= Trabecular number, TbSp=

Trabecular spacing, SAA= South African Africans, *= Significant median differences $p \leq 0.05$, **= Significant median differences $p < 0.0001$.

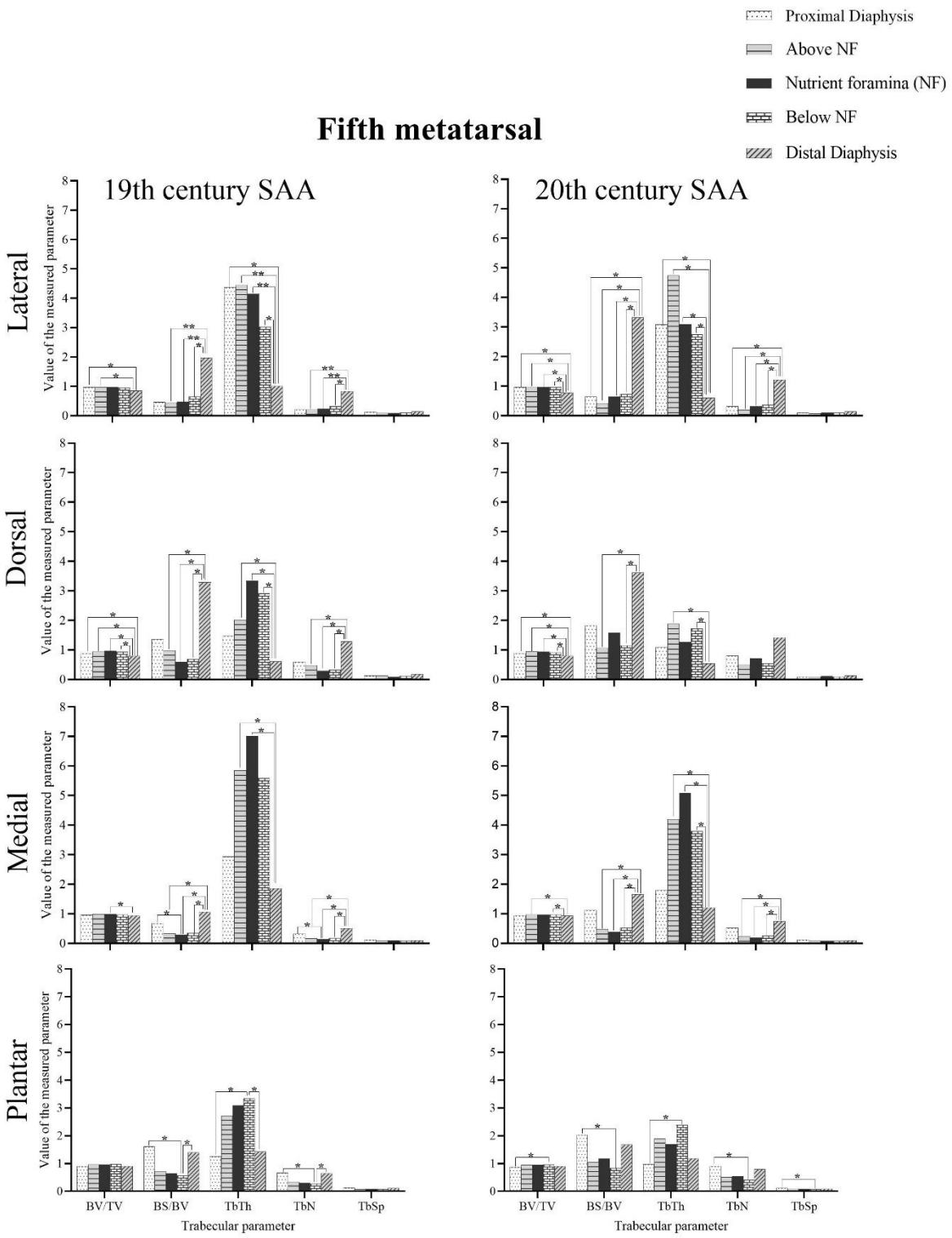


Figure 7: A plate of graphs showing trabecular quality indicators at different levels of the fifth metatarsal bone within the 19th century and 20th century population groups in pooled age

groups. Bars indicate median trabecular values. BV/TV= Bone volume fraction, BS/BV= Bone surface volume, TbTh= Trabecular thickness, TbN= Trabecular number, TbSp= Trabecular spacing, SAA= South African Africans, *= Significant median differences $p \leq 0.05$, **= Significant median differences $p < 0.0001$.

3.3. Variations of trabecular morphologic parameters on the first and fifth metatarsal bone surfaces in the pooled population, sex, and age sample.

The median comparisons of each trabecular morphologic parameter at the different levels and surfaces of the first and fifth metatarsal bones are shown in Figure 8. The NF was located on the lateral and medial surfaces of the first and fifth metatarsal bones, respectively. On the first metatarsal bones, statistically significant differences in the trabecular morphologic parameters and the bone surfaces were only found at the distal diaphysis region, where the medial surface had statistically significantly higher BS/BV and TbN but lower BV/TV and TbTh than the dorsal *(p<0.0001)*, plantar *(p<0.0001)* and lateral *(p<0.0001)* surfaces. On the fifth metatarsal bone, the medial surface had statistically significantly higher BV/TV and TbTh but lower BS/BV, TbN and TbSp than the dorsal *(p<0.0001)*, plantar *(p<0.0001)* and lateral *(p<0.0001)* surfaces at all levels of the bone (Fig. 8).

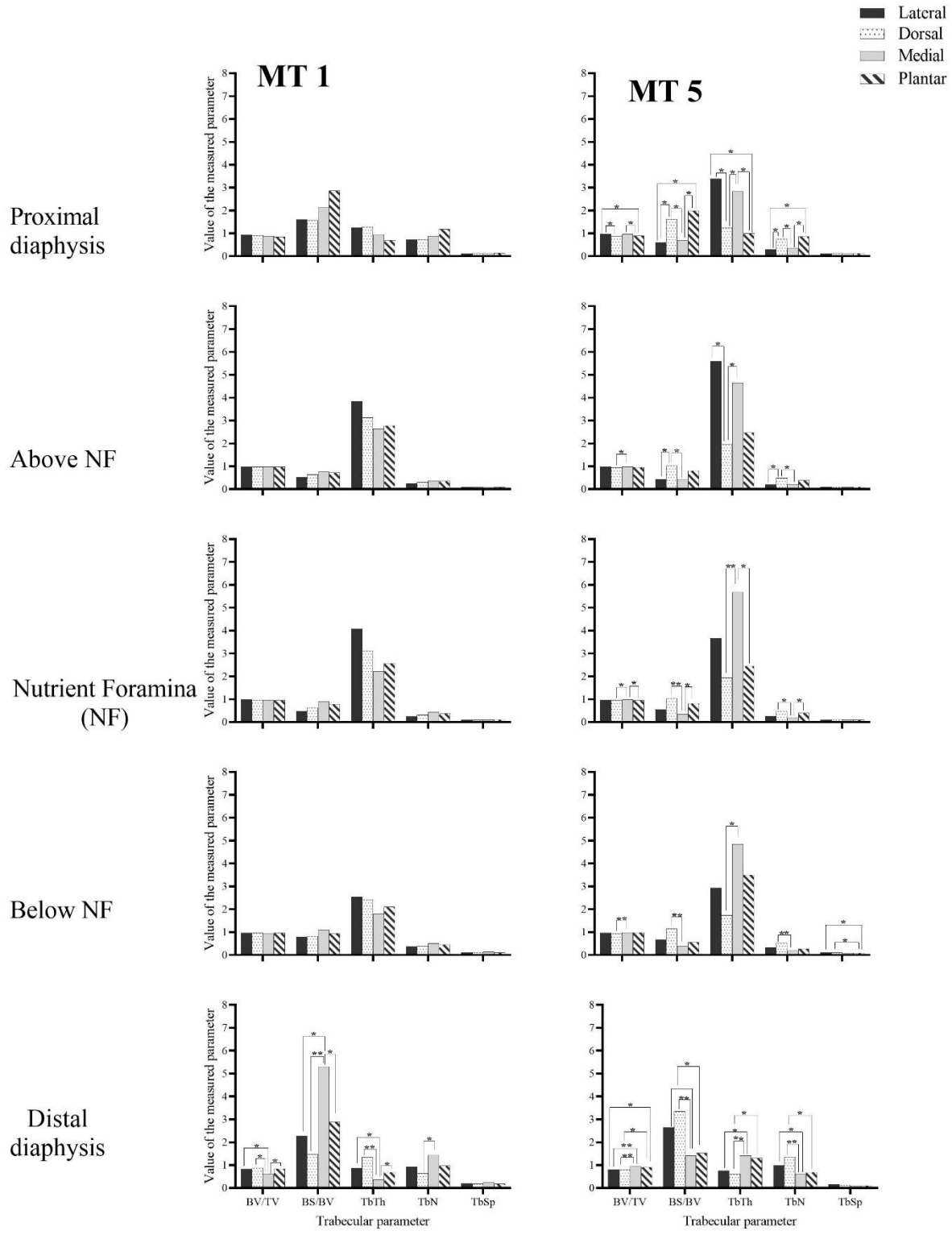


Figure 8: A plate of graphs showing variations of trabecular bone quality on the first and fifth metatarsal bone surfaces in a pooled population and age group. Bars indicate median trabecular values. MT1= First metatarsal bone, MT5= Fifth metatarsal bone, BV/TV= Bone volume fraction, BS/BV= Bone surface volume, TbTh= Trabecular thickness, TbN=

Trabecular number, TbSp= Trabecular spacing. *= Significant median differences $p \leq 0.05$, **= Significant median differences $p < 0.0001$.

3.4 Variations in the volumetric local bone density distribution in the first and fifth metatarsal bones between the study populations

The cross-sections of segmented μCT scans and colour maps of the distribution of local bone density on the first and fifth metatarsal bones are indicated in Figures 9 and 10, respectively. The local bone density showed no statistically significant ontogenetic differences at all levels and on all surfaces of the first and fifth metatarsal bones in the 19th and 20th century SAA populations *(p>0.05)*, but showed a gradual decrease from the 18-29 year group through to 50-65 year group in both population samples.

In a pooled population, sex, and age sample, the local bone density increased from the proximal diaphysis towards the NF level and then decreased towards the distal diaphysis level in both the first and fifth metatarsal bones. The surfaces of the distal diaphysis level of the first metatarsal bone showed statistically significant differences on the local bone density with the lateral *(p<0.0001)* and dorsal *(p<0.0001)* surfaces having higher local bone density compared to the medial surface. All levels of the fifth metatarsal bone diaphysis showed statistically significant differences on the bone density except on the proximal diaphysis level. At the ANF, NF, BNF and distal diaphysis levels, the local bone density was higher on the medial surface compared to the lateral *(p<0.0001)*, dorsal *(p<0.0001)*, and plantar *(p<0.0001)* surfaces. Generally, the local bone density was higher on the surfaces where the nutrient foramen was located (lateral on the first metatarsal and medial on the fifth metatarsal) in all population, sex, and age groups than on the other surfaces.

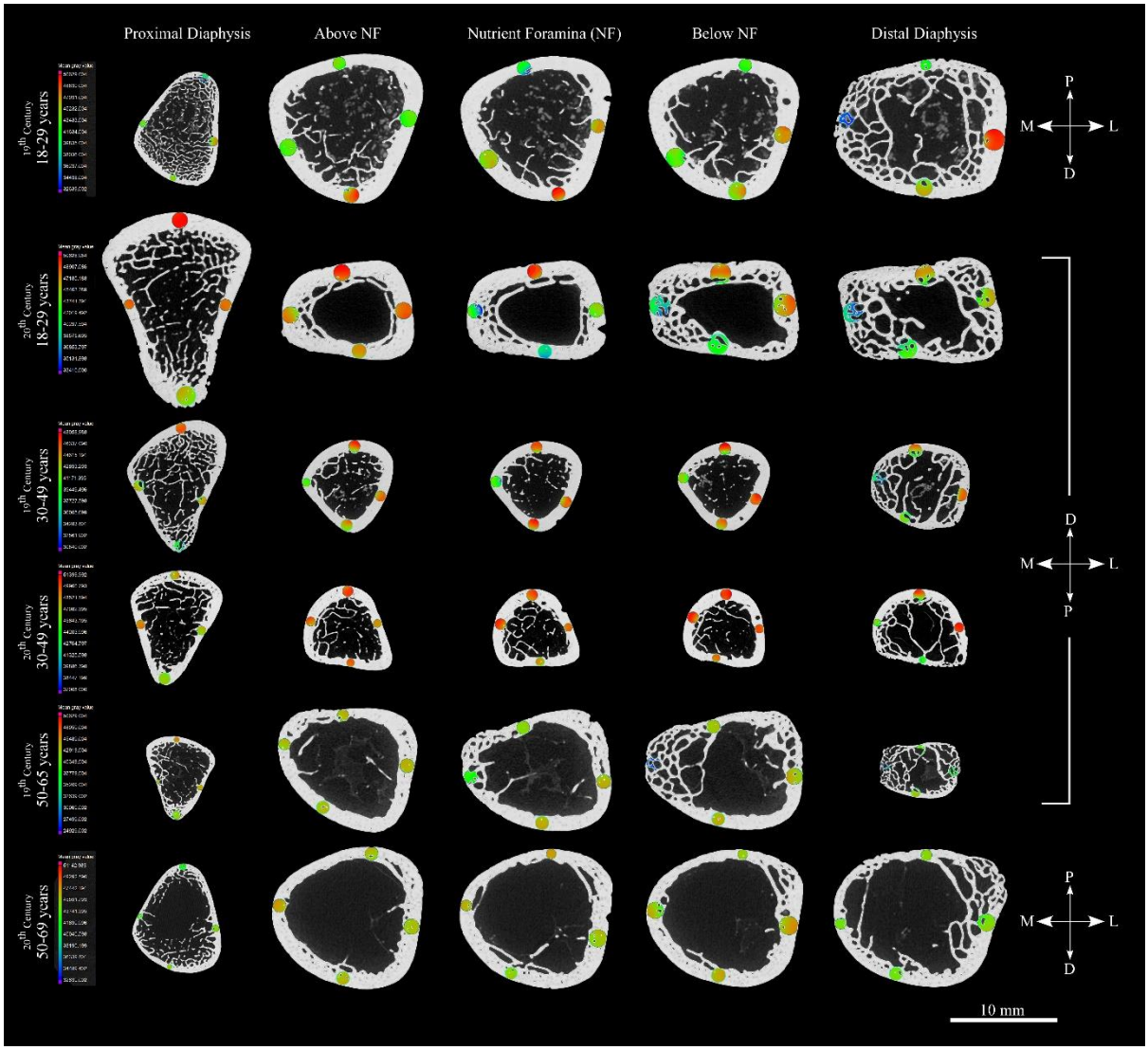


Figure 9: A plate of µCT photographs of the first metatarsal bone showing local bone densities (colour maps) at different levels of the metatarsal bone across different age groups within each population group. A higher mean gray value (reddish colour) indicates more dense areas and a low mean gray value (blueish colour) indicates less dense areas of the trabeculated bone. The nutrient foramen is located on the lateral surface. M= Medial surface, L= Lateral surface, D= Dorsal surface, P= Plantar surface.

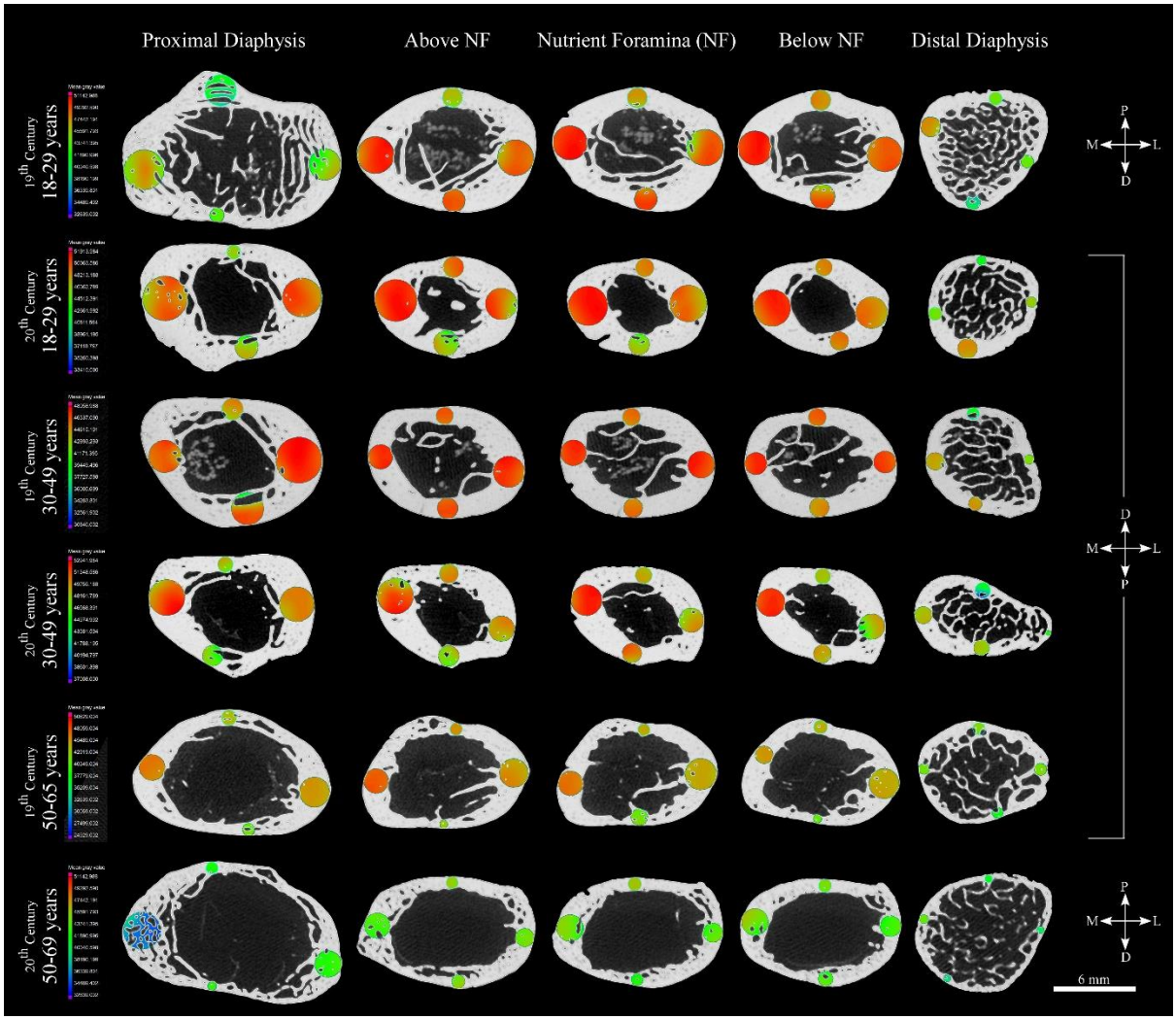


Figure 10: A plate of µCT photographs of the fifth metatarsal bone showing local bone densities (colour maps) at different levels of the trabeculated bone of the metatarsal bone across different age groups within each population group. A higher mean gray value (reddish colour) indicates more dense areas and a low mean gray value (blueish colour) indicates less dense areas of the trabeculated bone. The nutrient foramen is located on the medial surface. M= Medial surface, L= Lateral surface, D= Dorsal surface, P= Plantar surface.

4. Discussion

The current study determined the nature of the trabecular microarchitecture around the level of nutrient foramen to detect any degree of trabecular bone weakening, ontogenetic trabecular morphologic changes and any population sample differences between the 19th century and 20th century South African Africans (SAA) individuals who lived in similar environmental conditions but are assumed to have practised different habitual locomotory behaviours. Knowledge of the trabecular structure aids in understanding the morpho-functional adaptations of the metatarsal bones and the relative risk of bone quality loss in different anatomical sites of the bone (Saers et al., 2016; Komza, 2017). Banse (2002) demonstrated that areas with similar BV/TV exhibited completely different structural organisation, suggesting that each trabecular quality and fragility indicator must be considered to comprehend the trabecular structure fully. In healthy adult bones, high trabecular bone quality is associated with a greater BV/TV and thicker (high TbTh), compact (less TbN and TbSp), and dense (high volumetric local bone density) trabeculae (Klintström et al., 2014; Saers et al., 2016; Ocak et al., 2022).

In the current study, there was no statistically significant sex or side of the body differences on the trabecular morphologic parameters examined, and this is similar to other studies in humans and primates (Saers et al., 2016; Tsegai et al., 2018). The lack of significant sex or side of body differences could be because the metatarsal bones are primarily for weight-bearing and transmission of loading forces during ambulation, and gait patterns are universal in both sexes in both 19th century and 20th century individuals (Ruff, 1987; Kristen et al., 2005; Al-Munajjed et al., 2016). Ontogenetic studies have shown that individuals have distinct trabecular morphology as they grow and advance in age (Ryan and Krovitz, 2006; Raichlen et al., 2015). Age also determines how the bone adapts to mechanical loading (Gosman and Ketcham, 2009; Tsegai et al., 2018). In the current study, the first metatarsal bone showed gradual ontogenetic trabecular morphologic changes, with the stronger trabecular bone in the 18-29 years group followed by the 30-49 years group. These gradual but continuous trabecular bone quality loss patterns from young adults through middle adults to old adults are similar to those previously reported in modern populations (Agarwal et al., 2004). In addition, significant ontogenetic differences were mainly observed between the 18-29 and 50-65 year groups, suggesting marked bone quality loss in older adults compared to younger adults, similar to reports from previous studies (Brickley and Howell, 1999; Agarwal et al., 2004).

The fifth metatarsal bone showed statistically non-significant but notable ontogenetic trabecular structure variation patterns between the two SAA populations. In the 19th century SAA, the trabecular bone was strongest in the 30-49 year group while in the 20th century SAA, the trabecular bone was strongest in the 18-29 year group. These patterns suggest that the 30-49 year group were more physically active in the 19th century SAA while the 18-29 year group were more physically active in the 20th century SAA. In the 19th century lifestyle, the 30-49 year group was probably more active through physically demanding activities such as farming and walking long distances to support their families as compared to the 18-29 year group which may have been dependent on their parents for support (Stock and Pfeiffer, 2001). The 20th century lifestyle may be considered more sedentary (Ruff et al., 2015; Chirchir et al., 2017). Individuals in the 30-49 year group in the 20th century may have access to improved means of transport due to technological advances affecting how they live and work compared to 19th century individuals. The 18-29 year group is an active group associated with physical activities like sporting activities compared to the 30-49 year group in the 20th century. This could possibly explain why the 18-29 year group appear relatively stronger than the other age groups in the 20th century SAA. The 30-49 years and 50-65 years period is marked by reduced osteoblast (bone-forming cells) activity and increased osteoclast (bone resorption cells) activity, hormonal deprivation and reduced physical activities, which may subsequently reduce the trabecular bone quality and lead to conditions like osteoporosis (Chan and Duque, 2002; Jain and Vokes, 2019; Patton et al., 2019). In the current study, the trabecular morphologic changes between the 30-49 years and 50-65 years groups were not very distinct between the two population groups, suggesting that there was a similar gradual decline in physical activities and subsequent trabecular bone quality consistent with age-related decline (Agarwal et al., 2004).

Chirchir et al. (2017) showed that modern humans (Holocene) have lower BV/TV in the proximal femur, distal tibial and metatarsal heads compared to pre-historical humans (pre-Holocene) due to different locomotor and lifestyle behaviours. The pre-Holocene individuals were more mobile hunter-gatherer/foragers while the Holocene individuals were more sedentary agriculturalists (Chirchir et al., 2015, 2017). However, other trabecular parameters including the BS/BV, TbTh, TbN and TbSp are yet to be investigated between Holocene and pre-Holocene individuals. In the current study, a minimum but significant population difference was observed on the fifth metatarsal bone only in the 30-49 year group, whereby the 20th SAA had higher TbN than the 19th SAA at the proximal diaphysis level. The BV/TV,

BS/BV, TbTh and TbSp did not show statistically significant population differences on all levels and surfaces of the two metatarsal bones. Thus, it may be concluded that the 19th century and 20th century SAA individuals exhibit similar trabecular bone morphology, though they practiced different habitual locomotory behaviours.

The typical human gait has three main phases: the rear foot (heel) strike, the mid-foot phase, and the forefoot (toe-off) phase (Altman and Davis, 2012). In the rear foot strike, the heels touch the ground first. In a mid-foot strike, the heel and the ball of the foot touch the ground at the same time. In a forefoot strike, the ball of the foot touches the ground before the heel (Chi and Schmitt, 2005; Lieberman et al., 2010; Altman and Davis, 2012). According to Lieberman et al. (2010), the main differences between shod and unshod walking primarily lie in foot loading during heel and mid-foot-strike phases. Modern footwear allows individuals to touch the ground with their heels as the footwear is built with a heel cushion that reduces the collision forces during the heel strike, but the most significant loading of metatarsal bones happens in the mid-foot strike (De Wit et al., 2000; Chi and Schmitt, 2005). The unshod gait usually skips the heel strike phase and lands on the flat foot or mid-foot strike, where the amount of load transmitted to the metatarsal bones is similar to that during the shod gait (De Clercq et al., 1994; De Wit et al., 2000; Lieberman et al., 2010). Thus, regardless of being shod or unshod, the compression and bending forces transmitted to the metatarsal diaphysis are almost the same, resulting in the shod and variably unshod populations exhibiting similar trabecular morphology as shown in the current study.

It is important to note that previous studies that demonstrated distinct secular changes on the trabecular bone morphology used bones of individuals who lived at least five centuries to millennia apart (Vogel et al., 1990; Kneissel et al., 1997; Brickley and Howell, 1999; Stock and Pfeiffer, 2001; Agarwal et al., 2004; Chirchir et al., 2015; Ryan and Shaw, 2015; Saers et al., 2016; Chirchir et al., 2017). Therefore, the current findings indicate that the distinct trabecular morpho-functional changes may not be evident in population groups that lived only a century apart but shared similar geographical (e.g. terrain) and environmental conditions like climate and diet (nutrition). A century is potentially a short period of time for trabecular morphologic parameters to show significant changes in secular trends since the changes in lifestyle, cultural innovations, and technological advances are gradual and require time to exert morphological changes on the bones (Ruff et al., 2015).

The current study demonstrated that the metatarsal diaphyseal levels ANF, NF and BNF showed the highest BV/TV, TbTh and volumetric local bone density but lower BS/BV, TbN, and TbSp than the proximal and distal diaphyses. However, the trabecular morphologic parameters at the ANF, NF and BNF levels did not show significant differences. These patterns were consistent in the first and fifth metatarsal bones of both the 19th century and 20th century SAA individuals. Saers et al. (2016) observed that the trabecular bone quality increased proximo-distally in the femur and tibia bones. The study by Saers et al. (2016) omitted the trabecular morphologic parameters at the middle diaphysis (midshaft). To comprehensively understand the trabecular morphologic changes along different segments of the long bone diaphysis, the current study included the areas around the middle diaphysis (ANF, NF, BNF) in addition to the proximal and distal segments. The current study's results showed that the trabecular bone quality increase from the proximal diaphysis, reaches a peak around the NF level (located at the midshaft) and then gradually decreases to the distal diaphysis in the metatarsal bones. Possibly, this is because the middle diaphysis of long bones resists bending and compression forces more than the proximal and distal diaphyses, making the middle diaphysis a strong area (Kontulainen et al., 2008; Popp et al., 2012). In addition, the middle diaphysis is the primary ossification centre during development and growth, making it stronger than the proximal and distal ends of the diaphysis (Brookes and Revell, 2012).

The volumetric local bone density colour maps demonstrate that the lateral surface of the first metatarsal and the medial surface of the fifth metatarsal bones are stronger (denser) than other bone surfaces in both population groups. This may be due to the presence of the NF on these surfaces (Manjatika et al., 2023). The area around the NF is metabolically active due to abundant blood supply from the nutrient vessels. The abundant blood supply promotes rapid bone growth and remodelling through adequate nourishment of the osteocytes and osteoclasts leading to more developed trabecular bone parameters on surfaces bearing the NF compared to non-bearing surfaces of the diaphysis (Nagel, 1993; Brookes and Revell, 2012). Trabecular bone morphology is also influenced by loading forces on the diaphysis (Stock and Pfeiffer, 2001; Kontulainen et al., 2008). On the first metatarsal bone, all the surfaces exhibited relatively similar trabecular morphology on most of the diaphyseal levels, suggesting that the surfaces of the first metatarsal bone are subjected to similar loading forces during ambulation (Kristen et al., 2005; Al-Munajjed et al., 2016; Hagihara and Nara, 2018). The trabecular morphology on the medial surface of the fifth metatarsal bone was also stronger compared to

other surfaces, possibly because the medial surface of the fifth metatarsal bone receives muscle attachments of the third plantar and fourth dorsal interosseus muscles and these muscles exert forces during the abduction and adduction of the metatarsal bones during walking (Kalin and Hirsch, 1987; Hirasaki and Oishi, 2018).

The main limitation of the current study is that it draws conclusions and trends particularly about sex differences based on a limited sample sized data. As such, a large sample size with an equal sex distribution is needed to corroborate on the current findings. Furthermore, the hypothetical prediction of different locomotor behaviours between 19th century and 20th century individuals needs to be considered when interpreting the trends in the current study.

5. Conclusion

The current study has shown that the first and fifth metatarsal diaphyses exhibit high BV/TV, TbTh, local bone density, but low BS/BV, TbN and TbSp around the NF region, indicating high trabecular bone quality compared to other parts of the diaphysis in all age and populations examined. The 19th century and 20th century population groups with different inferred locomotor behaviours exhibit similar trabecular bone quality at all levels of the bone in all age groups. There is no significant bone quality loss regardless of habitual locomotor behaviours like variably unshod and shod. This study also suggests that a century difference is minimal for evident trabecular bone secular changes to manifest. So far, this is the first study to report on the trabecular bone structure around the NF of the metatarsal bones between the 19th century and 20th century populations, providing a new understanding of the ontogenetic changes coupled with time and the risk of bone fragility at different anatomical sites of the metatarsal bones.

Acknowledgements

The authors would like to thank the Raymond A. Dart Collection of Modern Human Skeletons curators for granting us access to the collection. The authors are also grateful to NESCA staff members for their assistance with µCT scanning and analysis. The authors also sincerely thank those who donated their bodies to science so that anatomical research could be performed.

Funding

This study was funded by the Smieszek fellowship (2022, 2023) and the University of the Witwatersrand Faculty research grant (2023) awarded to A.T. Manjatika.

Declaration of competing interest

There are no conflicts of interest regarding the publication of this paper.

Ethical approval: The current study was conducted under the ethical clearance waiver number W-CBP-220504-01 and was covered by the Human Tissue Act (No. 65 of 1983) and the National Health Act (No. 61 of 2003) on the use of human specimens for research and teaching purposes.

Author contributions: ATM: Project development, data collection, data analysis, manuscript writing. EFH: Manuscript review. PM: Project development, manuscript review. JGD: Project development, manuscript review. All authors have read and approved the final manuscript.

References

Agarwal, S.C., 2012. The past of sex, gender, and health: Bioarchaeology of the aging skeleton. Am. Anthropol. 114 (2), 322-335. https://doi.org/10.1111/j.1548-1433.2012.01428.x.

Agarwal, S.C., 2021. What is normal bone health? A bioarchaeological perspective on meaningful measures and interpretations of bone strength, loss, and aging. Am. J. Hum. Biol. 33 (5), e23647. https://doi.org/10.1002/ajhb.23647.

Agarwal, S.C., Dumitriu, M., Tomlinson, G.A., Grynpas, M.D., 2004. Medieval trabecular bone architecture: the influence of age, sex, and lifestyle. Am. J. Phys. Anthropol. 124 (1), 33-44. https://doi.org/10.1002/ajpa.10335.

Agarwal, S.C., Grynpas, M.D., 1996. Bone quantity and quality in past populations. Anat. Rec. 246 (4), 423-432.

Al-Munajjed, A.A., Bischoff, J.E., Dharia, M.A., Telfer, S., Woodburn, J., Carbes, S., 2016. Metatarsal loading during gait—a musculoskeletal analysis. J. Biomech. Eng. 138 (3), 034503. https://doi.org/10.1115/1.4032413.

Altman, A R., Davis, I.S., 2012. A kinematic method for footstrike pattern detection in barefoot and shod runners. Gait Posture. 35 (2), 298-300. https://doi.org/10.1016/j.gaitpost.2011.09.104.

Banse, X., 2002. When density fails to predict bone strength. Doctoral dissertation, UCL-Université Catholique de Louvain.

Barak, M.M., Lieberman, D.E., Hublin, J.-J. 2011. A Wolff in sheep's clothing: trabecular bone adaptation in response to changes in joint loading orientation. Bone. 49 (6), 1141-1151. https://doi.org/10.1016/j.bone.2011.08.020.

Bartl, R., Bartl, C., Bartl, R., Bartl, C., 2017. Modelling and remodelling of bone. Bone Disorders: Biology, Diagnosis, Prevention, Therapy, Springer. pp 21-30.

Brickley, M., Howell, P., 1999. Measurement of changes in trabecular bone structure with age in an archaeological population. J. Archaeol. Sci. 26 (2), 151-157. https://doi.org/10.1006/jasc.1998.0313.

Brookes, M., Revell, W.J., 2012. Blood supply of bone: scientific aspects. Springer Science & Business Media.

Cakir, H., Van Vliet-Koppert, S., Van Lieshout, E., De Vries, M., Van Der Elst, M., Schepers, T., 2011. Demographics and outcome of metatarsal fractures. Arch. Orthop. Trauma Surg. 131, 241-245. https://doi.org/10.1007/s00402-010-1164-6.

Chan, G.K., Duque, G., 2002. Age-related bone loss: old bone, new facts. Gerontology, 48 (2), 62-71.

Chi, K.-J., Schmitt, D., 2005. Mechanical energy and effective foot mass during impact loading of walking and running. J. Biomech. 38 (7), 1387-1395. https://doi.org/10.1016/j.jbiomech.2004.06.020.

Chirchir, H., Kivell, T.L., Ruff, C.B., Hublin, J.-J., Carlson, K.J., Zipfel, B., Richmond, B.G., 2015. Recent origin of low trabecular bone density in modern humans. Proc. Natl. Acad. Sci. 112 (2), 366-371. https://doi.org/10.1073/pnas.1411696112.

Chirchir, H., Ruff, C.B., Junno, J.A., Potts, R., 2017. Low trabecular bone density in recent sedentary modern humans. Am. J. Phys. Anthropol. 162 (3), 550-560. https://doi.org/10.1002/ajpa.23138.

Craig, J.G., Widman, D., van Holsbeeck, M., (2003. Longitudinal stress fracture: patterns of edema and the importance of the nutrient foramen. Skeletal Radiol. 32 (1), 22-27. https://doi.org/10.1007/s00256-002-0597-6.

Da Silva, A.M.H., Alves, J.M., da Silva, O.L., da Silva Junior, N.F., 2014. Two and three-dimensional morphometric analysis of trabecular bone using X-ray microtomography (μCT). Braz. J. Biomed. Eng. 30 (2), 93-101. http://dx.doi.org/10.1590/rbeb.2014.011.

Dayal, M.R., Kegley, A.D., Štrkalj, G., Bidmos, M.A., Kuykendall, K.L., 2009. The history and composition of the Raymond A. Dart Collection of human skeletons at the University of the Witwatersrand, Johannesburg, South Africa. Am. J. Phsy. Anthropol. 140 (2), 324-335. https://doi.org/10.1002/ajpa.21072.

De Clercq, D., Aerts, P., Kunnen, M., 1994. The mechanical characteristics of the human heel pad during foot strike in running: an in vivo cineradiographic study. J. Biomech. 27(10), 1213-1222. https://doi.org/10.1016/0021-9290(94)90275-5.

De Wit, B., De Clercq, D., Aerts, P., 2000. Biomechanical analysis of the stance phase during barefoot and shod running. J. Biomech. 33 (3), 269-278. https://doi.org/10.1016/S0021-9290(99)00192-X.

Eckstein, F., Matsuura, M., Kuhn, V., Priemel, M., Müller, R., Link, T.M., Lochmüller, E.M., 2007. Sex differences of human trabecular bone microstructure in aging are site-dependent. J. Bone Miner. Res. 22 (6), 817-824. https://doi.org/10.1359/JBMR.070301.

Gosman, J.H., Ketcham, R.A., 2009. Patterns in ontogeny of human trabecular bone from SunWatch village in the Prehistoric Ohio valley: General features of microarchitectural change. Am. J. Phys. Anthropol. 138 (3), 318-332. https://doi.org/10.1002/ajpa.20931.

Götzen, N., Cross, A.R., Ifju, P.G., Rapoff, A.J., 2003. Understanding stress concentration about a nutrient foramen. J. Biomech. 36 (10), 1511-1521. https://doi.org/10.1016/S0021-9290(03)00130-1.

Hagihara, Y., Nara, T., 2018. Diaphyseal cross-sectional geometry of the metatarsal bones in the Jomon population. Am. J. Phys. Anthropol. 166 (3), 745-752. https://doi.org/10.1002/ajpa.23463.

Hill, P., 1998. Bone remodelling. Br. J. Orthod. 25 (2), 101-107.

Hirasaki, E., Oishi, M., 2018. Arrangement of foot interosseous muscles in African great apes. Am. J. Phys. Anthropol. 167 (4), 924-929. https://doi.org/10.1002/ajpa.23685.

Jain, R.K., Vokes, T., 2019. Physical activity as measured by accelerometer in NHANES 2005–2006 is associated with better bone density and trabecular bone score in older adults. Arch. Osteoporos. 14, 1-7. https://doi.org/10.1007/s11657-019-0583-4.

Kadambande, S., Khurana, A., Debnath, U., Bansal, M., Hariharan, K., 2006. Comparative anthropometric analysis of shod and unshod feet. Foot, 16 (4), 188-191. https://doi.org/10.1016/j.foot.2006.06.001.

Kalin, P.J., Hirsch, B.E., 1987. The origins and function of the interosseous muscles of the foot. J. Anat. 152, 83-91.

Kivell, T.L., 2016. A review of trabecular bone functional adaptation: what have we learned from trabecular analyses in extant hominoids and what can we apply to fossils? J. Anat. 228 (4), 569-594. https://doi.org/10.1111/joa.12446.

Klintström, E., Smedby, Ö., Klintström, B., Brismar, T., Moreno, R., 2014. Trabecular bone histomorphometric measurements and contrast-to-noise ratio in CBCT. Dentomaxillofac. Radiol. 43 (8), 20140196. http://dx.doi.org/10.1259/dmfr.20140196.

Kneissel, M., Roschger, P., Steiner, W., Schamall, D., Kalchhauser, G., Boyde, A., Teschler-Nicola, M., 1997. Cancellous bone structure in the growing and aging lumbar spine in a historic Nubian population. Calcif. Tissue Int. 61 (2), 95-100.

Komza, K., 2017. A unique form of locomotion in Swartkrans hominins: An analysis of the trabecular structure of the first metatarsal. Masters dissertation, University of Kent.

Kontulainen, S., Johnston, J., Liu, D., Leung, C., Oxland, T., McKay, H., 2008. Strength indices from pQCT imaging predict up to 85% of variance in bone failure properties at tibial epiphysis and diaphysis. J. Musculoskelet. Neuronal Interact. 8 (4), 401-9.

Kothapalli, J., 2018. Nutrient foramina architecture in metacarpal and metatarsal bones. Int. J. Anat. Res. 6 (4.2), 5848-52. https://dx.doi.org/10.16965/ijar.2018.359.

Kristen, K.H., Berger, K., Berger, C., Kampla, W., Anzböck, W., Weitzel, S., 2005. The first metatarsal bone under loading conditions: a finite element analysis. Foot Ankle Clin. 10 (1), 1-14. https://doi.org/10.1016/j.fcl.2004.11.003.

Lieberman, D.E., Venkadesan, M., Werbel, W.A., Daoud, A.I., D'andrea, S., Davis, I.S., Mang'Eni, R.O., Pitsiladis, Y., 2010. Foot strike patterns and collision forces in habitually barefoot versus shod runners. Nature. 463 (7280), 531-535. https://doi.org/10.1038/nature08723.

Manjatika, A.T, Mazengenya, P., Davimes, J., 2023. Topographical anatomy and clinical implications of the metatarsal diaphyseal nutrient foramina across South African populations. Surg. Radiol. Anat. 45, 1213-1226. https://doi.org/10.1007/s00276-023-03233-5.

Moore, N.F., 2018. Metatarsal fracture management', Orthop. Trauma, 32 (6), 428-436. https://doi.org/10.1016/j.mporth.2018.09.008.

Nagel, A., 1993. The clinical significance of the nutrient artery', Orthop. Rev. 22 (5), 557-561.

Nagel, A., Fernholz, F., Kibele, C., Rosenbaum, D., 2008. Long distance running increases plantar pressures beneath the metatarsal heads: a barefoot walking investigation of 200 marathon runners. Gait Posture. 27 (1), 152-155. https://doi.org/10.1016/j.gaitpost.2006.12.012.

Ocak, H., Çelik, H.H., Ocak, M., Geneci, F., 2022. Evaluation of trabecular structure of hamate using micro-computed tomography. Int. J. Exp. Clin. Anat. 16 (2), 62-68. https://doi.org/10.2399/ana.22.2210175.

Onywera, V.O., Scott, R.A., Boit, M.K., Pitsiladis, Y.P., 2006. Demographic characteristics of elite Kenyan endurance runners. J. Sports Sci. 24(4), 415-422. https://doi.org/10.1080/02640410500189033.

Paruk, F., Matthews, G., Cassim, B., 2017. Osteoporotic hip fractures in Black South Africans: a regional study. Arch. Osteopor. 12, 1-6. https://doi.org/10.1007/s11657-017-0409-1.

Paruk, F., Tsabasvi, M., Kalla, A., 2021. Osteoporosis in Africa—where are we now. Clin. Rheumatol. 40 (9), 3419-3428. https://doi.org/10.1007/s10067-020-05335-6.

Patton, D.M., Bigelow, E.M., Schlecht, S.H., Kohn, D.H., Bredbenner, T.L., Jepsen, K.J., 2019. The relationship between whole bone stiffness and strength is age and sex dependent. J. Biomech. 83, 125-133. https://doi.org/10.1016/j.jbiomech.2018.11.030.

Petrisor, B.A., Ekrol, I., Court-Brown, C., 2006. The epidemiology of metatarsal fractures. Foot Ankle Int. 27 (3), 172-174.

Pfeiffer, S.K., Lazenby, R.A., 1994. Low bone mass in past and present aboriginal populations. Nutrition and Osteoporosis, Springer. pp. 35-51. https://doi.org/10.1007/978-1-4757-9092-4_2.

Popp, A.W., Windolf, M., Senn, C., Tami, A., Richards, R.G., Brianza, S., Schiuma, D., 2012. Prediction of bone strength at the distal tibia by HR-pQCT and DXA. Bone, 50 (1), 296-300. https://doi.org/10.1016/j.bone.2011.10.033.

Raichlen, D.A., Gordon, A.D., Foster, A.D., Webber, J.T., Sukhdeo, S.M., Scott, R.S., Gosman, J.H., Ryan, T.M., 2015. An ontogenetic framework linking locomotion and trabecular bone architecture with applications for reconstructing hominin life history. J. Hum. Evol. 81, 1-12. https://doi.org/10.1016/j.jhevol.2015.01.003.

Ruff, C., 1987. Sexual dimorphism in human lower limb bone structure: relationship to subsistence strategy and sexual division of labor. J. Hum. Evol. 16 (5), 391-416. https://doi.org/10.1016/0047-2484(87)90069-8.

Ruff, C., Holt, B., Niskanen, M., Sladek, V., Berner, M., Garofalo, E., Garvin, H. M., Hora, M., Junno, J.A., Schuplerova, E., 2015. Gradual decline in mobility with the adoption of food production in Europe. Proc. Natl. Acad. Sci. 112 (23), 7147-7152. https://doi.org/10.1073/pnas.1502932112.

Ruff, C., Holt, B., Trinkaus, E., (2006. Who's afraid of the big bad Wolff?:“Wolff's law” and bone functional adaptation. Am. J. Phys. Anthropol. 129 (4), 484-498. https://doi.org/10.1002/ajpa.20371.

Ruff, C., Trinkaus, E., Walker, A., Larsen, C.S., 1993. Postcranial robusticity in Homo. I: temporal trends and mechanical interpretation. Am. J. Phys. Anthropol. 91 (1), 21-53.

Ryan, T.M., Krovitz, G.E., 2006. Trabecular bone ontogeny in the human proximal femur. J. Hum. Evol. 51 (6), 591-602. https://doi.org/10.1016/j.jhevol.2006.06.004.

Ryan, T.M., Shaw, C.N., 2012. Unique suites of trabecular bone features characterize locomotor behavior in human and non-human anthropoid primates. PloS one, 7 (7), e41037. https://doi.org/10.1371/journal.pone.0041037.

Ryan, T.M., Shaw, C.N., 2015. Gracility of the modern Homo sapiens skeleton is the result of decreased biomechanical loading. Proc. Natl. Acad. Sci. 112 (2), 372-377. https://doi.org/10.1073/pnas.1418646112.

Saers, J.P., Cazorla-Bak, Y., Shaw, C.N., Stock, J.T., Ryan, T.M., 2016. Trabecular bone structural variation throughout the human lower limb. J. Hum. Evol. 97, 97-108. https://doi.org/10.1016/j.jhevol.2016.05.012.

Saers, J.P., Ryan, T.M., Stock, J.T., 2019. Trabecular bone functional adaptation and sexual dimorphism in the human foot. Am. J. Phys. Anthropol. 168 (1), 154-169. https://doi.org/10.1002/ajpa.23732.

Sarpong, N.O., Swindell, H.W., Trupia, E.P., Vosseller, J.T., 2018. Metatarsal fractures. Foot Ankle Orthop. 3 (3), 2473011418775094. https://doi.org/10.1177/2473011418775094.

Scherf, H., Harvati, K., Hublin, J.-J., 2013. A comparison of proximal humeral cancellous bone of great apes and humans. J. Hum. Evol. 65 (1), 29-38. https://doi.org/10.1016/j.jhevol.2013.03.008.

Silva, A., Alves, J., Da Silva, O., Junior, N.S., Gazziro, M., Pereira, J., Lasso, P., Vaz, C., Pereira, C., Leiva, T., 2011. Microstructural assessment of cancellous bone using 3D microtomography. J. Phys. 313 (1), 012008. https://doi.org/10.1088/1742-6596/313/1/012008.

Stock, J., Pfeiffer, S., 2001. Linking structural variability in long bone diaphyses to habitual behaviors: foragers from the southern African later stone age and the Andaman Islands. Am. J. Phys. Anthropol. 115 (4), 337-348. https://doi.org/10.1002/ajpa.1090.

Tommy, K.A., 2018. A comparative study of trabecular architecture in the distal tibia of humans, hominoids and australopiths from South Africa. Masters dissertation, University of the Witwatersrand, Faculty of Science.

Tsegai, Z.J., Skinner, M.M., Pahr, D.H., Hublin, J.J., Kivell, T.L., 2018. Ontogeny and variability of trabecular bone in the chimpanzee humerus, femur and tibia. Am. J. Phys. Anthropol. 167 (4), 713-736. https://doi.org/10.1002/ajpa.23696.

Vogel, M., Hahn, M., Caselitz, P., Woggan, J., Pompesius-Kempa, M., Delling, G., 1990. Comparison of trabecular bone structure in man today and an ancient population in Western Germany. Bone morphometry, . Japan: Nishimura Co. pp. 220-223.

Wallace, I., Kwaczala, A., Judex, S., Demes, B., Carlson, K., 2013. Physical activity engendering loads from diverse directions augments the growing skeleton. J. Musculoskelet. Neuronal Interact. 13 (3), 283-288.

Ward, K.A., Madanhire, T., Marenah, K., Micklesfield, L.K., Gregson, C.L., 2024. Disparities in fragility fracture and osteoporosis care in Africa. Lancet Diabetes Endocrinol. 12 (5), 294-296. https://doi.org/10.1016/S2213-8587(24)00073-1.

Willems, C., Stassijns, G., Cornelis, W., D'Août, K., 2017. Biomechanical implications of walking with indigenous footwear. Am. J. Phys. Anthropol. 162 (4), 782-793. https://doi.org/10.1002/ajpa.23169.

Xue, Z., Ding, H., Hu, C., Xu, H., An, Z., 2016. An anatomical study of the nutrient foramina of the human humeral diaphysis. Med. Sci. Monit. 22, 1637-1645. https://doi.org/10.12659%2FMSM.898361.

Yang, T.-L., Shen, H., Liu, A., Dong, S.-S., Zhang, L., Deng, F.-Y., Zhao, Q., Deng, H.-W. 2020.A road map for understanding molecular and genetic determinants of osteoporosis. Nat. Rev. Endocrinol. 16 (2), 91-103. https://doi.org/10.1038/s41574-019-0282-7.

Zipfel, B., 2004. Morphological variation in the metatarsal bones of selected recent and pre-pastoral humans from South Africa. Doctoral dissertation, University of the Witwatersrand.

Zipfel, B., Berger, L.R., 2007. Shod versus unshod: the emergence of forefoot pathology in modern humans. Foot. 17 (4), 205-213. https://doi.org/10.1016/j.foot.2007.06.002.

Zwitser, E., Breederveld, R., 2010. Fractures of the fifth metatarsal; diagnosis and treatment. Injury. 41 (6), 555-562. https://doi.org/10.1016/j.injury.2009.05.035.

Chapter 8: Discussion and conclusion

8.1 Introduction

This thesis examined the topographical variations of the metatarsal diaphyseal nutrient foramen/foramina (NF) in three South African population groups, making it the largest sample-sized study to date with population, sex, age, and laterality specific to this group. Further, this thesis examined the sex estimation potential of the dimensions/measurements around the metatarsal diaphyseal NF. Given that internal bone morphology aids in predicting the degree of bone fragility and loss, this thesis also examined the trabecular structural changes around the metatarsal diaphyseal NF in 19th century and 20th century individuals. The subsequent subsections of this chapter summarise the main findings in relation to each study's aim, followed by describing the study limitations, recommendations and conclusions for the whole thesis.

8.2 Topographical variation of the metatarsal diaphyseal nutrient foramina (NF)

Chapter 2, Manjatika et al. (2023) provided a comprehensive topography of the metatarsal diaphyseal NF. The topographical variations studied included the NF number, position, location, size, and direction. This study has shown that the number of NF may be up to five per bone. This contradicts previous studies that observed the maximum number of metatarsal NF as three (Singh, 1960; Patake and Mysorekar, 1977; Malukar and Joshi, 2011; Sandhya and Singh, 2017; Kothapalli, 2018). These previous studies, however, did not describe the dimensions of the viable nutrient canal. Therefore, it may be suggested that the differences between current and previous studies are not population-specific; some very small NF may have been overlooked in the previous studies, and their sample sizes were too small to detect the number of all viable NF. The high number of NF in the metatarsal bones is similar to that observed in other long bones like the femur, demonstrating that the metatarsal bones are well vascularised and that metatarsal fractures may have a good prognosis.

Manjatika et al. (2023) have further shown that the main location of the NF is in the middle third of the metatarsal diaphysis, similar to previous studies (Monreal-Redondo and Fernández-Camacho, 2003; Anamika et al., 2015; Kothapalli, 2018). This is true for first through fifth metatarsal bones. However, some NF may also be located in the proximal and distal segments of the metatarsal diaphysis. Notably, there is no significant side of the body

or sex or population variations regarding the location of the metatarsal diaphyseal NF. Similarly, the position of the NF is also not dependent on the side of the body, sex or population affinity. However, the predominant position of the NF is variable, depending on the metatarsal bone.

Manjatika et al. (2023) show that the size of the NF correlates with bone size and its relative metabolic demands due to its position and biomechanical forces like muscle attachment. This was evident as the relatively large or big metatarsal bones (first and fifth) had predominantly large-sized NF. In contrast, the relatively small metatarsal bones (second through fourth) had predominantly small-sized NF. This study has also laid out the methodology for describing and classifying the size of the metatarsal diaphyseal NF using hypodermic needles for future studies. The nutrient canals in all the metatarsal bones obeyed the growing end theory, similar to previous studies (Anamika et al., 2015; Kothapalli, 2018). In the metacarpal bones, the direction of the nutrient canal is also similar to that described in the current study (Singh, 1959; Patake and Mysorekar, 1977; Malukar and Joshi, 2011; Singla et al., 2017). However, in the other long bones with two epiphyses e.g. the femur, tibia, and fibula, the direction of the nutrient canal is highly variable.

In general, Manjatika et al. (2023) examined the topographical variations of the metatarsal diaphyseal NF using a large sample across three South African populations with known postcranial skeletal variability (Steyn and İşcan, 1997). However, this study showed no significant topographical variations with respect to the side of the body (laterality), sex, and or within and between population groups. The lack of significant population variations on the metatarsal diaphyseal NF could be because the NF provide blood supply to the bone, a fundamental and universal physiological function shared by all populations. Additionally, the metatarsal bones are used for weight-bearing during ambulation in all populations, making them less likely to be influenced by environmental and lifestyle factors. Clinically, knowledge of the findings from the present study may help identify the nutrient foramina and preserve blood supply during surgeries to the metatarsal bones.

8.3 The utility of the dimension around the nutrient foramina (NF) in estimating sex

In Chapter 3, Manjatika et al. (2024a) described the utility of the dimensions around the metatarsal diaphyseal NF in estimating sex in the SAED populations. Generally, sex estimation equations are population-specific, and equations generated from a certain

population may not be applicable to other populations (Bidmos et al., 2021). Therefore, it is important to generate population-specific equations to accurately identify individuals within a population. There were no sex estimation equations for the South African population using metatarsal NF dimensions or other metatarsal dimensions such as the head and base measurements. It was shown that the measurements around the metatarsal diaphyseal NF are sexually dimorphic, with DFA and LRA producing classification accuracy rates of 83.1-88.7%, which are appropriate for use in forensic settings (Krogman and İşçan, 1986; Steyn and İşcan, 1997). Up to ten univariables also demonstrated high classification rates of over 75%, suggesting that these dimensions may be used in fragmentary skeletal remains. The width/breadth measurements (e.g. CNF, MLNF and DPNF) were better predictors of sex than length (NFPE and TL) measurements.

In Chapter 4, Manjatika et al. (2024b) examined the utility of the dimension around the NF in the SAA population, which is the largest SA population group and has the highest numbers of murder victims across South Africa (Bidmos et al., 2021). It was demonstrated that the dimensions around the metatarsal diaphyseal NF of the SAA population are sexually dimorphic, with males showing higher mean values than females. The multivariable DFA and LRA yielded average classification accuracy rates of 75-80.5%, while the univariable DFA models yielded 53.5–75.5% classification accuracy rates. Thus, only the classification rates of the multivariable DFA and LRA are considered appropriate for use in forensic settings (Bidmos et al., 2021).

In Chapter 5, Manjatika et al. (2024c) tested and described the utility of the dimension around the NF in the SAMA populations. The SAMA population have disproportionately high victim rates for murder within South Africa, and this makes the generation of novel and effective sex estimation equations relevant (Silber and Geffen, 2009). It has been demonstrated that the dimensions around the metatarsal diaphyseal NF of the SAMA are sexually dimorphic, with males showing higher mean values than females. The multivariable DFA and LRA yielded average classification accuracy rates of 75%–83.7%, while the univariable DFA models yielded 60.8–80% classification accuracy rates. Thus, only the classification rates of the multivariable DFA and LRA are considered appropriate for use in forensic settings (Bidmos et al., 2021).

The three above studies (chapters 3-5) have shown that the measurements around the metatarsal diaphyseal NF exhibit sexual dimorphism in the SAED, SAA and SAMA

populations. The multivariable functions performed better in all population groups compared to the univariable functions. These findings further support the need to develop multivariable functions instead of relying on univariable functions to improve sex estimation accuracy from recovered metatarsal bones (Krüger et al., 2017; Shakoane et al., 2021). The width measurements (MLNF, DPNF and CNF) performed better than the length measurements (NFPE and TL) in most univariable and multivariable functions, similar to other studies (Black III, 1978; Safont et al., 2000; Garcia, 2012; Krüger et al., 2017). The advantage of the width measurements is that they allow the metatarsal diaphyseal NF to be of forensic utility in intact and fragmented remains. Interestingly, DFA and LRA yielded comparable average classification rates. However, the data in the current studies was primarily non-parametric, implying that the generated LRA equations are more applicable than the DFA equations in all population groups.

There were, however, varied degrees of sexual dimorphism, which supports that population groups manifest sexual dimorphism differently (İşcan and Steyn, 2013). Notably, population-specific differences are attributable to genetic variations, climatic conditions, and geographical and environmental adaptations (Tawha et al., 2020). Environmental adaptations may be influenced by socioeconomic status, habitual physical activities, technology, and diet. Thus, some populations may exhibit higher sex estimation accuracy rates than others while using exact measurements. The SAED sex classification rates are similar to previous studies (Bidmos and Dayal, 2003; Fasemore et al., 2018; Sallie et al., 2022), suggesting that the metatarsal NF dimensions can be used as an alternative method of sex estimation. Unlike the SAED, the classification rates in the SAA and SAMA are lower than those from previous studies using the measurements around the head, midshaft, base and total length of the metatarsal bones in different populations (Robling and Ubelaker, 1997; Case and Ross, 2007; Moneim et al., 2008; Mountrakis et al., 2010; Bidmos et al., 2021). This shows that the measurements around the NF of the metatarsal bones are relatively weaker predictors of sex in the SAA and SAMA populations, and they can only be recommended for forensic use cautiously or in cases of commingling or recovery of an isolated foot. Notably, it may be important to assess the potential of estimating the population affinity using the metatarsal bones in order to select the appropriate population-specific equations that have been generated in the current study. In cases where population affinity can not be assessed, it may be recommended to generate universal equations that combine the metatarsal bones of the three studied South African population groups.

The current study supports previous reports where SAED usually presents higher sex estimation classification accuracies than the SAA and SAMA (Stull et al., 2014; Krüger et al., 2017; Mokoena et al., 2017; Fasemore et al., 2018). Population data suggest low rates of intra-group variations in the SAED (i.e., SAED is more homogenous in terms of population affinity) compared to the SAA and SAMA populations which explains why SAED classification rates are usually higher in most bones than in other SA populations (Krüger et al., 2017; Fasemore et al., 2018).

In general, the current studies have shown that the measurements around the metatarsal diaphyseal NF are sexually dimorphic, and the average sex classification accuracy rates were higher in the SAED, followed by the SAMA, and least in the SAA. This phenomenon is unsurprising as sexual dimorphism is less pronounced in some populations than in others (Bidmos and Dayal, 2004; Bidmos and Asala, 2004). In the current study, the multivariate functions used in each population group varied, further supporting that sexual dimorphism in some postcranial skeletons is population-specific. Exceptions, however, need to be noted as other postcranial bones, such as the pelvic bones, are intrinsically sexually dimorphic, and the sexing methods of the pelvis may apply to other populations globally (Steyn and Patriquin, 2009; Klales, 2020).

8.4 Trabecular microarchitectural changes around the metatarsal diaphyseal nutrient foramen (NF)

The nutrient foramen (NF) is widely known in the literature as a potential weak area that predisposes the long bone to fractures (Kizilkanat et al., 2007; Mazengenya and Fasemore, 2015). The trabecular morphology of the metatarsal diaphysis, especially around the NF, was examined in the current study to determine the degree of bone weakening, ontogenetic and sex-related changes and population differences in the 20th century South African populations. In addition, the trabecular morphology was assessed and compared between the 19th century and 20th century South African Africans (SAA) to determine the effects of inferred locomotory behaviours on metatarsal bone microarchitecture over time. Notably, there was limited literature describing the distinct habitual locomotory behaviours between the 19th century and 20th century SAA individuals. As such, the inference of the locomotory behaviours was based on hypothetical predictions that the 19th century and 20th century SAA had different access to habitual footwear. Previous studies have described the age, population

and locomotory behaviour changes related to the trabecular morphology. For instance, Saers et al. (2016), Chirchir et al. (2017), and (Saers et al., 2019) observed trabecular bone loss from the hunter-gatherer populations through the agriculturists to the recent modern populations, suggesting secular trends in trabecular microarchitecture. Generally, trabecular morphology is affected by genetics, age, diet, mechanical loading, temperature/climate and sex (Agarwal, 2021). However, most of these concepts are poorly accounted for when interpreting the trabecular morphometric findings. Hence, these factors may be potential confounders. In the 19th century, most SAA individuals were hunters/gatherers and practised subsistence farming, making them reliant on locally available foods, which may have resulted in a limited nutrition profile (Wadley, 1996). In the 20th century, most SAA individuals had access to urban jobs and relocated to urban settings with improved terrain and industrialized agriculture. Technological advances in the 20th century also increased the availability of diverse processed foods, leading to a rich nutrition profile (Wadley, 1996). In the current study, the 19th and 20th century SAA populations may be considered to have shared similar genetic and climatic factors but different nutrition and lifestyle factors. However, in the 20th century, SAED, SAMA, and SAA may be considered to share the same environmental, nutrition, and climatic conditions. This approach enabled a possible assessment of the effect of age and morpho-functional adaptations over a time period.

Chapter 6 (Manjatika et al., under review) described the ontogenetic or age-related trabecular morphologic changes along different levels of the metatarsal diaphysis across the SAED, SAA and SAMA of the 20th century individuals. The comparisons across the three populations were age-matched to determine if one population group is at a higher risk of bone fragility than another. When using all trabecular bone quality indicators (BS/BV, BV/TV, TbSp, TbN, TbTh, and local bone density), it was demonstrated that the areas around the NF exhibit higher trabecular bone quality compared to the proximal and distal diaphyses. This observation is true irrespective of sex, age, side of the body, or population groups, as there were no significant differences. It has also been shown that there is a gradual increase in trabecular bone quality from 0-10 years until the bone reaches peak trabecular bone quality in the 21-30 year group, and bone loss starts in the 31-40 year group in all the populations examined.

Chapter 7 (Manjatika et al., under review) described the morpho-functional adaptations and changes related to the trabecular morphology along different levels of the metatarsal diaphysis of the 19th century and 20th century SAA individuals. The 19th century and 20th

century SAA individuals were age-matched to determine the effect of different inferred habitual locomotory behaviours on the trabecular bone morphology. When using all trabecular bone quality indicators (BS/BV, BV/TV, TbSp, TbN, TbTh, and local bone density), it was demonstrated that the areas around the NF show higher trabecular bone quality compared to the proximal and distal diaphyses, similar to those reported in Chapter 6. This observation is true irrespective of sex, age, side of the body, and population groups (19^{th} vs 20^{th} century individuals), as there were no considerable significant differences. It has also been shown that there is a gradual decrease in trabecular bone quality from 18-29 years towards the 50-65 year group, and the gradual bone losses were mainly statistically non-significant.

Chapters 6 and 7 show that the areas around the NF have the highest trabecular bone quality compared to other parts of the metatarsal diaphysis. Contrary to this observation, topographical studies traditionally considered the area around the NF as potentially the weakest, predisposing the bone to high fracture risk (Campos et al., 1987; Gümüsburun et al., 1994; Kizilkanat et al., 2007; Mazengenya and Billings, 2016; Manjatika et al., 2023). These studies, however, made their conclusions without examining the microarchitecture of the bone diaphysis. Götzen et al. (2003) studied the cortical bone around the NF of equine metacarpals and reported the absence of cortical bone weakening around the NF. The current study has further expanded the understanding of the area around the NF by reporting trabecular findings similar to those reported in cortical bone (Götzen et al., 2003). As evidenced by the current study, the area around the NF is likely to be less fragile due to its high trabecular bone quality. This is because it houses the nutrient artery; hence, it is a highly vascularised and metabolically active area compared to other levels of bone diaphysis (Nagel, 1993; Brookes and Revell, 2012).

Craig et al. (2003) observed fractures at the level of NF and suggested that the fractures were due to the intrinsic weakness of the diaphyseal area. Given the findings of the current study, it may be suggested that the fractures at the level of NF, as observed by Craig et al. (2003), could be caused by the mechanism of injury or due to pathological/physiological conditions, e.g. bone fatigue. For instance, the common mechanisms of metatarsal injuries are twisting injury and direct trauma (Sarpong et al., 2018). Twisting injuries occur when one segment, e.g., the distal end of the diaphysis, is fixed to the ground, and the foot suddenly experiences rotational movements. Direct trauma injuries occur when high energy forces, e.g. from falls, road traffic accidents and repetitive loading, are exerted on a bone. Thus, it is likely that the

fractures around the proximal and distal diaphysis of the metatarsal bones could result from both mechanisms, while that of the area at the NF (midshaft) could be due to direct high-energy trauma (Owen et al., 1995; Singer et al., 2008).

Limited studies assessed the ontogenetic and sex-related changes between modern and past populations (Vogel et al., 1990; Kneissel et al., 1997; Brickley and Howell, 1999; Agarwal et al., 2004). This is because of the difficulties in obtaining accurate ages from the exhumed skeletal remains and the lack of age or sex-matched samples. The current study, however, utilised specimens from the Raymond A. Dart Collection of Modern Human Skeletons with documented records of age, sex, and population characteristics (Dayal et al., 2009). The current study has shown that the trabecular structure of the children (young) populations is weaker than that of the adult populations, suggesting that children have a higher risk of fracture development than adults. This observation is not surprising because the trabecular morphology in children is still developing and undergoing the 'modelling phase' and has not yet attained the peak trabecular maturity levels, making it weak. Once a bone reaches adult maturity, the trabecular bone undergoes constant remodelling to adapt to mechanical stressors in more variable ways, like increasing thickness in response to increased loading or reducing the thickness in areas of lower loading (Saparin et al., 2011). Thus, the current study explains why metatarsal fractures have twice the incidence in children as in adults, as reported in epidemiological studies (Rammelt et al., 2004; Petrisor et al., 2006; Moore, 2018; Sarpong et al., 2018).

Previous studies demonstrated population-related differences in the trabecular microarchitecture between South African populations and other populations of the world with regards to the iliac, radius, ulnar and vertebral bones (Schnitzler et al., 1990; Cauley, 2011; Cole et al., 2015). However, most of these differences were observed in the bone mineral density, with few differences in some trabecular bone quality indicators. The bone mineral density differences between populations are expected as they indicated nutritional disparities with individuals of low socioeconomic status exhibiting low bone mineral density compared to those from high-income societies. The current study stratified the research samples by age to ensure a uniform comparison and possibly reduce the effect of age on bone microarchitecture. The current study shows no major differences across the three 20th century South African populations in all age groups, levels and surfaces of the first and fifth metatarsal bone diaphysis. These findings support previous studies that observed only minor differences in the South African populations on the trabecular microarchitecture of the iliac

bone (Schnitzler et al., 1990). The apparent lack of major population differences in the three populations studied herein may be attributable to living in the same environment at the same time (20th century) and sharing similar nutrition and climatic conditions. In addition, similarities in trabecular microarchitecture among the three populations may reflect shared occupational characteristics and mobility patterns, including sporting activities.

Comparison of the modern and historical samples is often challenging, partly due to various radiological scanning and analysis systems constraints, resulting in a lack of unified methodology and reporting. Previous studies mainly used BV/TV and BS/BV as trabecular bone quality indicators, making it challenging to compare trabecular morphological differences between modern and historical populations (Chirchir et al., 2015, 2017). Bouxsein et al. (2010) reported that the method of analysis of the trabecular data affects the findings and subsequently their interpretations. More recent studies utilised high-resolution 3-dimensional scanning modalities compared to older studies which often used 2-dimensional histomorphometry (Chappard et al., 2005; Bouxsein et al., 2010). These technical-methodological differences make it challenging to observe the secular changes in the trabecular morphology between historical and modern populations. In the current study, however, the metatarsal bones of both the 19th and 20th century individuals were scanned and analysed using the same scanning modalities i.e., μCT on the entire sample. This approach minimised potential biases during the interpretation of the findings. Additionally, more than one indicator of trabecular bone quality i.e., BS/BV, BV/TV, TbSp, TbN, TbTh, and volumetric local bone density was assessed, giving a detailed understanding of the performance of trabecular morphology at each level of the bone. The SAA of the 19th and 20th centuries shared the same geographical location and climatic conditions. They also share the same genetic makeup. Thus, genetic and environmental co-factors and variations may be somewhat reduced, allowing a larger focus on mechanical factors like inferred habitual locomotory behaviours. The current study has shown that the trabecular microarchitecture of the 19th and 20th century SAA individuals is similar, suggesting that the variably unshod and shod locomotory behaviours were not distinct enough to show secular changes in the trabecular morphology. Additionally, a century difference may be considered too small for significant secular trends on trabecular morphology to manifest, as changes in lifestyle, culture, and technological advances are gradual. Hence, minor differences observed in the trabecular microarchitecture may have arisen due to chance and may not have morpho-functional and clinical relevance (Su et al., 2013; Wallace et al., 2017).

8.5 Study limitations

The current study has presented findings in relation to the topography, morphometry and trabecular morphological changes around the metatarsal diaphyseal nutrient foramen across different age, sex, and population groups within South Africa. However, the findings must be considered in light of some methodological limitations, especially the analysis of the trabecular morphology aspects. The study's cross-sectional nature represents a snapshot in time, and large sample size studies are required to avoid any associated biases like selective mortality and frailty (Agarwal, 2021). However, the small sample sizes utilised for the µCT in the current study showed similar trends in all ages, sexes, side of the body, populations, and bones, enabling an understanding of the trabecular morphologic changes along the diaphysis of the metatarsal bones. Nutritional and disease prevalences, which also affect the trabecular morphology, were not directly accounted for, especially those that do not present with gross macroscopic evidence. This was because the sampled individuals' medical and occupational histories were unavailable. However, the clear developmental trabecular patterns in the current study suggest that the bones utilised in the current study had no underlying bone diseases.

The sex and side of the body sample sizes within each age group were low and could not allow for robust statistical comparisons. Hence, sex and side of the body comparisons were assessed only in the pooled samples. However, the lack of significant sex or side of the body differences in both 19th and 20th century individuals could be because the metatarsal bones are primarily used for weight-bearing and locomotion, a universal functional activity performed by all individuals. The notion that the 19th SAA were variably unshod and the 20th SAA were shod was a theoretical prediction based on the literature and understanding of the SAA historical context. Thus, assessment of the effect of locomotory behaviours on the trabecular morphology between 19th and 20th century individuals utilised the SAA only, disregarding the SAED and SAMA populations. The locomotory habits of the SAED and SAMA in the 19th century were unknown partly because of migration from various geographical locations and lack of documented evidence on the mobility patterns. Moreover, the 19th century SAED and SAMA specimens were unavailable in the Raymond A. Dart Collection of Modern Human Skeletons. All aspects (topography, morphometry, and

trabecular structure) of the current study disregarded South Africans of Indian descent due to the limited sample size that could not allow meaningful statistical comparisons.

8.6 Recommendations for further studies

As demonstrated in the current study, the utility of the dimensions around the NF still requires further validation using other defined populations globally. Further validation will bring to light the population specificity of the generated equations. In settings with limited skeletal collections, further studies could potentially use metatarsal bones from living individuals by employing non-invasive 3D computerised tomography images that are routinely kept in most hospitals, though the measurements may slightly differ when compared to direct bone measurements (Ujaddughe et al., 2024).

To fully comprehend the trabecular morphologic changes and patterns around the NF, it is recommended that the internal morphology of the diaphysis of other long bones be further studied using the reference points described in the current study. Given that there is no degree of trabecular bone weakening, future studies may also need to examine the cross-sectional cortical geometry around the NF of the metatarsal bones to achieve a holistic understanding of the internal bone morphology around the NF in humans.

The current study did not observe differences between the variably unshod and the shod populations, as the transmission of weight-bearing forces during the stands phase is similar during shod and unshod walking. Nevertheless, the transmission of forces through the articular structures could be different because, in unshod walking, the base and head of the metatarsal bones land simultaneously. In contrast, in shod walking, the forces are transmitted sequentially from the heel, through the base and to the head of the metatarsal bones (De Clercq et al., 1994; De Wit et al., 2000; Lieberman et al., 2010). Thus, in future studies, examining the trabecular structure around the epiphyses (articular ends of the long bones) is imperative to determine if unshod and shod walking may exhibit significant trabecular differences.

8.7 Conclusions, novelty and significance of the current study

In conclusion, the topographical part of this study has provided a comprehensive understanding of the NF, with a new understanding of the number and size distribution of NF on each of the metatarsal bones. Overall, the study has also shown that topographical variations are not dependent on sex, laterality, or population, disproving previous claims that the variations of metatarsal diaphyseal NF are population-specific. These findings may aid in informing decisions during preoperative planning to determine the position and location of the NF, and how to best approach the fractured area to avoid iatrogenic injuries to the arteries.

The current study is the first to demonstrate that the dimensions around the metatarsal diaphyseal NF are sexually dimorphic. This was demonstrated by using three different South African populations, which aided in validating this novel methodology on the metatarsal bones. The sex classification accuracy rates are population-specific, indicating their utility in other populations must be done cautiously or combined with other known sexually dimorphic bones to achieve accurate sex estimation in archaeological and forensic settings. This new methodology of sex estimation is advantageous, particularly in South Africa, where crime rates are high, and there are limited resources and expertise, and the need for new sex estimation methods is apparent.

The current study also employed advanced imaging to determine the intrinsic bone quality differences between the three distinct and age-matched samples from 19th and 20th century individuals. For the first time, this study has shown that the area around the NF has the greatest trabecular bone quality, implying that it is less fragile, thereby disproving the speculations from topographical studies that considered the area around the NF the most fragile. It has also been shown that the metatarsal diaphysis undergoes gradual trabecular bone quality increase from 0-10 years, reaches trabecular skeletal peak quality around 21-30 years, and gradually undergoes bone loss afterwards, regardless of the population group. This study has also shown that secular trends in the trabecular structure between the contemporary (19th and 20th century) individuals do not exist, though these individuals are believed to practise different locomotor behaviours.

8.8 References

Agarwal, S. C. (2021) What is normal bone health? A bioarchaeological perspective on meaningful measures and interpretations of bone strength, loss, and aging. *American Journal of Human Biology,* 33(5)**,** pp. 23647.

Agarwal, S. C., Dumitriu, M., Tomlison, G. A. & Grynpas, M. D. (2004) Medieval trabecular bone architecture: the influence of age, sex, and lifestyle. *American Journal of Physical Anthropology.* 124(1)**,** pp. 33-44.

Anamika, K., Murlimanju, B., Divya, P., Prabhu, L. V., Saralaya, V., Rai, A. R. & Joy, T. (2015) Morphology of nutrient foramina in human metatarsals and their clinical importance. *Medicine & Health,* 10(1)**,** pp. 37-47.

Bidmos, M., Adebesin, A., Mazengenya, P., Olateju, O. & Adegboye, O. (2021) Estimation of sex from metatarsals using discriminant function and logistic regression analyses. *Australian Journal of Forensic Sciences,* 53(5)**,** pp. 543-556.

Bidmos, M. & Dayal, M. (2004) Further evidence to show population specificity of discriminant function equations for sex determination using the talus of South African blacks. *Journal of Forensic Sciences,* 49(6)**,** pp. JFS2003431.

Bidmos, M. A. & Asala, S. A. (2004) Sexual dimorphism of the calcaneus of South African blacks. *Journal of Forensic Sciences,* 49(3)**,** pp. JFS2003254.

Bidmos, M. A. & Dayal, M. R. (2003) Sex determination from the talus of South African whites by discriminant function analysis. *The American Journal of Forensic Medicine and Pathology,* 24(4)**,** pp. 322-328.

Black III, T. K. (1978) A new method for assessing the sex of fragmentary skeletal remains: femoral shaft circumference. *American Journal of Physical Anthropology,* 48(2)**,** pp. 227-231.

Bouxsein, M. L., Boyd, S. K., Christiansen, B. A., Guldberg, R. E., Jepsen, K. J. & Müller, R. (2010) Guidelines for assessment of bone microstructure in rodents using micro–computed tomography. *Journal of Bone and Mineral Research,* 25(7)**,** pp. 1468-1486.

Brickley, M. & Howell, P. (1999) Measurement of changes in trabecular bone structure with age in an archaeological population. *Journal of Archaeological Science,* 26(2)**,** pp. 151-157.

Brookes, M. & Revell, W. J. (2012) *Blood supply of bone: scientific aspects*, Springer Science & Business Media.

Campos, F. F., Pellico, L. G., Alias, M. G. & Fernandez-Valencia, R. (1987) A study of the nutrient foramina in human long bones. *Surgical and Radiologic Anatomy,* 9**,** pp. 251-255.

Case, D. T. & Ross, A. H. (2007) Sex determination from hand and foot bone lengths. *Journal of Forensic Sciences,* 52(2)**,** pp. 264-270.

Cauley, J. A. (2011) Defining ethnic and racial differences in osteoporosis and fragility fractures. *Clinical Orthopaedics and Related Research®,* 469(7)**,** pp. 1891-1899.

Chappard, D., Retailleau-Gaborit, N., Legrand, E., Baslé, M. F. & Audran, M. (2005) Comparison insight bone measurements by histomorphometry and μCT. *Journal of Bone and Mineral Research,* 20 (7)**,** pp. 1177-1184.

Chirchir, H., Kivell, T. L., Ruff, C. B., Hublin, J.-J., Carlson, K. J., Zipfel, B. & Richmond, B. G. (2015) Recent origin of low trabecular bone density in modern humans. *Proceedings of the National Academy of Sciences,* 112(2)**,** pp. 366-371.

Chirchir, H., Ruff, C. B., Junno, J. A. & Potts, R. (2017) Low trabecular bone density in recent sedentary modern humans. *American Journal of Physical Anthropology,* 162(3)**,** pp. 550-560.

Cole, T. J., Rousham, E. K., Hawley, N. L., Cameron, N., Norris, S. A. & Pettifor, J. M. (2015) Ethnic and sex differences in skeletal maturation among the birth to twenty cohort in South Africa. *Archives of Disease in Childhood,* 100(2)**,** pp. 138-143.

Craig, J. G., Widman, D. & Van Holsbeeck, M. (2003) Longitudinal stress fracture: patterns of edema and the importance of the nutrient foramen. *Skeletal Radiology,* 32**,** pp. 22-27.

Dayal, M. R., Kegley, A. D., Štrkalj, G., Bidmos, M. A. & Kuykendall, K. L. (2009) The history and composition of the Raymond A. Dart Collection of human skeletons at the

University of the Witwatersrand, Johannesburg, South Africa. *American Journal of Physical Anthropology,* 140(2)**,** pp. 324-335.

De Clercq, D., Aerts, P. & Kunnen, M. (1994) The mechanical characteristics of the human heel pad during foot strike in running: an in vivo cineradiographic study. *Journal of Biomechanics,* 27(10)**,** pp. 1213-1222.

De Wit, B., De Clercq, D. & Aerts, P. (2000) Biomechanical analysis of the stance phase during barefoot and shod running. *Journal of Biomechanics,* 33(3)**,** 269-278.

Fasemore, M. D., Bidmos, M. A., Mokoena, P., Imam, A., Billings, B. K. & Mazengenya, P. (2018) Dimensions around the nutrient foramina of the tibia and fibula in the estimation of sex. *Forensic Science International,* 287**,** pp. 222. e1-222. e7.

Garcia, S. (2012) Is the circumference at the nutrient foramen of the tibia of value to sex determination on human osteological collections? Testing a new method. *International Journal of Osteoarchaeology,* 22(3)**,** pp. 361-365.

Götzen, N., Cross, A. R., Ifju, P. G. & Rapoff, A. J. (2003) Understanding stress concentration about a nutrient foramen. *Journal of Biomechanics,* 36(10)**,** pp. 1511-1521.

Gümüsburun, E., Yücel, F., Ozkan, Y. & Akgün, Z. (1994) A study of the nutrient foramina of lower limb long bones. *Surgical and Radiologic Anatomy,* 16(4)**,** pp. 409-412.

Iscan, M. Y. & Steyn, M. (2013) *The human skeleton in forensic medicine,* Charles C Thomas Publisher.

Kizilkanat, E., Boyan, N., Ozsahin, E. T., Soames, R. & Oguz, O. (2007) Location, number and clinical significance of nutrient foramina in human long bones. *Annals of Anatomy,* 189(1)**,** pp. 87-95.

Klales, A. R. (2020) Sex estimation using pelvis morphology. *In Sex estimation of the human skeleton.* Academic Press, pp. 75-93.

Kneissel, M., Roschger, P., Steiner, W., Schamall, D., Kalchhauser, G., Boyde, A. & Teschler-Nicola, M. (1997) Cancellous bone structure in the growing and aging lumbar spine in a historic Nubian population. *Calcified Tissue International,* 61**,** pp. 95-100.

Kothapalli, J. (2018) Nutrient foramina architecture in metacarpal and metatarsal bones. *International Journal of Anatomy Research,* 6(4)**,** pp. 5848-5852.

Krogman, W. M. & Isçan, M. Y. (1986) The human skeleton in forensic medicine, Charles C. *Thomas, Springfield, IL,* 15**,** pp. 202-08.

Krüger, G. C., L'abbé, E. N. & Stull, K. E. (2017) Sex estimation from the long bones of modern South Africans. *International Journal of Legal Medicine,* 131**,** pp. 275-285.

Lieberman, D. E., Venkadesan, M., Werbel, W. A., Daoud, A. I., D'andrea, S., Davis, I. S., Mang'eni, R. O. & Pitsiladis, Y. (2010) Foot strike patterns and collision forces in habitually barefoot versus shod runners. *Nature,* 463**,** pp. 531-535.

Malukar, O. & Joshi, H. (2011) Diaphysial nutrient foramina in long bones and miniature long bones. *National Journal of Integrated Research in Medicne,* 12**,** pp. 14-17.

Manjatika, A., Mazengenya, P. & Davimes, J. (2023) Topographical anatomy and clinical implications of the metatarsal diaphyseal nutrient foramina across South African populations. *Surgical and Radiologic Anatomy*, 45, pp. 1213-1226.

Manjatika, A. T., Davimes, J. G. & Mazengenya, P. (2024a) Estimation of sex using dimensions around the metatarsal diaphyseal nutrient foramen: application of discriminant function analysis and logistic regression models. *Legal Medicine***,** 68, pp. 102417.

Manjatika, A. T., Mazengenya, P. & Davimes, J. G. (2024b) Utility of the metatarsal diaphyseal nutrient foramen in estimating sex in the South African Africans population. *Translational Research in Anatomy***,** 37, pp. 100327.

Manjatika, A. T., Davimes, J. G. & Mazengenya, P. (2024c) Application of discriminant function analysis and logistic regression models to estimate sex using the dimensions around the metatarsal diaphyseal nutrient foramen in the South Africans of Mixed ancestry. *Australian Journal of Forensic Sciences*, pp. 1-15.

Mazengenya, P. & Billings, B. (2016) Topographic and morphometric features of the nutrient foramina of the fibula in the South African mixed-ancestry population group and their surgical relevance. *European Journal of Anatomy,* 20(4)**,** pp. 329-336.

Mazengenya, P. & Fasemore, M. D. (2015) Morphometric studies of the nutrient foramen in lower limb long bones of adult black and white South Africans. *European Journal of Anatomy,* 19(2)**,** pp. 155-163.

Mokoena, P., Billings, B. K., Bidmos, M. A. & Mazengenya, P. (2017) Sex estimation using dimensions around the nutrient foramen of the long bones of the arm and forearm in South Africans. *Forensic Science International,* 278**,** pp. 404. e1-404. e5.

Moneim, W. M. A., Hady, R. H. A., Maaboud, R. M. A., Fathy, H. M. & Hamed, A. M. (2008) Identification of sex depending on radiological examination of foot and patella. *The American Journal of Forensic Medicine and Pathology,* 29(2)**,** pp. 136-140.

Monreal-Redondo, D. & Fernández-Camacho, F. (2003) Diaphyseal nutrient foramina in the first metatarsals in normal and hallux valgus feet: location and surgical implications. *Surgical and Radiologic Anatomy,* 25**,** pp. 234-240.

Moore, N. F. (2018) Metatarsal fracture management. *Orthopaedics and Trauma,* 32**,** pp. 428-436.

Mountrakis, C., Eliopoulos, C., Koilias, C. G. & Manolis, S. K. (2010) Sex determination using metatarsal osteometrics from the Athens collection. *Forensic Science International,* 200**,** pp. 178. e1-178. e7.

Nagel, A., Fernholz, F., Kibele, C. & Rosenbaum, D. (2008) Long distance running increases plantar pressures beneath the metatarsal heads: a barefoot walking investigation of 200 marathon runners. *Gait & Posture,* 27(1)**,** pp. 152-155.

Owen, R., Hickey, F. & Finlay, D. (1995) A study of metatarsal fractures in children. *Injury,* 26(8)**,** pp. 537-538.

Patake, S. & Mysorekar, V. (1977) Diaphysial nutrient foramina in human metacarpals and metatarsals. *Journal of Anatomy,* 124(2)**,** pp. 299-304.

Petrisor, B. A., Ekrol, I. & Court-Brown, C. (2006) The epidemiology of metatarsal fractures. *Foot & Ankle International,* 27(3)**,** pp. 172-174.

Rammelt, S., Heineck, J. & Zwipp, H. (2004) Metatarsal fractures. *Injury,* 35(2)**,** pp. 77-86.

Robling, A. G. & Ubelaker, D. H. (1997) Sex estimation from the metatarsals. *Journal of Forensic Science,* 42(6)**,** pp. 1062-1069.

Saers, J. P., Cazorla-Bak, Y., Shaw, C. N., Stock, J. T. & Ryan, T. M. (2016) Trabecular bone structural variation throughout the human lower limb. *Journal of Human Evolution,* 97**,** pp. 97-108.

Saers, J. P., Ryan, T. M. & Stock, J. T. (2019) Trabecular bone functional adaptation and sexual dimorphism in the human foot. *American Journal of Physical Anthropology,* 168**,** pp. 154-169.

Safont, S., Malgosa, A. & Subirà, M. E. (2000) Sex assessment on the basis of long bone circumference. *American Journal of Physical Anthropology,* 113**,** pp. 317-328.

Sallie, S., Bidmos, M. A. & Mazengenya, P. (2022) Estimation of sex from the metacarpal dimensions at the nutrient foramen in white South Africans. *Australian Journal of Forensic Sciences,* 54(4)**,** pp. 533-545.

Sandhya, K. & Singh, K. (2017) A morphometric study on the nutrient foramen of metatarsal bones in the Jharkhand population. *Journal of Dental and Medical Sciences,* 16(6)**,** pp. 31-34.

Saparin, P., Scherf, H., Hublin, J. J., Fratzl, P. & Weinkamer, R. (2011) Structural adaptation of trabecular bone revealed by position resolved analysis of proximal femora of different primates. *The Anatomical Record,* 294**,** pp. 55-67.

Sarpong, N. O., Swindell, H. W., Trupia, E. P. & Vosseller, J. T. (2018) Metatarsal fractures. *Foot & Ankle Orthopaedics,* 3(3)**,** pp. 1-8.

Schnitzler, C., Pettifor, J., Mesquita, J., Bird, M., Schnaid, E. & Smyth, A. (1990) Histomorphometry of iliac crest bone in 346 normal black and white South African adults. *Bone and Mineral,* 10(3)**,** pp. 183-199.

Shakoane, G. P., Dussault, M. C. & L'abbé, E. N. (2021) Estimating sex among South African groups using the dentition. *Forensic Science International: Reports,* 4**,** pp. 100233.

Silber, G. & Geffen, N. (2009) Race, class and violent crime in South Africa: dispelling the'Huntley thesis'. *SA Crime Quarterly,* 2009 (30)**,** pp. 35-43.

Singer, G., Cichocki, M., Schalamon, J., Eberl, R. & Höllwarth, M. E. (2008) A study of metatarsal fractures in children. *Journal of Bone and Joint Surgery,* 90(4)**,** pp. 772-776.

Singh, I. (1959) Variations in the metacarpal bones. *Journal of anatomy,* 93(2)**,** pp. 262-267.

Singh, I. (1960) Variations in the metatarsal bones. *Journal of Anatomy,* 94(3)**,** pp. 345-350.

Singla, A., Kalsi, G., Masih, N., Gupta, T. & Sharma, M. (2017) Morphological and topographical anatomy of nutrient foramens in human metacarpals and their surgical importance. *Surgical and Radiologic Anatomy,* 39**,** pp. 1227-1233.

Steyn, M. & İşcan, M. Y. (1997) Sex determination from the femur and tibia in South African whites. *Forensic Science International,* 90**,** pp. 111-119.

Steyn, M. & Patriquin, M. (2009) Osteometric sex determination from the pelvis—does population specificity matter? *Forensic Science International,* 191**,** pp. 113. e1-113. e5.

Stull, K. E., Kenyhercz, M. W. & L'abbé, E. N. (2014) Ancestry estimation in South Africa using craniometrics and geometric morphometrics. *Forensic Science International,* 245**,** pp. 206. e1-206. e7.

Su, A., Wallace, I. J. & Nakatsukasa, M. (2013) Trabecular bone anisotropy and orientation in an Early Pleistocene hominin talus from East Turkana, Kenya. *Journal of Human Evolution,* 64(6)**,** pp. 667-677.

Tawha, T., Dinkele, E., Mole, C. & Gibbon, V. E. (2020) Assessing zygomatic shape and size for estimating sex and ancestry in a South African sample. *Science & Justice,* 60**,** pp. 284-292.

Ujaddughe, O. M., Haberfeld, J., Bidmos, M. A. & Olateju, O. I. (2024) Cranial measurements obtained by three-dimensional computed tomography technique in the estimation of sex of contemporary Black South Africans. *Forensic Imaging,* 37**,** pp. 200585.

Vogel, M., Hahn, M., Caselitz, P., Woggan, J., Pompesius-Kempa, M. & Delling, G. (1990) Comparison of trabecular bone structure in man today and an ancient population in Western Germany. *Bone Morphometry***,** Japan, Nishimura Co, pp. 220-223.

Wadley, L., (1996) Changes in the social relations of precolonial hunter–gatherers after agropastoralist contact: an example from the Magaliesberg, South Africa. *Journal of Anthropological Archaeology*, 15, pp. 205-217.

Wallace, I. J., Demes, B. & Judex, S. (2017) 10 Ontogenetic and genetic influences on bone's responsiveness to mechanical signals. *Building bones: Bone formation and development in anthropology*, 77**,** pp. 233-253.

UNIVERSITY OF THE WITWATERSRAND, JOHANNESBURG | FACULTY OF HEALTH SCIENCES | Anatomical Sciences

SCHOOL OF ANATOMICAL SCIENCES ETHICS WAIVER CLEARANCE LETTER

Faculty of Health Sciences
School of Anatomical Sciences
University of the Witwatersrand
Johannesburg

Re: In terms of Chapter 8, sections 62-64 of the National Health Act No 61 of 2003 donated bodies and their tissues may be used for, among other purposes, health, and research. Use of such Material is subject only to permission from the responsible person in the School of Anatomical Sciences – the Head or person designated by the Head of School.

Human Research Ethics Committee (Medical) Clearance Certificate:

W-CBP-220504-01

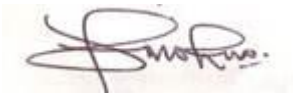
This letter serves to confirm that the Head of School, based in the School of Anatomical Sciences, Faculty of Health Sciences, has reviewed the research proposal entitled:

"Examination of the metatarsal diaphyseal nutrient foramina: implications for forensic analysis and morpho-functional adaptations in 19th and 20th century individuals"

by principal investigator: Arthur Manjatika

and supervisor/collaborators: Joshua Davimes & Pedzisai Mazengenya

and has granted approval for the ethics waiver to conduct the above-mentioned research study.



_____
Professor Amadi O. Ihunwo
Head, School of Anatomical Sciences
Faculty of Health Sciences

__21-November-2022__
Dated

School of Anatomical Sciences
7 York Rd, Parktown, 2193, South Africa, Private Bag 3, WITS 2050
Tel: +27 11 717 2405/2305 | www.wits.ac.za/anatomicalsciences/

UNIVERSITY OF THE WITWATERSRAND, JOHANNESBURG	HUMAN RESEARCH ETHICS COMMITTEE (MEDICAL)

Office of the Deputy Vice-Chancellor (Research & Innovation)

TO: Professor AO Ihunwo
School: Anatomical Sciences
Department:
Medical School
University

E-mail: Amadi.Ihunwo@wits.ac.za

CC: Supervisor: <>
and <HREC-Medical.ResearchOffice@wits.ac.za>

FROM: Mr Iain Burns
Human Research Ethics Committee (Medical)
Tel: 011 717 1252

E-mail: Iain.Burns@wits.ac.za

DATE: 04/05/2022

REF: *R14/49*

PROTOCOL NO: W-CBP-220504-01 (This is your ethics application study reference number. Please quote this reference number in all correspondence relating to this study)

PROJECT TITLE: *Research on cadaveric material*
Research conducted on donated bodies and their tissues
under sections 62-64 under the National Health Act No.61 of 2003
Formerly W-CJ-140604-1

Please find attached the Ethics Waiver Certificate for the above project. I hope it goes well and that an article in a recognized publication comes out of it. This will reflect well on your professional standing and contribute to the Government funding of the University.



MSWorks2000/Iain0007/ClearScanWaiver.wps

UNIVERSITY OF THE WITWATERSRAND, JOHANNESBURG	HUMAN RESEARCH ETHICS COMMITTEE (MEDICAL)

Office of the Deputy Vice-Chancellor (Research & Innovation)

04/05/2022

Ref: W-CBP-220504-01

TO WHOM IT MAY CONCERN

Waiver: This certifies that the following research does not require clearance from the Human Research Ethics Committee (Medical)

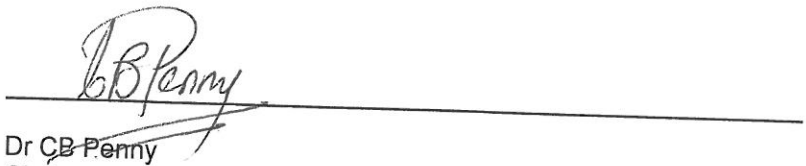
Investigator: Professor AO Ihunwo
Student No. (if appropriate):
Staff No. (if appropriate): 00500193

Supervisor:

School: Anatomical Sciences
Department:
Medical School
University

Project title: *Research on cadaveric material*
Research conducted on donated bodies and their tissues
under sections 62-64 under the National Health Act No.61 of 2003
Formerly W-CJ-140604-1

Reason: Statutory waiver
No human participants will be involved in the study



Dr CB Penny
Chairperson: Human Research Ethics Committee (Medical)

Research Office Secretariat:
Third Floor, Phillip Tobias Building, corner of St Andrews and York Roads, Parktown, Johannesburg 2193
Postal address: Private Bag 3, Wits 2050
Tel Nos: +27 (0)11 717 1234/1252/2656/2700
Office E-mail: HREC-Medical.ResearchOffice@wits.ac.za
Website:
https://www.wits.ac.za/research/researcher-support/research-ethics/ethics-committees/

Arthur Manjatika 2228141_PhD Turn it in report.docx

ORIGINALITY REPORT

21%	12%	16%	9%
SIMILARITY INDEX	INTERNET SOURCES	PUBLICATIONS	STUDENT PAPERS

PRIMARY SOURCES

1	Submitted to University of Witwatersrand Student Paper	6%
2	link.springer.com Internet Source	2%
3	kar.kent.ac.uk Internet Source	1%
4	Arthur Tsalani Manjatika, Joshua Gabriel Davimes, Pedzisai Mazengenya. "Estimation of sex using dimensions around the metatarsal diaphyseal nutrient foramen: application of discriminant function analysis and logistic regression models", Legal Medicine, 2024 Publication	1%
5	Arthur Tsalani Manjatika, Pedzisai Mazengenya, Joshua Gabriel Davimes. "Topographical anatomy and clinical implications of the metatarsal diaphyseal nutrient foramina across South African populations", Surgical and Radiologic Anatomy, 2023	1%

Declaration: Student's contribution to article(s) and agreement of co-author(s)

I, Arthur Tsalani Manjatika, student number 2228141, declare that this Thesis is my own work and that I contributed adequately towards research findings published in the article(s) stated below which are included in my Thesis.

Signature of Student:  **Date:** 08 August 2024.

Name of Primary Supervisor: Dr Joshua Gabriel Davimes.

Signature of Primary Supervisor .....  .....**Date**.....08/08/2024.....

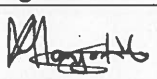
Agreement by co-authors: By signing this declaration, the co-authors listed below agree to the use of the article(s) by the student as part of his Thesis. In cases where the student is not the 1st author of a published article, the primary supervisor must explain (under comments) why the student is entitled to use the paper for his degree purposes.

Article 1: Title: Topographical anatomy and clinical implications of the metatarsal diaphyseal nutrient foramina across South African populations.
Journal name, year, volume and page numbers: Surgical and Radiologic Anatomy (2023) 45:1213–1226.

Authors	Name	Signature	Date
1st author	Arthur Tsalani Manjatika		08/08/2024
2nd author	Pedzisai Mazengenya		08/08/2024
3rd author	Joshua Gabriel Davimes		08/08/2024

Article 2: Title: Estimation of sex using dimensions around the metatarsal diaphyseal nutrient foramen: Application of discriminant function analysis and logistic regression models.

Journal name, year, volume and page numbers: Legal Medicine (2024) 68:102417.

Authors	Name	Signature	Date
1st author	Arthur Tsalani Manjatika		08/08/2024
2nd author	Joshua Gabriel Davimes		08/08/2024
3rd author	Pedzisai Mazengenya		08/08/2024

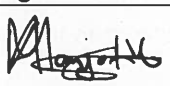
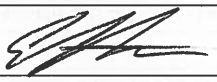
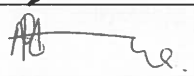
Article 3: Title: Utility of the metatarsal diaphyseal nutrient foramen in estimating sex in the South African Africans population.
Journal name, year, volume and page numbers: Translational Research in Anatomy (2024) 37:100327.

Authors	Name	Signature	Date
1st author	Arthur Tsalani Manjatika		29/07/2024
2nd author	Pedzisai Mazengenya		08/08/2024
3rd author	Joshua Gabriel Davimes		08/08/2024

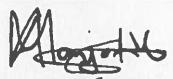
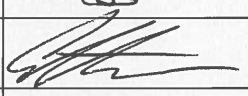
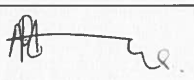
Article 4: Title: Application of discriminant function analysis and logistic regression models to estimate sex using the dimensions around the metatarsal diaphyseal nutrient foramen in the South Africans of Mixed ancestry.
Journal name, year, volume and page numbers: Australian Journal of Forensic Sciences (In Press)

Authors	Name	Signature	Date
1st author	Arthur Tsalani Manjatika		08/08/2024
2nd author	Joshua Gabriel Davimes		08/08/2024
3rd author	Pedzisai Mazengenya		08/08/2024

Article 5: Title: Age-related trabecular morphologic changes around the metatarsal diaphyseal nutrient foramina: implications for risk of fracture assessment.
Journal name, year, volume and page numbers: (Under review)

Authors	Name	Signature	Date
1st author	Arthur Tsalani Manjatika		08/08/2024
2nd author	Erin Frances Hutchinson		13/08/2024
3rd author	Pedzisai Mazengenya		08/08/2024
4th author	Joshua Gabriel Davimes		08/08/2024

Article 6: Title: Morpho-functional adaptations of the trabecular microarchitecture around the metatarsal diaphyseal nutrient foramina of the 19th and 20th century individuals.
Journal name, year, volume and page numbers: (Under review)

Authors	Name	Signature	Date
1st author	Arthur Tsalani Manjatika		08/08/2024
2nd author	Erin Frances Hutchinson		13/08/2024
3rd author	Joshua Gabriel Davimes		08/08/2024
4th author	Pedzisai Mazengenya		08/08/2024

Appendix 4: Permissions from the journal

SPRINGER NATURE LICENSE
TERMS AND CONDITIONS

Aug 05, 2024

This Agreement between Arthur Tsalani Manjatika ("You") and Springer Nature ("Springer Nature") consists of your license details and the terms and conditions provided by Springer Nature and Copyright Clearance Center.

License Number	5833860050773
License date	Jul 21, 2024
Licensed Content Publisher	Springer Nature
Licensed Content Publication	Surgical and Radiologic Anatomy
Licensed Content Title	Topographical anatomy and clinical implications of the metatarsal diaphyseal nutrient foramina across South African populations
Licensed Content Author	Arthur Tsalani Manjatika et al
Licensed Content Date	Aug 22, 2023
Type of Use	Thesis/Dissertation
Requestor type	academic/university or research institute
Format	electronic
Portion	full article/chapter
Will you be translating?	no
Circulation/distribution	1 - 29

Author of this Springer Nature content	yes
Title of new work	Examination of the metatarsal diaphyseal nutrient foramina: implications for forensic analysis and morpho-functional adaptations in 19th and 20th century individuals
Institution name	University of the Witwatersrand
Expected presentation date	Jul 2024
The Requesting Person / Organization to Appear on the License	Arthur Tsalani Manjatika
Requestor Location	Arthur Manjatika David Webster Hall, University of the Wi 1 Jan Smuts Avenue, Braamfontein Johannesburg, Gauteng 2001 South Africa Attn: Arthur Tsalani Manjatika
Billing Type	Invoice
Billing Address	Arthur Manjatika David Webster Hall, University of the Wi 1 Jan Smuts Avenue, Braamfontein Johannesburg, South Africa 2001 Attn: Arthur Tsalani Manjatika
Total	0.00 USD

Terms and Conditions

Springer Nature Customer Service Centre GmbH Terms and Conditions

The following terms and conditions ("Terms and Conditions") together with the terms specified in your [RightsLink] constitute the License ("License") between you as Licensee and Springer Nature Customer Service Centre GmbH as Licensor. By clicking 'accept' and completing the transaction for your use of the material ("Licensed Material"), you confirm your acceptance of and obligation to be bound by these Terms and Conditions.

1. Grant and Scope of License

1. 1. The Licensor grants you a personal, non-exclusive, non-transferable, non-sublicensable, revocable, world-wide License to reproduce, distribute, communicate to the public, make available, broadcast, electronically transmit or create derivative works using the Licensed Material for the purpose(s) specified in your RightsLink Licence Details only. Licenses are granted for the specific use requested in the order and for no other use, subject to these Terms and Conditions. You acknowledge and agree that the rights granted to you under this License do not include the right to modify, edit, translate, include in collective works, or create derivative works of the Licensed Material in whole or in part unless expressly stated in your RightsLink Licence Details. You may use the Licensed Material only as permitted under this Agreement and will not reproduce, distribute, display, perform, or otherwise use or exploit any Licensed Material in any way, in whole or in part, except as expressly permitted by this License.

1. 2. You may only use the Licensed Content in the manner and to the extent permitted by these Terms and Conditions, by your RightsLink Licence Details and by any applicable laws.

1. 3. A separate license may be required for any additional use of the Licensed Material, e.g. where a license has been purchased for print use only, separate permission must be obtained for electronic re-use. Similarly, a License is only valid in the language selected and does not apply for editions in other languages unless additional translation rights have been granted separately in the License.

1. 4. Any content within the Licensed Material that is owned by third parties is expressly excluded from the License.

1. 5. Rights for additional reuses such as custom editions, computer/mobile applications, film or TV reuses and/or any other derivative rights requests require additional permission and may be subject to an additional fee. Please apply to journalpermissions@springernature.com or bookpermissions@springernature.com for these rights.

2. Reservation of Rights

Licensor reserves all rights not expressly granted to you under this License. You acknowledge and agree that nothing in this License limits or restricts Licensor's rights in or use of the Licensed Material in any way. Neither this License, nor any act, omission, or statement by Licensor or you, conveys any ownership right to you in any Licensed Material, or to any element or portion thereof. As between Licensor and you, Licensor owns and retains all right, title, and interest in and to the Licensed Material subject to the license granted in Section 1.1. Your permission to use the Licensed Material is expressly conditioned on you not impairing Licensor's or the applicable copyright owner's rights in the Licensed Material in any way.

3. Restrictions on use

3. 1. Minor editing privileges are allowed for adaptations for stylistic purposes or formatting purposes provided such alterations do not alter the original meaning or intention of the Licensed Material and the new figure(s) are still accurate and representative of the Licensed Material. Any other changes including but not limited to, cropping, adapting, and/or omitting material that affect the meaning, intention or moral rights of the author(s) are strictly prohibited.

3. 2. You must not use any Licensed Material as part of any design or trademark.

3. 3. Licensed Material may be used in Open Access Publications (OAP), but any such reuse must include a clear acknowledgment of this permission visible at the same time as the figures/tables/illustration or abstract and which must indicate that the Licensed Material is not part of the governing OA license but has been reproduced with permission. This may be indicated according to any standard referencing system but must include at a minimum 'Book/Journal title, Author, Journal Name (if applicable), Volume (if applicable), Publisher, Year, reproduced with permission from SNCSC'.

4. STM Permission Guidelines

4. 1. An alternative scope of license may apply to signatories of the STM Permissions Guidelines ("STM PG") as amended from time to time and made available at https://www.stm-assoc.org/intellectual-property/permissions/permissions-guidelines/.

4. 2. For content reuse requests that qualify for permission under the STM PG, and which may be updated from time to time, the STM PG supersede the terms and conditions contained in this License.

4. 3. If a License has been granted under the STM PG, but the STM PG no longer apply at the time of publication, further permission must be sought from the Rightsholder. Contact journalpermissions@springernature.com or bookpermissions@springernature.com for these rights.

5. Duration of License

5. 1. Unless otherwise indicated on your License, a License is valid from the date of purchase ("License Date") until the end of the relevant period in the below table:

Reuse in a medical communications project	Reuse up to distribution or time period indicated in License
Reuse in a dissertation/thesis	Lifetime of thesis
Reuse in a journal/magazine	Lifetime of journal/magazine
Reuse in a book/textbook	Lifetime of edition
Reuse on a website	1 year unless otherwise specified in the License
Reuse in a presentation/slide kit/poster	Lifetime of presentation/slide kit/poster. Note: publication whether electronic or in print of presentation/slide kit/poster may require further permission.
Reuse in conference proceedings	Lifetime of conference proceedings
Reuse in an annual report	Lifetime of annual report
Reuse in training/CME materials	Reuse up to distribution or time period indicated in License
Reuse in newsmedia	Lifetime of newsmedia
Reuse in coursepack/classroom materials	Reuse up to distribution and/or time period indicated in license

6. Acknowledgement

6. 1. The Licensor's permission must be acknowledged next to the Licensed Material in print. In electronic form, this acknowledgement must be visible at the

same time as the figures/tables/illustrations or abstract and must be hyperlinked to the journal/book's homepage.

6. 2. Acknowledgement may be provided according to any standard referencing system and at a minimum should include "Author, Article/Book Title, Journal name/Book imprint, volume, page number, year, Springer Nature".

7. Reuse in a dissertation or thesis

7. 1. Where 'reuse in a dissertation/thesis' has been selected, the following terms apply: Print rights of the Version of Record are provided for; electronic rights for use only on institutional repository as defined by the Sherpa guideline (www.sherpa.ac.uk/romeo/) and only up to what is required by the awarding institution.

7. 2. For theses published under an ISBN or ISSN, separate permission is required. Please contact journalpermissions@springernature.com or bookpermissions@springernature.com for these rights.

7. 3. Authors must properly cite the published manuscript in their thesis according to current citation standards and include the following acknowledgement: '*Reproduced with permission from Springer Nature*'.

8. License Fee

You must pay the fee set forth in the License Agreement (the "License Fees"). All amounts payable by you under this License are exclusive of any sales, use, withholding, value added or similar taxes, government fees or levies or other assessments. Collection and/or remittance of such taxes to the relevant tax authority shall be the responsibility of the party who has the legal obligation to do so.

9. Warranty

9. 1. The Licensor warrants that it has, to the best of its knowledge, the rights to license reuse of the Licensed Material. **You are solely responsible for ensuring that the material you wish to license is original to the Licensor and does not carry the copyright of another entity or third party (as credited in the published version).** If the credit line on any part of the Licensed Material indicates that it was reprinted or adapted with permission from another source, then you should seek additional permission from that source to reuse the material.

9. 2. EXCEPT FOR THE EXPRESS WARRANTY STATED HEREIN AND TO THE EXTENT PERMITTED BY APPLICABLE LAW, LICENSOR PROVIDES THE LICENSED MATERIAL "AS IS" AND MAKES NO OTHER REPRESENTATION OR WARRANTY. LICENSOR EXPRESSLY DISCLAIMS ANY LIABILITY FOR ANY CLAIM ARISING FROM OR OUT OF THE CONTENT, INCLUDING BUT NOT LIMITED TO ANY ERRORS, INACCURACIES, OMISSIONS, OR DEFECTS CONTAINED THEREIN, AND ANY IMPLIED OR EXPRESS WARRANTY AS TO MERCHANTABILITY OR FITNESS FOR A PARTICULAR PURPOSE. IN NO EVENT SHALL LICENSOR BE LIABLE TO YOU OR ANY OTHER PARTY OR ANY OTHER PERSON OR FOR ANY SPECIAL, CONSEQUENTIAL, INCIDENTAL, INDIRECT, PUNITIVE, OR EXEMPLARY DAMAGES, HOWEVER CAUSED, ARISING OUT OF OR IN CONNECTION WITH THE DOWNLOADING, VIEWING OR USE OF THE LICENSED MATERIAL REGARDLESS OF THE FORM OF ACTION, WHETHER FOR BREACH OF CONTRACT, BREACH OF WARRANTY, TORT, NEGLIGENCE, INFRINGEMENT OR OTHERWISE (INCLUDING, WITHOUT LIMITATION, DAMAGES BASED ON LOSS OF

PROFITS, DATA, FILES, USE, BUSINESS OPPORTUNITY OR CLAIMS OF THIRD PARTIES), AND WHETHER OR NOT THE PARTY HAS BEEN ADVISED OF THE POSSIBILITY OF SUCH DAMAGES. THIS LIMITATION APPLIES NOTWITHSTANDING ANY FAILURE OF ESSENTIAL PURPOSE OF ANY LIMITED REMEDY PROVIDED HEREIN.

10. Termination and Cancellation

10. 1. The License and all rights granted hereunder will continue until the end of the applicable period shown in Clause 5.1 above. Thereafter, this license will be terminated and all rights granted hereunder will cease.

10. 2. Licensor reserves the right to terminate the License in the event that payment is not received in full or if you breach the terms of this License.

11. General

11. 1. The License and the rights and obligations of the parties hereto shall be construed, interpreted and determined in accordance with the laws of the Federal Republic of Germany without reference to the stipulations of the CISG (United Nations Convention on Contracts for the International Sale of Goods) or to Germany´s choice-of-law principle.

11. 2. The parties acknowledge and agree that any controversies and disputes arising out of this License shall be decided exclusively by the courts of or having jurisdiction for Heidelberg, Germany, as far as legally permissible.

11. 3. This License is solely for Licensor's and Licensee's benefit. It is not for the benefit of any other person or entity.

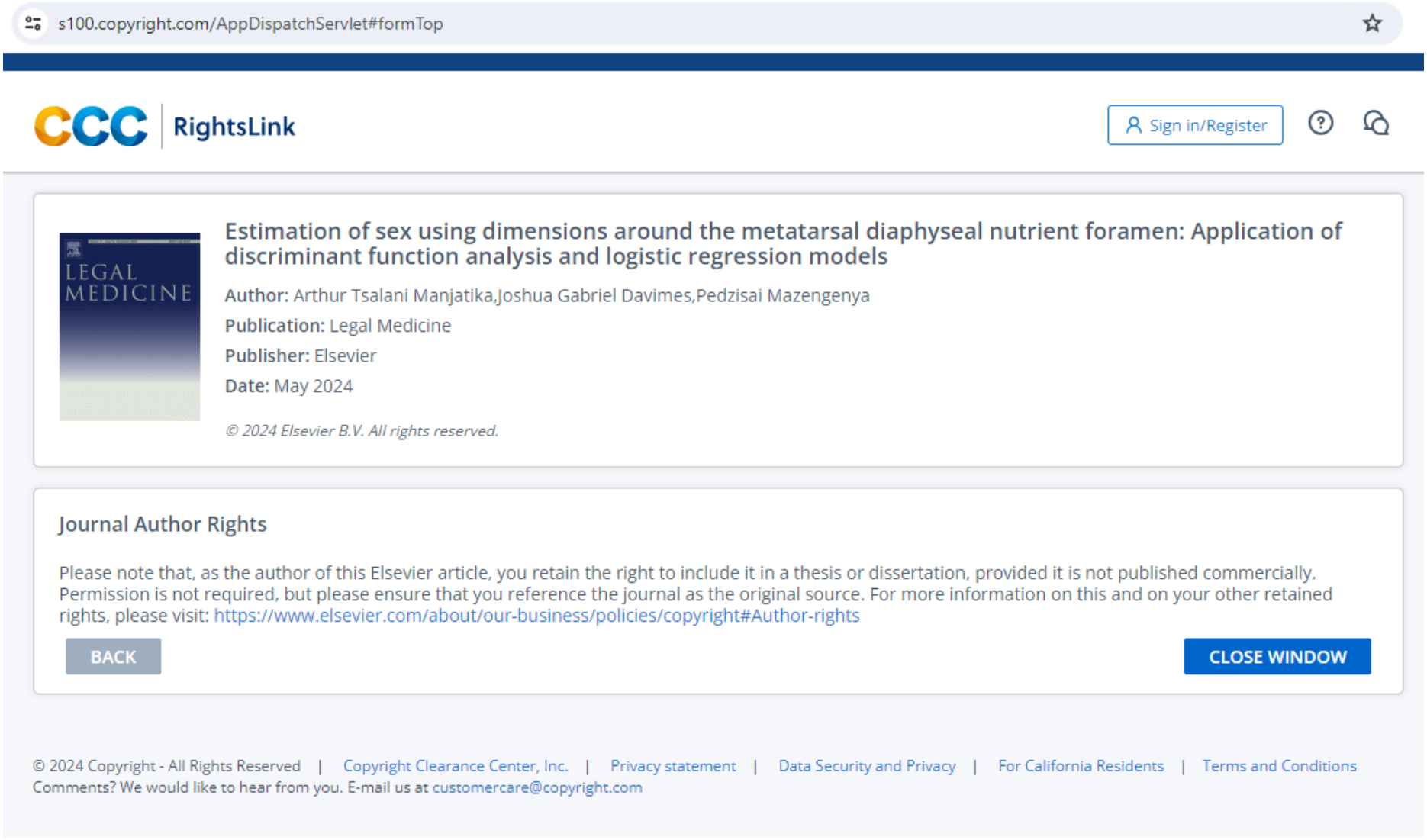
Questions? For questions on Copyright Clearance Center accounts or website issues please contact springernaturesupport@copyright.com or +1-855-239-3415 (toll free in the US) or +1-978-646-2777. For questions on Springer Nature licensing please visit https://www.springernature.com/gp/partners/rights-permissions-third-party-distribution

Other Conditions:

Version 1.4 - Dec 2022

Questions? customercare@copyright.com.

Chapter 3: No permission required



Chapter 4: No permission required

